

For Reference

NOT TO BE TAKEN FROM THIS ROOM

Ex LIBRIS
UNIVERSITATIS
ALBERTAENSIS





Digitized by the Internet Archive
in 2023 with funding from
University of Alberta Library

<https://archive.org/details/Purvis1972>

THE UNIVERSITY OF ALBERTA

AN EXPERIMENTAL AND SIMULATION STUDY OF THE DEPLETION OF
RETROGRADE HYDROCARBON MIXTURES FROM POROUS MEDIA

By



ROSS ALLAN PURVIS

A THESIS

SUBMITTED TO THE FACULTY OF GRADUATE STUDIES AND RESEARCH
IN PARTIAL FULFILMENT OF THE REQUIREMENTS FOR THE DEGREE
OF DOCTOR OF PHILOSOPHY
IN PETROLEUM ENGINEERING

DEPARTMENT OF CHEMICAL AND PETROLEUM ENGINEERING

EDMONTON, ALBERTA

FALL, 1972

Thesis
72F-87D

THE UNIVERSITY OF ALBERTA
FACULTY OF GRADUATE STUDIES AND RESEARCH

The undersigned certify that they have read, and
recommend to the Faculty of Graduate Studies and Research,
for acceptance, a thesis entitled AN EXPERIMENTAL AND SIM-
ULATION STUDY OF THE DEPLETION OF RETROGRADE HYDROCARBON
MIXTURES FROM POROUS MEDIA submitted by Ross Allan Purvis
in partial fulfilment of the requirements for the degree of
Doctor of Philosophy.

ABSTRACT

The efficient recovery of hydrocarbons from reservoirs which exhibit retrograde behavior is a matter of great commercial importance. There has been some concern and controversy about the effects porous media have on phase behavior in these reservoirs. An apparatus was constructed to study some of the effects porous media have on phase behavior and fluid recovery in retrograde systems. The apparatus could be used for a variety of experiments, however, the experimental work was concentrated on photographing the condensation and vaporization of retrograde liquids from binary mixtures in packs of uniform spheres. It was found that phase equilibrium was always maintained while liquids were condensing, but that it was very difficult to assure equilibrium during vaporization. The tendency for non-equilibrium during vaporization was traced to the nature of the changes in coexisting phase fugacities with composition.

A computer program was written to simulate the depletion performance of binary and ternary retrograde hydrocarbon mixtures. The vapor-liquid equilibria calculations were based on the Chao-Seader correlation. An interpolation procedure was developed to extend the pressure range of the Chao-Seader correlation to the convergence pressure of the mixture. The phase density calculations were based on equation of state approximations which were developed for some well-known corresponding states correlations.

ACKNOWLEDGEMENT

The author wishes to express his gratitude and appreciation to the following persons and organizations:

Professor P. M. Dranchuk -- for serving as thesis supervisor;

Professors D. B. Robinson, A. E. Mather, D. L. Flock and C. M. Rodkiewicz -- for serving on the thesis committee and for numerous beneficial discussions;

The machine shop and DACS center personnel of the Department of Chemical and Petroleum Engineering -- for their assistance and co-operation;

Fellow graduate students -- for their discussions with regard to this work;

The National Research Council of Canada, the Petroleum Recovery Research Institute of Calgary and the Aid to Education Fund -- for their financial support of this work;

His wife -- for her understanding and for typing the manuscript;

His family -- for their patience.

TABLE OF CONTENTS

	Page
LIST OF TABLES	iv
LIST OF FIGURES	vii
Chapter 1. INTRODUCTION	
1.1 Terminology for Retrograde Systems	1
1.2 Characteristics of Naturally Occuring Systems	2
1.3 Recovery Methods for Retrograde Gas Reservoirs	4
1.4 Literature Review of Experiments to Simulate Retrograde Reservoir Processes	7
(a) Effect of Porous Media	7
(b) Two-Phase Flow Considerations	11
(c) Effect of Connate Water	13
1.5 Objectives and Procedures	13
Chapter 2. EXPERIMENTAL APPARATUS AND OPERATING PROCEDURE	
2.1 General Description of Apparatus	15
2.2 Sampling and Analyses	17
2.3 Loading and Mixing a New Charge	20
2.4 Unpacked Cell Depletion	21
2.5 Packed Cell Depletion	22
2.6 Simultaneous Packed Cell and Unpacked Cell Dew or Bubble Point Determination	22
2.7 Vaporization of Retrograde Liquid from the Packed Cell	23
Chapter 3. EXPERIMENTAL RESULTS AND DISCUSSION OF RESULTS	
3.1 Materials	26
3.2 Calibrations and Sources of Error	27
3.3 Methane and n-Butane Mixtures	29
3.4 Methane and n-Pentane Mixtures	33
3.5 Methane and n-Hexane Mixture	42
3.6 Role of Fugacity in Attaining Equilibrium . .	45
3.7 Simultaneous Packed Cell and Unpacked Cell Dew or Bubble Point Measurements	50
3.8 Vaporization of a Retrograde Liquid by Contacting with Methane	52
3.9 Photographs of Retrograde Liquid Structures .	55
Chapter 4. CALCULATION OF VAPOR-LIQUID EQUILIBRIA	
4.1 Foreword	57
4.2 The N.G.A.A. K-Value Charts	57
4.3 The Critical Composition Method of Estimating Convergence Pressure	63
4.4 The Chao-Seader Method	65
4.5 Combined Chao-Seader and Critical Composition Methods	70

Table of Contents (cont.)

Page

Chapter 5. CALCULATION OF VAPOR AND LIQUID DENSITIES

5.1	Foreword	74
5.2	Some Equation of State Features	75
5.3	A General Method for Analytical Representation of Compressibility Factor Correlations	84
5.4	Application of the Generalized Equation of State Method to the Lydersen et al. Correlation	87
	(a) Saturated Liquid Densities	87
	(b) Vapor Pressure Equation	89
	(c) Saturated Vapor Densities	90
	(d) Single-Phase Region - Isochores	92
	(e) Discussion	95
	(f) Conclusions	98
5.5	Application of Some Reduced Equations of State to the Standing and Katz Correlation	99
5.6	Application of Some Reduced Equations of State to the Rowlinson Correlation	105

Chapter 6. SIMULATION OF EXPERIMENTAL RESULTS AND
SELECTED LITERATURE DATA

6.1	Foreword	110
6.2	Simulation of Experimental Results	110
	(a) Methane and n-Butane Mixtures	111
	(b) Methane and n-Pentane Mixtures	115
	(c) Methane and n-Hexane Mixture	120
6.3	Simulated Depletion Performance of Some Ternary Mixtures	124
	(a) Methane, Propane and n-Butane Mixtures	125
	(b) Methane, Propane and n-Pentane Mixtures	129
	(c) Methane, Propane and Decane Mixtures	132
	(d) Methane, n-Butane and Decane Mixtures	137

Chapter 7. CONCLUSIONS AND RECOMMENDATIONS

7.1	Conclusions	147
7.2	Recommendations	149

NOMENCLATURE

REFERENCES

APPENDIX A - LEAST SQUARES FITTING TECHNIQUES

A.1	Foreword	A-1
A.2	Computer Program	A-2

APPENDIX B - TWO-PARAMETER EQUATIONS OF STATE

B.1	Foreword	B-1
B.2	van der Waals Equation	B-1

Table of Contents (cont.)	Page
B.3 Berthelot Equation	B-7
B.4 Dieterici Equation	B-9
B.5 Redlich-Kwong Equation	B-15
APPENDIX C - COMPUTER PROGRAMS FOR CORRESPONDING STATES DENSITY CORRELATIONS	
APPENDIX D - COMPUTER PROGRAM TO SIMULATE THE DEPLETION PERFORMANCE OF A CONSTANT VOLUME RESERVOIR	
APPENDIX E - COMPUTER PRINTOUT FOR SIMULATION OF DEPLETION PERFORMANCE RUNS	
APPENDIX F - CORRELATION OF CRITICAL COMPRESSIBILITY FACTORS AND CRITICAL PRESSURES FOR BINARY MIXTURES	
F.1 Foreword	F-1
F.2 Correlation of Critical Compressibility Factors	F-2
F.3 Correlation of Critical Pressures	F-4
APPENDIX G - DENSITY BALANCE CALIBRATION AND DATA REDUCTION PROGRAM	
G.1 Foreword	G-1
G.2 Density Balance Calibration	G-1
G.3 Density Balance Data Reduction Progam	G-7
APPENDIX H - INSTRUMENT CALIBRATION DATA	
APPENDIX I - PHOTOGRAPHS OF RETROGRADE LIQUID CAPILLARY STRUCTURES	

LIST OF TABLES

Table No.		Page
3-1	SUMMARY OF POROUS MEDIA AND PACKED CELL DATA	28
3-2	COMPOSITION AND PER CENT LIQUID DATA FOR METHANE AND N-BUTANE MIXTURES	30
3-3	COMPOSITION AND PER CENT LIQUID DATA FOR METHANE AND N-PENTANE MIXTURES	35
3-4	COMPOSITION AND PER CENT LIQUID DATA FOR THE METHANE AND N-HEXANE MIXTURE	43
3-5	SIMULTANEOUS PACKED CELL AND UNPACKED CELL DEW OR BUBBLE POINT MEASUREMENTS	51
5-1	COMPARISON OF CALCULATED DENSITIES WITH THE DATA SOURCE	94
6-1	RUN NO. 4, METHANE AND N-BUTANE AT 100°F	112
6-2	RUN NO. 3, METHANE AND N-PENTANE AT 100°F	117
6-3	RUN NO. 7, METHANE AND N-HEXANE AT 100°F	122
6-4	METHANE, PROPANE AND N-BUTANE MIXTURE AT 40°F	126
6-5	METHANE, PROPANE AND N-PENTANE MIXTURE AT 100°F	130
6-6	METHANE, PROPANE AND N-DECANE MIXTURE AT 100°F	134
6-7	METHANE, N-BUTANE AND N-DECANE MIXTURE AT 160°F	140
B-1	TABLE OF PERCENTAGE DIFFERENCES BETWEEN CORRE- LATION AND VAN DER WAALS EQUATION	B-5
B-2	TABLE OF PERCENTAGE DIFFERENCES BETWEEN CORRE- LATION AND VAN DER WAALS EQUATION	B-6
B-3	SUMMARY OF TWO-PARAMETER EQUATION OF STATE APPROXIMATIONS FOR THE z_T ISOCHORES OF ROWLINSON'S CORRELATION	B-8
B-4	TABLE OF PERCENTAGE DIFFERENCES BETWEEN CORRE- LATION AND BERTHELOT EQUATION	B-10
B-5	TABLE OF PERCENTAGE DIFFERENCES BETWEEN CORRE- LATION AND BERTHELOT EQUATION	B-11
B-6	TABLE OF PERCENTAGE DIFFERENCES BETWEEN CORRE- LATION AND DIETERICI EQUATION	B-13
B-7	TABLE OF PERCENTAGE DIFFERENCES BETWEEN CORRE- LATION AND DIETERICI EQUATION	B-14

Table No.	Page
B-8 TABLE OF PERCENTAGE DIFFERENCES BETWEEN CORRELATION AND REDLICH-KWONG EQUATION	B-17
B-9 TABLE OF PERCENTAGE DIFFERENCES BETWEEN CORRELATION AND REDLICH-KWONG EQUATION	B-19
E-1 RUN NO. 5, METHANE AND N-BUTANE AT 100°F	E-1
E-2 RUN NO. 13, METHANE AND N-BUTANE AT 100°F	E-3
E-3 RUN NO. 1, METHANE AND N-PENTANE AT 99.5°F	E-5
E-4 RUN NO. 2, METHANE AND N-PENTANE AT 99.7°F	E-7
E-5 RUN NO. 8, METHANE AND N-PENTANE AT 100°F	E-9
E-6 RUN NO. 9, METHANE AND N-PENTANE AT 100°F	E-11
E-7 RUN NO. 10, UHP METHANE AND N-PENTANE AT 100°F	E-13
E-8 RUN NO. 11, METHANE AND N-PENTANE AT 160°F	E-15
E-9 RUN NO. 12, METHANE AND N-PENTANE AT 100°F	E-17
E-10 METHANE, PROPANE AND N-BUTANE MIXTURE AT 100°F	E-19
E-11 METHANE, PROPANE AND N-BUTANE MIXTURE AT 160°F	E-21
E-12 METHANE, PROPANE AND N-PENTANE MIXTURE AT 160°F	E-23
E-13 METHANE, PROPANE AND N-PENTANE MIXTURE AT 220°F	E-25
E-14 METHANE, PROPANE AND N-DECANE MIXTURE AT 280°F	E-27
E-15 METHANE, N-BUTANE AND N-DECANE MIXTURE AT 280°F	E-29
F-1 CRITICAL STATE DATA FOR SOME METHANE BINARIES	F-6
F-2 CRITICAL STATE DATA FOR SOME ETHANE BINARIES	F-11
F-3 CRITICAL STATE DATA FOR SOME PROPANE BINARIES	F-14
F-4 CRITICAL STATE DATA FOR SOME MISCELLANEOUS BINARIES	F-17
G-1 DENSITY BALANCE CALIBRATIONS USING HELIUM	G-3
G-2 DENSITY BALANCE CALIBRATIONS USING METHANE	G-4
G-3 DENSITY BALANCE CALIBRATIONS USING NITROGEN	G-5
G-4 DENSITY BALANCE CALIBRATION USING UHP METHANE AND UHP CARBON DIOXIDE	G-6

Table No.	Page
H-1 PRESSURE GAUGE CALIBRATIONS	H-1
H-2 THERMOCOUPLE CALIBRATION	H-2

LIST OF FIGURES

Figure No.		Page
1-1	Schematic Phase Diagram Illustrating Nomenclature for Retrograde Systems	3
2-1	Schematic Diagram of Apparatus for Study of Retrograde Phenomenon in Porous Media	16
2-2	Schematic Diagram of Sample Analysis Section .	18
2-3	Typical Chart for Dew Point Determinations in Packed and Unpacked Cells	24
3-1	Pressure-Composition Isotherms for the Methane and n-Butane System at 100°F	32
3-2	Retrograde Liquid Saturation for Differential Depletion of Methane-n-Butane Mixtures	34
3-3	Pressure-Composition Isotherms for the Methane and n-Pentane System at 100°F	39
3-4	Retrograde Liquid Saturation for Differential Depletion of Methane-n-Pentane Mixtures	41
3-5	Pressure-Composition Isotherms for the Methane and n-Hexane System at 100°F	44
3-6	Examples Showing the Effect of Pressure on Fugacity in the Two-Phase Region	47
3-7	Effect of Composition on the Fugacity of n-Butane in the Two-Phase Region	49
3-8	Pentane Recovery by Contacting with Methane .	53
3-9	Typical Photographs of Sphere Packs	56
4-1	Equilibrium Ratios for the Methane-n-Pentane System at 100°F	60
4-2	Pressure-Temperature Diagram Illustrating the Critical Composition Method for Calculating Convergence Pressure in Multicomponent Systems	66
4-3	Correction Factors for Methane K-values from the Chao-Seader Correlation at 100°F	71
5-1	Isochoric Diagram Showing The Vapor Pressure Curve	76
5-2	Temperature Isochoric Diagram Showing the Two-Phase Envelope	82

Figure No.	Page
5-3 Pressure Isochoric Diagram Showing the Two-Phase Envelope	83
5-4 Isochoric Diagrams with the Saturated State Taken as a Datum	85
5-5 Compressibility Factor Diagram for the Lydersen, Greenkorn and Hougen Correlation	96
5-6 Compressibility Factor Diagram for the Standing and Katz Correlation	101
5-7 Compressibility Factor Diagram for the Rowlinson Correlation	108
6-1 Comparison of Calculated and Literature Equilibrium Ratios for the Methane-n-Butane System at 100°F	114
6-2 Comparison of Calculated and Literature Phase Densities for the Methane-n-Butane System at 100°F	116
6-3 Comparison of Calculated and Literature Equilibrium Ratios for the Methane-n-Pentane System at 100°F	119
6-4 Comparison of Calculated and Literature Phase Densities for the Methane-n-Pentane System at 100°F	121
6-5 Comparison of Calculated and Literature Equilibrium Ratios for the Methane-Propane-n-Butane Mixtures of Table 6-4	128
6-6 Comparison of Calculated and Literature Equilibrium Ratios for the Methane-Propane-n-Pentane Mixtures of Table 6-5	133
6-7 Comparison of Calculated and Literature Equilibrium Ratios for the Methane-Propane-Decane Mixtures of Table 6-6	136
6-8 Loci of Phase Compositions for the Simulated Depletion Performance of the Mixtures Given in Tables 6-6 and E-14	138
6-9 Comparison of Calculated and Literature Equilibrium Ratios for the Methane-n-Butane-Decane Mixtures of Table 6-7	143
6-10 Loci of Phase Compositions for the Simulated Depletion Performance of the Mixtures Given in Tables 6-7 and E-15	144

Figure No.	Page
6-11 Volume Per Cent Retrograde Liquid for the Example Depletion Calculations Presented in Tables 6-7 and E-15	146
F-1 z_c Excess Values for Binary Mixtures Containing Methane	F-21
F-2 Correlation of z_{cij} with $ T_{ci} - T_{cj} $ for Binary Mixtures Containing Methane	F-22
F-3 z_c Excess Values for Binary Mixtures Containing Ethane	F-23
F-4 z_c Excess Values for Binary Mixtures Containing Propane	F-24
I-1 Photographs of Liquid Capillary Structures Formed During Pressure Depletion of the Methane-n-Butane Mixture in Run 4	I-1
I-2 Photographs of Liquid Capillary Structures Formed During Pressure Depletion of the Methane-n-Butane Mixture in Run 5	I-2
I-3 Photographs of Liquid Capillary Structures Formed During Pressure Depletion of the Methane-n-Hexane Mixture in Run 7	I-3
I-4 Photographs of Liquid Capillary Structures Formed During Pressure Depletion of the Methane-n-Butane Mixture in Run 13	I-4

Chapter 1. INTRODUCTION

1.1 Terminology for Retrograde Systems

The adjective "retrograde" is used to designate a direction or a condition which is contrary to a previous direction or an earlier condition. Katz and Kurata¹ reported that the first use of retrograde in connection with phase behavior was by Kuenen at Leiden in 1892. Kuenen used the term "retrograde condensation" to describe the appearance and subsequent disappearance of a liquid phase during isothermal compression of binary mixtures at temperatures above their critical. Katz and Kurata have given some rules for nomenclature which are now generally used to describe retrograde phenomena in phase behavior. Their rules are:

1. Condensation is interpreted as the formation of a more dense or liquid phase, and vaporization is interpreted as the formation of a less dense or vapor phase when the system is on or within the border curve for the two phase system.

2. The term "retrograde" is used to earmark phase changes in which the direction of temperature or pressure travel causing the phase change is backward from that which causes the phase change for normal cases, such as pure substances or mixtures at low pressure.

3. Only isothermal or isobaric changes are considered retrograde, since a change in phase accompanying a combined variation of pressure and temperature has no standard of comparison.

4. If two liquid phases form during an isothermal or isobaric process, then the word "double" will prefix the name

such as double isobaric retrograde condensation.

Figure 1-1 is a schematic phase diagram for a multicomponent hydrocarbon mixture which illustrates the preferred nomenclature to describe retrograde behavior. It should be noted that the term "revaporization" is not required under these rules. The border curve in Figure 1-1 is such that both the bubble point and dew point lines reverse slope to join at the critical point. Hence, retrograde condensation can occur between dew points such as points D and D', and is sometimes called condensation of the first kind. Similarly retrograde condensation can occur between bubble points which is sometimes referred to as condensation of the second kind. In some mixtures only the bubble point line or the dew point line reverses to the critical point, and just one retrograde region occurs.

In oil-field terminology underground accumulations of hydrocarbons are broadly classified as gas or oil reservoirs. Gas reservoirs are multicomponent mixtures which exist in the gaseous state under initial reservoir pressure and temperature and can be further classified as: (a) gas-condensate or retrograde gas, (b) wet gas, and (c) dry gas.

1.2 Characteristics of Naturally Occuring Systems

To be classified as a retrograde gas, the reservoir temperature must lie between the critical and cricondentherm points of the phase diagram for the original mixture. Since the reservoir production process occurs at essentially constant temperature, only isothermal retrograde condensation or

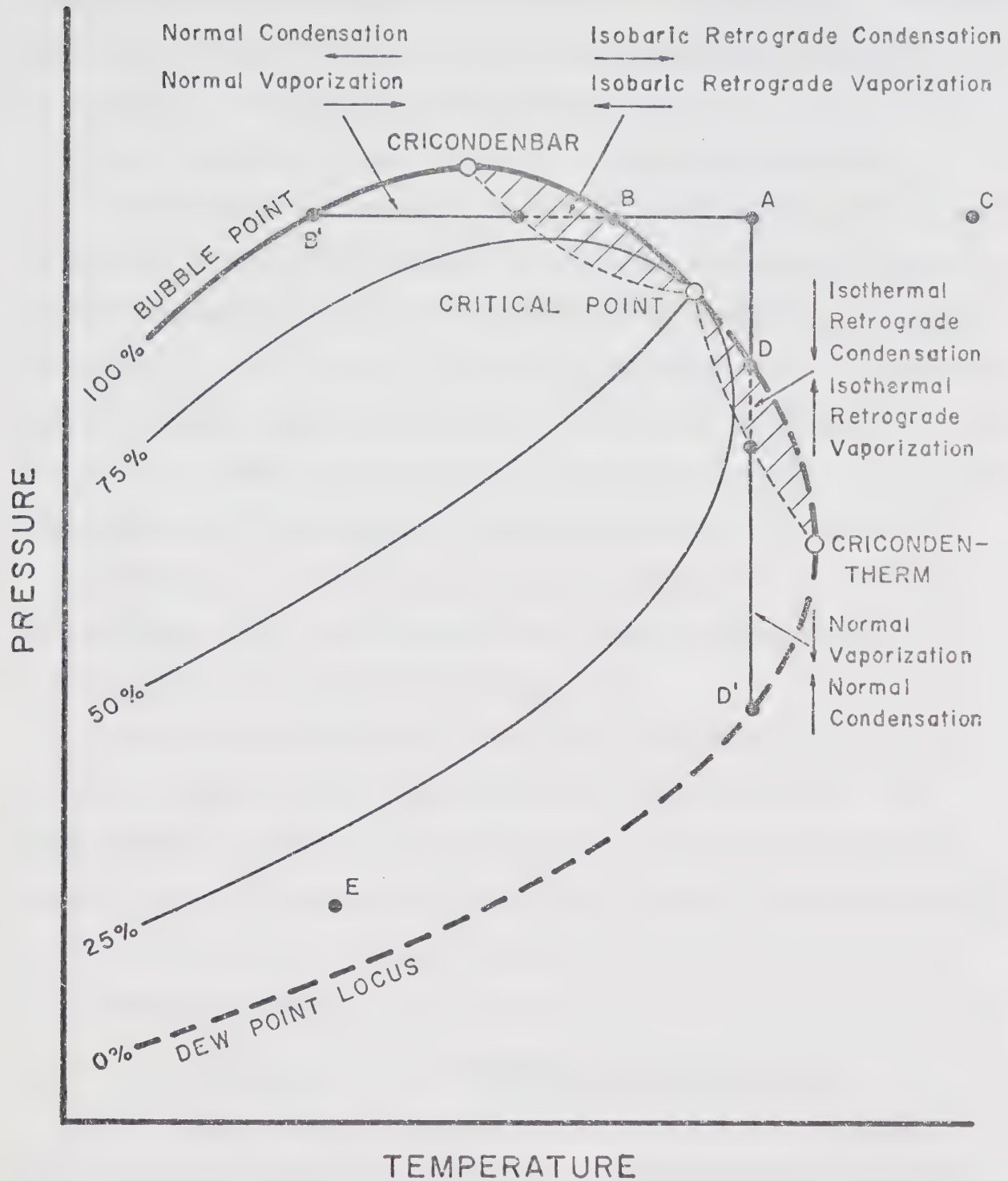


Figure 1-1. Schematic Phase Diagram Illustrating Nomenclature for Retrograde Systems.

vaporization are of interest to reservoir engineers. A reservoir temperature and initial reservoir pressure corresponding to point A of Figure 1-1, and pressure decline along the path A-D' are typical of a gas-condensate or retrograde gas.

Wet gas reservoirs have reservoir temperatures which are in excess of the cricondentherm, and therefore always remain in the single phase gaseous region in the reservoir. Point C of Figure 1-1 is typical of the initial conditions of pressure and temperature for such systems. The term "wet" results from the fact that the system is in the two phase region at surface separator conditions such as those of point E in Figure 1-1. The separator liquid from a wet gas contains fewer heavy hydrocarbons than a retrograde gas, and the quantity of separator liquid recovered is usually less.

Dry gas reservoirs are comprised principally of methane with only minor amounts of intermediate hydrocarbons. No hydrocarbon liquids condense from these mixtures, either in the reservoir or surface facilities. However, water vapor is usually removed to prevent formation of gas hydrates in gas pipelines and distribution systems.

1.3 Recovery Methods for Retrograde Gas Reservoirs

The exploitation schemes for wet gas or dry gas reservoirs are much different than those for retrograde gas reservoirs. In the former, a decline in reservoir pressure with continued gas production does not result in the formation of a liquid phase within the reservoir. Therefore, the composition of the produced gas and remaining reservoir gas never

changes. In retrograde gas reservoirs the formation of a reservoir liquid which is rich in the heavier components causes the produced gas and remaining reservoir vapor-liquid mixture to have continuously changing compositions. As the two phase mixture in the reservoir becomes richer in the heavier components, the critical point, and the entire pressure-temperature phase diagram shifts to the right (higher temperature region). This results in a reduced dew point pressure at reservoir temperature which may not be reached at the abandonment pressure. Thus, some of the retrograde liquid is not vaporized, but remains in the reservoir at abandonment.

At the present time there are three general procedures for recovering gas-condensate fluids from constant volume reservoirs (reservoirs in which there is no water influx or other change in reservoir volume). The first and simplest is to produce and market all production after it has been processed into pipeline or residue gas, liquified petroleum gas (LPG), and stabilized condensate. This depletion procedure is characterized by: (a) minimum initial capital investment, (b) high initial cash flow, (c) low recovery of retrograde liquids, and (d) numerous operating problems in the later stages of depletion due to low deliverability and liquid accumulations in producing wells. This method is currently practiced only when the initial retrograde gas is lean, or when the reservoir is too small to justify the expense of an enhanced recovery method.

A second method which was originally investigated by Standing, Lindblad, and Parsons² is to initially produce the

reservoir as in the first method, but to initiate residue gas cycling after partial depletion. There are several advantages to this method: (a) minimum initial capital investment, (b) high initial cash flow, (c) good retrograde liquid recovery, (d) deferred capital investment for a compressor plant, (e) compressor plant construction costs are reduced as the design pressure is much less than the original reservoir pressure, and (f) there are fewer operating problems during the later stages of depletion.

The third and most common method of recovery is to initiate residue gas cycling at the start of production, and to continue cycling until the fluid from producing wells becomes largely diluted with injected residue gas. If full pressure maintenance is to be attained makeup gas must be purchased or otherwise be available, since some gas is used for compressor fuel, and the LPG and condensate are sold. The advantages of this method are: (a) the reservoir process is a miscible gas-gas displacement, (b) there is complete recovery of natural gas liquids from that portion of the reservoir swept by dry gas, (c) flow capacity is sustained since a minimum of retrograde condensation occurs in the reservoir, and (d) there are few operational problems during the "blow down" after cycling is stopped. The disadvantages are: (a) large initial capital investment in cycling facilities, (b) higher operating costs, (c) long project life, and (d) deferred gas sales. Some of these disadvantages can be offset by a recently investigated³ variation which permits gradually declining reservoir pressure by cycling only part of the residue gas.

1.4 Literature Review of Experiments to Simulate Retrograde Reservoir Processes

The isothermal retrograde condensation and vaporization processes which occur during the depletion of a reservoir are approximated in commercial laboratories by stepwise differential depletions. A reservoir sample is charged to a PVT cell and the system is brought to reservoir temperature and original pressure. A portion of the equilibrium vapor is then removed from the top of the cell, the system equilibrated, and measurements of pressure, liquid volume, and phase composition are made. The procedure is repeated to some arbitrary lower pressure. The PVT cells used for these density and vapor-liquid equilibria measurements do not contain a porous medium. Thus there has been some concern as to whether the results of experiments in unpacked cells are representative of the actual behavior in the interstices of the reservoir rock. There are three major differences between experimental and actual reservoir conditions which have caused concern.

1.4 (a) Effect of Porous Media

The effect of a porous medium on the geometry of the vapor-liquid interface is neglected. The first experimental work with retrograde fluids in the presence of a porous medium was reported in 1948 by Weinaug and Cordell⁴. They depleted binary mixtures of methane-butane and methane-pentane from unconsolidated Ottawa sand packs without a connate water saturation. The results were compared to the depletion of methane-butane mixtures from an unpacked cell over similar time periods. This comparison indicated that vaporization of retrograde liquids was aided by the presence of the sand. The

improved vaporization from the sand was probably a result of increased interfacial area rather than being related to the curved vapor-liquid interface. Oxford and Huntington⁵ performed a series of depletion and constant pressure vaporization experiments with nitrogen-hexane, nitrogen-heptane, and a nitrogen-natural condensate mixture in unconsolidated Wilcox sand packs. They concluded that condensates could be vaporized from sands, and that depletion rate, connate water or initial hydrocarbon liquid saturation have a negligible effect on the performance. These conclusions are largely qualitative since the mixtures studied did not exhibit retrograde behavior under experimental conditions, but simply the solubility of hydrocarbons in nitrogen.

The next phase behavior work in a porous medium involved bubble point measurements in crude oil systems. Gimatudinov and Shedlovsky⁶ devised a sensitive technique for determining bubble points within cores from a break in the pressure-volume curve. The technique used formation water as an intermediate fluid, and gas pressure rather than piston movement to effect a change in volume and pressure. They found bubble points to be 4 to 5 atm. higher in natural sandstone cores (permeabilities ranged from 0.1 to 2.0 darcies) than the corresponding bubble points (30 to 70 atm.) in unpacked cells. Tindy and Raynal⁷ reported similar increases in bubble point pressures for crude oils in unconsolidated packs of sand, glass beads, powdered steel and pumice. They observed that for porous media composed of glass beads with grain diameter varying from 145 microns to 5 mm., that the increase in saturation pressure

was insensitive to grain diameter. They also noted that the chemical nature of the porous medium did not have a marked effect on the magnitude of the increase in saturation pressure.

Two Russian papers^{8, 9} reported a method for determining the initial condensation pressure (upper dew point) for retrograde gases in unconsolidated sand packs under flowing conditions. A change in apparent permeability with pressure was observed. The pressure corresponding to the maximum permeability, on a pressure versus permeability diagram, was taken to be the dew point. These pressures were from 8 to 15 atm. higher than the corresponding dew points (206 to 255 atm.) under static conditions in an unpacked cell. Dissertation work by Mamedov¹⁰ also indicated higher upper dew point pressures for gas-condensate mixtures in a porous medium.

A new apparatus¹¹ for comparing the behavior of retrograde gas mixtures in packed and unpacked cells was reported in 1965, and has been used in several Russian studies of condensate recovery. Trebin and Zadora¹² depleted retrograde gas mixtures from an unpacked cell and from packed cells having specific surface areas of 563, 1307 and 3415 $\text{cm.}^2/\text{cm.}^3$. They tried various depletion rates and found that $4 \text{ kg./cm.}^2/\text{hr.}$ resulted in equilibrium between phases. Their data indicated that: (a) the gas produced from a packed cell always contained less recoverable condensate than the gas from an unpacked cell, (b) increasing the specific surface of the porous medium caused a decrease in the condensate content of the produced gas and in the total condensate recovered by depletion to atmospheric pressure, (c) the richer the initial retrograde gas

mixture, the greater the effect of the porous medium, and (d) the effect of the porous medium on depletion performance decreases with increased temperature.

Smith and Yarborough¹³ reported experiments on vaporization of retrograde liquids from unconsolidated sand packs by dry gas injection at 1500 psi and 100°F. Three runs with the methane-pentane system showed that a retrograde liquid saturation of approximately 6.5 per cent could be vaporized by contacting with 2.5 pore volumes of methane. Pentane recovery was found to be independent of sand wettability and connate water saturation. A vaporization run with 7.2 per cent retrograde liquid saturation from a simulated sour gas-condensate (pentane and heptane were used for heavy components) was performed in a sand pack without a connate water saturation. The injected dry gas was a methane-hydrogen sulfide mixture. The pentane was completely recovered by injecting four pore volumes of dry gas, however, six pore volumes of dry gas were required to vaporize all the heptane. It was concluded that retrograde liquids could be completely recovered if they were contacted with sufficient dry gas. A Russian paper¹⁴ reported experiments with a particular gas-condensate mixture at 20°C where no vaporization of the retrograde liquid occurred within a packed column. A chemical analysis of the mixture was not reported, so it can only be assumed that the mixture consisted of high boiling point hydrocarbons with very few intermediates. Standing, Lindblad and Parsons² reported some calculations to estimate the quantity of dry gas required to vaporize a retrograde

liquid from a reservoir fluid. They stated that laboratory tests were performed to confirm calculations that a retrograde liquid saturation of 7.8 per cent could be vaporized by three pore volumes of dry injection gas at 1310 psia and 195°F.

Other papers in the Russian literature^{15, 16} show that effects on phase behavior similar to those for a porous medium can be obtained by adding an inert gas such as helium to the initial mixture to be tested. The helium helps to maintain equilibrium between phases during depletion and increases the dew and bubble point pressures.

Clark¹⁷ showed that the volumetric behavior of pure substances (methane, ethane and propane) are significantly affected by adsorption on sand-clay mixtures when the temperature was below the critical temperature of the substance. However, he noted little if any adsorption when a connate water was present.

Although there is a significant amount of work showing that phase behavior is affected by the presence of a porous medium, the reasons for the effects are largely unknown. Anomalies are usually attributed to curvature of the vapor-liquid interface, and qualitatively explained in terms of capillary, adsorption or other physicochemical phenomena.

1.4 (b) Two-Phase Flow Considerations

The reservoir depletion process is simulated in unpacked cells by repeated withdrawals of a portion of the vapor phase. Thus, it is assumed that the retrograde liquid deposited in the porous medium is immobile. This assumption is valid provided that the total liquid saturation (connate

water plus retrograde liquid) never exceeds the minimum liquid flow saturation (MLFS) required to initiate liquid flow. Ham and Eilerts¹⁸ developed a special core holder which was used in experiments to show that the MLFS is a function of the porous medium, flowing fluids, pressure and flow velocity. In their experiments with a nitrogen-natural condensate fluid, the MLFS varied from 22 to 36 per cent for a sandstone core, and from 8 to 11 per cent for a limestone core. Efros¹⁹ studied the effect liberation of solution gas had on gas and liquid relative permeabilities. He presented a two-parameter permeability relationship which was a function of saturation, pressure gradient and gas-liquid viscosity ratio.

The maximum retrograde liquid volumes for naturally occurring systems seldom exceed ten per cent, so the assumption that retrograde liquids are immobile is usually valid for the bulk of the reservoir. The logarithmic nature of pressure profiles for radial flow causes retrograde liquids to condense and accumulate near the well bore. Thus, a region of two-phase flow often develops around producing wells. Hurst, Goodson and Leeser²⁰ have shown that deliverability can be seriously affected by these liquid accumulations.

1.4 (c) Effect of Connate Water

Formation water is not present in unpacked cells, but is always present in reservoir rocks. Water is left out of commercial PVT studies because it complicates analyses and can result in severe corrosion if the mixture contains acid gases. The chief concern with water centers around the solubility of reservoir fluids in it. The paraffin hydrocarbons are very

slightly soluble in water, however, carbon dioxide²¹ and hydrogen sulfide²² are moderately soluble, and their release from connate water with declining pressure may cause a considerable difference in composition between experimental and reservoir conditions.

It is also known that in binary hydrocarbon-water systems the critical point between gas and hydrocarbon rich liquid occurs at a higher pressure²³ than the critical pressure for the pure hydrocarbon. Assuming the critical pressure of a multicomponent mixture is also higher, one would also expect the bubble and dew point pressures to be higher. This may account for the anomalous increase in bubble and dew point pressures in the presence of a porous medium having a connate water saturation.

Another factor to be considered is that most reservoir rocks are water wet. Thus water will occupy the smallest pore spaces. This has the effect of decreasing the adsorption of gas-condensate fluids^{24, 25}. Connate water also reduces the quantity of retrograde liquid required to exceed the MLFS.

1.5 Objectives and Procedures

The purpose of this work was twofold. The first objective was to devise and conduct some experiments which would answer some of the questions concerning the effects of porous media on retrograde behavior that were discussed previously. This work was concentrated on experiments to study the effects of curvature on vapor-liquid equilibria of well defined binary hydrocarbon systems. Identical samples were depleted from

packed and unpacked cells and the results compared. Bubble or dew point pressures were also measured in packed and unpacked cells. Photographs were taken of the retrograde liquid capillary structures which formed during the depletion of a binary mixture from a pack of uniform spheres. A theoretical analysis of the liquid structures may be found in another report²⁶.

The second objective was to develop a computer phase behavior routine capable of simulating the depletion performance of high-pressure retrograde systems. The vapor-liquid equilibria portion of the computer program used a combination of several well-known methods. The Chao and Seader²⁷ correlation was used to generate compositionally dependent equilibrium ratios which were extrapolated to the system convergence pressure using an approximating formula proposed by Green and Hachmuth²⁸. The system convergence pressure was determined in accordance with a definition given by Rowe²⁹. The vapor phase density was calculated from an approximation developed for the well-known Standing and Katz correlation³⁰ for natural gases. The density of the liquid phase was calculated from a new approximation method which was applied to the corresponding states correlation of Lydersen, Greenkorn and Hougen³¹.

Chapter 2. EXPERIMENTAL APPARATUS AND OPERATING PROCEDURE

2.1 General Description of Apparatus

An apparatus was designed and constructed which permitted the phase behavior of a mixture in a PVT cell packed with a porous medium to be directly compared to the phase behavior of the same mixture in an unpacked cell. This involved the comparison of vapor phase compositions at equal pressures for the packed and unpacked cells. It also involved the comparison of simultaneous bubble or dew point pressures in packed and unpacked cells. The same apparatus was used to obtain photographs of liquid structures formed by retrograde liquids in various packs of uniform spheres.

Three 60 ml. windowed cells (Jerguson Model 19T40) were arranged as shown in Figure 2-1. The cells were mounted on an inner frame suspended by several springs. The inner frame could be vibrated with an eccentric drive assembly which was rotated with a variable speed electric motor. Mixing between phases in the two vertical cells was achieved through mercury splashing during vibration. The cells were enclosed in a constant temperature air bath. Two large double windows in the air bath allowed full view of the cells and auxilliary fittings. The air bath temperature was maintained with a Hallikainen controller (Model 1253A) connected to a 2 KW heater load, while up to 3 KW of constant heater load could be supplied directly through a separate voltage regulator. A ten inch fan was used to circulate air within the bath. This resulted in temperature control within $\pm 0.1^\circ\text{F}$ at 100°F where most of

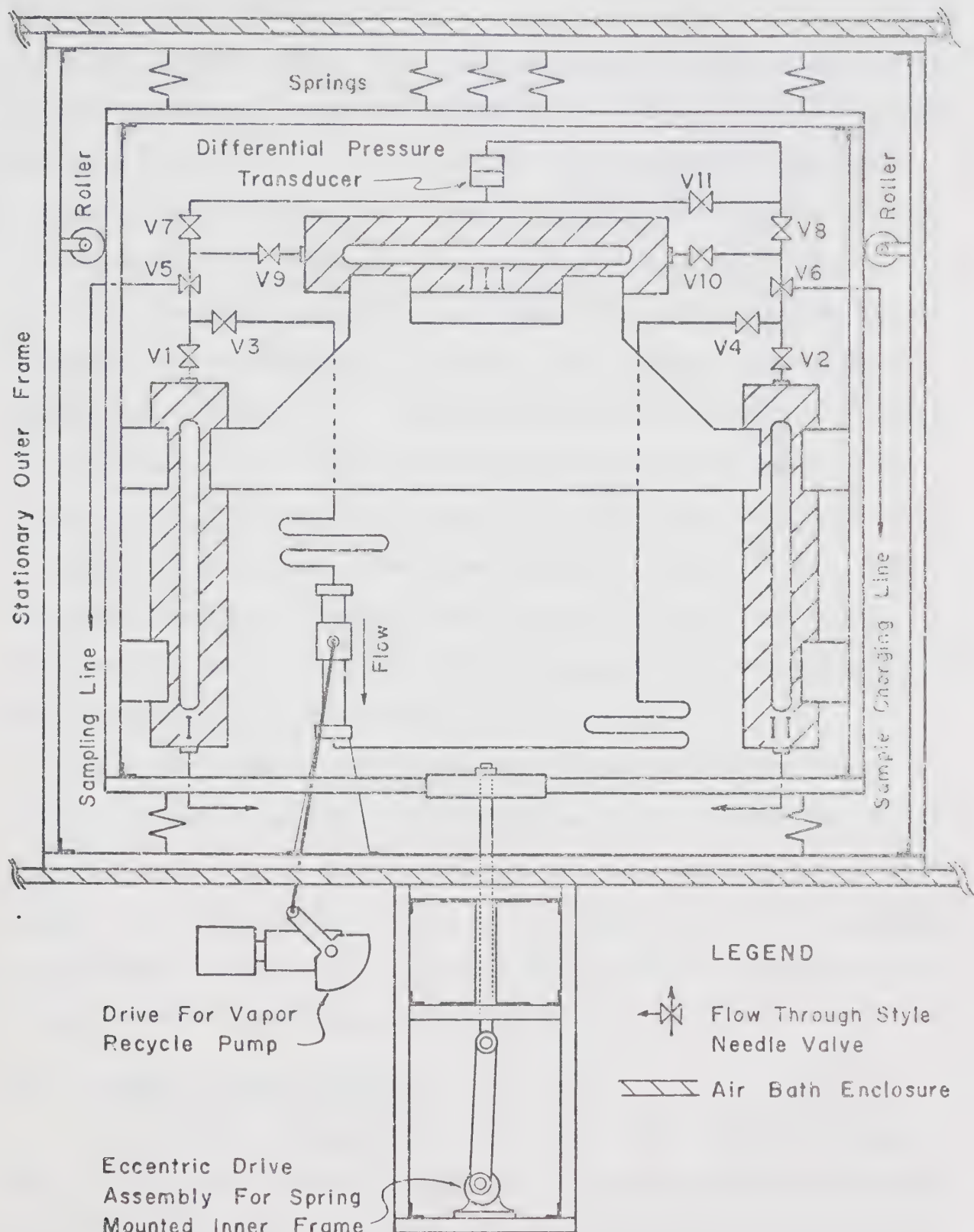


Figure 2-1. Schematic Diagram of Apparatus for Study of Retrograde Phenomenon in Porous Media.

the data were taken.

All valves within the air bath were manually operated by reaching through long-sleeve insulated gloves attached to the wall of the bath. By working through the gloves, the bath temperature was not altered while operating valves or taking photographs with a camera mounted inside the air bath.

The mercury volume in each vertical cell could be simultaneously or independently varied with a Ruska proportioning pump (Model 2218 WII). The pressure in the two vertical cells was measured with precision Bourdon tube gauges (Heise, 16 inch dial). Two gauges (0-1500 psi and 0-5000 psi) were connected to the mercury line from each cell, and the dial readings corrected for the variable mercury head in the cells. The temperature in each cell was measured with a thermocouple which protruded into the cell.

The horizontal cell always contained a pack of glass beads or ball bearings. To equilibrate the retrograde liquid in this cell, vapor was circulated with a Ruska vapor recycle pump. The flow through the pump was always in the direction indicated on Figure 2-1 to avoid any possible accumulation of liquids within the pump or lines.

2.2 Sampling and Analyses

A schematic diagram of the vacuum system used to transfer vapor phase samples directly to either an electro-magnetic gas density balance or a research chromatograph is shown in Figure 2-2. Vapor samples were admitted to the sample system by opening the micro-needle valve V5. Valve V5 featured a

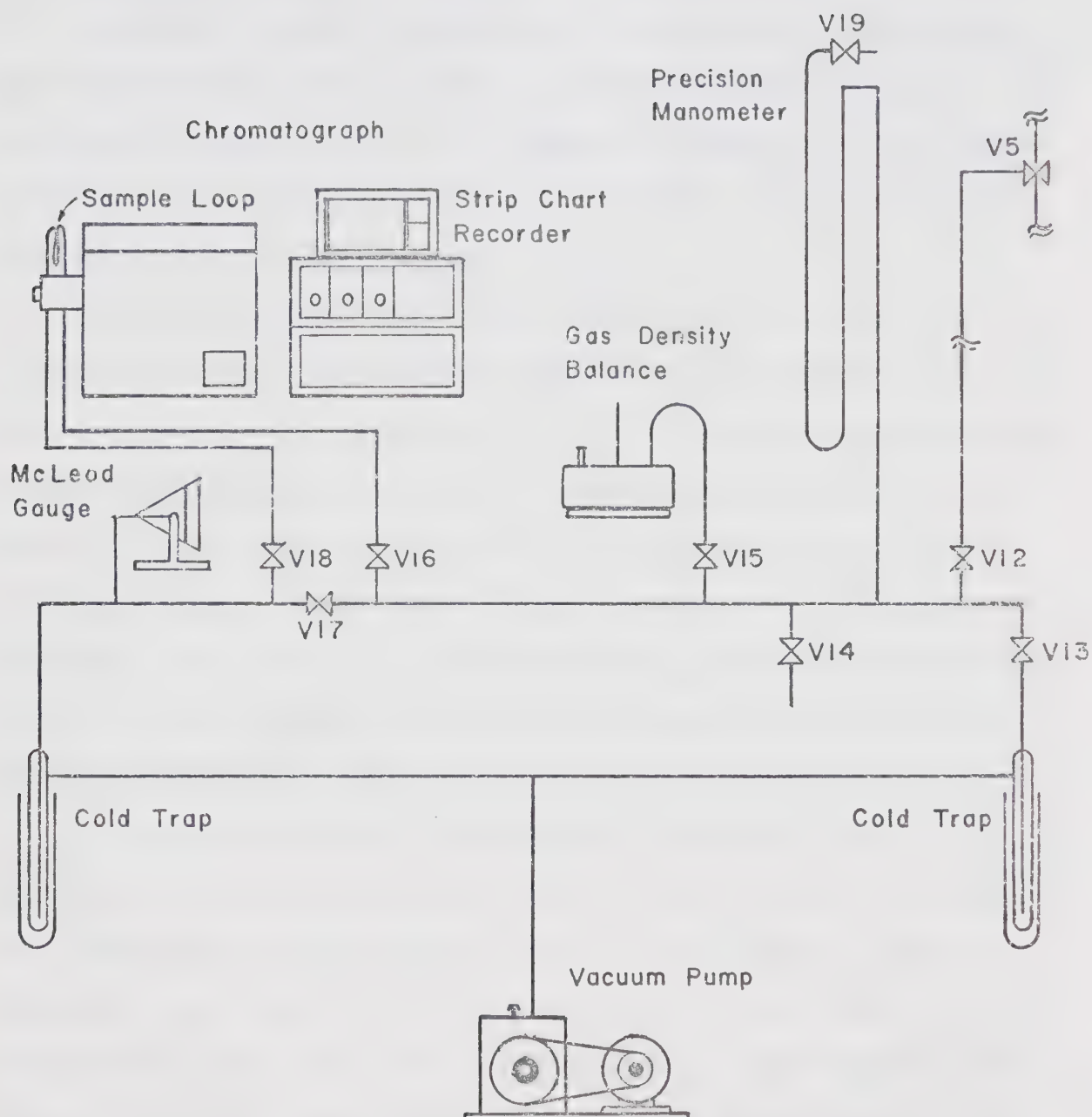


Figure 2-2. Schematic Diagram of Sample Analysis Section

flow-through design which eliminated sampling stagnant vapor from dead-end lines or fittings. The need for external heating to prevent liquid condensation from samples was avoided by keeping the sample system at subatmospheric pressure. The precision manometer gave the absolute pressure in the sample system as the space between valve V19 and the mercury column was kept under a high vacuum.

To prepare the system for a new sample all the valves in Figure 2-2 were opened except valves V5, V14 and V19, and the entire system was evacuated to less than five microns (McLeod gauge reading). If a sample was to be taken for density balance analysis valves V12 and V15 were opened and all other valves closed. Then, valve V5 was opened until the desired pressure was observed on the manometer. Several measurements could be made on the same sample by simply opening valve V13 for an instant to reduce the pressure on the sample system.

If a chromatograph sample was to be taken, valves V12 and V16 were opened and all other valves closed. The sample was admitted through valve V5 until a particular reference pressure was observed on the manometer. Then, valve V16 was closed and the sample was introduced into the chromatograph. After the sample was introduced into the chromatograph the lines connecting the sample loop to valves V16 and V18 became filled with carrier gas (helium). This gas was evacuated through valve V18 without contaminating the remaining sample which could be used for a duplicate analysis.

The micro-metering valve V15 was used to introduce reference gases for calibration of the density balance and

chromatograph.

2.3 Loading and Mixing a New Charge

Prior to loading a new charge, all of the valves in Figure 2-1 were opened except V5 and V6. The entire system was then purged with methane and vented to atmospheric pressure. Next, the least volatile component in the mixture (butane, pentane, or hexane) was admitted through valve V6. Sample valve V5 was opened and closed as required to control the quantity of least volatile component admitted to the system. If a ternary mixture was being prepared the intermediate component was added next, otherwise methane was added.

Sufficient mercury was pumped into cells I and II to increase the system pressure above the upper dew point of the mixture. The mixture was then circulated through the packed cell with the vapor recycle pump. During circulation, the contents of cells I and II were periodically injected, withdrawn, and reinjected into the system to ensure a homogeneous mixture.

After mixing, a sample was taken through valve V5 and the composition of the mixture determined. If the desired composition was not attained, the mercury level was brought to the top of cell II and valves V4, V8 and V10 closed. The pressure in cell II was lowered by withdrawing mercury and more of the deficient component added to cell II. Mercury was again pumped into cell II until the pressure was equal to that in the other cells. Valves V4, V8 and V10 were then opened and the components mixed as before. This process was

repeated until the desired composition was attained.

2.4 Unpacked Cell Depletion

After mixing, all of the contents of cell II and all but about 15 ml. of the contents of cell I were compressed into cell III and the vapor recycle pump. Then valves V3, V4, V9 and V10 were closed, and valves V1, V2, V7, V8 and V11 left open. This procedure stored a charge having the same initial composition for a subsequent run in which the packed cell was depleted.

The depletion of a constant volume gas-condensate reservoir is a differential process which can be approximated as a series of flash liberations. The series of flashes was performed as follows. Valve V1 was closed, and mercury was withdrawn from cell I while shaking to maintain equilibrium between phases. After the pressure in cell I was lowered to some predetermined value, mercury was withdrawn from cell II until both cells were at equal pressure. Then valve V1 was opened and mercury simultaneously added to cell I and withdrawn from cell II until the mercury level in cell I was restored to its initial level. Valve V1 was closed again and the amount of retrograde liquid in cell I was measured with a cathetometer. A vapor sample was then expanded into the composition analysis section through valve V5. This procedure was repeated until either all the retrograde liquid had vaporized, or the system pressure was depleted to some arbitrary lower limit. Whenever the withdrawals from cell I had nearly filled cell II, valve V8 was closed and the contents of cell

II were vented through valve V6.

2.5 Packed Cell Depletion

After depleting the unpacked cell, valves V1, V7 and V8 were closed. Next, the mercury level in cell II was raised to the top of the cell and the contents vented through valve V6. Then valves V3, V4, V9 and V10 were opened. The pressure drop caused by opening these valves was usually about 300 psi so that the charge, previously stored in the packed cell and recycle pump, remained above its dew point. The vapor recycle pump was then started, and after about an hour of mixing an initial sample was taken.

The differential depletion of the packed cell was performed by slowly withdrawing mercury (2.5 to 15.0 ml./hr.) from cell II. Vapor samples were taken at regular intervals of pressure, and in some experiments photographs were taken of the liquid capillary structures which formed at the window of the Jerguson cell. Whenever the mercury level reached the bottom of cell II, valves V4 and V10 were closed and the contents of cell II were vented through valve V6.

2.6 Simultaneous Packed Cell and Unpacked Cell Dew or Bubble Point Determination

An initial charge was prepared and sampled as previously described. Then the system volume was adjusted so that cell I was full of mercury and the space above the mercury in cell II was slightly greater than the pore volume of cell III. If necessary, part of the charge was bled through valve V6 until the system pressure was about 100 psi above the estimated dew

or bubble point.

Valves V3, V4, V10 and V11 were then closed and the run started by slowly withdrawing mercury from cells I and II at equal rates, typically 2.5 to 10.0 ml./hr. The differential pressure between the unpacked system (cell II) and the other system (consisting of cell I and the packed cell III) was measured by recording the output voltage from a sensitive differential pressure transducer (75 psi span) on a strip chart recorder. A typical chart is shown in Figure 2-3. The differential pressure between the two systems could be estimated from the chart within 1 psi. Two event markers on the recorder were used to record every 10 psi pressure drop in the open and packed systems as indicated by the Heise gauges. Since the packed system had a smaller initial cell volume than the unpacked system, and the rate of volume increase was equal for both cells, the bubble or dew point was reached first in the packed cell. The formation of two phases of different density caused a break in the pressure-volume curve traced by the recorder. Later, a similar break resulted from the formation of two phases in the unpacked cell. This differential technique provided a sensitive method of determining if the presence of a porous medium had any significant effect on the bubble or dew point pressures of the mixtures studied.

2.7 Vaporization Of Retrograde Liquid from the Packed Cell

An experiment to model the vaporization of a retrograde liquid from a porous medium by contacting with dry gas at

MIXTURE: 0.888 Methane, 0.112 n-Pentane
 TEMPERATURE: 100° F.
 CHART SPEED: 0.2 inches/min.

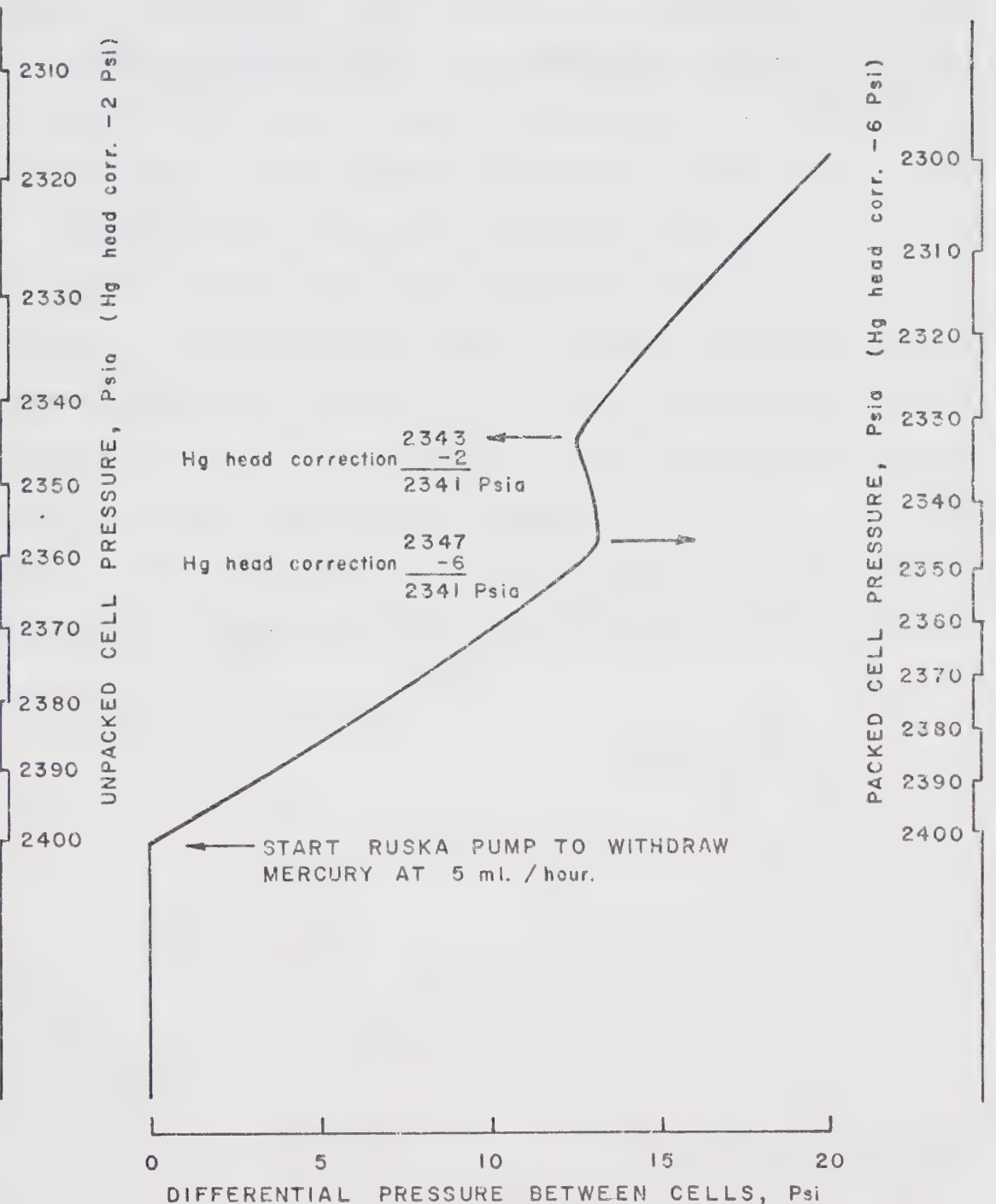


Figure 2-3. Typical Chart for Dew Point Determinations in Packed and Unpacked Cells.

constant pressure was performed as follows. An initial charge was prepared and sampled as previously described. After partially depleting the packed cell, valves V3, V4, V9 and V10 were closed and the contents of cells I and II vented and purged with methane. Cell II was then filled with methane at a pressure equal to the final depletion pressure of cell III, while cell I was filled with mercury. To start the run, valves V7 and V8 were closed and valves V9 and V10 were opened. Mercury was simultaneously added to cell II and withdrawn from cell I at the same rate (usually 2.5 or 5.0 ml./hr.). Samples of produced vapor from the packed cell were taken at regular intervals. Removal of a sample would cause a small decrease in system pressure which could be restored by temporarily stopping the mercury withdrawal from cell I. By using this procedure the number of pore volumes of dry gas required to vaporize a particular retrograde liquid could be determined.

Chapter 3. EXPERIMENTAL RESULTS AND DISCUSSION OF RESULTS

3.1 Materials

Matheson CP grade methane was used without further purification on all runs except Run 10. The manufacturer claims 99.0 per cent minimum purity for CP grade. Mass spectrometer and chromatograph analyses also indicated 99.0 per cent purity with the following impurities: 0.7 mole per cent nitrogen, 0.2 per cent ethane, and 0.1 mole per cent carbon dioxide.

The n-butane used was Matheson instrument grade for which the manufacturer stated 99.5 per cent minimum purity for the liquid phase. A liquid sample was transferred to a stainless steel cylinder and the sample was repeatedly cooled in a liquid air bath and evacuated to less than five microns (McLeod gauge) to remove non-condensibles. Chromatograph analysis of this liquid sample indicated approximately 0.1 mole per cent of each of the following: i-butane, i-pentane and n-pentane.

The n-pentane and n-hexane used were Phillips pure grade with a minimum stated purity of 99.0 per cent. Chromatograph analysis indicated the n-pentane to contain 0.4 mole per cent i-pentane and 0.2 mole per cent of an isomer of hexane. A similar analysis of the n-hexane revealed 0.8 mole per cent of a higher boiling point isomer of hexane. The pentane and hexane were not further purified except to strip any entrapped air prior to loading by slowly bubbling methane through the loading burette on the charging system.

Run 10 was made with Matheson UHP methane (99.97 per cent purity) and the middle cut of distilled Phillips pure

grade n-pentane.

The materials used to simulate porous media and other packed cell data are summarized in Table 3-1. These materials were thoroughly washed with acetone prior to packing. After the packed cell was mounted on the apparatus it was flushed with pentane.

3.2 Calibrations and Sources of Error

Static pressures were measured with Heise gauges which were found to be linear within 0.1 per cent of full scale when calibrated against a Ruska dead weight tester. Pressures in the range from 40 to 1300 psia could be estimated to within 1 psi after correcting for the variable mercury head in the cells. Pressures in the range from 1300 to 4000 psia are believed to be accurate within 3 psi. Other pressure calibration data are summarized in Appendix H.

The iron-constantan thermocouples in each cell were calibrated in a water bath with a precision mercury thermometer. The calibration data are given in Appendix H. The reference junction and potentiometer used for calibration were also used to take the data. The calibration was believed to be accurate within 0.05°F, however the air bath enclosure could only be controlled to within 0.1°F.

The electro-magnetic gas density balance was calibrated with the following gases: helium, methane, nitrogen and carbon dioxide. The calibration data in Appendix G indicate the same slope of current versus density for all gases after adjusting the molecular weights for trace impurities. The

TABLE 3-1
SUMMARY OF POROUS MEDIA AND PACKED CELL DATA

30-40 US Mesh Glass Beads:

Density of glass beads	2.515	gm./cc.
Weight of beads in the pack	89.60	gm.
Volume of beads in the pack	35.63	ml.
Valve-to-valve volume of cell . . .	60.30	ml.
Cell volume packed with beads . . .	56.30	ml.
Porosity	36.70	%

3/32 inch Chrom-steel Ball Bearings:

Density of ball bearings	7.716	gm./cc.
Weight of bearings in the pack . .	268.34	gm.
Volume of bearings in the pack . .	34.83	ml.
Valve-to-valve volume of cell . . .	60.9	ml.
Cell volume packed with bearings .	58.4	ml.
Porosity	40.4	%

1 mm. Stainless Steel Ball Bearings:

Density of ball bearings	7.701	gm./cc.
Weight of bearings in the pack . .	290.57	gm.
Volume of bearings in the pack . .	37.73	ml.
Valve-to-valve volume of cell . . .	60.9	ml.
Cell volume packed with bearings .	58.4	ml.
Porosity	35.5	%

vapor phase analyses tabulated in this chapter were all calculated from density measurements. Repeatability of analyses was 0.1 mole per cent or better. The largest source of error in density balance analyses was caused by approximately one mole per cent of impurities in all runs except Run 10. For density balance calculations methane and the light impurities were treated as a pseudo-component with a molecular weight of 16.2. True molecular weights were used for the heavy components since their impurities were generally isomers with the same molecular weight. True molecular weights were used for Run 10 and good agreement was observed with other runs where the pseudo-light component molecular weight was used.

3.3 Methane and n-Butane Mixtures

Four runs at 100°F were made with the methane and n-butane system and the results are summarized in Table 3-2. The same packing material (3/32 inch diameter ball bearings) was used in all runs. Both packed and unpacked cell depletions were performed in Runs 4, 5 and 13. Run 14 was a repeat of the packed cell depletion in Run 13 to resolve the composition difference between the packed and unpacked cells and to obtain improved photographs of the retrograde liquid structures.

A comparison of the vapor compositions for the packed and unpacked cells indicates that equilibrium was not always maintained during the vaporization portion of the depletions. This is particularly evident in Run 5 at pressures below 600 psia where the produced vapor compositions differ by as much as 12 mole per cent. Photographs of liquid structures from

TABLE 3-2

COMPOSITION AND PER CENT LIQUID DATA FOR
METHANE AND N-BUTANE MIXTURES

Run 4. 3/32 in. Sphere Pack Temperature 100°F					Run 5. 3/32 in. Sphere Pack Temperature 100°F				
Press. Psia	Mole Frac. CH ₄		Liquid Volume		Press. Psia	Mole Frac. CH ₄		Liquid Volume	
	Unpack- ed Cell	Packed Cell	Meas. %	Calc. %		Unpack- ed Cell	Packed Cell	Meas. %	Calc. %
Initial	0.864	0.864	0.0	0.0		0.816	0.815	0.0	0.0
1750	0.862	0.865	0.0	0.0		0.828	0.828	2.1	7.5
1500	0.867	0.867	Trace	0.91		0.868	0.865	9.7	10.0
1250	0.881	0.881	1.10	1.70		0.881	0.880	9.7	9.2
1000	0.884	0.885	0.95	1.42		0.885	0.883	8.2	7.9
800	0.881	0.881	0.95	1.01		0.880	0.882	6.8	6.9
600	0.863	0.866	0.47	0.41		0.865	0.874	6.0	5.8
400	0.840	0.854	0.0	0.0		0.828	0.857	3.7	4.5
200	0.835	0.859				0.708	0.747	1.0	2.0
150						0.637	0.758	0.6	1.2
100						0.607	0.671	0.0	0.0
Run 13. 3/32 in. Sphere Pack Temperature 100°F					Run 14. 3/32 in. Sphere Pack Temperature 100°F				
Press. Psia	Mole Frac. CH ₄		Liquid Volume		Press. Psia	Mole Frac. CH ₄		Liquid Volume	
	Unpack- ed Cell	Packed Cell	Meas. %	Calc. %		Unpack- ed Cell	Packed Cell	Meas. %	Calc. %
Initial	0.849	0.858	0.0	0.0				0.855	0.0
1500	0.868	0.865	0.32	3.39				0.863	
1250	0.882	0.881	1.77	3.74				0.881	
1000	0.884	0.883	1.45	3.19				0.885	
800	0.881	0.880	0.97	2.62				0.880	
600	0.865	0.866	0.32	1.89				0.868	
400	0.829	0.829	Trace	0.83				0.836	
300		0.800						0.798	
200	0.803	0.800		0.0				0.798	

Run 5 indicated liquid rings of varying sizes with gravity segregation (liquid accumulation along the bottom of the horizontal cell). The two prime factors contributing to non-equilibrium were that the depletion rate was too rapid and the sphere size too large. Although the depletion rate was comparable to that in the other runs, the liquid saturation (equilibrium data predict a maximum saturation of 9 per cent) was from three to six times greater. The large sphere size could not support all the liquid and gravity segregation resulted causing reduced interfacial area for mass transfer.

The composition isotherms for equilibrium phases in binary mixtures are fixed, and experimental results can be directly compared with other published data. Figure 3-1 makes this comparison for vapor phase compositions and good agreement with the data of Sage, Hicks and Lacey³² is observed. The data of Weinaug and Cordell⁴ were obtained by depleting a retrograde mixture from an Ottawa sand pack in nine hours. The short vertical lines give the average composition of a vapor sample removed during the indicated pressure drop.

The calculated compositions shown on Figure 3-1 were obtained from equilibrium flash calculations and are discussed further in Chapter 6.

Two values are reported in Table 3-2 for the liquid volume. The "measured per cent" column gives the percentage of retrograde liquid observed in the unpacked cell by sighting with a cathetometer. This measurement was not very precise for liquid saturations less than about 10 per cent. It was

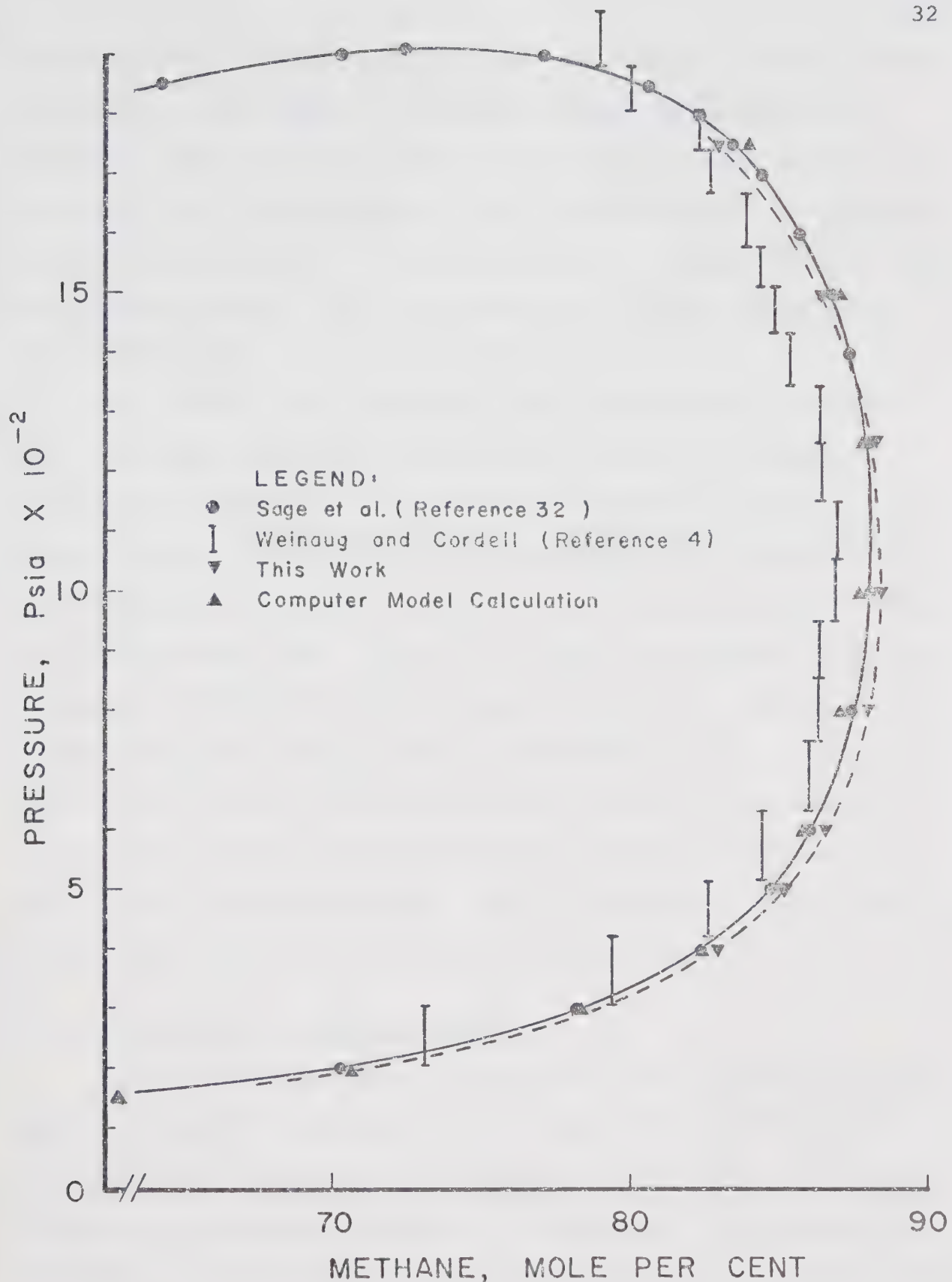


Figure 3-1. Pressure-Composition Isotherms for the Methane and n-Butane System at 100°F.

very difficult to distinguish the true meniscus, and it would take up to three hours for all the liquid to settle after shaking. Readings were taken a few minutes after shaking was stopped. The "calculated per cent" column gives the per cent liquid from a series of flash calculations which modelled the depletion process in the unpacked cell. These calculations and results are discussed in Chapter 6.

The packed cell depletions were differential processes. For retrograde systems a differential depletion results in less liquid than that obtained from a series of flash liberations. Thus, the equilibrium retrograde liquid saturations in the packed cell would be smaller than the observed saturations in the unpacked cell. Figure 3-2 shows retrograde liquid saturations for a differential depletion process. The two-phase equilibrium and density data of reference 32 were used to prepare this figure. It should be noted that large changes in liquid saturations result from minor changes in the composition of the initial mixture. This figure may be used to estimate the liquid saturations in the packed cell.

3.4 Methane and n-Pentane Mixtures

Eight runs were made with methane and n-pentane mixtures and the results are summarized in Table 3-3. Runs 1 and 2 were shakedown runs, and the temperature was less than 100°F because the reference junction was not used in an early thermocouple calibration. Attempts to photograph the liquid structures in these two runs were unsuccessful because of multiple reflections of the flood lamps on the glass beads. The

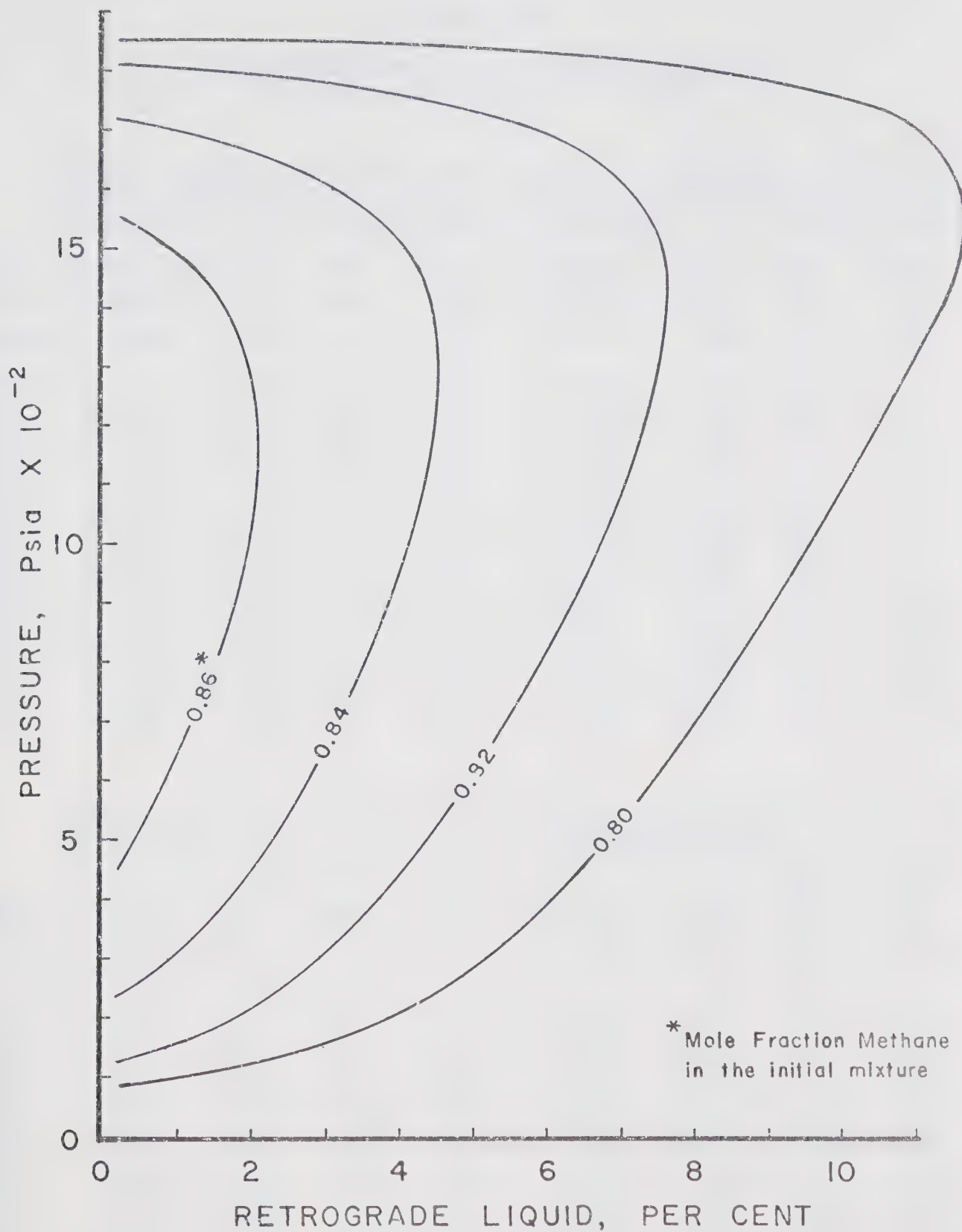


Figure 3-2. Retrograde Liquid Saturation for Differential Depletion of Methane-n-Butane Mixtures.

TABLE 3-3

COMPOSITION AND PER CENT LIQUID DATA FOR
METHANE AND N-PENTANE MIXTURES

Run 1. 30-40 U.S. Mesh Glass Beads, Temperature 99.5°F				Run 2. 30-40 U.S. Mesh Glass Beads, Temperature 99.7°F			
Press. Psia	Mole Frac. CH ₄ Unpack- ed Cell	Liquid Volume Packed Cell	Meas. % Calc. %	Mole Frac. CH ₄ Unpack- ed Cell	Liquid Volume Packed Cell	Meas. % Calc. %	
Initial	0.881	0.882	0.0 0.0	0.911	0.912	0.0 0.0	0.0 0.0
2250	0.911	0.910	4.8 10.8	0.911	0.911	0.0 0.0	0.0 0.0
2000	0.934	0.934	13.1 11.6	0.936	0.939	4.4 6.5	3.7 5.2
1750	0.947	0.950	13.5 11.6	0.949	0.953	6.5 7.1	5.1 5.1
1500	0.956	0.958	13.7 10.7	0.954	0.959	7.1 6.8	5.1 4.9
1250	0.960	0.949	13.9 9.9	0.964	0.965	6.8 6.5	4.9 4.5
1000	0.964	0.964	13.5 9.1	0.964	0.967	6.5 6.5	4.5 4.5
800	0.963	0.966	12.2 8.5	0.954	0.965	6.1 6.1	4.2 4.2
600	0.961	0.962	11.3 7.9	0.961	0.964	5.0 5.0	3.9 3.9
400	0.953	0.954	10.6 7.2	0.951	0.955	4.4 4.4	3.4 3.4
200	0.921	0.919	9.6 6.4	0.923	0.928	2.8 2.8	2.8 2.8
150	0.898	0.898	9.6 6.1	0.903	0.907	2.5 2.5	2.6 2.6
100	0.853	0.854	8.9 5.8	0.858	0.871	2.1 2.1	2.2 2.2
80	0.787	0.832	8.5 5.6	0.802	0.842	1.3 1.3	2.1 2.1
60	0.764	0.765	8.3 5.3	0.705	0.805	1.1 1.1	1.8 1.8
40	0.627	0.598	8.0 4.9	0.633	0.724	0.5 0.5	1.4 1.4
Run 3. 3/32 in. Sphere Pack Temperature 100°F				Run 8. 1 mm. Sphere Pack Temperature 100°F			
Press. Psia	Mole Frac. CH ₄ Unpack- ed Cell	Liquid Volume Packed Cell	Meas. % Calc. %	Mole Frac. CH ₄ Unpack- ed Cell	Liquid Volume Packed Cell	Meas. % Calc. %	
Initial	0.935	0.937	0.0 0.0	0.936	0.936	0.0 0.0	0.0 0.0
2250	0.936		0.0 0.0	0.936	0.936	0.0 0.0	0.0 0.0
2000	0.935	0.938	0.0 0.0	0.936	0.936	0.0 0.0	0.0 0.0
1750	0.946	0.946	1.11 0.90	0.942	0.947	1.29 1.94	0.74 1.22
1500	0.954	0.955	2.22 1.36	0.951	0.955	1.94 2.10	1.22 1.39
1250	0.957	0.959	2.69 1.51	0.957	0.957	2.10 1.77	1.39 1.39
1000	0.960	0.962	2.06 1.50	0.960	0.958	1.77 1.29	1.39 1.29
800	0.961	0.961	2.22 1.39	0.960	0.958	1.29 1.29	1.29 1.29
600	0.959	0.958	1.11 1.20	0.958	0.960	0.65 0.65	1.10 1.10
400	0.950	0.950	0.79 0.90	0.948	0.954	0.48 0.48	0.80 0.80
200	0.915	0.941	0.79 0.30	0.915	0.928	0.32 0.16	0.22 0.02
150	0.889	0.942	0.95 0.11	0.891	0.920	0.16 0.0	0.02 0.0
100	0.840	0.924	0.63 0.0	0.837	0.844	0.0 0.0	0.0 0.0
80	0.802	0.908	0.0	0.810	0.909	0.0 0.0	
60	0.746	0.886		0.758	0.789		

TABLE 3-3 (Cont.)

COMPOSITION AND PER CENT LIQUID DATA FOR
METHANE AND N-PENTANE MIXTURESRun 10. 1 mm. Sphere Pack
Temperature 100°FRun 12. 1 mm. Sphere Pack
Temperature 100°F

Press. Psia	Mole Frac. CH ₄		Liquid Volume		Mole Frac. CH ₄		Liquid Volume	
	Unpack- ed Cell	Packed Cell	Meas. %	Calc. %	Unpack- ed Cell	Packed Cell	Meas. %	Calc. %
Initial	0.925	0.927	0.0	0.0	0.927	0.929	0.0	0.0
2000	0.931	0.931	0.48	0.40	0.932	0.933	Trace	0.0
1750	0.946	0.944	2.90	2.53	0.946	0.946	2.26	2.17
1500	0.952	0.952	3.39	2.78	0.954	0.955	3.23	2.47
1250	0.957	0.959	3.55	2.79	0.960	0.960	2.74	2.50
1000	0.959	0.962	3.23	2.66	0.961	0.963	2.42	2.41
800	0.958	0.961	3.06	2.48	0.961	0.963	2.10	2.24
600	0.960	0.957	2.74	2.22	0.959	0.963	1.77	2.00
400	0.948	0.956	1.61	1.86	0.949	0.958	1.13	1.65
200	0.909	0.940	0.97	1.21	0.914	0.949	0.65	1.01
150	0.903	0.951	0.48	1.01	0.892	0.943	0.48	0.81
100	0.834	0.947	0.32	0.70	0.841	0.934	0.16	0.50
80	0.820	0.895	0.24	0.54	0.800	0.852	0.08	0.35
60	0.734	0.892	0.16	0.31	0.739	0.832	0.0	0.12
40	0.632	0.684	0.0	0.0	0.614	0.760	0.0	0.0

Run 9. 1 mm. Sphere Pack
Temperature 100°FRun 11. 1 mm. Sphere Pack
Temperature 160°F

Press. Psia	Mole Frac. CH ₄		Liquid Volume		Mole Frac. CH ₄		Liquid Volume	
	Unpack- ed Cell	Packed Cell	Meas. %	Calc. %	Unpack- ed Cell	Packed Cell	Meas. %	Calc. %
Initial	0.878	0.877	0.0	0.0	0.882	0.882	0.0	0.0
2250	0.901	0.898	11.1	12.0	0.882	0.881	0.0	0.0
2000	0.931	0.931	16.5	12.4	0.880	0.882	0.0	0.0
1750	0.947	0.944	16.6	12.3	0.900	0.897	2.90	1.48
1500	0.955	0.953	15.7	11.3	0.909	0.910	3.87	1.90
1250	0.959	0.958	15.0	10.4	0.915	0.916	3.71	1.75
1000	0.962	0.962	13.7	9.6	0.915	0.916	3.23	1.50
800	0.962	0.963	13.1	8.9	0.910		2.58	1.17
600	0.958	0.959	11.8	8.3	0.897		1.61	0.68
400	0.948	0.957	10.8	7.6	0.867		0.32	0.0
200	0.914	0.949	10.0	6.6	0.788		0.0	0.0
150	0.890	0.893	9.2	6.4				
100	0.832	0.844	8.7	6.0				
80	0.790	0.803	8.1	5.8				
60	0.715	0.740	7.4	5.5				

unpacked cells in Runs 1 and 2 were depleted over ten hour intervals with equilibration (mercury and liquid splashing) times of approximately 20 minutes prior to taking samples. The packed cells in Runs 1 and 2 were depleted over 16 and 13 hour intervals, respectively. There is good agreement between unpacked and packed cell vapor compositions in Run 1, particularly in view of the high liquid saturations. The slightly shorter packed cell depletion time for Run 2 seems to have caused a disproportionate increase in the differences between compositions of the produced vapor.

Runs 3 and 8 had nearly the same initial compositions, but different sized sphere packs. Equilibrium was maintained between phases in both runs at pressures down to about 400 psia. Departures from equilibrium at pressures below 400 psia were the largest in Run 3 which had the smaller interfacial surface area because of the larger sphere size. The depletion times for the packed cells in Runs 3 and 8 were 17 and 19 hours respectively, with both unpacked cells depleted over 12 hour intervals. It may be noted that changes in vapor composition continued after there was no visible liquid in the unpacked cell. Liquid was apparently adsorbed on the walls and in the interstices of the confining cells. This wetting of the walls contributed to the difficulty in obtaining reliable per cent liquid values, especially at the lower liquid saturations.

The depletion times for the packed cells in Runs 10 and 12 were increased to 20 and 27 hours, respectively, however departures from equilibrium were not decreased. Thus it

may be concluded that the formation of new surface area by agitation in the unpacked cell is much more effective for mass transfer than longer time periods with forced convection of the vapor phase in the packed cell.

The high liquid saturations of Run 9 resulted in gravity segregation in the packed cell and non-equilibrium between phases despite a 26 hour depletion time over a period of three days. The higher liquid saturations did, however, result in improved equilibrium for the unpacked cell depletion which was performed in only 11 hours.

Run 11 was performed at 160°F and the packed cell was only partially depleted to deposit a liquid saturation for a subsequent vaporization run by contacting with methane. The vaporization run is discussed in Section 3.8.

A comparison of the methane-n-pentane vapor compositions at 100°F with other published data is made in Figure 3-3. The results of this work show a critical pressure some 55 psi less than that reported by Sage, Reamer, Olds and Lacey³³, but in good agreement with Wagner and Leach³⁴ who state that it could not be greater than 2420 psia. The vapor phase compositions are approximately 1.3 per cent richer in methane than those of Sage et al. It should be noted that this relatively small change in equilibrium composition causes very large changes in dew point pressure. The vapor compositions reported by Weinaug and Cordell⁴ are also rich in methane compared to the data of Sage et al. The shaded portion of Figure 3-3 shows the region of non-equilibrium data for the packed cell

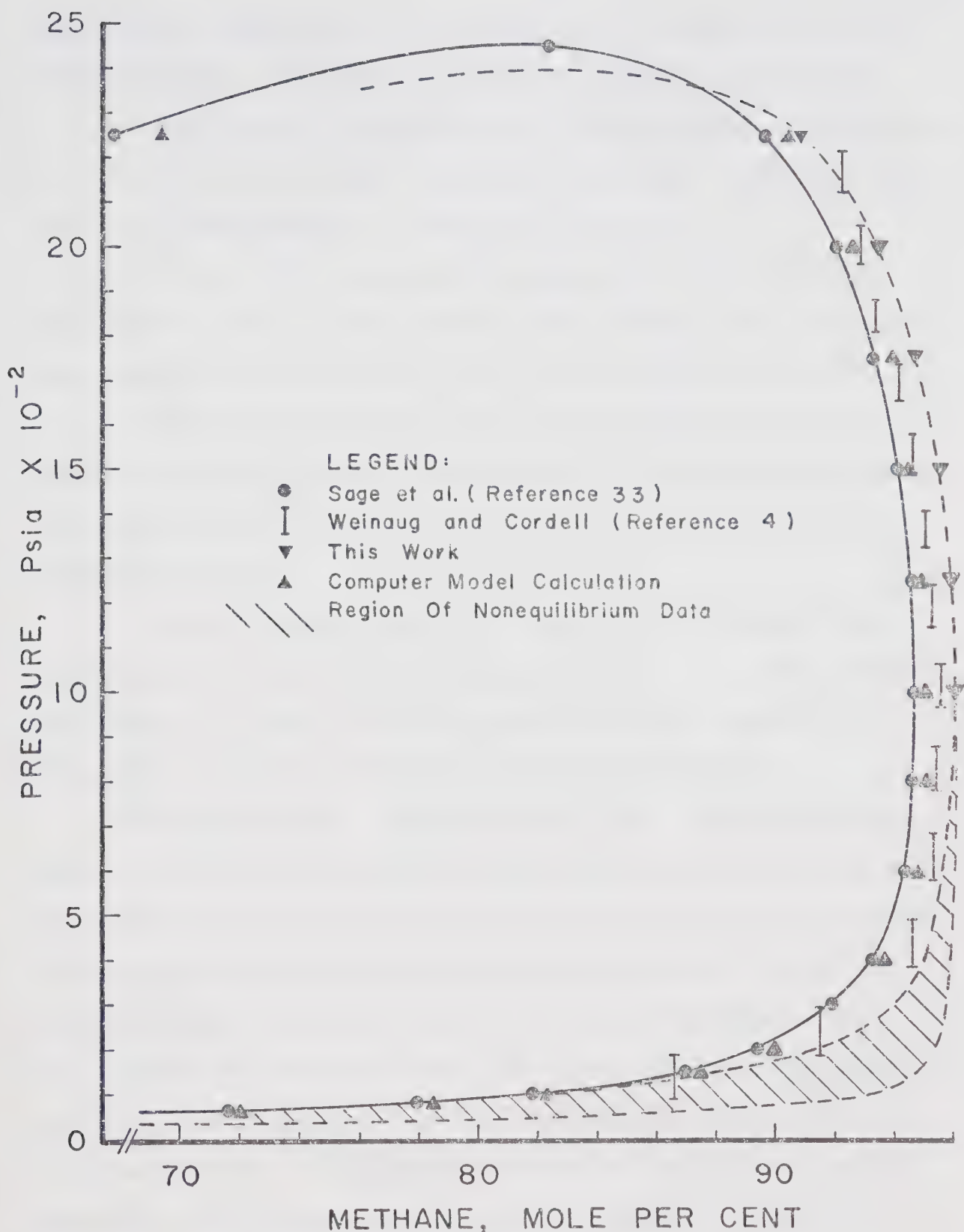


Figure 3-3. Pressure-Composition Isotherms for the Methane and n-Pentane System at 100°F.

depletions. The data in this region were usually very scattered, however, the following generalizations can be made:

1. Equilibrium was maintained during liquid condensation irrespective of the rate of pressure decrease (often 200 psi/hour), or the diameter of the packing material.

2. During the vaporization portion of the depletion, equilibrium could not be assured even when the rate of pressure decrease in the packed cell was as small as 20 psi/hour.

3. All data (including those of Weinaug and Cordell) indicate that decreasing the diameter of the packing material improves the approach to equilibrium during vaporization by pressure depletion.

4. Forced convection of the vapor phase through the sphere pack did not seem to improve the mass transfer during vaporization. Thus, it would appear that the controlling resistance to mass transfer is in the liquid phase

The comments made in Section 3.3 about the liquid volume data of Table 3-2 also apply to the measured and calculated per cent liquid columns of Table 3-3. The liquid saturations for the differential process used to deplete the packed cell can be estimated from the curves presented in Figure 3-4. This figure was prepared using the vapor compositions shown for this work in Figure 3-3 and the specific volume reported in reference 33. A comparison of Figure 3-4 with Figure 3-2 shows that the reduced volatility of n-pentane delays the vaporization of the retrograde liquid.

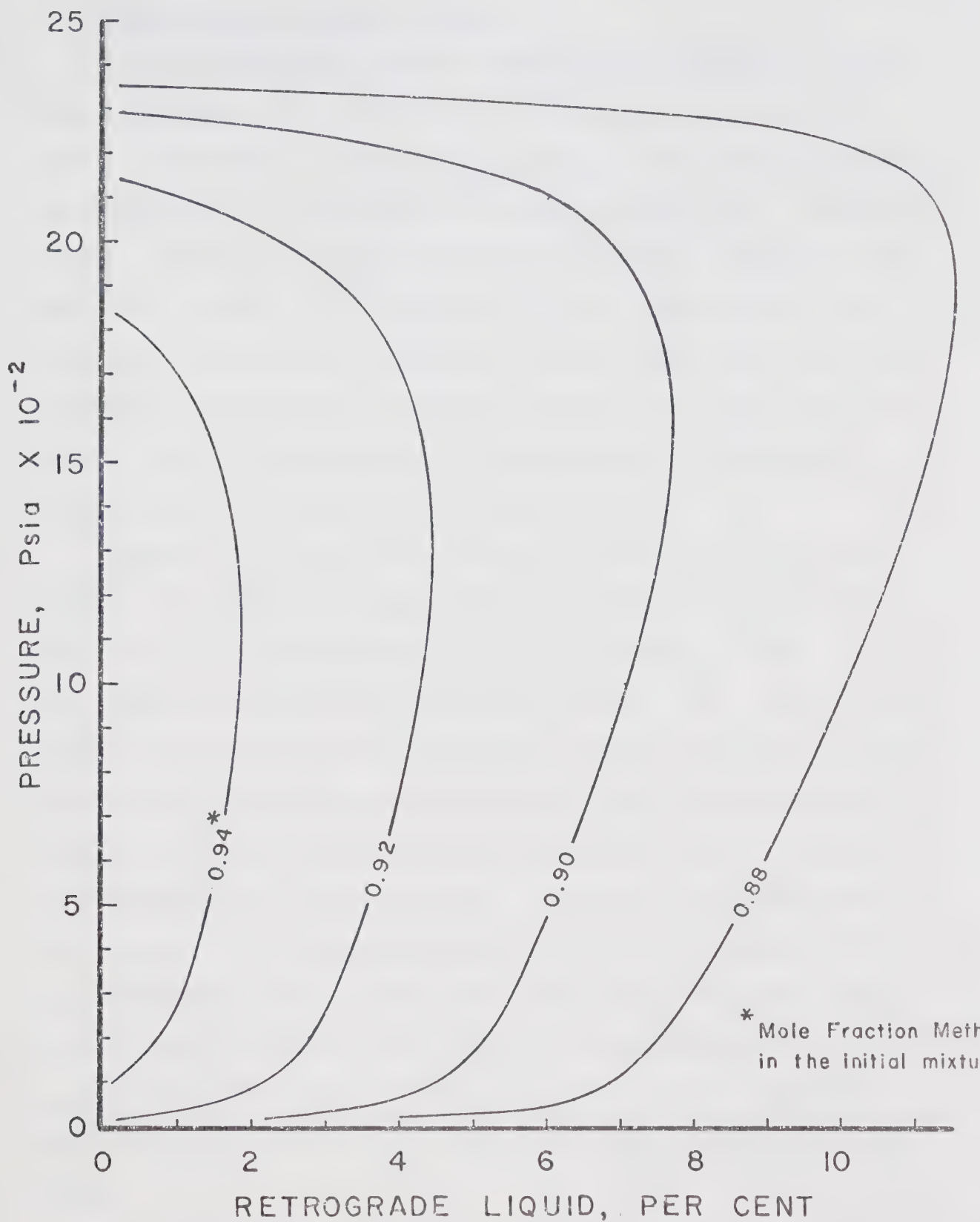


Figure 3-4. Retrograde Liquid Saturation for Differential Depletion of Methane-n-Pentane Mixtures.

3.5 Methane and n-Hexane Mixture

A single run was made with the methane-n-hexane system and the results are summarized in Table 3-4. The unpacked cell was depleted in one 12 hour period, while the packed cell was depleted in a total of 24 operating hours over a four day period. Table 3-4 indicates relatively small differences between the unpacked and packed cell vapor compositions, and it might be concluded that there was little departure from thermodynamic equilibrium. However, reference to Figure 3-5 indicates that it is doubtful if equilibrium was obtained in either cell at pressures below 1500 psia.

The data of Poston and McKetta³⁵ shown on Figure 3-5 indicate an unusually sharp reversal of the retrograde dew point locus to the reported critical pressure of 2902 psia. The vapor compositions of this work at 2500 psia and 2700 psia tend to indicate that the pressure-composition diagram should have more curvature at high pressure. Other methane-alkane binaries exhibit a more gradual reversal of the dew point locus toward the critical state. A comparison of the data of Run 7 during the vaporization portion of the depletion with the equilibrium data of Shim and Kohn³⁶ indicates that very little vaporization of the retrograde liquid occurred. The nearly constant value for the measured per cent liquid in Table 3-4 confirms that the retrograde liquid vaporized very slowly.

The conditions for liquid vaporization were the least favorable in Run 7 since the largest sphere size and the least

TABLE 3-4

COMPOSITION AND PER CENT LIQUID DATA FOR
THE METHANE AND N-HEXANE MIXTURE

Run 7. 3/32 in. Sphere Pack Temperature 100°F				
Press. Psia	Mole Frac. CH ₄ Unpack- ed Cell	Packed Cell	Liquid Volume Meas. %	Liquid Volume Calc. %
Initial	0.930	0.930	0.0	0.0
2750	0.936		5.9	5.81
2700		0.946		
2500	0.960	0.959	10.1	7.02
2250	0.971	0.969	11.7	8.25
2000	0.975	0.977	11.9	8.58
1750	0.984	0.979	13.7	8.24
1500	0.985	0.986	12.4	7.95
1250	0.988	0.989	12.0	7.62
1000	0.988	0.990	11.2	7.27
800	0.990	0.989	10.8	6.96
600	0.988	0.988	10.4	6.64
400	0.985	0.986	9.9	6.29
200	0.975	0.980	9.2	5.85
100	0.954	0.956	8.8	5.53
50	0.894	0.910	7.9	5.27
25	0.690	0.715	7.5	5.02

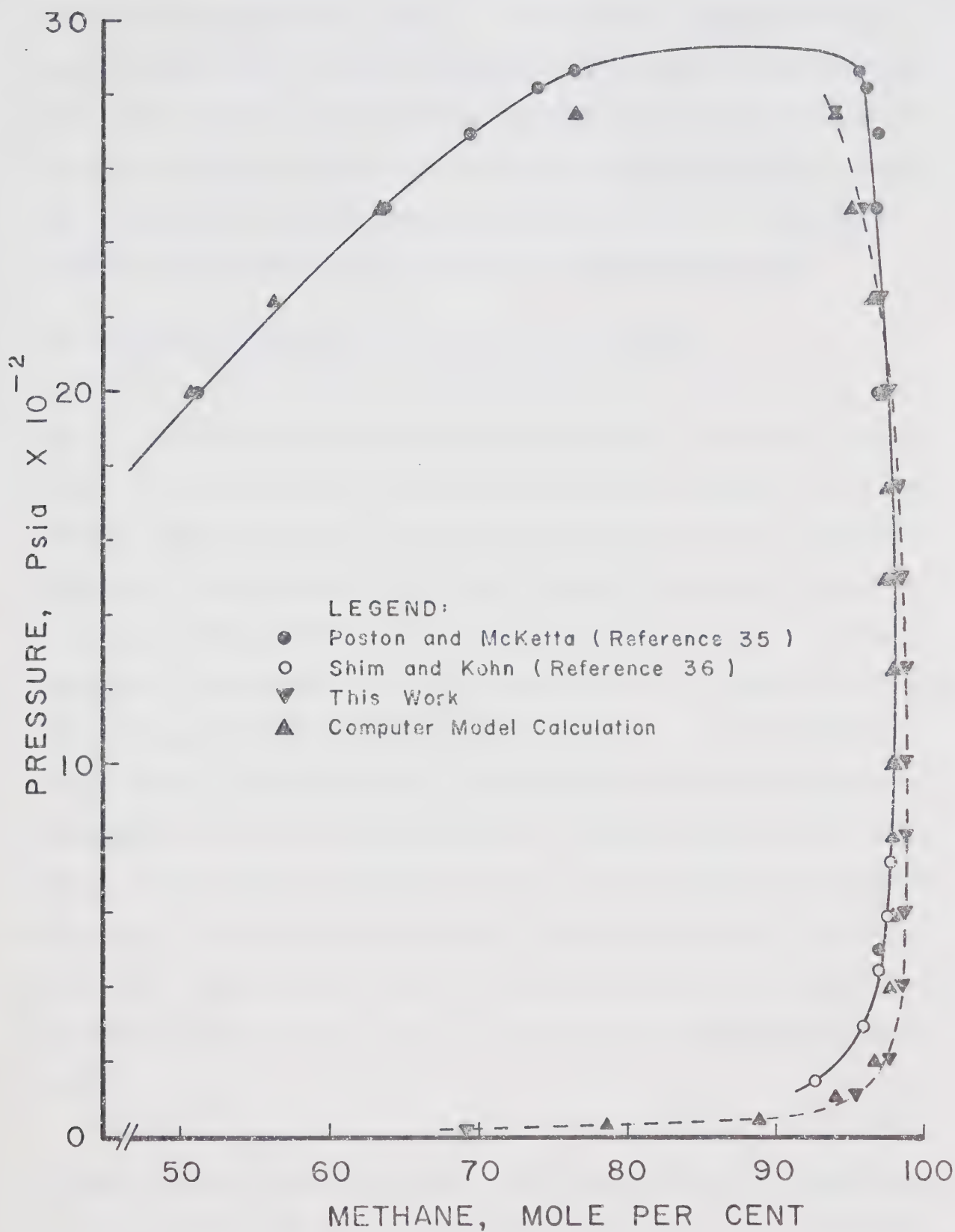


Figure 3-5. Pressure-Composition Isotherms for the Methane and n-Hexane System at 100°F.

volatile component were used. All evidence suggests that equilibrium is not readily attained, and that the problem becomes more severe with decreased volatility. It may be that the intermediate components in multicomponent mixtures reduce the resistance to mass transfer for the heavier components, however, this would have to be verified by experiment.

3.6 Role of Fugacity in Attaining Equilibrium

The previous sections pointed out the difficulty of maintaining equilibrium during the vaporization portion of depletions. The packed cell depletions were carried out under conditions where material and momentum fluxes existed between phases so equilibrium in its more general sense was never attained. The transfer of material between phases involves transport properties which are assumed to be a function of the thermodynamic state of the phase at a point. When several fluxes occur simultaneously, the interrelation of transport phenomena are given by irreversible thermodynamics. Unfortunately, irreversible thermodynamics has not been sufficiently developed to permit calculations for phase behavior at high pressure. The driving force which causes interphase mass transfer is the fugacity and it needs to be examined in more detail.

The fugacity of any component i in a phase is a measure of its escaping tendency, therefore the fugacity of component i must be the same in all equilibrated phases. The fugacity of a component depends upon the pressure, temperature and composition of the system. The total differential of the fugacity of component i in a system of m components is given

by

$$df_i = \left[\frac{\partial f_i}{\partial P} \right]_{T,x} dP + \left[\frac{\partial f_i}{\partial T} \right]_{P,x} dT + \left[\frac{\partial f_i}{\partial x_j} \right]_{P,T,x_k} dx_j$$

$k = 1, \dots, j-1, j+1, \dots, m-1$

(3-1)

For a binary mixture the change in fugacity of component i with pressure at constant temperature is given by

$$\left[\frac{\partial f_i}{\partial P} \right]_T = \left[\frac{\partial f_i}{\partial P} \right]_{T,x} + \left[\frac{\partial f_i}{\partial x_j} \right]_{P,T} \left[\frac{dx_j}{dP} \right]_T$$
(3-2)

The derivative on the left side of Equation 3-2 gives the change in the fugacity of component i with pressure for the coexisting phases of a binary mixture. Fugacities have been published^{32, 33} for the coexisting phases of the methane-n-butane and methane-n-pentane systems. These data have been replotted and the n-butane and n-pentane fugacities are shown in Figure 3-6. It is apparent that under the experimental conditions of 100°F the fugacities of these two components are nearly invariant with pressure, and that the derivative on the left side of Equation 3-2 will be of small magnitude.

The first term on the right hand side of Equation 3-2 can be evaluated from partial volumetric data by the thermodynamic relation

$$\left[\frac{\partial \ln(f_i)}{\partial P} \right]_{T,P} = \frac{v_i}{RT}$$
(3-3)

The second term on the right hand side involves the product of two derivatives. The first derivative is of particular interest since it shows how fugacity changes with composition at constant temperature and pressure. Thus, when the

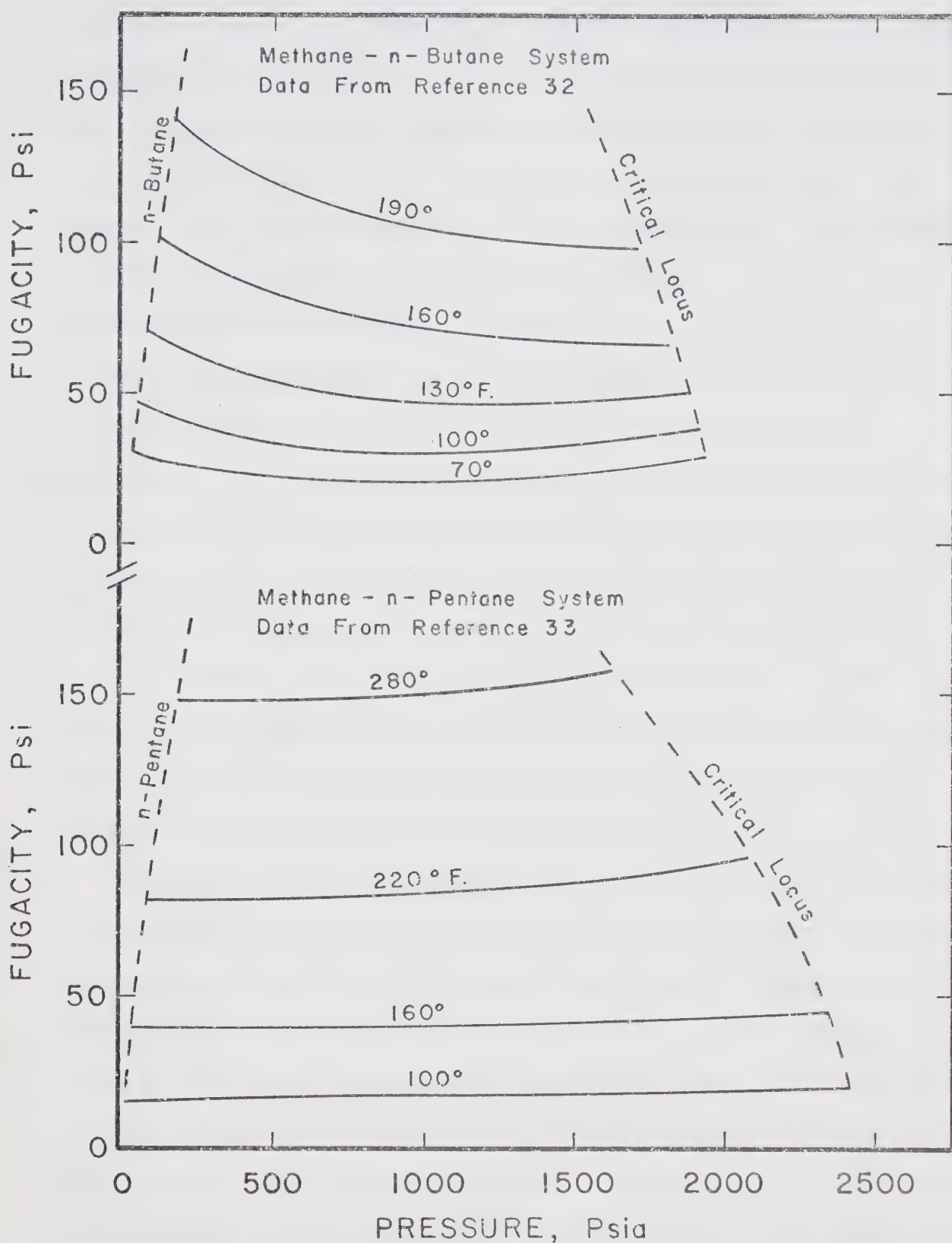


Figure 3-6. Examples Showing the Effect of Pressure on Fugacity in the Two Phase Region.

coexisting vapor and liquid are not in equilibrium (i.e. the composition is perturbed from the equilibrium value) this term gives the magnitude of the driving force for mass transfer to re-establish equilibrium. The second derivative gives the change in the coexisting equilibrium composition with pressure and can be evaluated by constructing tangents to a pressure-composition isotherm such as Figure 3-1.

The following results are presented even though it is clearly hazardous to evaluate some of the derivatives in Equation 3-2 by graphical methods. The extensive tables for the methane-n-butane system in references 32 and 37 were used to calculate the effect of composition upon the fugacity of n-butane. The derivative $(\partial f_i / \partial x_j)_{T,P}$ was calculated for both the liquid and vapor phases at temperatures of 100°F and 160°F. The results of these calculations are shown in Figure 3-7, and their significance with respect to establishing equilibrium may be explained as follows.

Consider the coexisting phases during a typical depletion run at 100°F. The mass transfer of n-butane during the pressure interval from the retrograde dew point to approximately 1000 psia is from the vapor (donor phase) to the liquid. During this pressure interval the curves of Figure 3-7 show that any departure of the vapor phase from the equilibrium composition causes a much larger change in fugacity than a corresponding departure from equilibrium in the liquid phase. Thus, the tendency is for both phases to stay very close to equilibrium. However, at pressures below 1000 psia n-butane is transferred

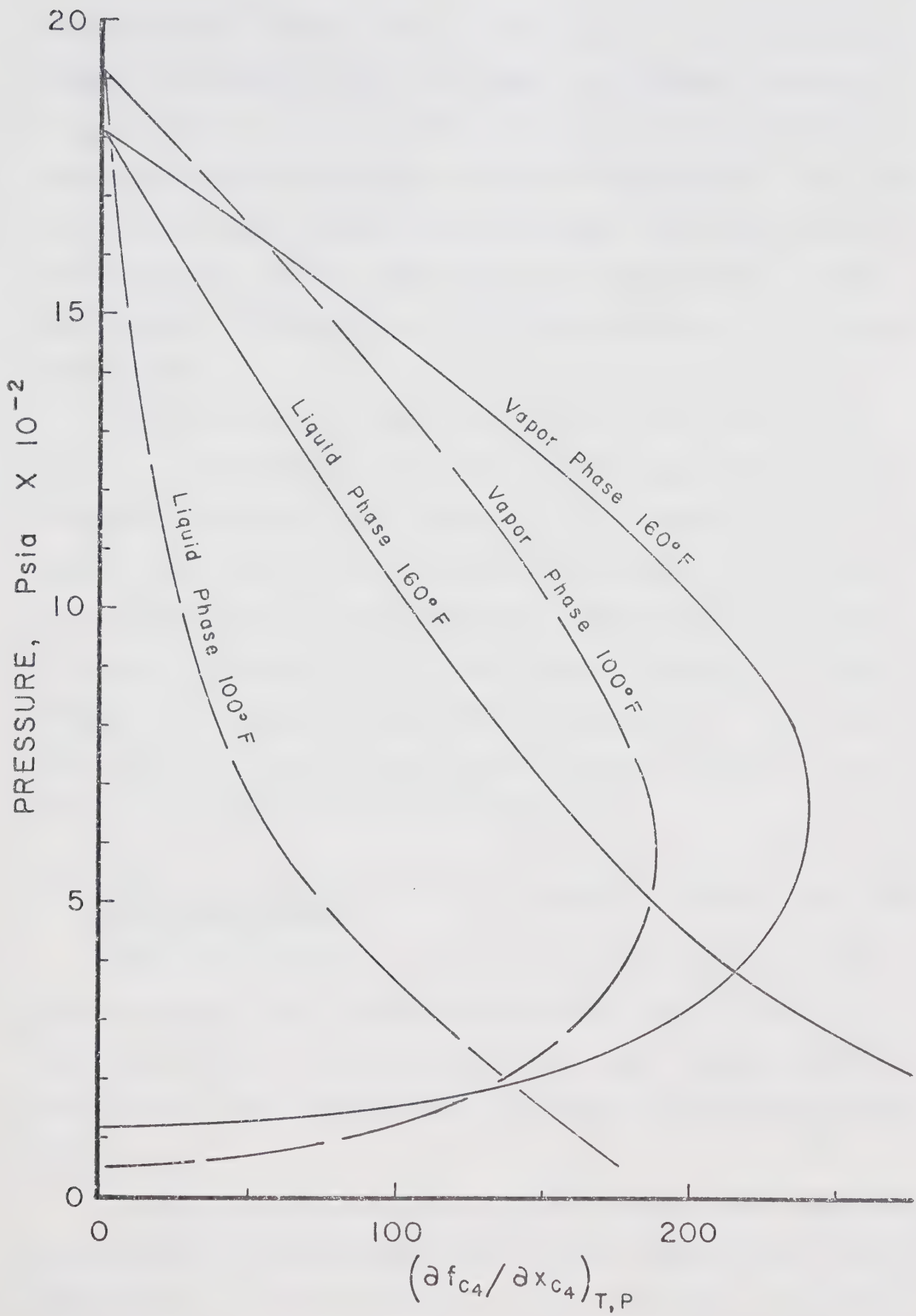


Figure 3-7. Effect of Composition on the Fugacity of n-Butane in the Two Phase Region.

from the liquid (donor phase) to the vapor. In the pressure interval from 1000 psia to 200 psia the tendency is towards non-equilibrium since the donor phase is not as sensitive to departures from equilibrium as the receiving phase. At pressures below 200 psia conditions are again favorable for equilibrium because of the rapid decline in sensitivity of the vapor phase to composition as the vapor pressure of n-butane is approached.

The conditions at 160°F in Figure 3-7 are similar to those at 100°F except that the point of equal sensitivity of the phases to composition occurs at approximately 375 psia instead of 200 psia. Thus, the pressure interval where there is a tendency to non-equilibrium is considerably smaller at the higher temperatures. If the trend continued for higher temperatures one might expect that supercritical components would exhibit a tendency to non-equilibrium during condensation, and equilibrium during vaporization.

3.7 Simultaneous Packed Cell and Unpacked Cell Dew or Bubble Point Measurements

Table 3-5 summarizes the simultaneous retrograde dew point or bubble point determinations in a pack of 30-40 U.S. Mesh glass beads. Any observed differences between packed and unpacked cells were within the limits of the experimental error.

For compositions near the critical state, dark opalescence was observed in the unpacked cell as the critical point was approached. The data in Table 3-5 are the basis for drawing

TABLE 3-5

SIMULTANEOUS PACKED CELL AND UNPACKED CELL DEW
OR BUBBLE POINT MEASUREMENTS

System: Methane and n-Pentane at 100°F

Pack: 30-40 U.S. Mesh Glass Beads

Composition Mole Frac. Methane	Dew (Bubble) Point Press., Psia		Remarks
	Unpacked Cell	Packed Cell	
0.899	2335	2335	Dew Point
0.783	2392	2392	Bubble Point
0.808	2395	2396	Bubble Point
0.827	2398	2399	Dark Opalescence
0.835	2398	2398	Dew Point
0.846	2401	2401	Dew Point
0.768	2356	2356	Bubble Point
0.820	2390	2390	Dark Opalescence
0.862	2376	2376	Dew Point
0.888	2341	2341	Dew Point
0.922	2200	2200	Dew Point

the pressure-composition isotherm in Figure 3-3 some 55 psi below the critical point reported in reference 33.

On the basis of a theoretical study by Morrow et al.²⁶, in which curvature effects at the vapor-liquid interface were investigated using a thermodynamic model, it was concluded that unless the particle size was less than a few microns, curvature effects on equilibrium pressures are negligible. It was also concluded that although reservoir rocks may contain a large proportion of fine pores, these pores would not be available to retrograde liquids since they would be occupied by formation water.

Therefore all the evidence of this work is that curvature effects on equilibrium pressures and compositions are negligible. The reported anomalous phase behavior in porous media discussed in Section 1.4 probably results from lack of equilibrium and/or from more than one flux operating so that meaningful interpretation lies in the field of irreversible thermodynamics.

3.8 Vaporization of a Retrograde Liquid by Contacting with Methane

The retrograde liquid saturation in the 1 mm. sphere pack of Run 11 was vaporized by contacting with methane at 1000 psia and 160°F. Figure 3-8 shows the mole percentage of n-pentane in the effluent from the packed cell versus pore volumes of injected methane. The results are qualitative since this was a shakedown run to test the apparatus for vaporization experiments. A slight increase in the n-pentane content of the effluent was observed just prior to breakthrough. A similar

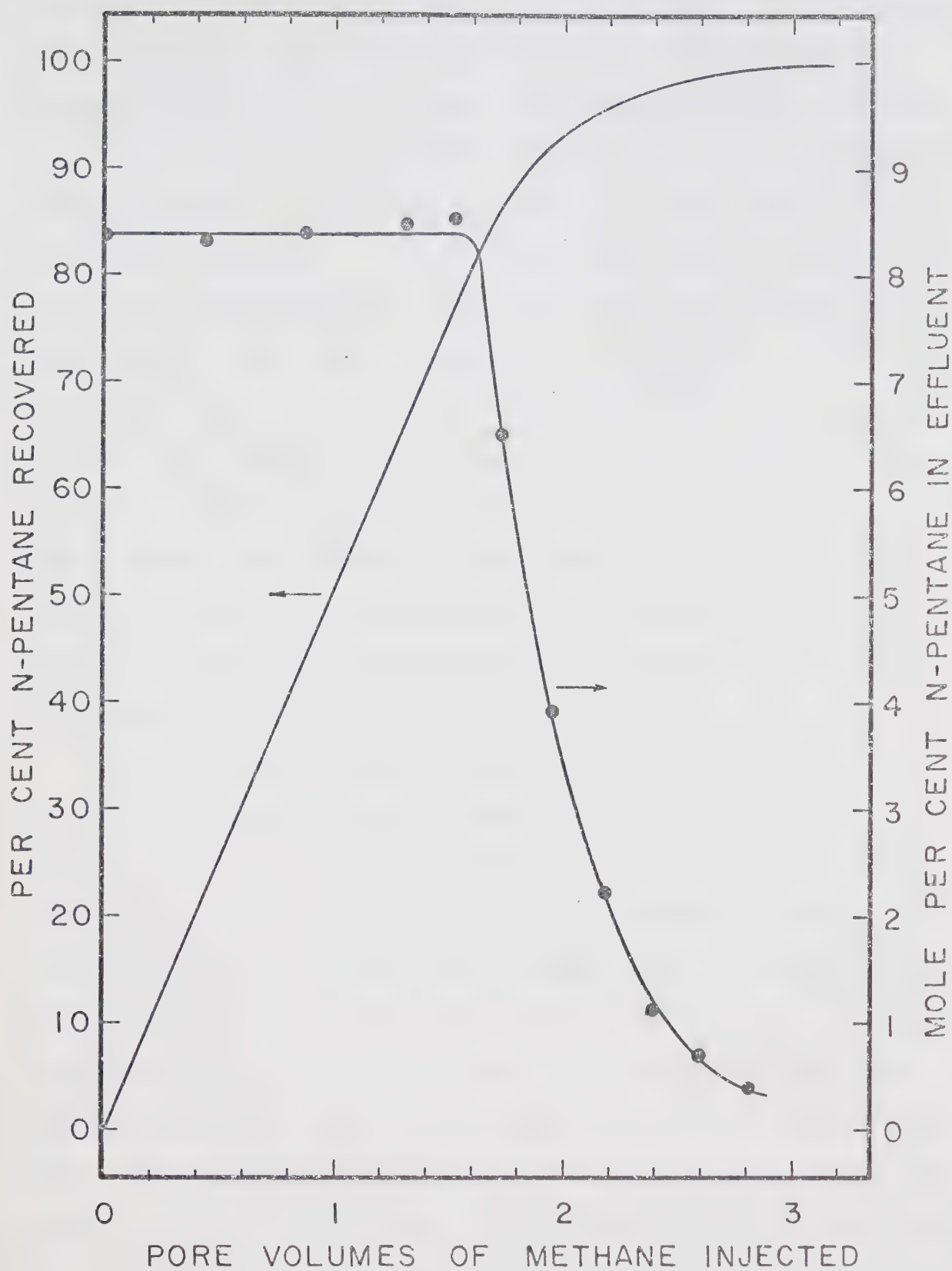


Figure 3-8. Pentane Recovery by Contacting with Methane.

increase was observed by Smith and Yarborough¹³, so it appears that a slightly enriched zone preceding breakthrough is a characteristic of the constant pressure vaporization process.

The decrease in n-pentane concentration after breakthrough shown in Figure 3-8 was not as abrupt as those observed by Smith and Yarborough¹³ for an Ottawa sand pack. This may have been due to channeling in the relatively coarse 1 mm. sphere pack used in this work, or because of unfavorable cell geometry. The length to cross-sectional area ratio was 17.7 cm.^{-1} in this work compared to 43.1 cm.^{-1} for the apparatus used by Smith and Yarborough. Figure 3-8 indicates a mixing zone (zone during which the n-pentane concentration in the effluent decreases to zero) in excess of one pore volume, whereas mixing zones of some 0.25 pore volumes were reported by Smith and Yarborough.

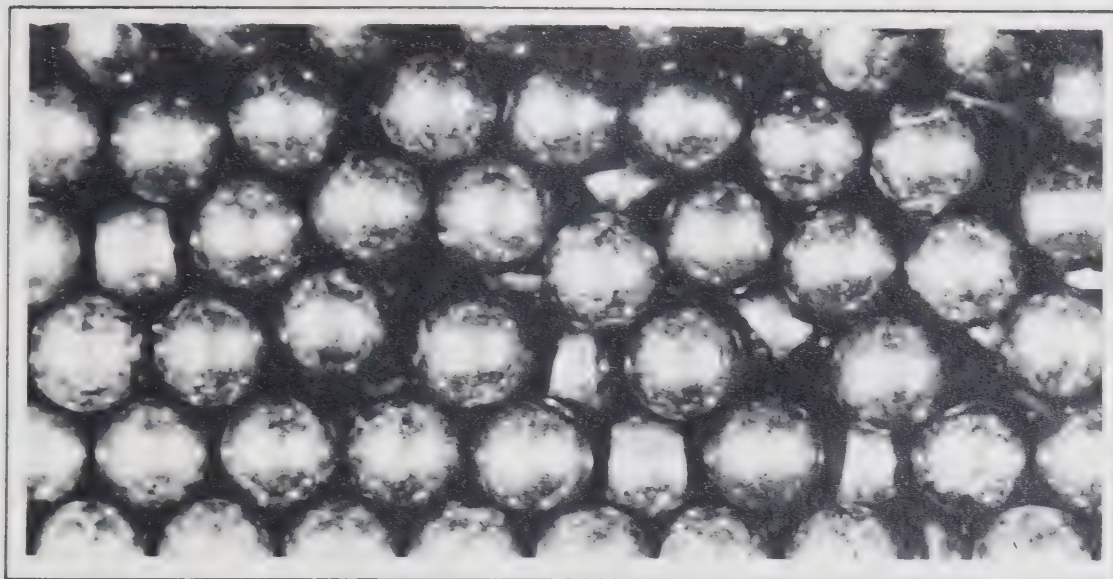
The curve of per cent n-pentane recovered versus pore volumes of methane injected shown in Figure 3-8 was plotted so that 100 per cent corresponds to a calculated n-pentane recovery of 25.6×10^{-6} moles. If the measured liquid saturation of 3.23 per cent for the unpacked cell depletion is applied to the packed cell, then there were 22.2×10^{-6} moles of n-pentane in the pack at the start of the vaporization run indicating a discrepancy of 13.3 per cent in the material balance. The density data of Sage, Reamer, Olds and Lacey³³ were used for these calculations. These data may not be applicable since the composition of the vapor phase in Run 11 was approximately two mole per cent richer in methane than the corresponding data of Sage et al.

3.9 Photographs of Retrograde Liquid Structures

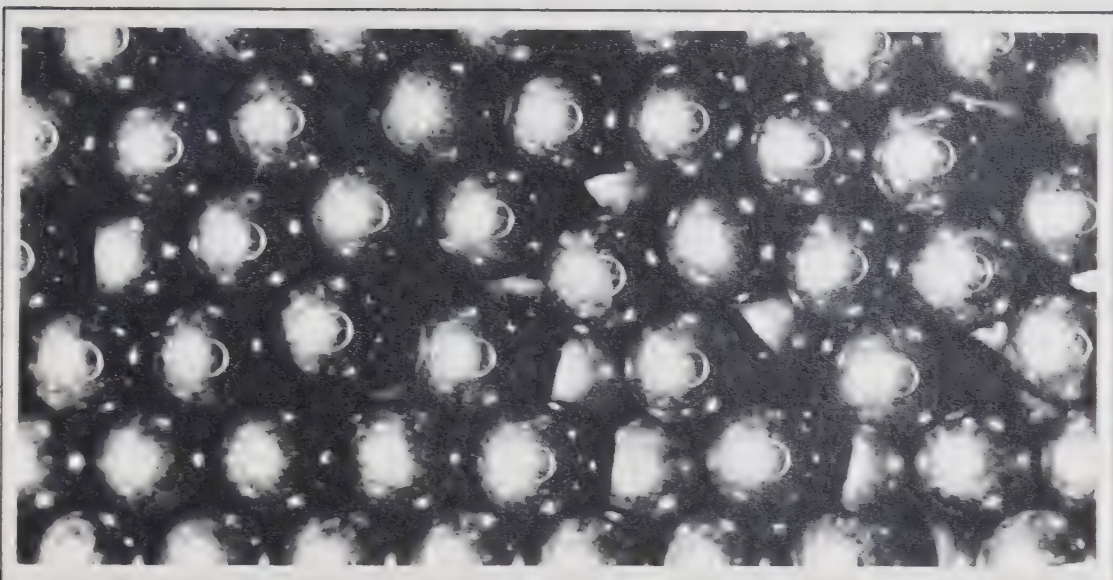
Photographs of condensed liquid structures were taken with a standard 35 millimeter camera equipped with an extension tube for increased magnification. Various exposure settings, film speeds, lighting arrangements and sphere sizes were tried in order to obtain satisfactory photographs of the liquid rings which formed at the contact points between the packing spheres and the window of the Jerguson cell.

Based on the theoretical analysis of Morrow et al.²⁶ it was concluded that the curvatures developed in sphere packs used in this work would have a negligible effect upon phase behavior. Having regard for this, and the fact that photograph quality improved with increased sphere size, several runs were made with 3/32 inch diameter sphere packs. Figure 3-9 shows two photographs of the same sphere pack; one at a pressure above the retrograde dew point without a retrograde liquid saturation, and another in the two-phase region with a retrograde liquid saturation.

Photographs were taken at regular pressure intervals during the packed cell depletions. The diameter of the liquid rings could be observed to increase as the pressure was decreased from the retrograde dew point to some intermediate pressure below which the diameter of the liquid rings would decrease as the liquid vaporized. If a particular composition resulted in too much retrograde liquid, the rings would grow until they joined together causing gravity segregation which retarded vaporization of the liquid. Suites of photographs for several runs are shown in Appendix I.



PHOTOGRAPH OF A 3/32 in. DIAMETER SPHERE PACK
WITHOUT A RETROGRADE LIQUID SATURATION



PHOTOGRAPH OF THE SAME SPHERE PACK SHOWING RETROGRADE
LIQUID RINGS WHERE THE SPHERES CONTACT THE CELL WINDOW

Figure 3-9. Typical Photographs of Sphere Packs.

Chapter 4. CALCULATION OF VAPOR-LIQUID EQUILIBRIA

4.1 Foreword

The reservoir engineer would like to be able to predict and compare the performances, fluid recoveries and resulting cash flows for various exploitation schemes. In order to be able to make these predictions, the composition and density of the vapor and liquid phases are required as functions of pressure. The vapor-liquid equilibria and density data for reservoir fluids are usually obtained from laboratory experiments. There is, however, a trend to use a digital computer to calculate these data starting with the initial composition and a minimum of laboratory data. These calculations require equilibrium ratios for every component and a suitable density correlation for the coexisting phases.

Equilibrium ratios, or K-values as they are more often called, are defined as the ratio of the mole fraction of component i in the vapor phase, y_i , to the mole fraction of the same component in the liquid phase, x_i , hence

$$K_i = y_i/x_i \quad (4-1)$$

These ratios are known to be functions of temperature, pressure and system composition. The common methods of correlating and calculating K-values are reviewed in this chapter.

4.2 The N.G.A.A. K-value Charts

The Natural Gasoline Association of America (N.G.A.A.) has prepared several different series of K-value charts for the normal alkanes. The first series was published in the

1951 N.G.S.M.A. Engineering Data Book³⁸ for pressures up to 800 psia. These charts were based on the fugacity tables of W. K. Lewis of the Massachusetts Institute of Technology.

In 1945 Hanson and Brown³⁹ compared the behavior of some mixtures containing light hydrocarbons which were selected to have critical pressures at the operating temperature. K-values for these mixtures could be measured for all pressures up to the critical where they were all observed to converge to unity. Thus, the "convergence pressure" was taken to be the pressure at which the K-values on a plot of $\log K_i$ versus $\log P$ converged to unity. For a binary mixture the convergence pressure, P_k , is exactly equal to the critical pressure.

Hanson and Brown also observed that the K-value for a particular component at a specified temperature and pressure was the same in different mixtures provided the mixtures had the same convergence pressure. This meant that the effect of composition on K-values could be accounted for by the convergence pressure concept. Based on this finding, the N.G.A.A. started to use convergence pressure as a correlating parameter. The 1957 N.G.S.M.A. Engineering Data Book⁴⁰ contained K-value charts for convergence pressures of 600, 800, 1000, 2000, 3000, 4000, 5000, 10000 and 20000 psia. The latest series was published in the 1966 N.G.P.A. Engineering Data Book⁴¹ and charts are provided for convergence pressures of 800, 1000, 2000, 4000 and 10000 psia. The number of convergence pressures covered by the latest series was reduced due to the lack of internal consistency in the earlier charts and the increased popularity of equation of state type

correlations which are easily programmed for computer solution.

In order to adapt the charts in the 1957 N.G.S.M.A. Data Book for computer usage K-values were approximated by the functional form

$$\ln(K_{ij} P) = \frac{1000}{T} \sum_{m=1}^4 \sum_{n=1}^7 A_{mni} \left(\frac{T}{1000} \right)^{m-1} \left(\frac{\ln P}{10} \right)^{n-1} \quad (4-2)$$

where: K_{ij} is the K-value for component i at convergence pressure j ,

A_{mni} are the N.G.P.A. curve fit coefficients for component i at convergence pressure j ,

P is the system pressure, psia,

T is the system temperature, °R.

The K-values evaluated from the N.G.P.A. coefficient deck⁴² deviate considerably from the charts when the ratio $P/P_k > 0.9$. Schlaudt⁴³ extended the surface fit to cover this region by assuming a linear relationship between $\log K_i$ and $\log P$ in the range $0.9 < P/P_k < 1.0$. The analytical representation for this range of pressure is

$$K_i = (P/P_k)^{\left(\frac{\log(K_{i,P/P_k=0.9}) - \log(0.9)}{\log(1.0) - \log(0.9)} \right)} \quad (4-3)$$

where: $K_{i,P/P_k=0.9}$ is the K-value of component i at the pressure ratio $P/P_k=0.9$

Since the convergence pressure is not a parameter in Equation 4-2 a suitable means for interpolation is required to calculate K-values for a specific convergence pressure.

Figure 4-1 shows the K-values for the methane-n-pentane system at 100°F for convergence pressures of 600, 800, 1000, 1500, 2000, 3000 and 5000 psia. This figure shows that

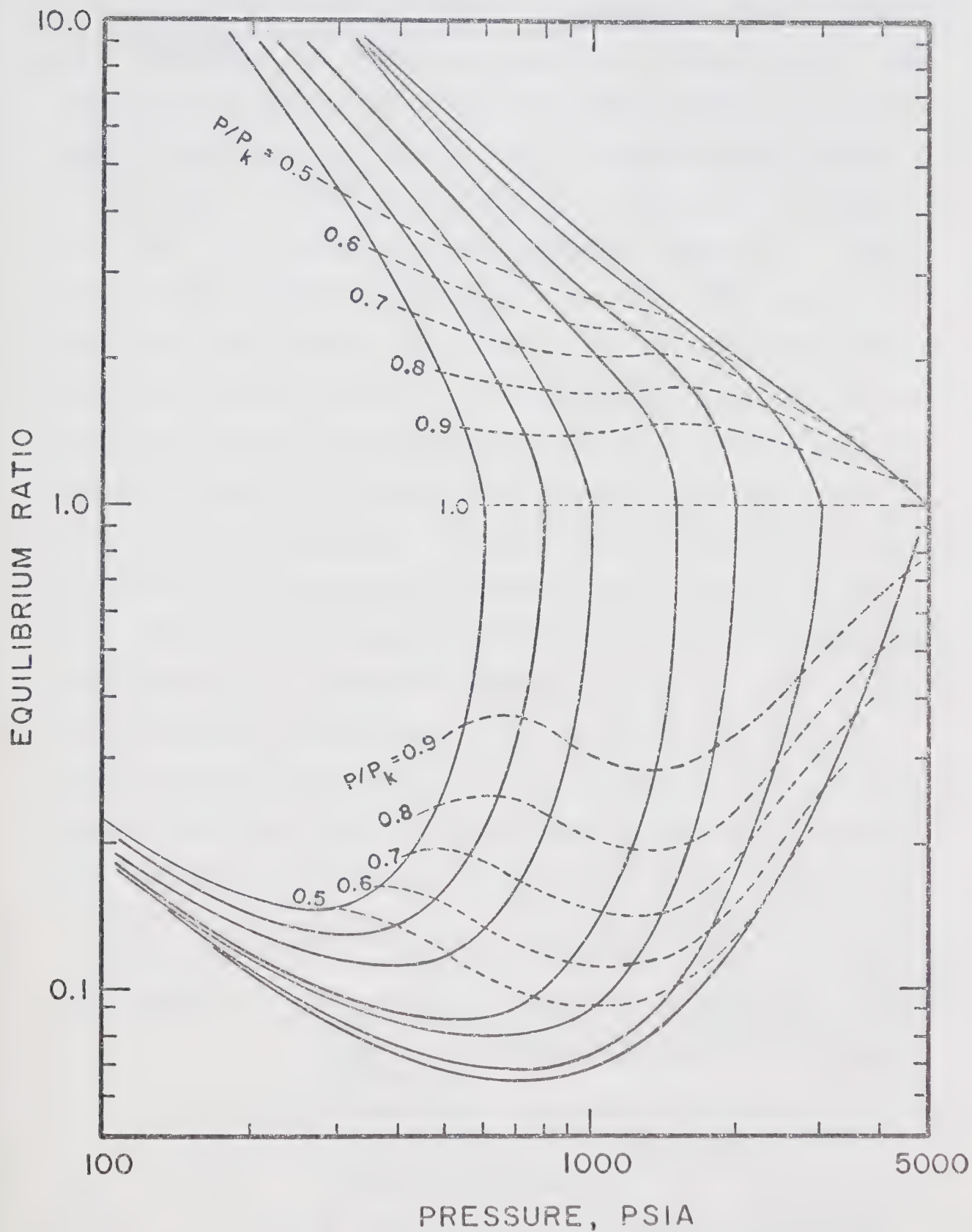


Figure 4-1. Equilibrium Ratios for the Methane-n-Pentane System at 100°F.

K-values are a strong function of composition (hence convergence pressure) for conditions near the critical state. Suppose that the K-value for n-pentane was required for a pressure of 1200 psia in a mixture with a convergence pressure of 1500 psia. Since a curve for $P_k = 1500$ psia is provided the value of 0.194 can be read directly. However, if the curve or corresponding surface fit for $P_k = 1500$ psia was not available, the K-value would have to be extrapolated from the K-value(s) corresponding to the next higher available convergence pressure(s). Extrapolation is required since K-values are not defined for convergence pressures which are less than the system pressure. Interpolation rather than extrapolation may be applied by an approach which uses the ratio P/P_k . This ratio is used to evaluate K-values for the available convergence pressures above and below the system convergence pressure. The dashed curves in Figure 4-1 give the loci of several P/P_k ratios. If it is assumed that the P/P_k locus between two adjacent convergence pressures is linear then the following interpolation formula can be used.

$$K_i = K_{i,1} \exp \left(\ln(K_{i,2}/K_{i,1}) \ln(P_k/P_{k,1}) / \ln(P_{k,2}/P_{k,1}) \right) \quad (4-4)$$

where: $P_{k,1}$ is the first available convergence pressure from the N.G.P.A. correlation which is less than the system convergence pressure,

$P_{k,2}$ is the first available convergence pressure from the N.G.P.A. correlation which is greater than the system convergence pressure,

$K_{i,1}$ is the K-value for component i evaluated at $P = (P/P_k)P_{k,1}$ and system temperature,

$K_{i,2}$ is the K-value for component i evaluated at $P = (P/P_k)P_{k,2}$ and system temperature.

Equations 4-3 and 4-4 may be used with fair success in the pressure range from $0.5 < P_k < 1.0$. The use of Equation 4-4 at pressures less than $0.5 P_k$ leads to large errors. Attempts to develop a single interpolation formula which could be applied over the full pressure range were unsuccessful. Interpolation schemes which used a combination of separate formulas lacked internal consistency as the change over point between formulas could be detected when the K-values were plotted. For these reasons the N.G.A.A. charts and approximating functions were not used in any of the phase simulation calculations in this work.

To this point no mention has been given to how the convergence pressure for a particular mixture may be calculated. The method of Hadden⁴⁴ is frequently used, and is recommended in the 1957 N.G.S.M.A. Engineering Data Book and the 1966 N.G.P.S.A. Engineering Data Book. In Hadden's method the convergence pressure is taken to be the critical pressure of a pseudo-binary mixture at the system temperature. The pseudo-binary mixture is composed of the most volatile component present in the mixture and a pseudo-heavy component comprising a weight average of all the components in the liquid phase except the most volatile component. The method is well-suited for hand calculations, but would be difficult to program for computer usage. A more rigorous method which can be adapted for computer use is considered in the next section.

4.3 The Critical Composition Method of Estimating Convergence Pressure

Rowe²⁹ presented a critical composition method which is a logical extension of the convergence pressure concept from binary to ternary, and from ternary to multicomponent mixtures. Rowe defined the convergence pressure to be "the critical pressure of a critical mixture which, when flashed to the operating pressure, will result in a tie line that passes through the over-all system composition for which the K-values are desired". The method is a trial and error procedure. First a convergence pressure is assumed so that K-values can be obtained from a correlation. Then flash calculations are performed to define a tie line from which a new convergence pressure is calculated. The procedure is repeated until the calculated convergence pressure is in good agreement with the convergence pressure used to obtain the K-values.

The critical composition method yields the same convergence pressures as Hadden's method for binary mixtures. However, it may yield significantly different values for convergence pressure in ternary or multicomponent mixtures. Thus, there may be cases where there is an inconsistency in data correlation when the critical composition method is used with existing K-value correlations which were not prepared with this definition of convergence pressure.

The accuracy of the critical composition method depends upon the accuracy of the critical temperature and critical pressure correlations with which it is used. A critical temperature correlation is used to locate the composition

along a tie line which has a critical temperature equal to the system temperature. Grieves and Thodos⁴⁵ found the locus of critical temperatures for ternary hydrocarbon mixtures to be linear on a compositional diagram. This fact simplifies the search for the composition of the critical mixture. The composition of the critical mixture is used in a critical pressure correlation to calculate the convergence pressure of the system.

The critical temperatures of paraffin hydrocarbon mixtures lie between the critical temperatures of the pure components. Also, the critical temperatures tend to be symmetric with respect to a composition variable and are therefore easily correlated. Several authors have reported accurate correlations for calculating critical temperatures^{46, 47, 48, 49, 50, 51}. The method of Etter and Kay⁵² was selected for this work because analytical expressions were provided which could be easily programmed for computer evaluation. This method is described further in Appendix D.

It is considerably more difficult to accurately predict the critical pressures of hydrocarbon mixtures than it is to predict their critical temperatures. Unlike critical temperatures, critical pressures may be much higher than the mole average critical pressure of the mixture. Also, critical pressures are not usually symmetric with respect to composition and may exhibit a sharp maximum, and/or a point of inflection. Several authors have presented critical pressure correlations^{46, 47, 49, 50, 51, 53, 54, 55, 56}. The method of

Etter and Kay⁵² was selected for this work, again because of the ease with which it could be programmed. A completely satisfactory critical pressure correlation was not available in the literature. Since the success of the critical composition method depends upon the accuracy of the critical pressure correlation, some work was done on correlating critical properties. This work is summarized in Appendix F.

Schlaudt⁴³ extended the critical composition method to multicomponent systems. The basis for the extension is best described by considering the pressure-temperature diagram for a two-phase reservoir fluid such as that shown in Figure 4-2. The critical points for the reservoir vapor and liquid phases are shown. A critical locus is also shown for all combinations of the coexisting vapor and liquid phases. To apply the critical composition method to this system, various proportions of the vapor and liquid phases are tried until an overall mixture is found which has a critical temperature equal to the reservoir temperature. The required convergence pressure is then the critical pressure of this mixture. The lack of dependable correlations for critical properties in multicomponent systems is the only factor preventing the critical composition method from receiving wide usage in natural reservoir systems.

4.4 The Chao-Seader Method

In 1961 Chao and Seader²⁷ published a general correlation for calculating compositionally dependent K-values for hydrocarbon mixtures. The correlation has received widespread

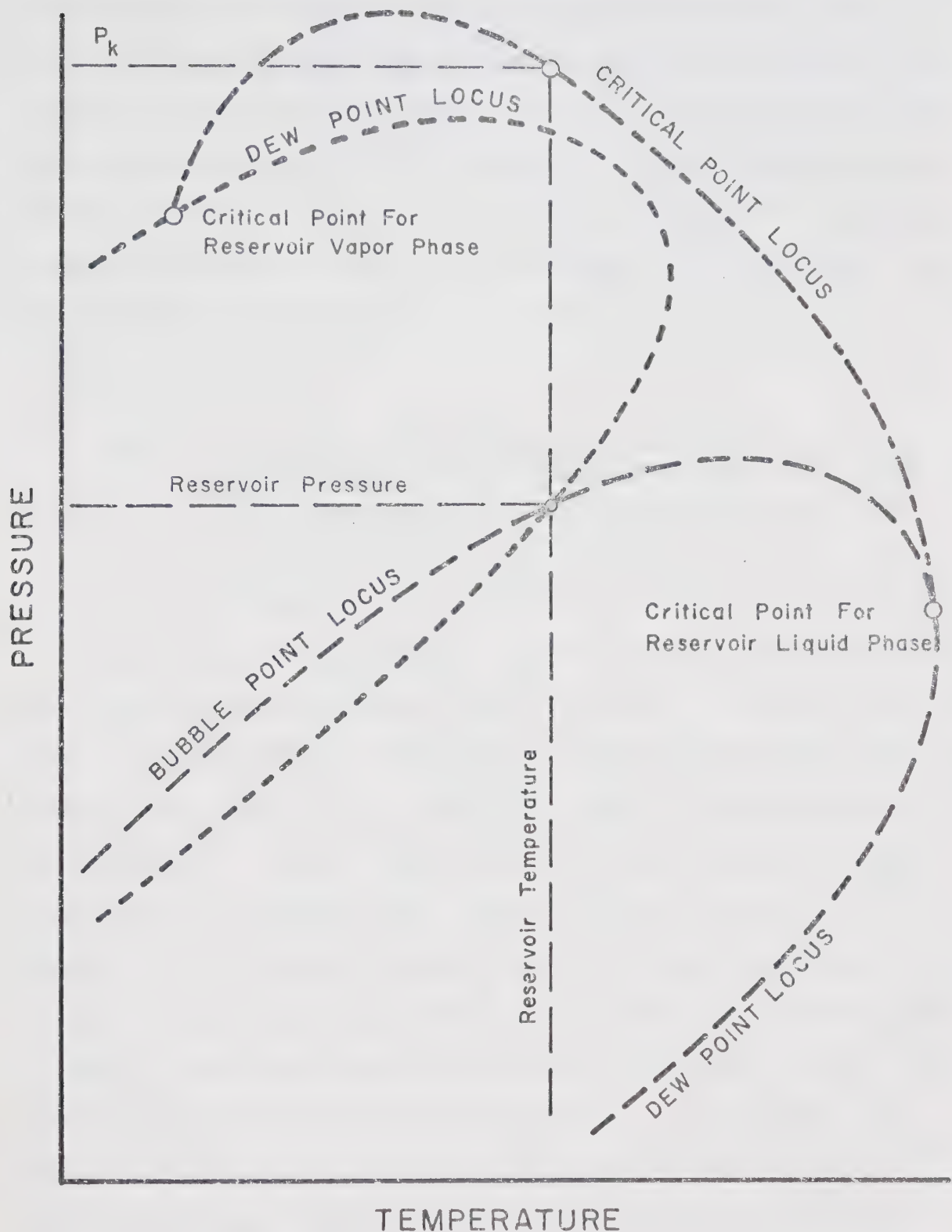


Figure 4-2. Pressure-Temperature Diagram Illustrating the Critical Composition Method for Calculating Convergence Pressure in Multicomponent Systems.

acceptance by the natural gas processing industry. The N.G.P.A. have extended the method to include sour gases, and offer a computer program which also calculates enthalpies for hydrocarbon mixtures. The correlation relates the non-ideal behavior of each component in coexisting phases to the properties of the pure components. K-values are calculated from the following equation

$$K_i = v_i \gamma_i / \phi_i \quad (4-5)$$

where: v_i is the liquid fugacity coefficient of pure component i at system conditions,

γ_i is the activity coefficient for pure component i in the liquid solution,

ϕ_i is the vapor fugacity coefficient of pure component i in the vapor mixture.

The liquid phase fugacity coefficient is well defined for any component provided the system pressure is greater than the vapor pressure of the component at system temperature, and the system temperature is less than the critical temperature of the component. Under these conditions the fugacity coefficient can be obtained from a generalized correlation^{31, 57}. However, if the system temperature or pressure are such that the pure liquid could not exist, a hypothetical fugacity must be used. Chao and Seader extended the Curl and Pitzer⁵⁷ correlation to these hypothetical regions using fugacity coefficients back calculated from experimental vapor-liquid equilibrium data. Thus, fugacity coefficients were correlated by the equation

$$\log v_i = \log v_i^{(0)} + \omega_i \log v_i^{(1)} \quad (4-6)$$

where: $v_i^{(0)}$ is the fugacity coefficient for a simple fluid,
 $v_i^{(1)}$ is a correction term for the departure of real fluids from the simple fluid model,
 ω_i is the acentric factor for component i.

The approximations for $v_i^{(0)}$ and $v_i^{(1)}$ are functions of the reduced temperature and reduced pressure for each component in the mixture. These approximations are empirical surface fits of the Curl and Pitzer correlation supplemented with some additional data covering the hypothetical regions.

The liquid phase activity coefficients are calculated from the Hildebrand⁵⁸ equation

$$\ln \gamma_i = v_i(\delta_i - \bar{\delta}_i)/RT \quad (4-7)$$

where: v_i is the molal volume of the saturated liquid,
 $\delta_i = \sqrt{\Delta E_v / V_i}$ the solubility parameter for component i,
 $\bar{\delta}_i$ is the volume weighted average value of the solubility parameter for the mixture,
 E_v is the change in internal energy during the vaporization of component i.

The Hildebrand equation is only valid for regular solutions where interactions between different sized molecules are small and may be neglected. Fortunately, the paraffin hydrocarbons approximate regular solutions over a considerable range of temperature, pressure and composition.

Vapor phase fugacity coefficients may be calculated from volumetric data or an equation of state by the thermodynamic relation

$$\ln \phi_i = \frac{1}{RT} \int_V^\infty \left[\left(\frac{\partial P}{\partial n_i} \right)_{T, V, n_j} - \frac{RT}{V} \right] dv - RT \ln z \quad (4-8)$$

where: V is the total volume of the vapor mixture,
 Z is the compressibility factor for the mixture
at system conditions.

Chao and Seader used the two constant Redlich-Kwong⁵⁹ equation to evaluate the derivative in Equation 4-8. The mixing rules for the Redlich-Kwong equation are simply

$$a = \sum y_i a_i \quad (4-9)$$

$$b = \sum y_i b_i \quad (4-10)$$

where: a_i , b_i are the Redlich-Kwong constants which can be evaluated from the critical properties of each component.

When Equation 4-8 is evaluated using the Redlich-Kwong equation of state and the mixing rules of Equations 4-9 and 4-10, Chao and Seader have shown that

$$\begin{aligned} \ln \phi_i = & (z - 1)b_i/b - \ln(z - bP) \\ & - a^2/b(2a_i/a - b_i/b) \ln(1 + bP/z) \end{aligned} \quad (4-11)$$

It is important to note that this relatively simple expression for ϕ_i is due to the simplicity of both the Redlich-Kwong equation of state and the mixing rules of Equations 4-9 and 4-10. The mixing rules establish the compositional dependence for the derivative in Equation 4-8. To be totally consistent with the development of the Chao-Seader correlation, the mixture Z in Equation 4-11 should be evaluated from the Redlich-Kwong equation. In practice, however, the Z can be calculated from a generalized corresponding states correlation.

The Chao-Seader correlation is generally applicable only for pressures below 2000 psia and therefore, is seldom used

for reservoir engineering calculations. The pressure limitation results from a restriction on the correlation that the pseudoreduced temperature of the liquid phase be less than about 0.93. The solubility of methane in the liquid increases with pressure to the point where this temperature restriction causes the correlation to breakdown.

Another difficulty with the Chao-Seader correlation is the failure of the Hildebrand equation to correctly predict methane behavior in the liquid mixture. Differences between experimental and calculated K-values for methane are systematic and Besserer⁶⁰ has shown that correction factors for methane K-values can be correlated with the critical temperature and critical pressure of the mixture. Figure 4-3 shows the correction factors for three methane binaries at 100°F. Application of these correction factors extends the pressure range of the Chao-Seader correlation, however, even with this correction the method is of limited use for reservoir engineering calculations. The next section outlines a calculation procedure which avoids this pressure limitation.

4.5 Combined Chao-Seader and Critical Composition Methods

The critical composition method provides a rigorous procedure for calculating the pressure at the point where the K-values on a plot of $\log K_i$ versus $\log P$ converge to unity. Thus, the possibility exists for calculating K-values over the full range of pressure by using the Chao-Seader method to generate a number of K-values for each component at the lower pressures and extrapolating these to the

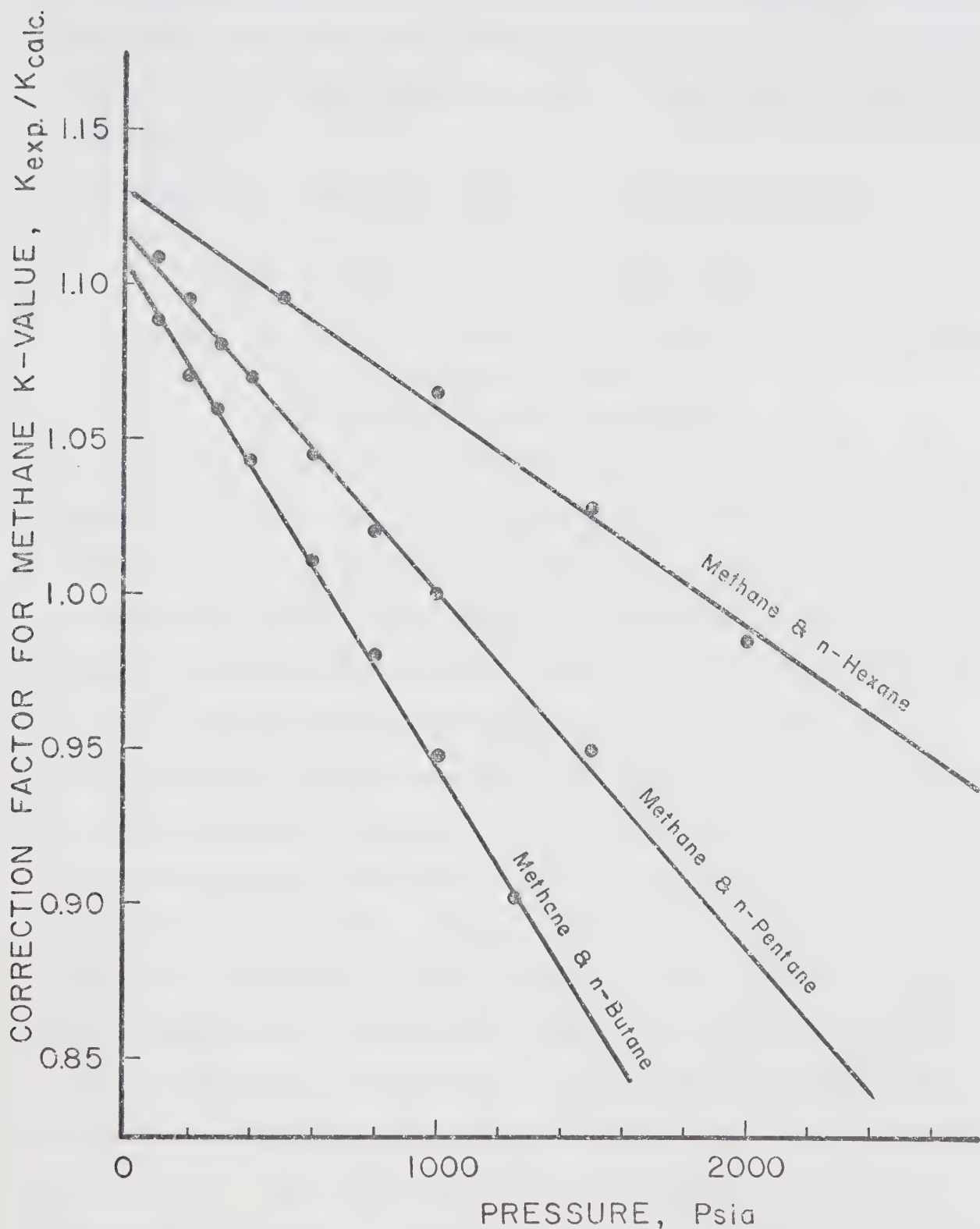


Figure 4-3. Correction Factors for Methane K -values from the Chao-Seader Correlation at 100°F.

convergence pressure given by the critical composition method. All that is required is a functional form which will suitably approximate the characteristic shape of the $\log K_i$ versus $\log P$ diagram.

Green and Hachmuth²⁸ used the empirical equation

$$K_i = C_{1i}(1 - P/P_k)^n + C_{2i}/P + C_{3i}P^2 + C_{4i} \quad (4-12)$$

where: C_{1i} , C_{2i} , C_{3i} and C_{4i} are empirical coefficients,
 P is the system pressure,
 P_k is the convergence pressure.

to correlate K-values for binary mixtures of paraffin hydrocarbons. The four coefficients were required to satisfy the conditions that K_i be unity at the vapor pressure and at the convergence pressure, and that K_i of the least volatile component pass through a minimum. The characteristic shape of a $\log K_i$ versus $\log P$ diagram for the more volatile components could be described with fewer coefficients, however, the same equation was used for all components. Green and Hachmuth tried various values for the exponent n and found that 0.25 gave the best average fit for binary mixtures of the normal paraffins. They correlated the four coefficients directly with the system composition and the physical properties of the pure components. In this work Equation 4-12 was only required to extrapolate K-values into the high pressure region. When the calculated convergence pressure was less than 3000 psia, the four coefficients in Equation 4-12 were calculated using the convergence pressure and K-values from the Chao-Seader correlation for pressures of 0.3 P_k ,

0.5 P_k and 0.7 P_k . When the convergence pressure was greater than 3000 psia, K-values corresponding to 0.1 P_k , 0.3 P_k and 0.5 P_k were used. After the four coefficients in Equation 4-12 were calculated for every component in the mixture it was possible to perform flash calculations throughout the high pressure region. A FORTRAN computer program for this calculation procedure is given in Appendix D.

Chapter 5. CALCULATION OF VAPOR AND LIQUID DENSITIES

5.1 Foreword

Computer programs for modelling the performance of petroleum reservoirs require a method for calculating fluid densities. This may be accomplished with a corresponding states correlation extended to mixtures through the use of the concept of pseudocritical properties.

In order to use corresponding states correlations, a suitable method must be found to adapt the information to computer use. This may involve interpolation techniques, fitting empirical functions to all or part of the data, or by using a reduced form of an equation of state. Interpolation techniques are considered the least desirable, because large-scale data storage and subsequent retrieval is an inefficient computer operation. The well-known equations of Beattie and Bridgeman⁶¹, and Benedict, Webb and Rubin⁶², have been applied in reduced form to generalized correlations by Su and Chang⁶³, Opfell, Sage and Pitzer⁶⁴, and Su and Viswanath⁶⁵.

Good accuracy has been achieved using these equations in the gaseous region, but unfortunately it has not been possible to find a single set of coefficients that will give good results over the entire liquid, gaseous and saturated regions. Hirschfelder, Buehler, McGee and Sutton⁶⁶ have developed a generalized equation of state in which different functions are used for the three regions defined as: (1) gas, where the reduced density is less than one; (2) dense gas,

where the reduced density is greater than one and the reduced temperature is greater than one; and (3) liquid, where the reduced density is greater than one and the reduced temperature is less than one. The functions increase in complexity for each of the three regions. The equations are density implicit, and a method for obtaining a solution when the reduced temperature and pressure are known was not reported.

Yen and Woods⁶⁷ have developed accurate empirical expressions for the saturated and compressed liquid regions when the reduced temperature is less than one for the Lydersen, Greenkorn and Hougen³¹ correlation. The expressions in their computer-oriented approach have the advantage of being density explicit, however, the equations are lengthy and more than 80 coefficients are required.

On the basis of these considerations, it was concluded that no generally applicable equation of state was available for representing fluid densities from generalized correlations. Furthermore, it appeared that previous attempts to develop equations of state for pure materials had not given sufficient recognition to the behavior of the reduced isochores, particularly along the saturation curve, when selecting the independent variable.

5.2 Some Equation of State Features

One of the most informative projections of PVT data is the isochoric plot shown on reduced coordinates in Figure 5-1. If all pure substances conformed to van der Waals' two-parameter theorem of corresponding states, all PVT data

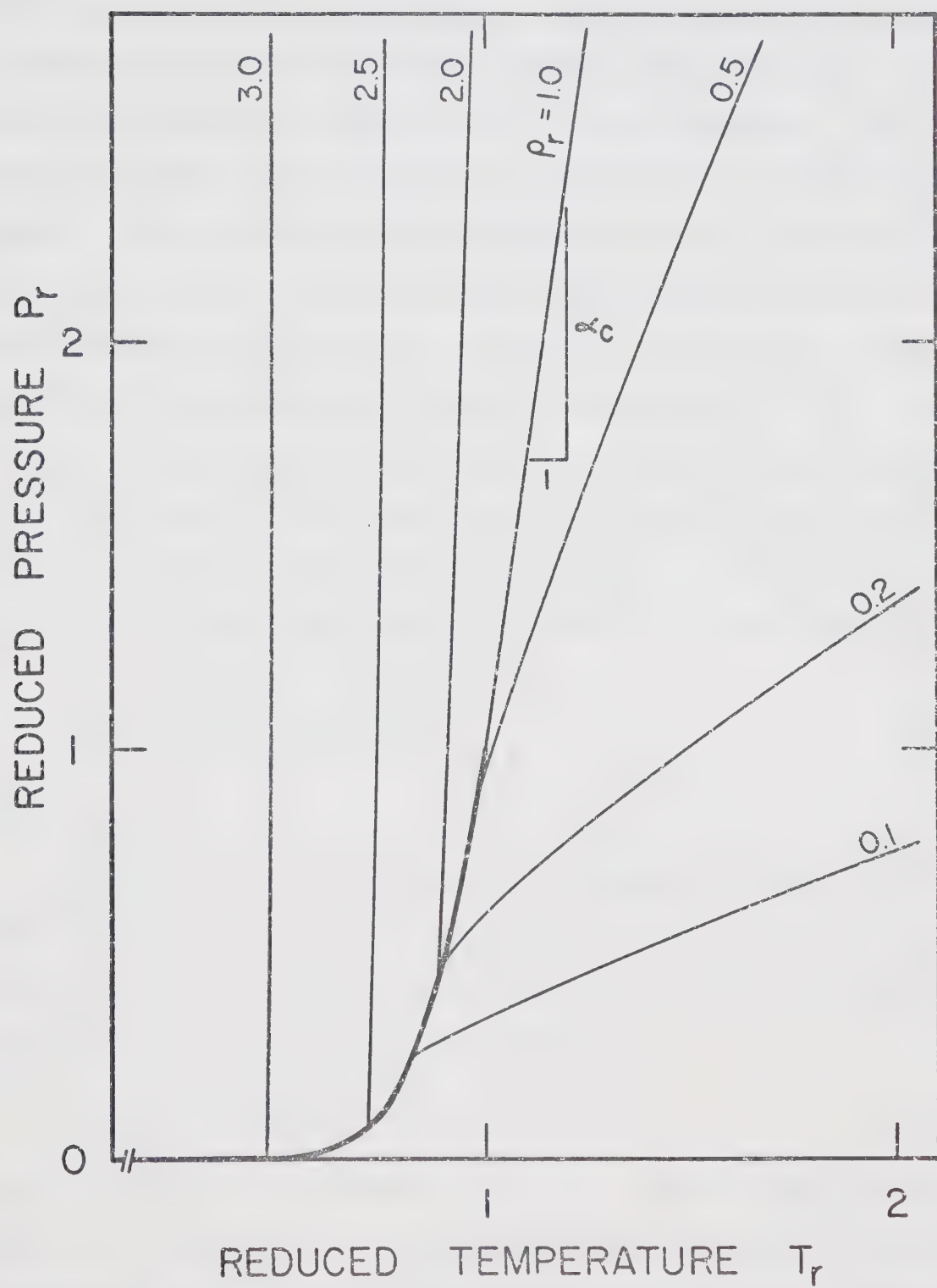


Figure 5-1. Isochoric Diagram Showing The Vapor Pressure Curve.

would lie on a single plot. In actual fact, however, the reduced critical point is the only point which is assured of being common for all substances. Various methods have been proposed to resolve the problem of departure from the two-parameter theorem by introducing a third parameter. For example, the acentric factor, ω , introduced by Pitzer⁶⁸ represents a method of describing the departure of a substance from the intermolecular potential function for a simple fluid with spherical molecules by observing the variation in reduced vapor pressure at a reduced temperature of 0.7. Riedel⁶⁹ developed a comprehensive corresponding states method by using the slope of the vapor pressure curve at the critical point as a third parameter. He defined α_c as the logarithmic slope of the vapor pressure curve at the critical point

$$\alpha_c = \frac{d(\ln P_r)}{d(\ln T_r)} = \frac{T_r \frac{dP_r}{dT_r}}{P_r \frac{dT_r}{dP_r}} \quad (5-1)$$

where $T_r = 1$.

Experimental evidence generally supports the observation from Figure 5-1 that the critical isochore is linear with a slope which is continuous with and equal to that of the vapor pressure curve. Hence one can write

$$(P_r)_{\rho_c} = 1 + \alpha_c (T_r - 1) \quad (5-2)$$

along the critical isochore, ρ_c . It is significant to note that the origin of both the parameters ω and α_c may be traced directly to the behavior of the substance along the vapor pressure curve. It may be concluded from this that the behavior of the substance along the vapor pressure curve

represents one of the major obstacles to developing an equation of state that is applicable to both the gaseous and liquid-like regions.

The isochores for a pure component are also linear in the region of very low density and in the region of high reduced temperature. The approximate linearity of the isochores has been used in developing most empirical equations of state. Beattie and Bridgeman⁶¹ and Benedict, Webb and Rubin⁶² used the form

$$(P_r)_{\rho_r} = A + B T_r + C T_r^{-2} \quad (5-3)$$

to describe the isochores. The term CT_r^{-2} diminishes with increasing temperature and satisfies the condition that the isochores become linear at high temperature. Martin and Hou⁷⁰ used the expression

$$(P_r)_{\rho_r} = A + B T_r + C \exp(-k T_r) \quad (5-4)$$

where k was found to be a universal constant.

The coefficients A , B and C in Equations 5-3 and 5-4 are functions of density. These equations can be applied to a range of densities if it is assumed that their functional dependence on density can be approximated by a power polynomial of degree n , namely

$$P_r = \sum_{i=1}^n (A_i + B_i T_r + C_i T_r^{-2}) \rho_r^i \quad (5-5)$$

and

$$P_r = \sum_{i=1}^n (A_i + B_i T_r + C_i \exp(-k T_r)) \rho_r^i \quad (5-6)$$

Some of the coefficients A_i , B_i and C_i may be evaluated

by imposing certain known limiting physical conditions such as:

- (i) the substance must exhibit ideal gas behavior as the pressure approaches zero so that $P_r z_c / (\rho_r T_r) = 1.0$ as $P_r \rightarrow 0$ for all T_r ;
- (ii) the slope of the critical isotherm is zero at the critical point so that $(\partial P_r / \partial \rho_r)_{T_r=1} = 0$;
- (iii) a point of inflection in the critical isotherm must exist at the critical point so that $(\partial^2 P_r / \partial \rho_r^2)_{T_r=1} = 0$.

The remaining coefficients are usually obtained by applying a least squares criterion to minimize the deviation between the predicted and observed pressures, or preferably the deviation between the predicted and observed densities^{71, 72}.

Equations 5-5 and 5-6 have the form of a truncated virial expansion. Thus, the assumption that the dependence of A_i , B_i and C_i on density could be approximated by a polynomial in density is tantamount to assuming that the temperature dependence of the second and higher virial coefficients can be represented by the same functional form as that of Equations 5-3 and 5-4. As these equations were intended to represent isochores, and not necessarily the temperature dependence of the virial coefficients, it is not surprising that Equations 5-5 and 5-6 fail at high densities.

The curvature of the isochores on a pressure-temperature diagram changes from concave downward to concave upward in passing through the critical density. At extremely high densities there is some evidence that the isochores straighten

and become concave downward. Thus, the coefficient $\sum_{i=1}^n C_i \rho_r^i$ in Equations 5-5 and 5-6 should change sign when crossing the critical density. This is one of the constraints implied by Equation 5-2. The additional constraints implied by Equation 5-2, namely that when $\rho_r = 1$, $\sum_{i=1}^n A_i = 1 - \alpha_c$ and $\sum_{i=1}^n B_i = \alpha_c$, are not normally used in equation of state development.

When the physical behavior of a system is not fully used in determining the form of, or the coefficients for an equation of state, one always faces the possibility of encountering correlated coefficients. Correlation of coefficients in approximating functions often occurs when variables are employed in an inappropriate form, or when improper variables are used. Correlation of coefficients is not desirable inasmuch as the coefficients become sensitive to the data set from which they were obtained. An improper functional form also prevents extrapolation outside the range of conditions for which data were available. Unfortunately, the coefficients in most equations of state tend to be correlated.

Consider, for example, the vapor pressure curve which is most conveniently described by a relationship between the variables $\log P_r$ and T_r^{-1} . As most equations of state do not employ the variables P_r and T_r in this form at saturation, a complicated interdependence among all coefficients is required if the vapor pressure is to be accurately predicted. Consider also the coefficient $\sum_{i=1}^n A_i \rho_r^i$, which may be thought of as an intercept or origin for the line approximating an isochore. Isochores have their origin at the

saturated state, and any other origin is an extrapolation into a hypothetical region. A computational scheme has been developed in this work which uses a vapor pressure equation at saturation, and eliminates the need for A_i coefficients to describe isochores.

The isochores of Figure 5-1 depict the derivative $(\partial P_r / \partial T_r)_{\rho_r}$. Figure 5-2 is also an isochoric diagram which has the advantage of showing the two phase envelope. The transformation relating Figure 5-1 to Figure 5-2 can be obtained by making the substitution

$$P_r = \rho_r z T_r / z_c \quad (5-7)$$

in the derivative with the result that

$$(\partial P_r / \partial T_r)_{\rho_r} = \rho_r / z_c (\partial (z T_r) / \partial T_r)_{\rho_r} \quad (5-8)$$

Hence, recalling the definition given in Equation 5-1, it may be shown that the slope of the critical isochore is $z_c \alpha_c$ on this diagram. The isochores of Figure 5-2 become linear at low densities, and exhibit a slope of one as the limiting condition of zero density is approached.

If Equation 5-7 is solved for T_r , and the substitution made in the derivative $(\partial T_r / \partial P_r)_{\rho_r}$, then

$$(\partial T_r / \partial P_r)_{\rho_r} = z_c / \rho_r (\partial (P_r / z) / \partial P_r)_{\rho_r} \quad (5-9)$$

and the pressure isochoric diagram illustrated in Figure 5-3 is obtained. On this diagram the critical isochore has a slope of $(z_c \alpha_c)^{-1}$ and the low-density isochores again exhibit a limiting slope of one.

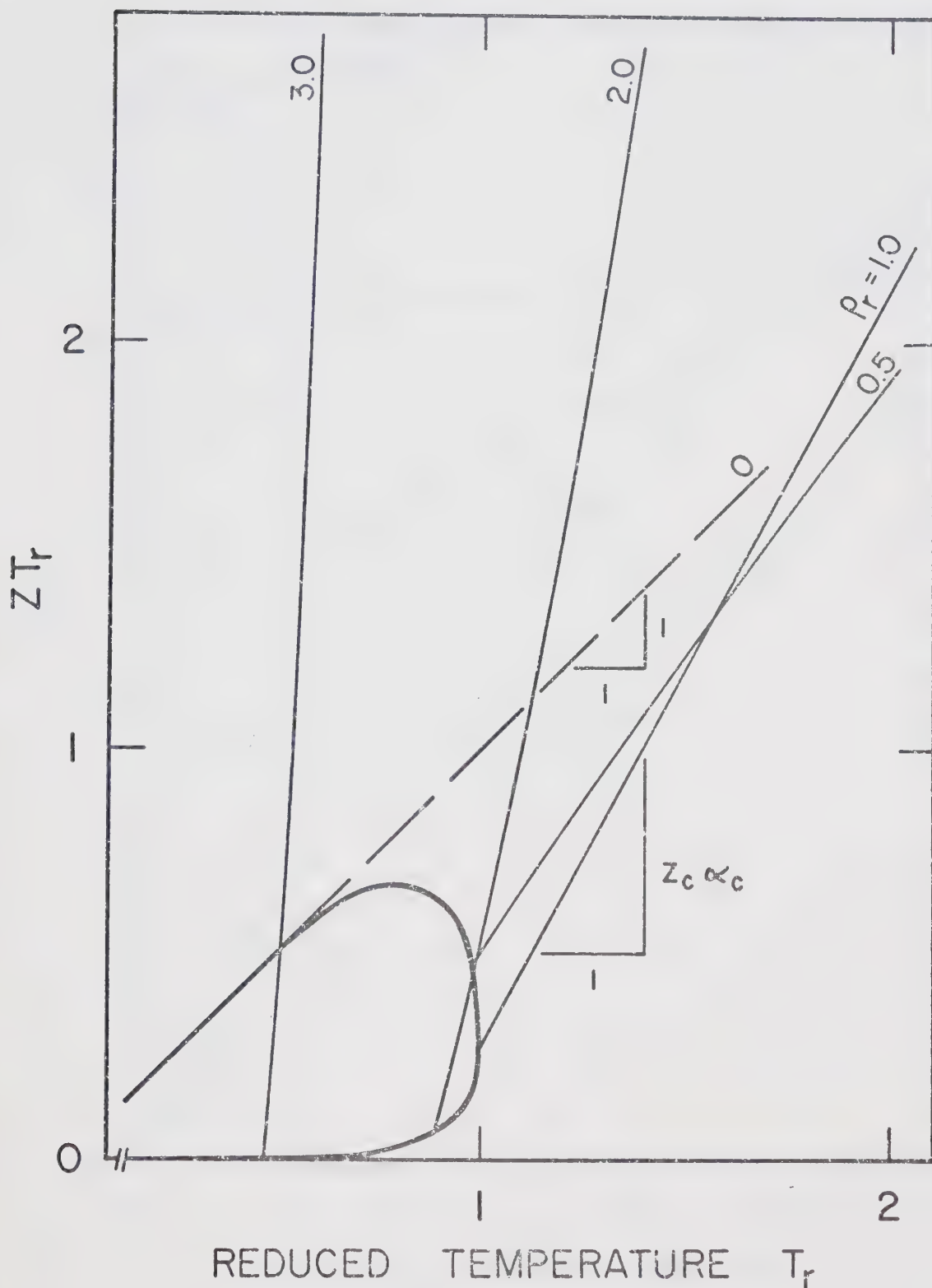


Figure 5-2. Temperature Isochoric Diagram Showing the Two-Phase Envelope.

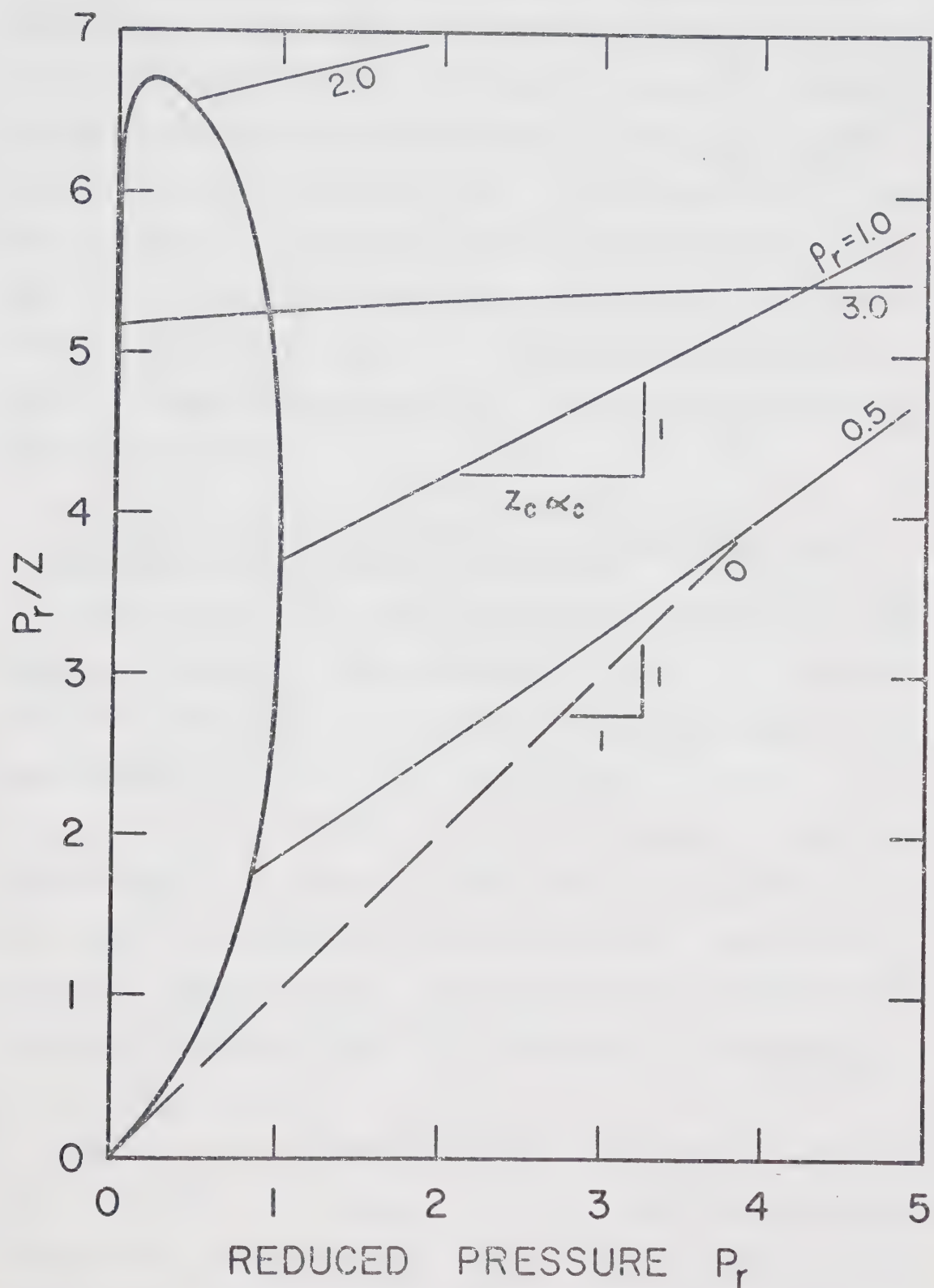


Figure 5-3. Pressure Isochoric Diagram Showing the Two-Phase Envelope.

By taking the saturated state as a datum, as suggested previously, the isochores of Figures 5-2 and 5-3 can be drawn from a common origin as shown in Figure 5-4. Because the isochores in Figure 5-4 all pass through the origin, an intercept term will not be required in any approximating expressions used to represent them. It should also be noted that the slopes of the isochores in Figure 5-3 are the reciprocals of those in Figure 5-2. This reciprocal feature is more apparent in Figure 5-4 and can be used to develop either a temperature-explicit or a pressure-explicit form for the isochores.

5.3 A General Method for Analytical Representation of Compressibility Factor Correlations

A procedure which uses independent equations for the saturated region and the isochores of Figure 5-4 has been developed. The use of independent equations results in the density-implicit forms $\rho_r = f(z_c, \alpha_c, \rho_r, T_r)$ and $\rho_r = g(z_c, \alpha_c, \rho_r, P_r)$ for the isochores of Figures 5-2 and 5-3, respectively. In principle these forms can be solved by any of the well-known iterative techniques. However, to guarantee convergence and retain simplicity, the method of interval halving was used. The procedure is outlined in the following steps:

1. Given z_c , α_c , P_r and T_r , two initial values of density $\rho_r^{(1)}$ and $\rho_r^{(2)}$, are required such that the two corresponding values of the function $F(\rho_r) = \rho_r - f(z_c, \alpha_c, \rho_r, P_r)$ have opposite sign. A choice of $\rho_r^{(1)} = 0$, results in $F(\rho_r^{(1)}) = -P_r z_c / T_c$, because $Z = 1.0$ at zero density. A choice of

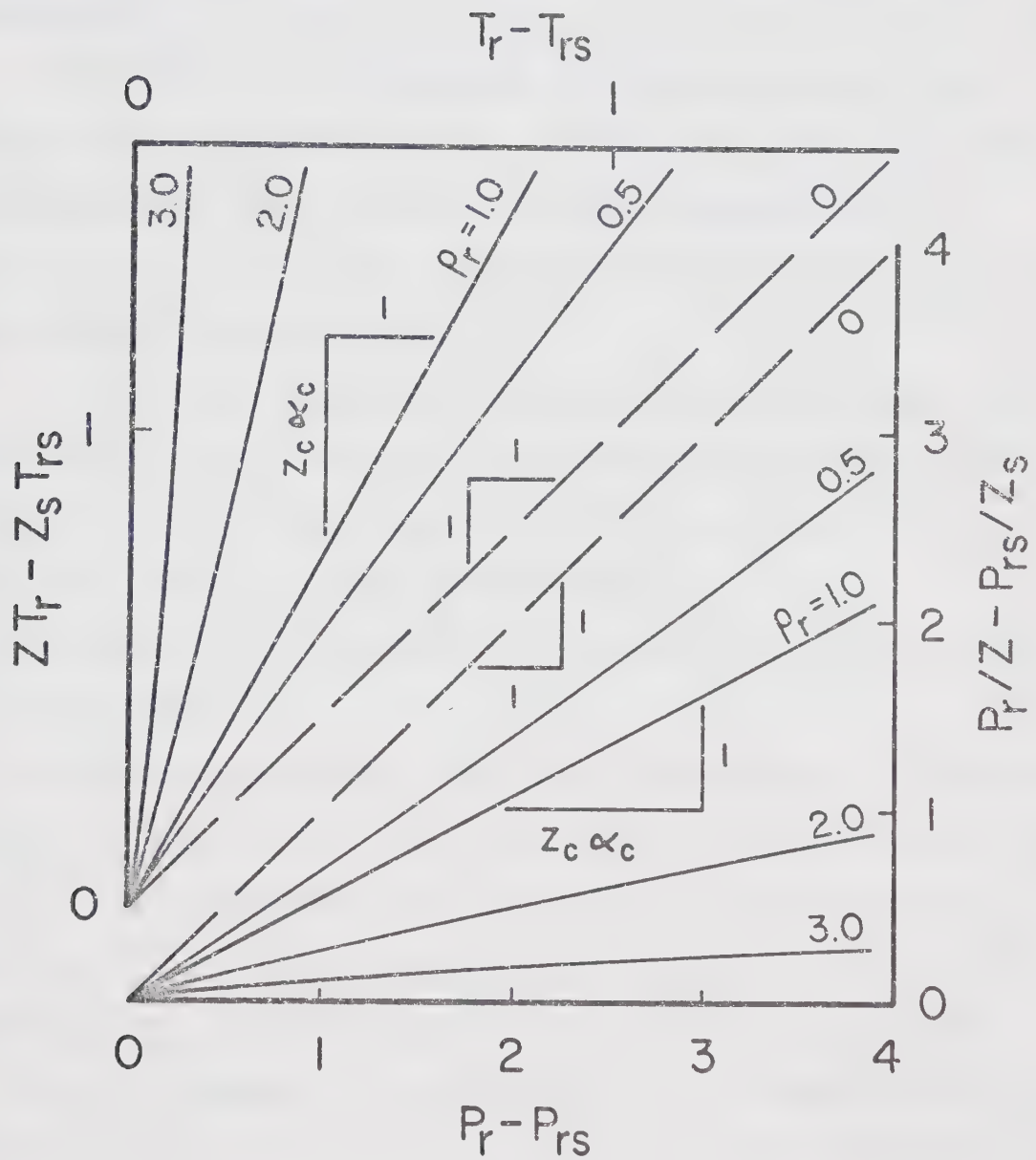


Figure 5-4. Isochoric Diagrams with the Saturated State Taken as a Datum.

$\rho_r^{(2)}$ equal to the highest density covered by the correlation will yield a positive value for $F(\rho_r^{(2)})$ if the solution lies in the range of the correlation.

2. An improved estimate of density, $\rho_r^{(3)}$, is calculated, and for the method of interval halving it is simply the average of $\rho_r^{(1)}$ and $\rho_r^{(2)}$, i.e. $\rho_r^{(3)} = (\rho_r^{(1)} + \rho_r^{(2)})/2$.

3. If $\rho_r^{(3)} > 1.0$, an equation for the saturated liquid region of the general form $\rho_{rs} = f(T_{rs})$ is solved for the temperature of the saturated liquid corresponding to $\rho_r^{(3)}$ from step 2. If $\rho_r^{(3)} < 1.0$, an equation for the saturated vapor region is solved for T_{rs} .

4. The vapor pressure corresponding to T_{rs} from step 3 is calculated from a vapor pressure equation for the substance or from a generalized vapor pressure equation with a parameter which characterizes the substance.

5. Equation 5-7 is applied to the saturated state and P_{rs}/Z_s is calculated.

6. An expression for the isochores of Figure 5-4 of the form $(P_r/Z - P_{rs}/Z_s) = f(Z_c, \alpha_c, \rho_r, P_r - P_{rs})$ is solved for Z , and $F(\rho_r^{(3)})$ is calculated. If $F(\rho_r^{(3)}) < 0$, the values of $\rho_r^{(1)}$ and $F(\rho_r^{(1)})$ in step 2 are replaced with $\rho_r^{(3)}$ and $F(\rho_r^{(3)})$, respectively, otherwise $\rho_r^{(2)}$ and $F(\rho_r^{(2)})$ are replaced.

7. Steps 2 through 6 are repeated until a convergence criterion, such as $|\rho_r^{(1)} - \rho_r^{(2)}|/\rho_r^{(1)} < \epsilon$, is satisfied where ϵ is some arbitrarily small value.

To utilize the above procedure, the following relationships are required:

(i) an equation relating the density of the saturated liquid

to the saturation temperature;
 (ii) a vapor pressure equation;
 (iii) an equation relating the density of the saturated vapor to the saturation temperature;
 (iv) an expression for the P_r/Z isochores illustrated in Figure 5-4.

Now that the theory and general procedure have been developed, the method will be demonstrated using a published corresponding states correlation as a data source.

5.4 Application of the Generalized Equation of State Method to the Lydersen et al. Correlation

The Lydersen, Greenkorn and Hougen³¹ correlation was selected as a data source because it presents data covering a wide range of densities with reduced temperatures from 0.3 to 15, and reduced pressures from saturation to 30. The correlation uses the critical compressibility factor as a third parameter, and tabular data are provided for Z_c values of 0.25, 0.27 and 0.29. The four relationships required to apply the generalized equation of state method to this correlation are discussed in the following sections.

5.4 (a) Saturated Liquid Densities

The two-phase region for a pure substance is specified by a single intensive variable. Most saturated liquid equations are explicit in density with either T_{rs} or P_{rs} as the independent variable. Since T_{rs} must be evaluated in every iteration of the solution procedure, an equation which is explicit in temperature would be preferable. Several equations for the saturated liquid state can be developed from

Taylor expansions about the critical point. A comprehensive discussion of Taylor expansions, the "law of rectilinear diameters"

$$\rho_{rL} + \rho_{rV} = 2 + D(1 - T_{rs}) \quad (5-10)$$

and the cubic coexistence curve

$$\rho_{rL} - \rho_{rV} = E(1 - T_{rs})^{1/3} \quad (5-11)$$

are given by Davis and Rice⁷³. Their tabulated values of D and E for various substances suggests that the form

$$\begin{aligned} \rho_{rL} = 1 + (D_1 + D_2 z_c) (1 - T_{rs}) \\ + (E_1/z_c) (1 - T_{rs})^{1/3} \end{aligned} \quad (5-12)$$

might be appropriate for representing the saturated liquid data of the Lydersen et al. correlation. When the coefficients D_1 , D_2 and E_1 were evaluated using a least-squares criterion, the average deviation from the data source was 0.78 per cent, indicating the forms to have some merit.

Rackett⁷⁴ recently reported the simple but accurate equation

$$\rho_{rL}^{-1} = z_c (1 - T_{rs})^{2/7} \quad (5-13)$$

This equation gave results differing from the data source by an average of 0.66, 0.37 and 1.31 per cent for z_c values of 0.25, 0.27 and 0.29, respectively. Rackett stated that a relation between z_c and the exponent 2/7 is not detectable from experimental evidence. However, to force a better correspondence with the data source, the modified form

$$\rho_{rL}^{-1} = (0.193 + 3.789 z_c^3) (1 - T_{rs})^{(0.220 + 3.52 z_c^3)} \quad (5-14)$$

was developed. Equation 5-14 differs from the data source by an average of 0.08, 0.14 and 0.23 per cent for the three respective z_c values. It may be noted that Equations 5-13 and 5-14 have a computational advantage when used in the proposed iterative method because T_{rs} can be calculated explicitly after taking the logarithm of both sides and solving for T_{rs} .

It was also demonstrated by Rackett that the saturated liquid data of Lydersen et al. can be calculated from the following equation by Riedel⁶⁹

$$\rho_{rL} = 1 + 0.85(1 - T_{rs}) + (1.93 + 0.2(\alpha_c - 7))(1 - T_{rs})^{1/3} \quad (5-15)$$

The saturated liquid density tabulations of the data source for z_c values of 0.25, 0.27 and 0.29 can be calculated from Equation 5-15 with standard errors of 0.07, 0.05 and 0.11 per cent, respectively. The α_c values which give these minimum differences are 8.0264, 6.8827 and 5.7045 for the respective z_c values. Since Equation 5-15 gave the best agreement with the data source, it was selected to describe the saturated liquid state.

5.4 (b) Vapor Pressure Equation

Because α_c is required in Equation 5-15 for the saturated liquid, and it will also be required for the slope of the critical isochore, it seems appropriate to use α_c for the vapor pressure calculation as well. Although α_c can be obtained from the definition expressed by Equation 5-1, it is usually obtained through application of Riedel's⁶⁹ generalized vapor pressure equation

$$\ln(P_r) = \alpha_c \ln(T_r) - 0.0838(\alpha_c - 3.75) \\ (36/T_r - 35 - T_r^6 + 42 \ln(T_r)) \quad (5-16)$$

at a convenient temperature such as the normal boiling point. Hence, Equation 5-16 was used for vapor pressure calculations in this work. Reid and Sherwood⁷⁵ have reviewed this equation and report an average maximum error of 5.3 per cent for pressures less than 1500 mm of Hg; for pressures greater than 1500 mm of Hg, the average maximum error was 1.7 per cent.

The Lydersen et al. correlation used Z_c rather than α_c as the third parameter, and consequently a relation between them is required. Riedel⁶⁹ reports the equation

$$\alpha_c = (Z_c^{-1} - 1.90)/0.26 \quad (5-17)$$

which relates the two parameters within ± 2 per cent. However, the α_c values from Equation 5-17 for Z_c values of 0.25, 0.27 and 0.29 do not agree with the ones which give the best correspondence between Equation 5-15 and the saturated liquid region of the data source. In order to be consistent, the same values of α_c given previously for use in Equation 5-15 were applied in Equation 5-16, and also in the expressions for the isochores.

5.4 (c) Saturated Vapor Densities

Attempts to solve for ρ_{rV} from modified forms of Equations 5-10 and 5-11 invariably resulted in large relative errors for values of $T_{rs} < 0.9$. The same difficulty was reported by Bradford and Thodos⁷⁶. These authors recommended using different equations for the temperature intervals $1.0 > T_{rs} \geq 0.9$ and $T_{rs} < 0.9$. They reported an average deviation

of 2.63 per cent between their equations and the experimental data for twelve hydrocarbons.

In the computational scheme previously outlined, any error in defining the saturated state is carried into the single-phase region. Unfortunately, all attempts to develop an accurate equation for the saturated vapor region of the data source have so far been unsuccessful.

In order to circumvent this difficulty, it was decided to try to use the gas branch of the critical isotherm as the reference condition rather than the saturated state which was used for $\rho_r > 1$. The saturated vapor curve and the critical isotherm coincide at the critical point. When the gaseous branch of the critical isotherm is used as a datum for the isochores, then the pressure difference $P_r - (P_r)_{T_r=1}$ gives the direction and magnitude of any departure from the critical isotherm along the isochores. If the pressure difference is negative, a test to see if $|P_r - P_{rs}| < \epsilon$ may be used to check if the specified T_r and P_r are within some small ϵ of the saturated vapor line.

Davis and Rice⁷³ derive the following equation for the gas branch of the critical isotherm

$$(P_r)_{T_r=1} = 1 - (5 - z_c^{-1})(1 - \rho_r)^4 + (4 - z_c^{-1})(1 - \rho_r)^5 \quad (5-18)$$

This equation gives pressures differing from the data source by standard errors of 0.77, 1.03 and 0.34 per cent, for z_c values of 0.25, 0.27 and 0.29, respectively. As Equation 5-18 gave better agreement with the data source than any of

the saturated vapor equations that were tried, it was used to calculate the datum for isochores when $\rho_r < 1$. There is also a computational advantage to Equation 5-18, because ρ_r is an independent variable in the proposed iterative procedure, thereby permitting explicit calculation of $(P_r)_{T_r=1}$.

5.4 (d) Single-Phase Region - Isochores

Analytical functions to approximate the pressure isochores of Figure 5-4 should satisfy the following requirements. They should yield curves which:

- (i) approach a limiting slope of one as $\rho_r \rightarrow 0$;
- (ii) are concave upward for $0 < \rho_r < 1.0$;
- (iii) become linear with a slope of $(z_c \alpha_c)^{-1}$ when $\rho_r = 1.0$;
- (iv) are concave downward for $\rho_r > 1.0$.

The functional form

$$\Delta(P_r/Z) = \Delta P_r \left(\frac{1}{z_c \alpha_c} \right)^{\rho_r} \{ G(\rho_r, z_c \alpha_c) + H(\Delta P_r, z_c \alpha_c) \} \quad (5-19)$$

where: $\Delta(P_r/Z) = P_r/Z - P_{rs}/Z_s$

and $\Delta P_r = P_r - P_{rs}$

satisfies these requirements. The function $G(\rho_r, z_c \alpha_c)$ controls the initial slope of the isochores at departure from the two-phase region. The change in slope of the isochores in the single-phase region is controlled by the function $H(\Delta P_r, z_c \alpha_c)$. Equation 5-19 gives a good approximation for the isochores with reduced densities greater than one, but is generally unsuitable for reduced densities less than one. For $\rho_r > 1.0$ it was found that for each of the three z_c values considered, the functions

$$G(\rho_r, z_c \alpha_c) = G_1 \rho_r^{1/2} + G_2 \rho_r + G_3 \rho_r^{3/2} \quad (5-20)$$

and

$$H(\Delta P_r, z_c \alpha_c) = H_1 (\Delta P_r)^{1/2} \quad (5-21)$$

give a satisfactory fit. The curvature coefficient, H_1 , was found to be invariant with $z_c \alpha_c$. It was also observed that a plot of $G(\rho_r, z_c \alpha_c)$ versus ρ_r for the three values of z_c results in three similar curves slightly displaced from each other by a distance approximately proportional to $(z_c \alpha_c)^{-1}$. Thus, it was possible to make a cross-correlation with z_c by a single coefficient G_4 , as follows:

$$G(\rho_r, z_c \alpha_c) = (G_1 \rho_r^{1/2} + G_2 \rho_r + G_3 \rho_r^{3/2}) (1 + G_4 \{(z_c \alpha_c)^{-1} - 0.53812\}) \quad (5-22)$$

Equation 5-22 simplifies to Equation 5-20 for $z_c = 0.27$ and $\alpha_c = 6.8827$, because the constant 0.53812 is the reciprocal of the product of these two parameters.

The non-linear least squares method proposed by Marquardt⁷⁷ was used to simultaneously calculate the following values of the coefficients in the functions $G(\rho_r, z_c \alpha_c)$ and $H(\Delta P_r, z_c \alpha_c)$ of Equation 5-19:

$$G_1 = 5.07301 \quad G_2 = -5.37068 \quad G_3 = 1.66199$$

$$G_4 = 5.47736 \quad H_1 = 0.042744$$

Table 5-1 makes a comparison of the fit obtained with these coefficients with respect to the 564 data points from which they were derived. Every point was given the same weighting, irrespective of its z_c value.

For the gaseous region, $0 < \rho_r < 1.0$, the slopes of the

TABLE 5-1
COMPARISON OF CALCULATED DENSITIES
WITH THE DATA SOURCE

ρ_r	z_c	No. of Points	T_r Range	P_r Range	Standard Error %		
					Average	Maximum	Points > 1.0%
>1	0.25	155	0.3 to 1.0	0.1 to 30.0	0.53	1.87	14
>1	0.27	254	0.3 to 3.0	0.1 to 30.0	0.77	3.53	38
>1	0.29	155	0.3 to 1.0	0.1 to 30.0	0.55	3.02	11
		564			0.65		
							Points > 2.0%
<1	0.25	104	1.0 to 2.0	0.1 to 1.15	2.40	18.31	16
<1	0.27	157	1.0 to 2.0	0.1 to 7.00	2.20	6.93	43
<1	0.29	104	1.0 to 2.0	0.1 to 1.15	2.03	15.20	15

isochores at departure from the two-phase region, or from the critical isotherm, were found to be a near linear function of density between the limiting values of one and $(z_c \alpha_c)^{-1}$. However, the change in the slope of the isochores with ΔP_r was more difficult to determine and approximate. Some of the difficulty rests with the data source, inasmuch as the data for $T_r > 2$, corresponding to large ΔP_r , were found to be rather scattered. Several functional forms were tried, but none were appreciably better than the following simple expression

$$\Delta(P_r/Z) = \frac{P_r - (P_r)_{T_r=1}}{1 + (z_c \alpha_c - 1) \rho_r^{0.8 + 0.05(P_r - (P_r)_{T_r=1})}} \quad (5-23)$$

A comparison of Equation 5-23 with the data source is also presented in Table 5-1.

5.4 (e) Discussion

A pictorial comparison of the analytical functions and the data source is given for the case $z_c = 0.27$ in Figure 5-5. A discrepancy with the data source occurs when the dots do not coincide with the intersections of the isotherms and isobars. Plotting PVT data on these coordinates represents a severe test of the data, because Z appears as the ordinate as well as in the denominator of the expression for the abscissa. Points from the data source for $T_r > 2$ were not plotted because they exhibited considerable scatter on this diagram.

An analogy between the compressibility factor diagrams associated with density-explicit and density-implicit formulations can be made. A conventional compressibility factor

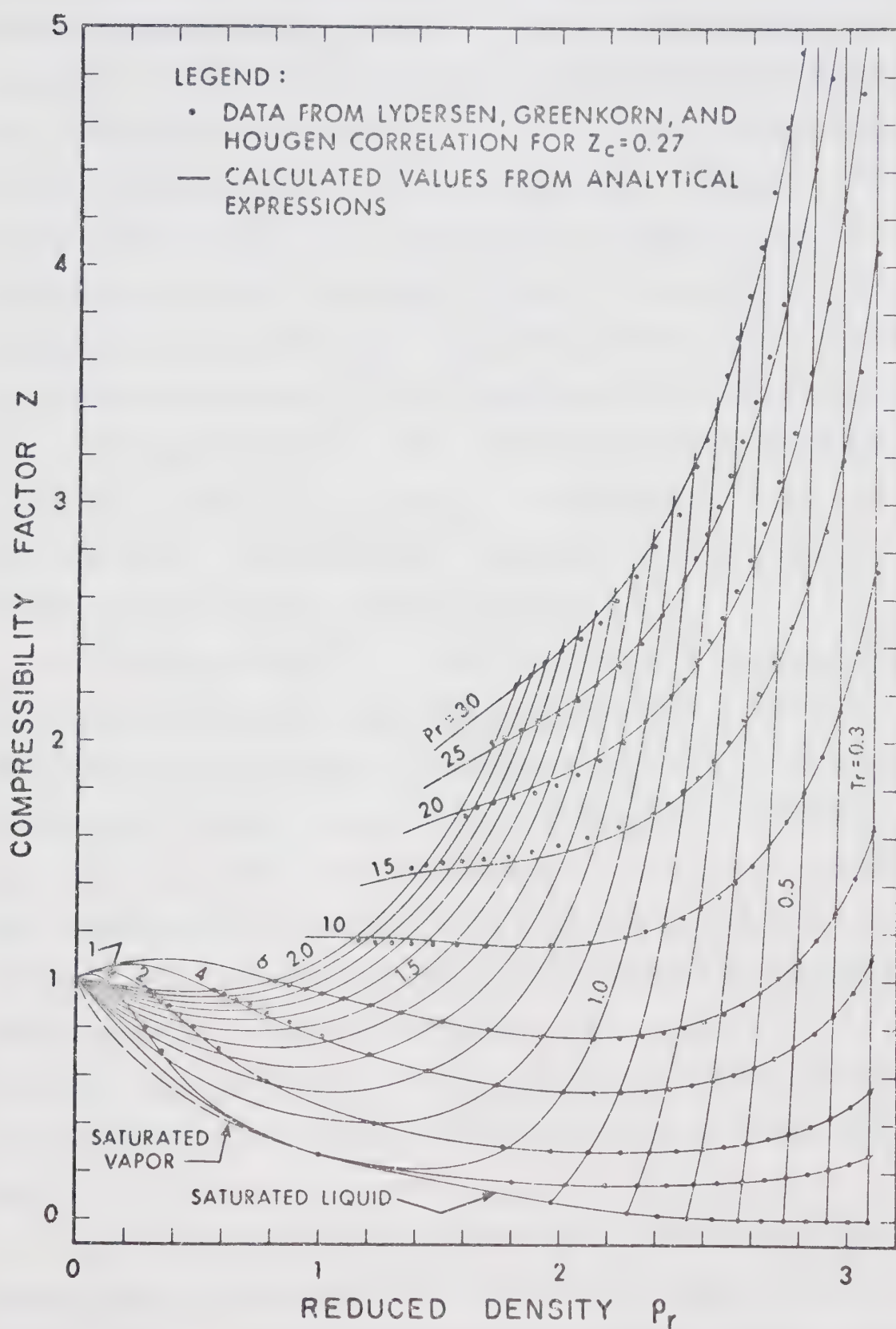


Figure 5-5. Compressibility Factor Diagram for the Lydersen, Greenkorn and Hougen Correlation.

diagram in which the dependent variable, Z , is the ordinate and the independent variables, P_r and T_r , are abscissa and parameter, respectively, reflects a density-explicit formulation. The chart is used only once to read the Z factor corresponding to the values of the independent variables. The coordinates of Figure 5-5 correspond to a density-implicit formulation in which the chart is read at every trial while converging to the solution. An initial value of Z is assumed so that an estimate of the independent variable ρ_r can be made using Equation 5-7. Then using independent variables of either ρ_r and P_r or ρ_r and T_r , a new value of Z is read from the chart. Based on this value, a better estimate of density is made and the process repeated.

Reid and Sherwood⁷⁵, in reviewing various corresponding states methods for calculating liquid densities, found the Lydersen et al. correlation to compare favorably with other methods, and to have an accuracy of about 2 to 5 per cent. For densities greater than the critical, the present formulation approximates the correlation with a standard error of 0.65 per cent, and can therefore be considered an analytical representation of the tabular data. It is important to note that this standard error is with respect to the normal independent variables P_r and T_r , as ρ_r is always obtained from Equation 5-7.

For reduced densities less than one, the present functions should be considered as a qualitative representation of the tables. A satisfactory representation for this region hinges upon developing a suitable saturated vapor equation,

and either smoothing the data for $T_r > 2$ or supplementing them with some additional data. The pressure range covered by the data source for Z_c values of 0.25 and 0.29 is too small to permit development of a cross-correlation with Z_c .

5.4 (f) Conclusions

A general method for developing an equation of state for a pure substance has been presented. The method has a good theoretical basis, and is capable of representing a wide range of densities with a minimum number of constants. Application of the method to the raw data for various substances will assist in developing better equations for the isochores of Figure 5-4. It will also help to give a better understanding of the cross-correlations with Z_c and α_c .

The method illustrates the need for more than one correlating parameter in corresponding states treatments. The critical compressibility factor has been shown^{31, 76} to be a good correlating parameter for the saturated vapor and liquid regions. It is also required to define the critical point. Riedel's factor is related to the slope of the isochores, and is fundamental to vapor pressure calculations using Equation 5-16.

Additional experience with the method, and the development of more accurate equations for the saturated vapor state will permit calculation of thermodynamic properties. In this connection the reciprocal feature illustrated in Figure 5-4, which shows the ability to express the isochores in their temperature-explicit or their pressure-explicit forms, will simplify the calculations.

A FORTRAN computer subroutine is given in Appendix C to solve the density-implicit form $f(z_c, \alpha_c, \rho_r, P_r) = 0$ by the method outlined in the text. The subroutine is used to calculate the density of the liquid-phase in the computer program developed to simulate the depletion of a constant volume reservoir.

5.5 Application of Some Reduced Equations of State to the Standing and Katz Correlation

The compressibility factor chart of Brown and Holcomb⁷⁸ was revised and extended by Standing and Katz³⁰ based on the density data from sixteen saturated multicomponent gases and a comparison with pure methane data. The correlation is presented in chart form with independent variables of pseudo-reduced pressure and pseudo-reduced temperature. Pseudo-critical properties based on Kay's Rule⁷⁹ were used to calculate the pseudo-reduced pressure

$$p_r^P = P / \sum_{i=1}^n y_i (P_c)_i \quad (5-24)$$

and the pseudo-reduced temperature

$$p_r^T = T / \sum_{i=1}^n y_i (T_c)_i \quad (5-25)$$

The correlation only applies to the vapor phase since pseudo-critical properties are not suitable correlating parameters in the vicinity of the critical point. The lowest pseudo-reduced temperature covered by the correlation is 1.05.

The Standing and Katz correlation has received wide acceptance and usage by the petroleum industry. The correlation has also been used to evaluate several commonly used integrals

for calculating gas flows^{80, 81}. Trube⁸² used the correlation to prepare a chart for the pseudo-reduced coefficient of compressibility, C_r , defined as

$$C_r = P_r^{-1} - z^{-1} \left(\frac{\partial z}{\partial P_r} \right)_{T_r} \quad (5-26)$$

Trube noted that it was progressively more difficult to estimate the values of the derivative as the critical temperature was approached.

A tabular form⁸³ of the Standing and Katz correlation was used to calculate pseudo-reduced densities at regular intervals from the relation

$$\rho_r = 0.27 P_r / (z T_r) \quad (5-27)$$

The value of $z_c = 0.27$ was arbitrary, but was considered representative of mixtures comprised chiefly of methane. Figure 5-6 is a plot of compressibility factor versus pseudo-reduced density and pseudo-reduced temperature. It should be noted that the isotherms for $T_r > 1.2$ plot as smooth curves, but that there are anomalous departures in the $T_r = 1.05, 1.10$ and 1.15 isotherms. These departures occur in the vicinity of the critical and may be due to experimental difficulties or more probably due to the failure of Kay's rule to correlate the data. Whatever the cause of the anomalies, it is apparent that a reduced form of an equation of state could not be expected to satisfactorily represent these isotherms. Hence, smooth and continuous curves were drawn for these isotherms and smoothed values obtained for analytical representation of the correlation.

The Benedict, Webb and Rubin⁶² (B-W-R) equation of

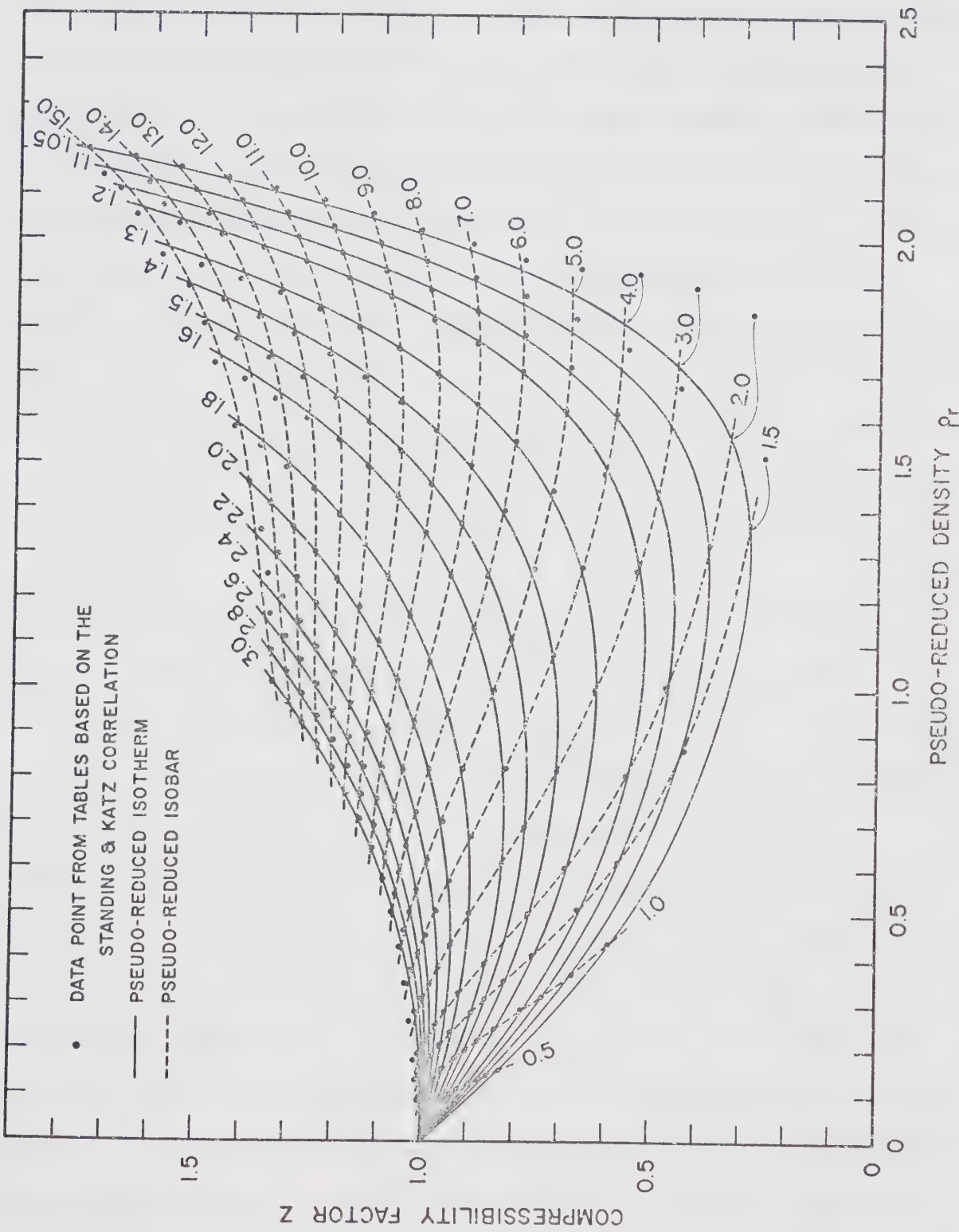


Figure 5-6. Compressibility Factor Diagram for the Standing and Katz Correlation.

state has been widely used to correlate the volumetric and thermodynamic properties of pure materials. Benedict et al. also proposed mixing rules for the eight coefficients in the equation so that it could be applied to gas mixtures. To apply the B-W-R equation to the Standing and Katz correlation the tabular data of reference 83 were treated as though they were reduced experimental data for a pure component. Since the correlation is in terms of the compressibility factor, the following form of the B-W-R equation was used to fit the data

$$Z = 1 + (A_1 + A_2/T_r + A_3/T_r^3) \rho_r + (A_4 + A_5/T_r) \rho_r^2 + A_5 A_6 \rho_r^5/T_r + A_7 \rho_r^2/T_r^3 (1 + A_8 \rho_r^2) \exp(-A_8 \rho_r^2) \quad (5-28)$$

The non-linear least squares method of Marquardt⁷⁷ was used to calculate the following values of the coefficients

$$\begin{array}{lll} A_1 = 0.31506237 & A_2 = -1.0467099 & A_3 = -0.57832727 \\ A_4 = 0.53530771 & A_5 = -0.61232032 & A_6 = -0.10488813 \\ A_7 = 0.68157001 & A_8 = 0.68446549 & \end{array}$$

These coefficients were obtained by minimizing the relative error in Z . When the independent variables are ρ_r and T_r the standard error in Z is 0.0101, or 0.87 per cent. When the normal independent variables of P_r and T_r are used with Equation 5-27 the standard error in Z is 0.00445, or 0.54 per cent with respect to the 1500 data points used to determine the coefficients. As with any equation of state, the region in the vicinity of the critical point is subject to the largest errors. The largest deviation was 7.15 per cent at the

point $T_r = 1.05$ and $P_r = 1.30$. There were six other points in this region where the correlation and the B-W-R approximation differed by more than two per cent. Since Trube⁸² had difficulty evaluating the pseudo-reduced coefficient of compressibility in this region it is likely that some of the discrepancies are inherent in the correlation. The Standing and Katz correlation was compared with some data not used in its development and was found to be accurate within 1.2 per cent⁸⁴. Thus, except for a small region along the $T_r = 1.05$ and 1.10 isotherms the B-W-R approximation gives an acceptable analytical representation of the correlation. A FORTRAN subroutine called ZKATZ is given in Appendix C for calculating vapor phase densities using Equations 5-27 and 5-28.

An attempt was made to improve the analytical representation in the region of the critical point. The approach used was based on the temperature isochoric diagram illustrated in Figure 5-2. The diagram suggests that any isotherm can be used as a datum for the isochores. Since the $T_r = 1.05$ isotherm had the largest discrepancies it was selected to be the datum and was fit to the B-W-R equation independent of the other isotherms. When Equation 5-28 is applied to a single isotherm it simplifies to the following expression.

$$Z = 1 + B_1 \rho_r + B_2 \rho_r^2 + B_3 \rho_r^5 + B_4 \rho_r^2 (1 + B_5 \rho_r^2) \exp(-B_5 \rho_r^2) \quad (5-29)$$

The following values of the coefficients

$$\begin{array}{lll} B_1 = -1.14078 & B_2 = -0.639247 & B_3 = 0.086445 \\ B_4 = 1.10566 & B_5 = 0.455115 & \end{array}$$

fit the 78 smoothed points from the $T_r = 1.05$ isotherm of the correlation with a standard error in Z of 0.0056, or 1.15 per cent. The largest discrepancy was 3.92 per cent which suggests faulty data since the B-W-R equation is capable of representing a single isotherm with much better accuracy.

With $T_r = 1.05$ taken as a datum for the isochores the temperature dependence for the product ZT_r is given by the following rearrangement of the B-W-R equation

$$ZT_r = (ZT_r)_{T_r=1.05} + (T_r - 1.05) (1 + B_6 \rho_r + B_7 \rho_r^2) \left(\frac{1}{T_r^2} - \frac{1}{1.05^2} \right) (B_8 \rho_r + B_9 \rho_r^2 (1 + B_{10} \rho_r^2) \exp(-B_{10} \rho_r^2)) \quad (5-30)$$

To evaluate the five constants in Equation 5-30, the appropriate values for $(ZT_r)_{T_r=1.05}$ were obtained by simply multiplying both sides of Equation 5-29 by 1.05. The following values for the coefficients were obtained by minimizing the relative error in ZT_r .

$$\begin{array}{lll} B_6 = 0.325610 & B_7 = 0.516982 & B_8 = -0.351376 \\ B_9 = 0.322333 & B_{10} = -0.270319 & \end{array}$$

With independent variables of ρ_r and T_r the standard error in ZT_r was 0.0215, or some 1.13 per cent. Thus, the approximation was not as accurate as Equation 5-28. However, the maximum error was reduced from 7.15 per cent for Equation 5-28 to 3.92 per cent for Equation 5-30. This slight advantage was not considered worthwhile in view of the two additional coefficients and the additional exponential term which were required in order to attain it.

The Standing and Katz correlation was also approximated

with the Martin and Hou⁷⁰ equation and various virial type equations of state. Although the results were encouraging, as many as 16 coefficients were required to obtain accuracy comparable with that of the B-W-R equation. Therefore, these equations were not pursued further.

5.6 Application of Some Reduced Equations of State to the Rowlinson Correlation

Rowlinson⁸⁵ presented a compressibility factor correlation based on some PVT data for the inert gases (neon, argon and xenon). The tabular correlation is a two-parameter corresponding states approach which uses the critical temperature and critical pressure for "reducing" the experimental values of Z . However, unlike most corresponding states correlations, Rowlinson used independent variables of reduced temperature and pseudo-reduced density defined by

$$\rho_r = 0.293 \frac{RT_c}{(P_c V)} \quad (5-31)$$

The utility of the correlation lies in the fact that it can be extended to other gases, with non-spherical molecules, by a single parameter, δ_c , which characterizes the effects of orientational forces between molecules. An approximate relationship between the parameter δ_c and Pitzer's⁶⁸ acentric factor is given by

$$\delta_c = \omega/2.4 \quad (5-32)$$

Rowlinson⁸⁶ showed that δ_c can be evaluated from a variety of data, including: vapor pressure, second virial coefficient, surface tension, Trouton's constant, heat capacity and rectilinear diameter. To use the correlation for a gas, with

non-spherical molecules, the apparent-reduced temperature, T_r' , and apparent-reduced density, ρ_r' , are obtained from the relations

$$T_r' = T_r - 2\delta_c(1 - T_r) \quad (5-33)$$

$$\rho_r' = \rho_r - \rho_r \delta_c (T_r^{-1} - 1) \quad (5-34)$$

These modified independent variables are then used to obtain Z directly from the tabular correlation.

Since Rowlinson's correlation was presented in terms of T_r and ρ_r , it is a convenient data source for comparing the relative accuracy of various equations of state. Some of the classical two-parameter equations of state were fitted to the correlation and the results are presented in Appendix B. The Redlich-Kwong equation was found to give the best approximation with a standard error of 1.92 per cent and a maximum error of 7.9 per cent.

The two-parameter equations did not yield the desired accuracy so equations with more coefficients were tried.

The following form of the Beattie-Bridgeman⁶¹ equation was used to approximate the correlation.

$$Z = 1 + (A_1 + A_2/T_r + A_3/T_r^3) \rho_r + (A_1 A_4 + A_2 A_5/T_r + A_1 A_3/T_r^3) \rho_r^2 + A_1 A_2 A_4 (\rho_r/T_r)^3 \quad (5-35)$$

The values of the coefficients obtained by minimizing the absolute error in Z were

$$A_1 = 0.5760164 \quad A_2 = -1.6027386 \quad A_3 = -0.07447406$$

$$A_4 = 0.1551410 \quad A_5 = -0.2115189$$

These coefficients give a standard error in Z of 0.0086, or

1.4 per cent, with a maximum error of 11.4 per cent at the point $p_r = 1.5$ on the critical isotherm. The Beattie-Bridgeman equation did not fit the critical isotherm as well as the Redlich-Kwong equation.

Next, the B-W-R equation was used to approximate the correlation. The following coefficients were obtained for Equation 5-28 by minimizing the relative error in Z .

$$\begin{array}{lll} A_1 = 0.3655669 & A_2 = -0.9993822 & A_3 = -0.5566062 \\ A_4 = 0.3538158 & A_5 = -0.4432745 & A_6 = -0.1024061 \\ A_7 = 0.5854692 & A_8 = 0.5468492 & \end{array}$$

These coefficients resulted in a standard error in Z of 0.651 per cent with a maximum error of 3.3 per cent. A pictorial comparison of this approximation with the correlation is made in Figure 5-7. The largest discrepancies occur along the high temperature isotherms ($T_r > 2.5$). A FORTRAN subroutine called ZROWL is given in Appendix C which can be used to calculate fluid densities from Equations 5-28 and 5-31.

The B-W-R approximation of the critical region of Rowlinson's correlation was much better than it was for the Standing and Katz correlation. It may be recalled that the $T_r = 1.05$ isotherm was taken as a datum for that correlation in a procedure to reduce the maximum errors. The same procedure was applied to Rowlinson's correlation only the critical isotherm was taken as the datum. In this case the more complex ten coefficient modification of the B-W-R equation resulted in slightly larger maximum errors. This result might have been anticipated since the B-W-R equation gave a good approximation in the vicinity of the critical. When

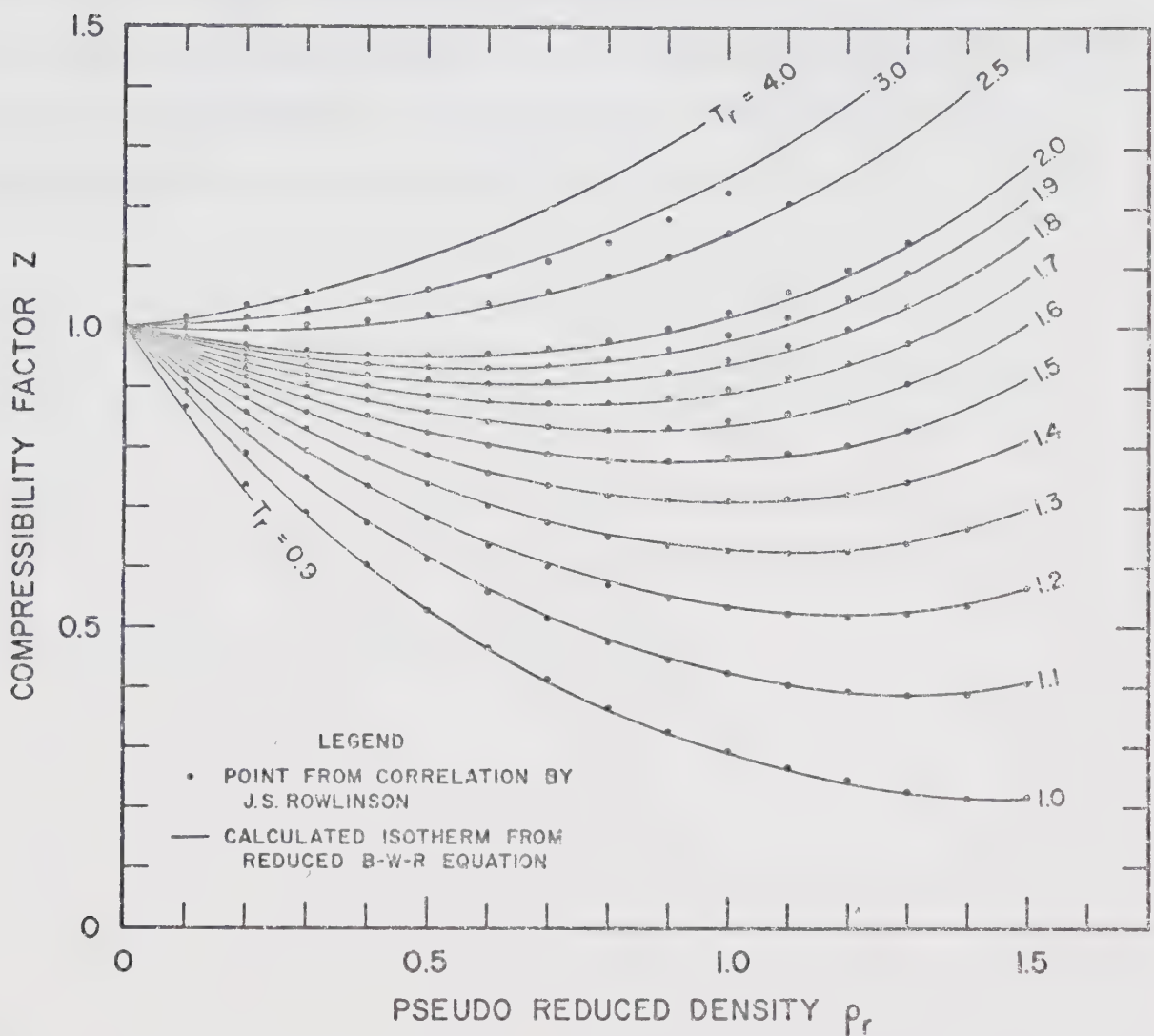


Figure 5-7. Compressibility Factor Diagram for the Rowlinson Correlation.

the B-W-R equation is applied in two stages, the coefficients become correlated since two separate objective functions are minimized. This problem can be avoided by evaluating the ten coefficients in Equation 5-30 simultaneously. One attempt was made at evaluating the coefficients simultaneously, however, the convergence was extremely slow and the cost of computing time did not justify further runs.

Chapter 6. SIMULATION OF EXPERIMENTAL RESULTS AND SELECTED LITERATURE DATA

6.1 Foreword

This chapter discusses computer simulation results for the depletion of a constant volume retrograde reservoir by vapor production. A computer model was developed which directly simulates the laboratory procedure described in section 2.4 for the depletion of the unpacked cell. The computer model and the experimental procedure both approximate the isothermal depletion process by a series of equilibrium flashes. The phase behavior portion of the computer model was described in Chapter 4 and the phase density portion was discussed in Chapter 5. A FORTRAN listing of the program is given in Appendix D.

6.2 Simulation of Experimental Results

The composition and density of the coexisting phases of equilibrium binary mixtures are fixed by specifying the system temperature and pressure. Thus, the volume per cent retrograde liquid is the only characteristic which is free to vary during the isothermal depletion of binary mixtures having different initial compositions. It may be recalled that experimental and calculated retrograde liquid volumes were compared in Tables 3-2, 3-3 and 3-4 of Chapter 3. The agreement between experimental and calculated retrograde liquid volumes was satisfactory considering that errors at any flash are carried forward in both the experimental procedure and the computer simulation.

The following sections discuss the computer model

approximations for K-values and phase densities of the binary mixtures used in the experiments.

6.2 (a) Methane and n-Butane Mixtures

The computer printout for the simulation of Run 4 is reproduced in Table 6-1. The first part of the print out is an echo check of some pure component data used in the calculations. The starting composition was 0.864 mole fraction methane and the first two flash calculations at 2000 psia and 1750 psia indicate the system to be in the single-phase region. The flash at 1500 psia results in two phases with a retrograde liquid volume of 0.91 per cent. The calculated K-values were 1.882 for methane and 0.249 for n-butane. At 1500 psia the vapor and liquid phase densities were calculated to be $0.138 \text{ ft.}^3/\text{lb.}$ and $0.0407 \text{ ft.}^3/\text{lb.}$, respectively. The results of flash calculations are presented at regular intervals in Table 6-1. The flash at 600 psia was the last to remain in the two-phase region. The computer print out for the other experimental runs with methane and n-butane are presented in Tables E-1 and E-2 of Appendix E.

Extensive data for the coexisting phases of the methane and n-butane system have been reported by Sage, Hicks and Lacey³². The simulation results can be directly compared with these data, since the phase rule requires that the composition and density of coexisting phases be invariant with system composition. The phase compositions were previously compared with published data in Figure 3-1. A comparison of the calculated K-values with those of Sage et al. is made in Figure 6-1. The close agreement for methane results from applying

TABLE 6-1

RUN NO. 4, METHANE AND N-BUTANE AT 100 F.
DEPLETION OF A CONSTANT VOLUME RESERVOIR BY VAPOR PRODUCTION

PURE COMPONENT DATA								
COMP	MOLE WT LB/MOLE	PC PSIA	VC FT**3	TC DEG R	ZC	PITZER OMEGA	RIEDEL ALPHA	
C1	16.042	669.7	1.590	343.13	0.282	0.000	5.860	
C4	58.120	550.7	4.080	765.29	0.274	0.195	6.770	
SIMULATED DEPLETION PERFORMANCE								
COMP	SYSTEM COMP	VAPOR COMP	LIQUID COMP	K VALUE	P, PK PSIA	LIO VOL %	VAPOR† CF/LB	LIQUID† CF/LB
C1	0.864	0.854	0.000	1.000	2000.	0.00	0.097	0.0000
C4	0.136	0.136	0.000	1.000				
MOLES	0.471	0.471	0.000		1912.	**		
C1	0.862	0.863	0.000	1.000	1750.	0.00	0.113	0.0000
C4	0.135	0.135	0.000	1.000				
MOLES	0.406	0.406	0.000		1934.			
C1	0.863	0.869	0.477	1.822	1500.	0.91	0.138	0.0407
C4	0.135	0.130	0.522	0.249				
MOLES	0.338	0.332	0.005		1934.			
C1	0.862	0.878	0.396	2.217	1250.	1.70	0.178	0.0373
C4	0.137	0.121	0.603	0.201				
MOLES	0.271	0.260	0.011		1934.			
C1	0.859	0.877	0.317	2.767	1000.	1.42	0.232	0.0348
C4	0.140	0.122	0.682	0.178				
MOLES	0.208	0.199	0.009		1934.			
C1	0.853	0.872	0.253	3.442	800.	1.01	0.298	0.0331
C4	0.146	0.127	0.746	0.170				
MOLES	0.161	0.154	0.006		1934.			
C1	0.847	0.858	0.188	4.554	600.	0.41	0.401	0.0318
C4	0.152	0.141	0.811	0.174				
MOLES	0.115	0.112	0.002		1934.			

† Cubic feet per pound, CF/LB

* System pressure, P

** Convergence pressure, P_K

TABLE 6-1 (CONT.)

RUN NO. 4, METHANE AND N-BUTANE AT 100 F.

SIMULATED DEPLETION PERFORMANCE									
COMP	SYSTEM COMP	VAPOR COMP	LIQUID COMP	K VALUE	P, PK PSIA	LIQ VOL %	VAPOR CF/LB	LIQUID CF/LB	
C1	0.843	0.843	0.000	1.000	400.	0.00	0.608	0.0000	
C4	0.156	0.156	0.000	1.000					
MOLES	0.072	0.072	0.000		1934.				
C1	0.843	0.843	0.000	1.000	200.	0.00	1.272	0.0000	
C4	0.156	0.156	0.000	1.000					
MOLES	0.034	0.034	0.000		1934.				
C1	0.843	0.843	0.000	1.000	150.	0.00	1.714	0.0000	
C4	0.156	0.156	0.000	1.000					
MOLES	0.025	0.025	0.000		1934.				

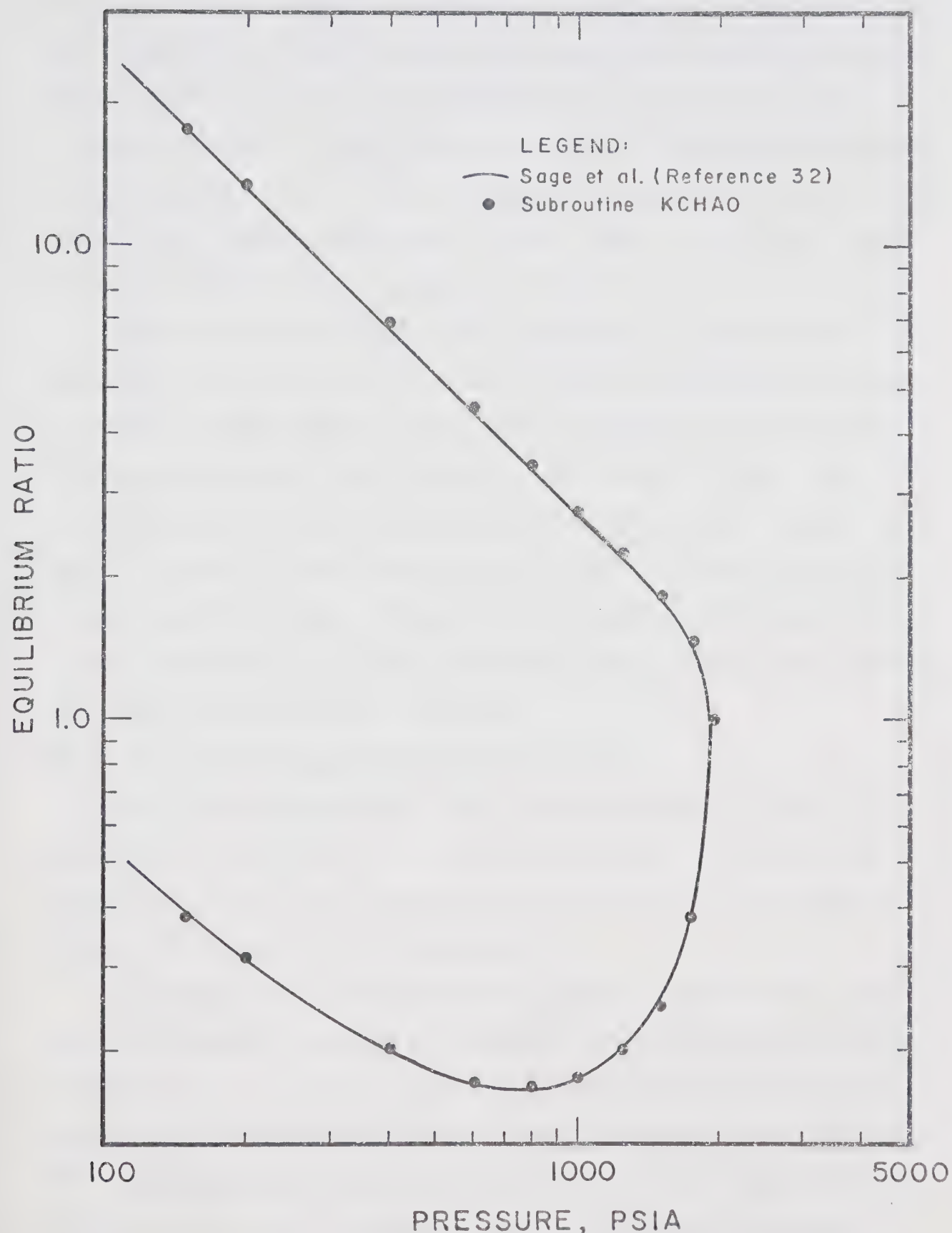


Figure 6-1. Comparison of Calculated and Literature Equilibrium Ratios for the Methane-n-Butane System at 100°F.

the correction ratios discussed in Section 4.4 and illustrated in Figure 4-3. The K-values for methane and n-butane at pressures above 1250 psia were obtained by extrapolating Chao-Seader K-values at lower pressures to the convergence pressure using Equation 4-12. The convergence pressure was calculated to be 1934 psia by subroutine CPRES, some 22 psi higher than the experimental value reported in reference 32.

Vapor phase densities are calculated in the computer model by subroutine ZKATZ and are used to determine the moles of vapor removed between equilibrium flashes. Liquid phase densities are obtained from subroutine COMPZ and are used to calculate the volume of retrograde liquid at each flash. Figure 6-2 makes a comparison of the calculated phase densities with literature data. There is a systematic discrepancy in liquid phase density which increases with pressure and amounts to about 8 per cent at 1750 psia.

6.2 (b) Methane and n-Pentane Mixtures

The computer printout for the simulation of Run 3 is reproduced in Table 6-2. Simulation results for the seven other runs, with the methane-n-pentane system, are given in Tables E-3 through E-9 of Appendix E.

A comparison of the calculated phase compositions with the experimental results and published data was presented in Figure 3-3. A comparison is made in Figure 6-3 between the calculated K-values and those of Sage, Reamer, Olds and Lacey³³. The excellent agreement of methane K-values was attributed to using the correction ratios presented in Figure 4-3. The discrepancies in the n-pentane K-values may be

LIQUID VOLUME, Cu. Ft./Lb.

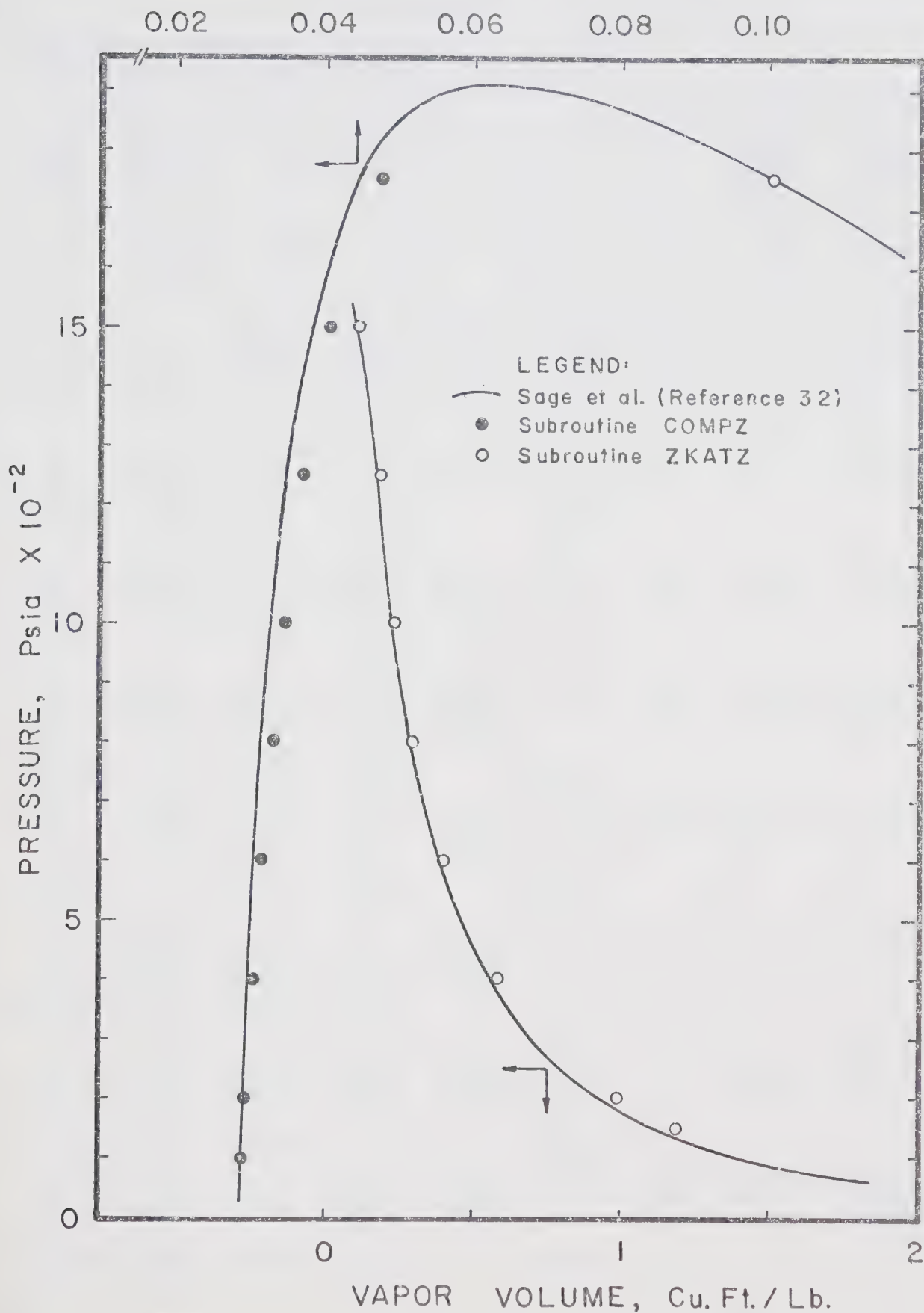


Figure 6-2. Comparison of Calculated and Literature Phase Densities for the Methane-n-Butane System at 100°F.

TABLE 6-2

RUN NO. 3, METHANE AND N-PENTANE AT 100 F.
DEPLETION OF A CONSTANT VOLUME RESERVOIR BY VAPOR PRODUCTION

PURE COMPONENT DATA							
COMP	MOLE WT LB/MOLE	PC PSIA	VC FT**3	TC DEG R	ZC	PITZER OMEGA	RIEDEL ALPHA
C1	16.042	669.7	1.590	343.13	0.288	0.000	5.860
C5	72.146	487.3	4.730	845.08	0.254	0.238	7.030
SIMULATED DEPLETION PERFORMANCE							
COMP	SYSTEM COMP	VAPOR COMP	LIQUID COMP	K VALUE	P, PK PSIA VOL %	VAPOR CF/LB	LIQUID CF/LB
C1	0.935	0.935	0.000	1.000	3100.	0.00	0.078
C5	0.065	0.065	0.000	1.000			0.0000
MOLES	0.649	0.649	0.000		2409.		
C1	0.934	0.934	0.000	1.000	2500.	0.00	0.093
C5	0.064	0.064	0.000	1.000			0.0000
MOLES	0.541	0.541	0.000		2409.		
C1	0.934	0.934	0.000	1.000	2000.	0.00	0.117
C5	0.064	0.064	0.000	1.000			0.0000
MOLES	0.432	0.432	0.000		2409.		
C1	0.934	0.940	0.513	1.831	1750.	0.90	0.139
C5	0.064	0.059	0.486	0.121			0.0355
MOLES	0.372	0.366	0.005		2409.		
C1	0.934	0.945	0.446	2.116	1500.	1.36	0.169
C5	0.065	0.054	0.553	0.098			0.0331
MOLES	0.312	0.304	0.008		2409.		
C1	0.931	0.949	0.379	2.502	1250.	1.51	0.212
C5	0.068	0.050	0.620	0.081			0.0312
MOLES	0.254	0.245	0.009		2409.		
C1	0.927	0.951	0.309	3.072	1000.	1.50	0.276
C5	0.072	0.048	0.690	0.070			0.0296
MOLES	0.198	0.189	0.009		2409.		

TABLE 6-2 (CONT.)

RUN NO. 3, METHANE AND N-PENTANE AT 100 F.

SIMULATED DEPLETION PERFORMANCE								
COMP	SYSTEM COMP	VAPOR COMP	LIQUID COMP	K VALUE	P, PK PSIA	LIQ VOL %	VAPOR CF/LB	LIQUID CF/LB
C1	0.921	0.951	0.251	3.779	800.	1.39	0.355	0.0284
C5	0.078	0.048	0.748	0.065				
MOLES	0.156	0.147	0.008		2409.			
C1	0.913	0.947	0.191	4.951	600.	1.20	0.482	0.0274
C5	0.086	0.052	0.808	0.064				
MOLES	0.115	0.107	0.007		2409.			
C1	0.900	0.937	0.128	7.288	400.	0.90	0.721	0.0264
C5	0.099	0.062	0.871	0.071				
MOLES	0.075	0.070	0.005		2409.			
C1	0.881	0.900	0.063	14.282	200.	0.30	1.340	0.0256
C5	0.118	0.099	0.936	0.105				
MOLES	0.036	0.034	0.001		2409.			
C1	0.860	0.875	0.046	18.936	150.	0.11	1.685	0.0254
C5	0.139	0.124	0.953	0.130				
MOLES	0.026	0.025	0.000		2409.			
C1	0.854	0.854	0.000	1.000	100.	0.00	2.428	0.0000
C5	0.145	0.145	0.000	1.000				
MOLES	0.017	0.017	0.000		2409.			
C1	0.854	0.854	0.000	1.000	80.	0.00	3.049	0.0000
C5	0.145	0.145	0.000	1.000				
MOLES	0.013	0.013	0.000		2409.			
C1	0.854	0.854	0.000	1.000	60.	0.00	4.084	0.0000
C5	0.145	0.145	0.000	1.000				
MOLES	0.010	0.010	0.000		2409.			
C1	0.854	0.854	0.000	1.000	40.	0.00	6.153	0.0000
C5	0.145	0.145	0.000	1.000				
MOLES	0.006	0.006	0.000		2409.			

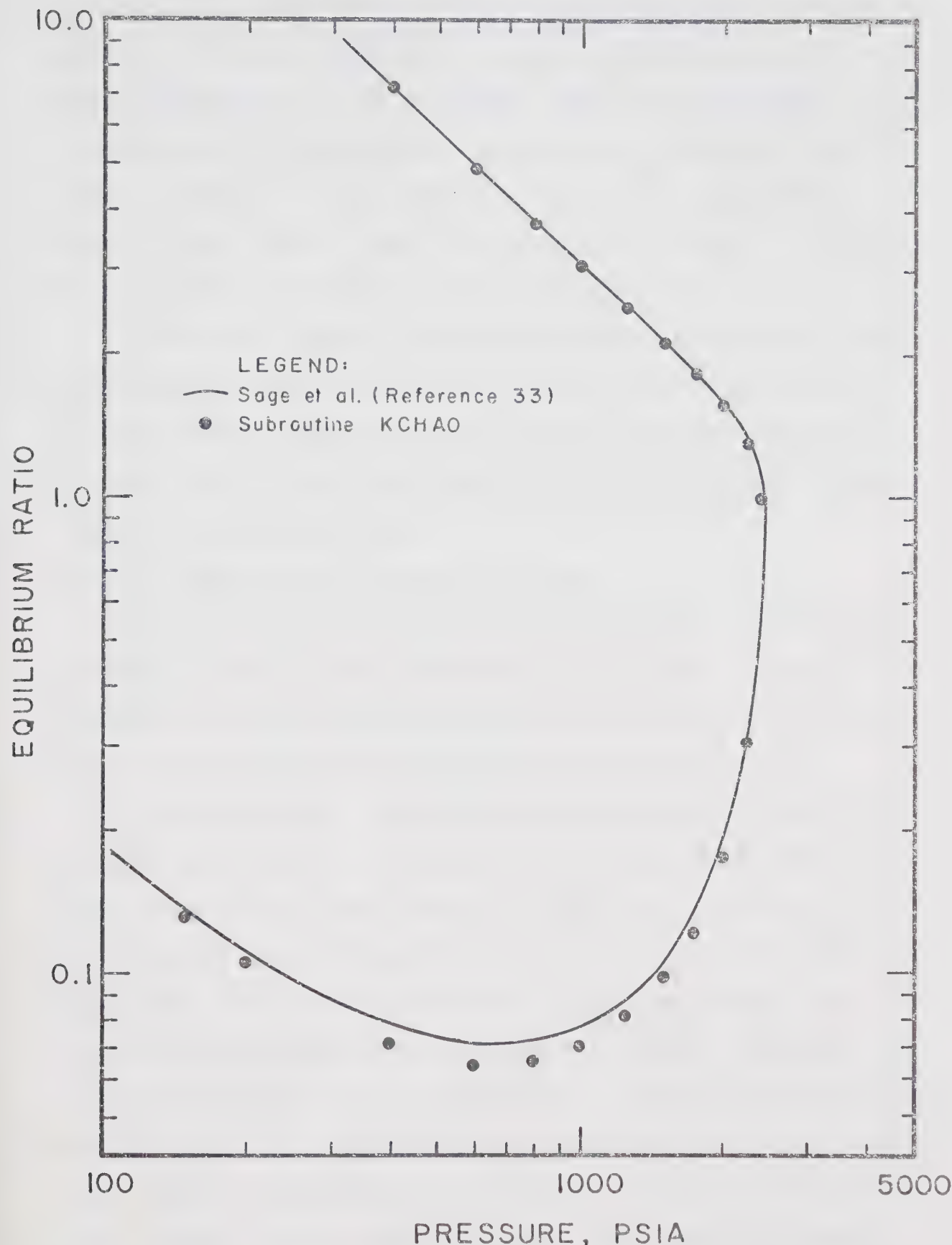


Figure 6-3. Comparison of Calculated and Literature Equilibrium Ratios for the Methane-n-Pentane System at 100°F.

caused by failure of the Redlich-Kwong equation to correctly predict the vapor phase fugacity coefficients in the Chao-Seader correlation. On the other hand, the calculated K-values result in vapor phase compositions which are about midway between those of Sage et al. and the experimental results of this work. Thus, there is some evidence to indicate that the data of Sage et al. may be in error.

Figure 6-4 makes a comparison between calculated phase densities and literature data. There is a systematic discrepancy which increases with pressure. The discrepancy at 2250 psia is 11.3 per cent for the liquid phase and 5.7 per cent for the vapor phase.

6.2 (c) Methane and n-Hexane Mixture

The print out for the computer simulation of the experimental run with methane and n-hexane is given in Table 6-3. The calculated critical pressure was 2852 psia, some 50 psi less than the value estimated by Poston and McKetta³⁵.

A comparison of calculated phase compositions with literature data was made in Figure 3-5 of Chapter 3. The calculated compositions and K-values differ from literature data at pressures below 200 psia, and at pressures above 2000 psia. The use of the correction ratios from Figure 4-3 forced good agreement between methane K-values, however, the calculated K-values for hexane deviate considerably from literature data. The discrepancy in convergence pressure would cause some of the difference in hexane K-values at high pressure. There is also the possibility that the vapor phase compositions of reference 25 are in error at high pressures.

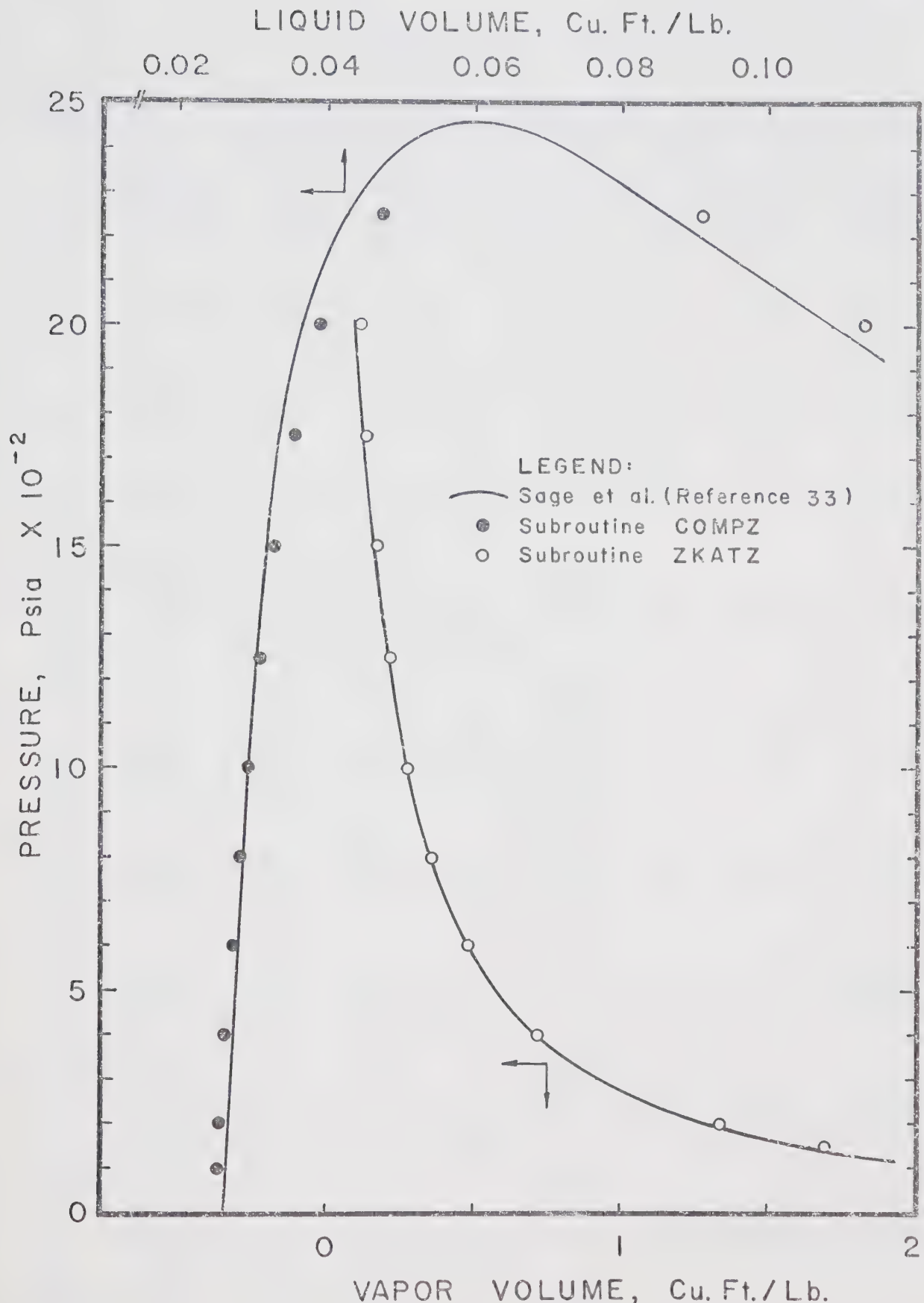


Figure 6-4. Comparison of Calculated and Literature Phase Densities for the Methane-n-Pentane System at 100°F.

TABLE 6-3

RUN NO. 7, METHANE AND N-HEXANE AT 100 F.
DEPLETION OF A CONSTANT VOLUME RESERVOIR BY VAPOR PRODUCTION

PURE COMPONENT DATA								
COMP	MOLE WT LB/MOLE	PC PSIA	VC FT**3	TC DEG R	ZC	PITZER OMEGA	RIEDEL ALPHA	
C1	16.042	669.7	1.590	343.13	0.288	0.000	5.260	
C6	86.172	436.6	5.930	913.14	0.264	0.292	7.270	
SIMULATED DEPLETION PERFORMANCE								
COMP	SYSTEM COMP	VAPOR COMP	LIQUID COMP	K VALUE	P, PK PSIA	LIQ VOL %	VAPOR CF/LB	LIQUID CF/LB
C1	0.930	0.930	0.000	1.000	3000.	0.00	0.074	0.0000
C6	0.070	0.070	0.000	1.000				
MOLES	0.643	0.643	0.000		2352.			
C1	0.929	0.940	0.762	1.232	2750.	5.81	0.083	0.0479
C6	0.070	0.059	0.237	0.252				
MOLES	0.594	0.557	0.037		2852.			
C1	0.929	0.952	0.633	1.505	2500.	7.02	0.097	0.0380
C6	0.070	0.047	0.366	0.128				
MOLES	0.539	0.495	0.044		2852.			
C1	0.926	0.964	0.563	1.711	2250.	8.25	0.114	0.0349
C6	0.073	0.035	0.436	0.081				
MOLES	0.483	0.432	0.050		2852.			
C1	0.922	0.971	0.508	1.911	2000.	8.58	0.134	0.0331
C6	0.077	0.028	0.491	0.052				
MOLES	0.428	0.377	0.051		2852.			
C1	0.916	0.973	0.457	2.128	1750.	8.24	0.157	0.0318
C6	0.083	0.026	0.542	0.043				
MOLES	0.374	0.326	0.047		2852.			
C1	0.907	0.976	0.404	2.414	1500.	7.95	0.189	0.0306
C6	0.092	0.023	0.595	0.039				
MOLES	0.319	0.274	0.044		2852.			

TABLE 6-3 (CONT.)

RUN NO. 7: METHANE AND n-HEXANE AT 100° F.

SIMULATED DEPLETION PERFORMANCE								
COMP	SYSTEM COMP	VAPOR COMP	LIQUID COMP	< VALU	P _{PK} PSIA	Liq VOL %	VAPOR CF/LB	LIQUID CF/LB
C1	0.895	0.978	0.347	2.812	1250.	7.62	0.235	0.0294
C6	0.104	0.021	0.652	0.022				
MOLES	0.265	0.223	0.041		2852.			
C1	0.879	0.980	0.287	3.407	1000.	7.27	0.304	0.0282
C6	0.120	0.019	0.712	0.027				
MOLES	0.213	0.174	0.032		2852.			
C1	0.854	0.980	0.236	4.150	800.	6.93	0.390	0.0273
C6	0.146	0.019	0.763	0.024				
MOLES	0.173	0.136	0.036		2852.			
C1	0.825	0.980	0.181	5.297	600.	6.64	0.532	0.0268
C6	0.174	0.019	0.818	0.023				
MOLES	0.134	0.100	0.033		2852.			
C1	0.780	0.977	0.124	7.862	400.	6.29	0.639	0.0261
C6	0.219	0.022	0.875	0.025				
MOLES	0.096	0.065	0.031		2852.			
C1	0.703	0.966	0.063	15.290	200.	5.85	1.585	0.0254
C6	0.296	0.033	0.936	0.036				
MOLES	0.060	0.032	0.028		2852.			
C1	0.545	0.940	0.021	30.142	100.	5.53	2.929	0.0250
C6	0.454	0.059	0.968	0.050				
MOLES	0.042	0.015	0.026		2852.			
C1	0.375	0.890	0.014	59.824	50.	5.27	5.006	0.0249
C6	0.624	0.109	0.985	0.111				
MOLES	0.032	0.007	0.024		2852.			
C1	0.227	0.787	0.006119.098		25.	5.02	7.710	0.0248
C6	0.772	0.212	0.993 0.213					
MOLES	0.027	0.003	0.023		2852.			

It may be recalled that the data of Poston and McKetta indicated an unusually sharp reversal of the dew point locus to the critical state. Coexisting phase density data for the methane-n-hexane system could not be found in the literature so a comparison with calculated phase densities was not possible.

6.3 Simulated Depletion Performance of Some Ternary Mixtures

The computer model was used to simulate the depletion performance of four ternary systems. Although the program could be used for any ternary mixture of alkanes from methane through decane, only systems for which there were PVT data in the literature were studied. Compositions of the initial mixtures were selected to result in typical retrograde behavior. For this work the Chao-Seader K-values for methane were used directly without applying correction ratios of the type discussed in Section 4.4.

The phase rule requires that three intensive properties be specified to define the two-phase region of a ternary mixture. Since three properties must be specified, some interpolation is usually required to make a comparison with literature data for ternary systems. This is particularly true for the simulation of the depletion performance of a retrograde system where the overall composition is continuously changing.

Literature data for ternary systems is often correlated in terms of a composition parameter, C, defined as

$$C = x_i / (x_i + x_h) \quad (6-1)$$

where: x_i is the mole fraction of intermediate component in the liquid phase,

x_h is the mole fraction of heavy component in the liquid phase.

This definition is useful when K-values are correlated with convergence pressures calculated by Hadden's method⁴⁴, but is of limited use when the critical composition method is used to calculate convergence pressures. The following sections compare the calculated results for the example depletions with literature data whenever possible.

6.2 (a) Methane, Propane and n-Butane Mixtures

Data on the phase equilibria in the methane, propane and n-butane system at temperatures of 40°, 100°, 160° and 220°F have been reported by Wiese, Jacobs and Sage⁸⁷. Example depletion performance calculations were made for this system at temperatures of 40°, 100° and 160°F. The computer printout for the example at 40°F is presented in Table 6-4. The printout for the examples at 100°F and 160°F may be found in Tables E-10 and E-11 of Appendix E.

Table 6-4 indicates a retrograde dew point of approximately 1600 psia and a calculated convergence pressure of 1801 psia. The calculated phase compositions do not agree very well with those of reference 87 for the pressures greater than 1000 psia. The calculated convergence pressure is the cause of the discrepancies. The data of reference 87 indicate the critical pressure of the critical composition for the mixture to be approximately 1600 psia. Thus, the calculated K-values for pressures greater than 1000 psia were obtained by extrapolation to a convergence pressure which was too high. Figure 6-5 illustrates the systematic deviation of

TABLE 6-4

METHANE, PROPANE, AND N-BUTANE MIXTURE AT 40 F.
DEPLETION OF A CONSTANT VOLUME RESERVOIR BY VAPOR PRODUCTION

PURE COMPONENT DATA							
COMP	MOLE WT LB/MOLE	PC PSIA	VC FT**3	TC DEG R	ZC	PITZER OMEGA	RIEDEL ALPHA
C1	16.042	669.7	1.590	343.13	0.288	0.000	5.860
C3	44.094	616.3	3.210	665.68	0.276	0.153	6.540
C4	58.120	550.7	4.080	765.29	0.274	0.195	6.770
SIMULATED DEPLETION PERFORMANCE							
COMP	SYSTEM COMP	VAPOR COMP	LIQUID COMP	K VALUE	P, PK PSIA VOL %	VAPOR CF/LB	LIQUID CF/LB
C1	0.825	0.825	0.000	1.000	1650.	0.00	0.081
C3	0.105	0.105	0.000	1.000			
C4	0.070	0.070	0.000	1.000			
MOLES	0.556	0.556	0.000		1801.		
C1	0.824	0.825	0.515	1.601	1600.	0.05	0.085
C3	0.104	0.104	0.235	0.445			
C4	0.069	0.069	0.249	0.280			
MOLES	0.536	0.536	0.000		1801.		
C1	0.824	0.842	0.479	1.756	1500.	3.34	0.099
C3	0.105	0.397	0.250	0.390			
C4	0.070	0.060	0.270	0.222			
MOLES	0.482	0.456	0.025		1801.		
C1	0.823	0.872	0.418	2.086	1250.	6.95	0.144
C3	0.105	0.084	0.278	0.303			
C4	0.071	0.042	0.302	0.141			
MOLES	0.371	0.319	0.052		1801.		
C1	0.808	0.888	0.361	2.458	1000.	7.57	0.206
C3	0.112	0.077	0.305	0.253			
C4	0.079	0.034	0.333	0.102			
MOLES	0.284	0.228	0.056		1801.		
C1	0.783	0.890	0.334	2.660	900.	7.35	0.237
C3	0.122	0.077	0.315	0.243			
C4	0.093	0.032	0.349	0.094			
MOLES	0.253	0.199	0.054		1801.		

TABLE 6-4 (CONT.)

METHANE, PROPANE, AND N-BUTANE MIXTURE AT 40 F.

SIMULATED DEPLETION PERFORMANCE									
COMP	SYSTEM COMP	VAPOR COMP	LIQUID COMP	K VALUE	P, PSIA	PK VOL %	LIQ	VAPOR CF/LB	LIQUID CF/LB
C1	0.770	0.890	0.305	2.914	800.	7.03	0.275	0.0334	
C3	0.128	0.077	0.326	0.238					
C4	0.100	0.032	0.368	0.087					
MOLES	0.223	0.172	0.051		1801.				
C1	0.755	0.887	0.273	3.242	700.	6.62	0.323	0.0327	
C3	0.134	0.079	0.335	0.237					
C4	0.109	0.032	0.390	0.083					
MOLES	0.195	0.147	0.048		1800.				
C1	0.735	0.882	0.239	3.681	600.	6.17	0.384	0.0320	
C3	0.143	0.083	0.344	0.242					
C4	0.121	0.033	0.416	0.081					
MOLES	0.167	0.123	0.044		1799.				
C1	0.711	0.873	0.203	4.300	500.	5.66	0.466	0.0312	
C3	0.152	0.089	0.350	0.255					
C4	0.135	0.036	0.445	0.082					
MOLES	0.141	0.100	0.040		1797.				
C1	0.681	0.858	0.164	5.232	400.	5.09	0.582	0.0305	
C3	0.164	0.099	0.354	0.280					
C4	0.154	0.041	0.481	0.086					
MOLES	0.115	0.079	0.036		1792.				
C1	0.641	0.832	0.122	6.792	300.	4.44	0.762	0.0297	
C3	0.179	0.115	0.351	0.330					
C4	0.179	0.051	0.526	0.097					
MOLES	0.089	0.058	0.031		1783.				
C1	0.586	0.782	0.078	9.924	200.	3.62	1.081	0.0289	
C3	0.197	0.145	0.332	0.436					
C4	0.216	0.072	0.588	0.123					
MOLES	0.063	0.038	0.024		1759.				
C1	0.505	0.650	0.033	19.347	100.	2.21	1.832	0.0280	
C3	0.219	0.204	0.265	0.769					
C4	0.275	0.145	0.700	0.207					
MOLES	0.034	0.019	0.014		1682.				

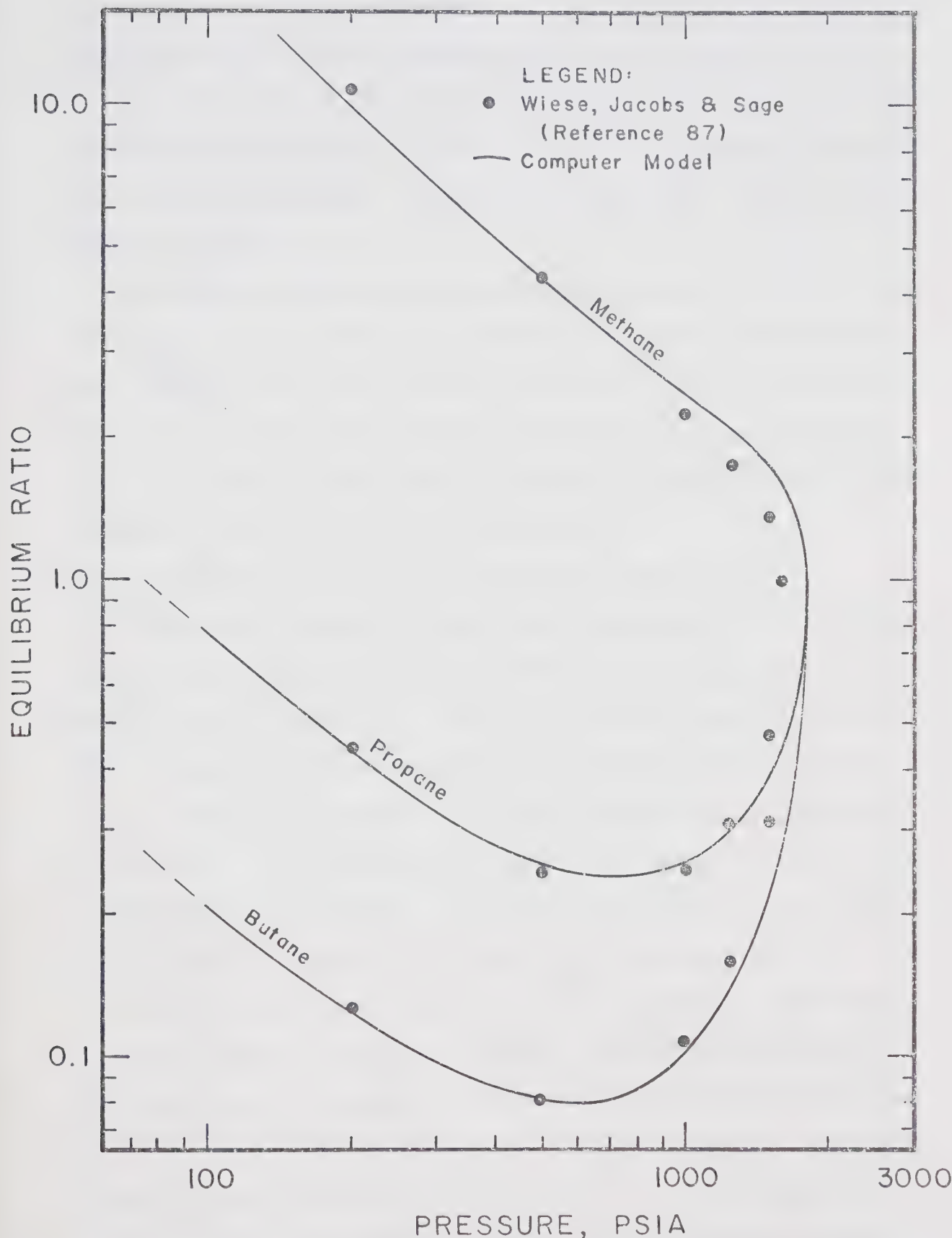


Figure 6-5. Comparison of Calculated and Literature Equilibrium Ratios for the Methane-Propane-n-Butane Mixtures of Table 6-4.

the K-values at high pressures. The circles on the figure represent the K-values interpolated from the data of Wiese et al. using composition parameters determined from the liquid phase compositions of Table 6-4. It is apparent that if the correct convergence pressure was used, the K-values would compare favorably.

The calculated convergence pressures were 1724 psia and 1443 psia for the examples at 100°F and 160°F, respectively. These values were also too high compared to the data of Wiese et al. which indicated critical pressures of approximately 1550 psia and 1300 psia for the critical compositions of the examples at 100°F and 160°F, respectively.

6.3 (b) Methane, Propane and n-Pentane Mixtures

Phase equilibria data have been reported for the methane, propane and n-pentane system at 100°F by Carter, Sage and Lacey⁸⁸, and at 160°F and 220°F by Dourson, Sage and Lacey⁸⁹. Three example depletion performance calculations were made, one for each of the temperatures for which there were experimental data. The computer printout for the example at 100°F is presented in Table 6-5. The examples for 160°F and 220°F may be found in Tables E-12 and E-13 of Appendix E.

The starting composition for the example at 100°F was 0.8 mole fraction methane, 0.12 mole fraction propane and 0.08 mole fraction n-pentane. The calculated retrograde dew point was approximately 1800 psia. The convergence pressure of the critical mixture was calculated to be 2088 psia compared to a value of 2200 psia interpolated from the experimental data of reference 88. Since the discrepancy in

TABLE 6-5

METHANE, PROPANE, AND N-PENTANE MIXTURE AT 100 F.
DEPLETION OF A CONSTANT VOLUME RESERVOIR BY VAPOR PRODUCTION

PURE COMPONENT DATA							
COMP	MOLE WT LB/MOLE	PC PSIA	VC FT**3	TC DEG R	ZC	PITZER OMEGA	RIEDEL ALPHA
C1	16.042	669.7	1.590	343.13	0.288	0.000	5.860
C3	44.094	616.3	3.210	665.68	0.276	0.153	6.540
C5	72.146	487.3	4.730	845.08	0.254	0.238	7.030
SIMULATED DEPLETION PERFORMANCE							
COMP	SYSTEM COMP	VAPOR COMP	LIQUID COMP	K VALUE	P, PK PSIA VOL %	VAPOR CF/LB	LIQUID CF/LB
C1	0.800	0.800	0.000	1.000	2000.	0.00	0.081
C3	0.120	0.120	0.000	1.000			
C5	0.080	0.080	0.000	1.000			
MOLES	0.513	0.513	0.000		2088.		
C1	0.799	0.818	0.447	1.828	1750.	3.82	0.101
C3	0.119	0.114	0.226	0.506			
C5	0.079	0.067	0.326	0.205			
MOLES	0.438	0.412	0.025		2088.		
C1	0.796	0.843	0.391	2.152	1500.	6.85	0.134
C3	0.120	0.106	0.242	0.441			
C5	0.082	0.049	0.365	0.135			
MOLES	0.362	0.317	0.045		2088.		
C1	0.787	0.855	0.344	2.486	1250.	7.46	0.176
C3	0.123	0.103	0.256	0.403			
C5	0.089	0.041	0.399	0.102			
MOLES	0.295	0.247	0.048		2088.		
C1	0.771	0.859	0.289	2.972	1000.	7.10	0.234
C3	0.128	0.103	0.265	0.389			
C5	0.099	0.037	0.444	0.083			
MOLES	0.233	0.188	0.045		2090.		
C1	0.748	0.856	0.239	3.580	800.	6.48	0.303
C3	0.135	0.106	0.268	0.398			
C5	0.116	0.036	0.492	0.074			
MOLES	0.186	0.145	0.040		2090.		

TABLE 6-5 (CONT.)

METHANE, PROPANE, AND N-PENTANE MIXTURE AT 100 F.

SIMULATED DEPLETION PERFORMANCE									
COMP	SYSTEM COMP	VAPOR COMP	LIQUID COMP	K VALUE	P, PK PSIA	LIQ VOL %	VAPOR CF/LB	LIQUID CF/LB	
C1	0.721	0.846	0.184	4.597	600.	5.67	0.413	0.0295	
C3	0.142	0.114	0.261	0.437					
C5	0.136	0.039	0.554	0.071					
MOLES	0.141	0.106	0.035		2088.				
C1	0.681	0.836	0.154	5.414	500.	5.24	0.495	0.0289	
C3	0.151	0.120	0.253	0.477					
C5	0.167	0.042	0.592	0.072					
MOLES	0.119	0.087	0.032		2084.				
C1	0.652	0.821	0.123	6.644	400.	4.75	0.613	0.0282	
C3	0.156	0.130	0.239	0.542					
C5	0.190	0.048	0.636	0.076					
MOLES	0.098	0.069	0.028		2075.				
C1	0.615	0.796	0.091	8.700	300.	4.21	0.797	0.0274	
C3	0.162	0.143	0.217	0.658					
C5	0.221	0.059	0.690	0.086					
MOLES	0.076	0.051	0.025		2058.				
C1	0.564	0.753	0.058	12.826	200.	3.54	1.125	0.0267	
C3	0.167	0.162	0.181	0.899					
C5	0.267	0.083	0.760	0.109					
MOLES	0.054	0.033	0.020		2025.				
C1	0.489	0.714	0.042	16.956	150.	3.14	1.413	0.0262	
C3	0.169	0.177	0.154	1.144					
C5	0.340	0.107	0.802	0.134					
MOLES	0.043	0.025	0.018		1991.				
C1	0.432	0.647	0.025	25.225	100.	2.62	1.905	0.0258	
C3	0.167	0.193	0.118	1.635					
C5	0.399	0.158	0.855	0.184					
MOLES	0.031	0.016	0.015		1933.				
ZKATZ	ITER = 0								
C1	0.353	0.490	0.009	50.016	50.	1.60	2.957	0.0253	
C3	0.158	0.196	0.063	3.111					
C5	0.488	0.313	0.927	0.337					
MOLES	0.017	0.008	0.009		1820.				

convergence pressure was about 5 per cent for this case, we might expect better agreement between the calculated and experimental K-values at high pressure. Figure 6-6 tends to confirm this expectation since there is satisfactory agreement for propane and n-pentane. Discrepancies in the methane K-values are likely caused by the type of systematic deviation that was discussed in Section 4.4.

There was satisfactory agreement between the data of reference 88 and the calculated data (convergence pressure and K-values) for the example at 160°F. However, the agreement between calculations and experimental data was not as good at 220°F. Propane was supercritical at 220°F so the Chao-Seader K-values were not as accurate as those at temperatures of 100°F and 160°F. A valid comparison of convergence pressure could not be made at 220°F since the experimental data are rather sparse at this temperature.

6.3 (c) Methane, Propane and Decane Mixtures

Phase equilibria data for the methane, propane and decane system at temperatures of 40°, 100°, 280°, 400° and 460°F were reported by Wiese, Reamer and Sage⁹⁰. Two example depletion performance calculations were performed; Table 6-6 gives the computer printout for an example at 100°F, and Table E-14 of Appendix E gives the printout for an example at 280°F.

Table 6-6 indicates a retrograde dew point of some 3400 psia. The calculated convergence pressure of 3957 psia compares favorably with a value of approximately 4100 psia from the experimental data of Wiese et al. Figure 6-7 makes a

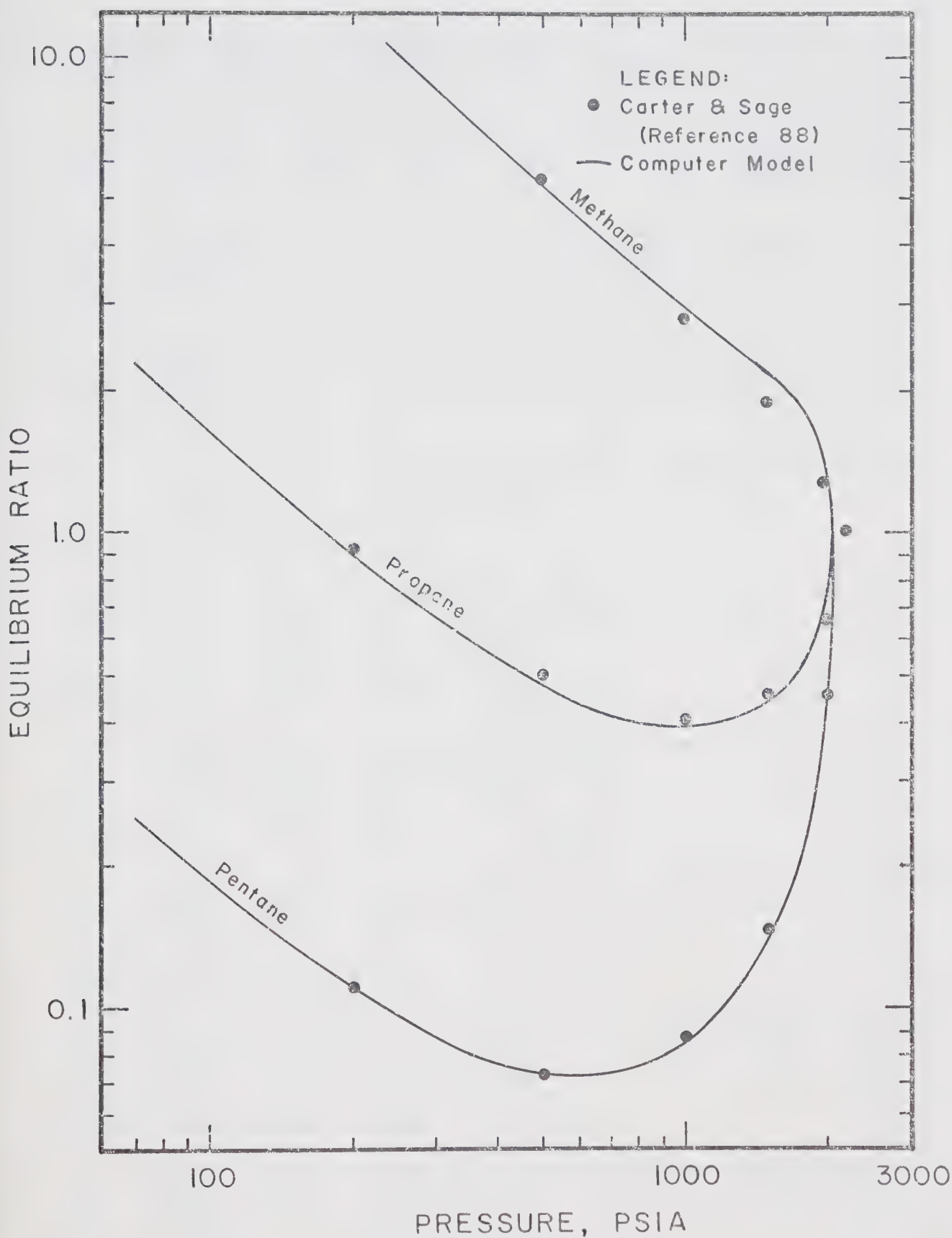


Figure 6-6. Comparison of Calculated and Literature Equilibrium Ratios for the Methane-Propane-n-Pentane Mixtures of Table 6-5.

TABLE 6-6.

METHANE, PROPANE, N-DECANE MIXTURE AT 100 F.
DEPLETION OF A CONSTANT VOLUME RESERVOIR BY VAPOR PRODUCTION

PURE COMPONENT DATA							
COMP	MOLE WT LB/MOLE	PC PSIA	VC FT**3	TC DEG R	ZC	PITZER OMEGA	RIEDEL ALPHA
C1	16.042	669.7	1.590	343.13	0.288	0.000	5.860
C3	44.094	516.3	3.210	665.68	0.276	0.153	6.540
C10	142.276	304.0	9.660	1111.70	0.246	0.486	8.180
SIMULATED DEPLETION PERFORMANCE							
COMP	SYSTEM COMP	VAPOR COMP	LIQUID COMP	K VALUE	P, PK PSIA VOL %	VAPOR CF/LB	LIQUID CF/LB
C1	0.900	0.900	0.000	1.0000	3750.	0.00	0.057
C3	0.060	0.060	0.000	1.0000			
C10	0.040	0.040	0.000	1.0000			
MOLES	0.759	0.759	0.000		3957.		
C1	0.899	0.899	0.000	1.0000	3500.	0.00	0.060
C3	0.059	0.059	0.000	1.0000			
C10	0.039	0.039	0.000	1.0000			
MOLES	0.729	0.729	0.000		3957.		
C1	0.899	0.910	0.609	1.4931	3250.	4.40	0.067
C3	0.059	0.058	0.103	0.5638			
C10	0.039	0.031	0.286	0.1094			
MOLES	0.681	0.657	0.024		3957.		
C1	0.899	0.921	0.575	1.6010	3000.	8.23	0.077
C3	0.060	0.056	0.108	0.5218			
C10	0.040	0.021	0.315	0.0678			
MOLES	0.629	0.584	0.044		3957.		
C1	0.897	0.937	0.513	1.8249	2500.	11.73	0.101
C3	0.060	0.054	0.118	0.4558			
C10	0.042	0.008	0.367	0.0219			
MOLES	0.526	0.466	0.059		3957.		
C1	0.889	0.945	0.446	2.1162	2000.	12.33	0.136
C3	0.061	0.052	0.130	0.4068			
C10	0.048	0.001	0.423	0.0031			
MOLES	0.422	0.363	0.059		3957.		

TABLE 6-6. (CONT.)

METHANE, PROPANE, N-DECANE MIXTURE AT 100 F.

SIMULATED DEPLETION PERFORMANCE									
COMP	SYSTEM COMP	VAPOR COMP	LIQUID COMP	K VALUE	P, PK PSIA	Liq VOL %	VAPOR CF/LB	LIQUID CF/LB	
C1	0.875	0.945	0.366	2.5842	1500.	11.36	0.138	0.0269	
C3	0.063	0.053	0.140	0.3765					
C10	0.060	0.000	0.492	0.0018					
MOLES	0.318	0.266	0.051		3957.				
C1	0.852	0.944	0.266	3.5465	1000.	10.33	0.297	0.0254	
C3	0.067	0.055	0.145	0.3790					
C10	0.080	0.000	0.588	0.0010					
MOLES	0.213	0.170	0.043		3951.				
C1	0.807	0.942	0.220	4.2791	800.	9.89	0.379	0.0247	
C3	0.073	0.057	0.142	0.4021					
C10	0.118	0.000	0.637	0.0008					
MOLES	0.173	0.133	0.039		3940.				
C1	0.776	0.938	0.170	5.5099	600.	9.43	0.516	0.0240	
C3	0.076	0.061	0.134	0.4548					
C10	0.146	0.000	0.694	0.0007					
MOLES	0.134	0.098	0.036		3916.				
C1	0.730	0.930	0.116	7.9885	400.	8.97	0.786	0.0233	
C3	0.081	0.068	0.119	0.5787					
C10	0.188	0.000	0.764	0.0006					
MOLES	0.097	0.064	0.033		3866.				
C1	0.653	0.913	0.059	15.4718	200.	8.46	1.573	0.0226	
C3	0.086	0.085	0.087	0.9826					
C10	0.260	0.000	0.353	0.0007					
MOLES	0.061	0.031	0.029		3744.				
C1	0.498	0.890	0.029	30.4896	100.	8.18	3.076	0.0221	
C3	0.086	0.108	0.059	1.8117					
C10	0.415	0.001	0.910	0.0011					
MOLES	0.043	0.015	0.027		3561.				
C1	0.338	0.860	0.014	60.5808	50.	8.01	5.909	0.0219	
C3	0.077	0.137	0.039	3.4799					
C10	0.584	0.001	0.946	0.0020					
MOLES	0.034	0.007	0.026		3321.				

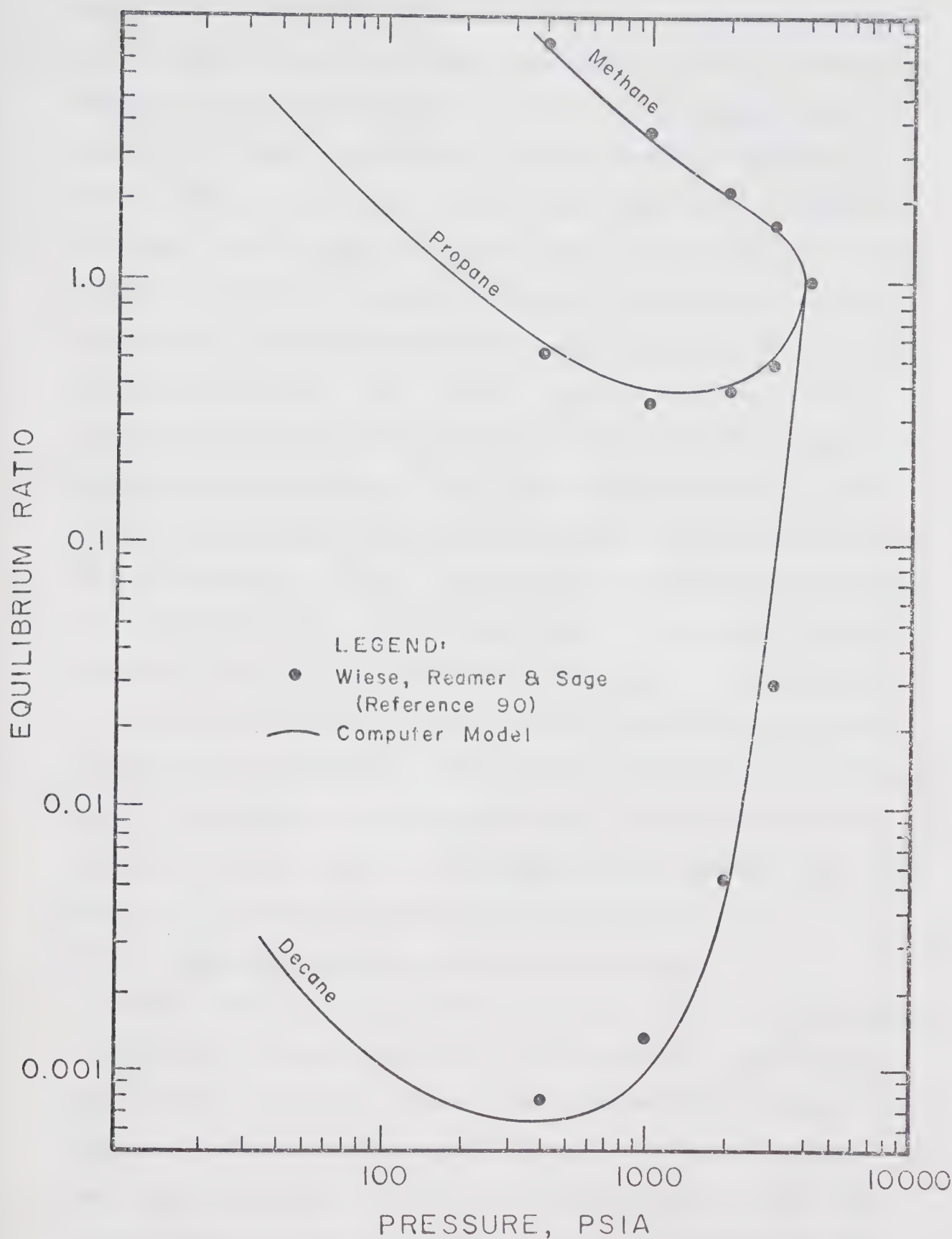


Figure 6-7. Comparison of Calculated and Literature Equilibrium Ratios for the Methane-Propane-Decane Mixtures of Table 6-6.

comparison between the calculated K-values and the experimental K-values interpolated from reference 90 using composition parameters calculated from the liquid phase compositions of Table 6-6. There was generally good agreement between K-values except for decane at 3000 psia, where the calculated value was 0.0678 compared to the experimental value of 0.03. This large error was caused by smaller percentage errors in the K-values calculated from the Chao-Seader correlation at the lower pressures. The smaller errors were magnified by the interpolation formula (Equation 4-12) used to extend the Chao-Seader correlation to the convergence pressure. Relatively large errors were also detected in the decane K-values for the example at 280°F. These errors could also be traced to systematic errors in the Chao-Seader correlation, particularly in the pressure range from 1200 psia to 2000 psia.

The loci of the calculated phase compositions for the two depletion performance calculations are presented in Figure 6-8. It should be noted that the vapor phase compositions vary only slightly whereas the liquid phase compositions vary widely and tend toward pure decane at low pressures.

6.3 (d) Methane, n-Butane and Decane Mixtures

Phase equilibria data have been reported for the methane, n-butane and decane system at 160°F by Reamer, Fiskin and Sage⁹¹ and at 280°F by Reamer, Sage and Lacey⁹². Example depletion performance calculations were performed for the same initial mixture (0.90 mole fraction methane, 0.06 mole fraction n-butane and 0.04 mole fraction decane) at temperatures of 160°F and 280°F. The computer printout for the

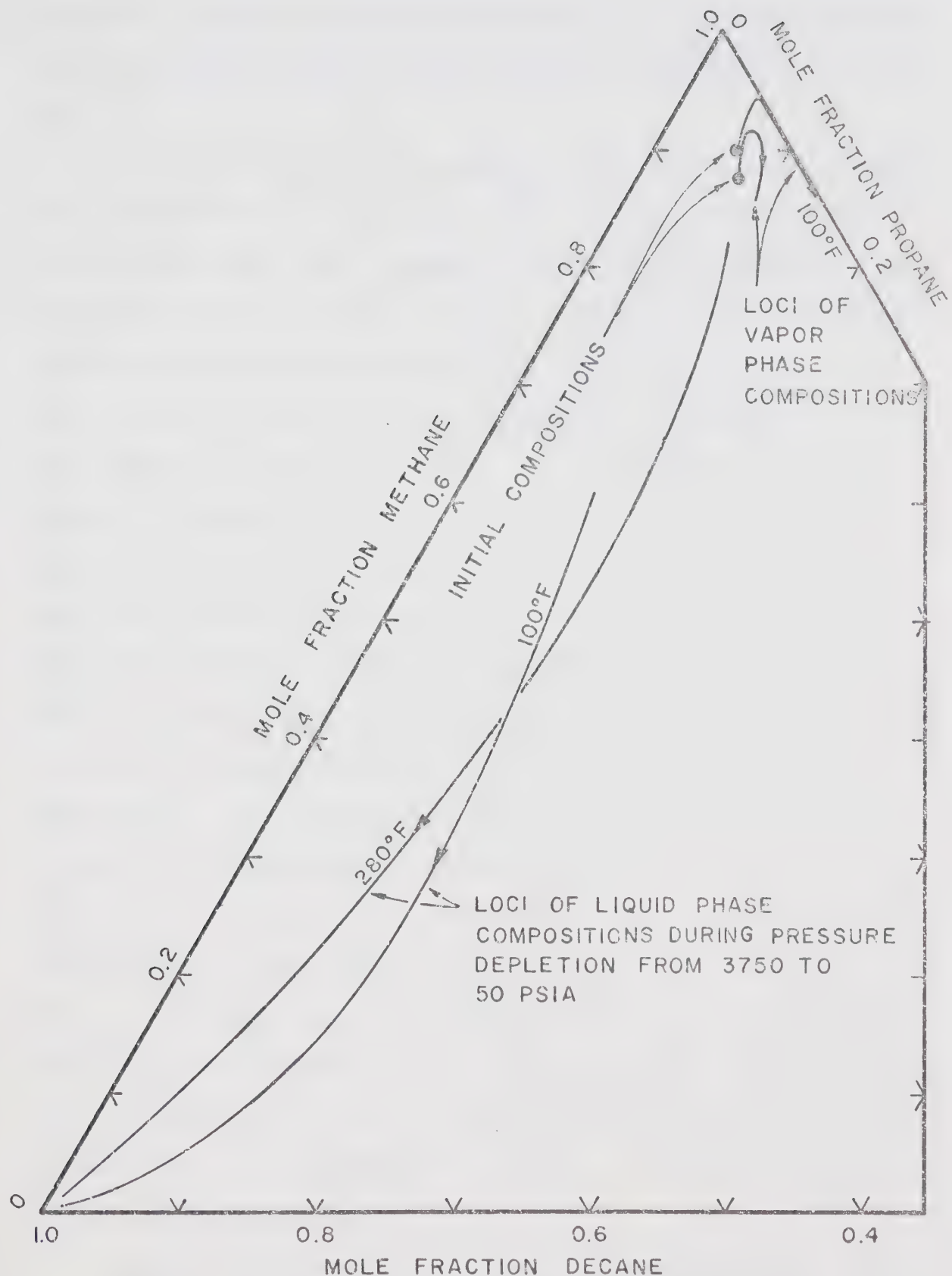


Figure 6-8. Loci of Phase Compositions for the Simulated Depletion Performance of the Mixtures given in Tables 6-6 and E-14.

example at 160°F is presented in Table 6-7, and the printout for the example at 280°F may be found in Table E-15 of Appendix E.

The data of Table 6-7 indicate the retrograde dew point to be approximately 3600 psia. The calculated convergence pressure was 3989 psia compared to an interpolated value of some 4100 psia from reference 91. A comparison of calculated K-values with the experimental data from reference 91 is shown in Figure 6-9. There is remarkable agreement for methane, however, there are systematic discrepancies in the n-butane and decane K-values. The Chao-Seader K-values for decane start to diverge from the experimental data at pressures above about 800 psia. Since the interpolation procedure used Chao-Seader K-values at pressures of 0.1 P_k , 0.3 P_k and 0.5 P_k (399, 1197 and 1995 psia, respectively), the errors in the low pressure K-values are carried into the high pressure region. The changeover point (0.5 P_k) from Chao-Seader K-values to interpolated K-values for decane is obvious in Figure 6-9. The dashed line shows the locus of the interpolation formula for a short interval below the changeover point. It is apparent that better results would have been obtained if the decane K-values at pressures corresponding to 0.05 P_k , 0.1 P_k and 0.2 P_k had been used to develop the coefficients for the interpolation formula. The example at 280°F showed similar behavior.

The loci of the calculated phase compositions for the two examples are shown in Figure 6-10. As expected, an increase in temperature caused the decane content of the vapor

TABLE 6-7.

METHANE, N-BUTANE, AND N-DECANE MIXTURE AT 160 F.
DEPLETION OF A CONSTANT VOLUME RESERVOIR BY VAPOR PRODUCTION

PURE COMPONENT DATA							
COMP	MOLE WT LB/MOLE	PC PSIA	VC FT**3	TC DEG R	ZC	PITZER OMEGA	RIEDEL ALPHA
C1	16.042	669.7	1.590	343.13	0.288	0.000	5.860
C4	58.120	550.7	4.080	765.29	0.274	0.195	6.770
C10	142.276	304.0	9.660	1111.70	0.246	0.486	8.180
SIMULATED DEPLETION PERFORMANCE							
COMP	SYSTEM COMP	VAPOR COMP	LIQUID COMP	K VALUE	P, PK PSIA VOL %	VAPOR CF/LB	LIQUID CF/LB
C1	0.900	0.904	0.663	1.3645	3500.	2.24	0.070
C4	0.060	0.058	0.122	0.4807			
C10	0.040	0.036	0.214	0.1696			
MOLES	0.614	0.602	0.012		3989.		
C1	0.899	0.917	0.518	1.4835	3250.	6.72	0.079
C4	0.060	0.055	0.130	0.4264			
C10	0.040	0.027	0.251	0.1077			
MOLES	0.571	0.535	0.035		3989.		
C1	0.898	0.927	0.580	1.5985	3000.	9.25	0.090
C4	0.060	0.053	0.138	0.3855			
C10	0.040	0.019	0.281	0.0693			
MOLES	0.528	0.481	0.047		3989.		
C1	0.896	0.935	0.544	1.7181	2750.	10.67	0.103
C4	0.060	0.051	0.145	0.3529			
C10	0.042	0.013	0.309	0.0419			
MOLES	0.486	0.433	0.053		3988.		
C1	0.892	0.941	0.508	1.8502	2500.	11.37	0.118
C4	0.061	0.050	0.153	0.3259			
C10	0.045	0.008	0.337	0.0243			
MOLES	0.445	0.390	0.054		3988.		
C1	0.888	0.946	0.472	2.0033	2250.	11.58	0.135
C4	0.062	0.049	0.161	0.3036			
C10	0.048	0.004	0.366	0.0129			
MOLES	0.402	0.348	0.054		3988.		

TABLE 6-7. (CONT.)

METHANE, N-BUTANE, AND N-DECANE MIXTURE AT 160 F.

SIMULATED DEPLETION PERFORMANCE									
COMP	SYSTEM COMP	VAPOR COMP	LIQUID COMP	K VALUE	P, PSIA	PK VOL %	VAPOR CF/LB	LIQUID CF/LB	
C1	0.882	0.949	0.433	2.1889	2000.	11.46	0.156	0.0300	
C4	0.064	0.048	0.170	0.2852					
C10	0.053	0.002	0.396	0.0061					
MOLES	0.360	0.308	0.052		3988.				
C1	0.874	0.948	0.391	2.4229	1750.	10.90	0.179	0.0291	
C4	0.066	0.048	0.179	0.2720					
C10	0.059	0.002	0.429	0.0055					
MOLES	0.317	0.269	0.048		3988.				
C1	0.864	0.948	0.346	2.7361	1500.	10.38	0.212	0.0282	
C4	0.068	0.049	0.187	0.2616					
C10	0.067	0.002	0.465	0.0048					
MOLES	0.274	0.229	0.044		3988.				
C1	0.851	0.948	0.298	3.1767	1250.	9.89	0.258	0.0274	
C4	0.071	0.049	0.194	0.2563					
C10	0.077	0.002	0.506	0.0040					
MOLES	0.230	0.189	0.040		3987.				
C1	0.832	0.946	0.246	3.8413	1000.	9.37	0.327	0.0265	
C4	0.075	0.051	0.199	0.2595					
C10	0.091	0.001	0.554	0.0034					
MOLES	0.187	0.149	0.037		3983.				
C1	0.806	0.943	0.201	4.6760	800.	8.97	0.414	0.0258	
C4	0.081	0.054	0.199	0.2729					
C10	0.112	0.001	0.599	0.0029					
MOLES	0.153	0.118	0.034		3974.				
C1	0.775	0.939	0.154	6.0737	600.	8.52	0.555	0.0251	
C4	0.087	0.059	0.193	0.3053					
C10	0.137	0.001	0.651	0.0027					
MOLES	0.119	0.087	0.031		3951.				
C1	0.730	0.935	0.129	7.1950	500.	8.30	0.666	0.0247	
C4	0.094	0.063	0.188	0.3353					
C10	0.174	0.001	0.681	0.0026					
MOLES	0.103	0.072	0.030		3929.				

TABLE 6-7. (CONT.)

METHANE, N-BUTANE, AND N-DECANE MIXTURE AT 160 F.

SIMULATED DEPLETION PERFORMANCE									
COMP	SYSTEM	VAPOR	LIQUID	K	P, PK	LIQ	VAPOR	LIQUID	
	COMP	COMP	COMP	COMP	PSIA	VOL %	CF/LB	CF/LB	
C1	0.697	0.929	0.104	8.8810	400.	8.06	0.829	0.0244	
C4	0.100	0.068	0.179	0.3835					
C10	0.202	0.001	0.715	0.0027					
MOLES	0.086	0.057	0.028		3892.				
C1	0.653	0.919	0.078	11.6986	300.	7.81	1.093	0.0240	
C4	0.105	0.077	0.166	0.4676					
C10	0.240	0.002	0.754	0.0029					
MOLES	0.070	0.043	0.027		3832.				
C1	0.592	0.903	0.052	17.3517	200.	7.52	1.596	0.0236	
C4	0.112	0.093	0.145	0.6411					
C10	0.295	0.002	0.802	0.0035					
MOLES	0.054	0.028	0.025		3719.				
C1	0.499	0.889	0.038	23.0153	150.	7.37	2.071	0.0234	
C4	0.118	0.107	0.131	0.8172					
C10	0.382	0.003	0.830	0.0042					
MOLES	0.046	0.021	0.024		3613.				
C1	0.430	0.865	0.025	34.3675	100.	7.19	2.964	0.0231	
C4	0.120	0.129	0.110	1.1717					
C10	0.449	0.004	0.863	0.0056					
MOLES	0.038	0.014	0.023		3435.				
C1	0.337	0.815	0.011	68.5303	50.	6.95	5.364	0.0229	
C4	0.117	0.175	0.078	2.2396					
C10	0.544	0.009	0.909	0.0099					
MOLES	0.029	0.007	0.022		3076.				

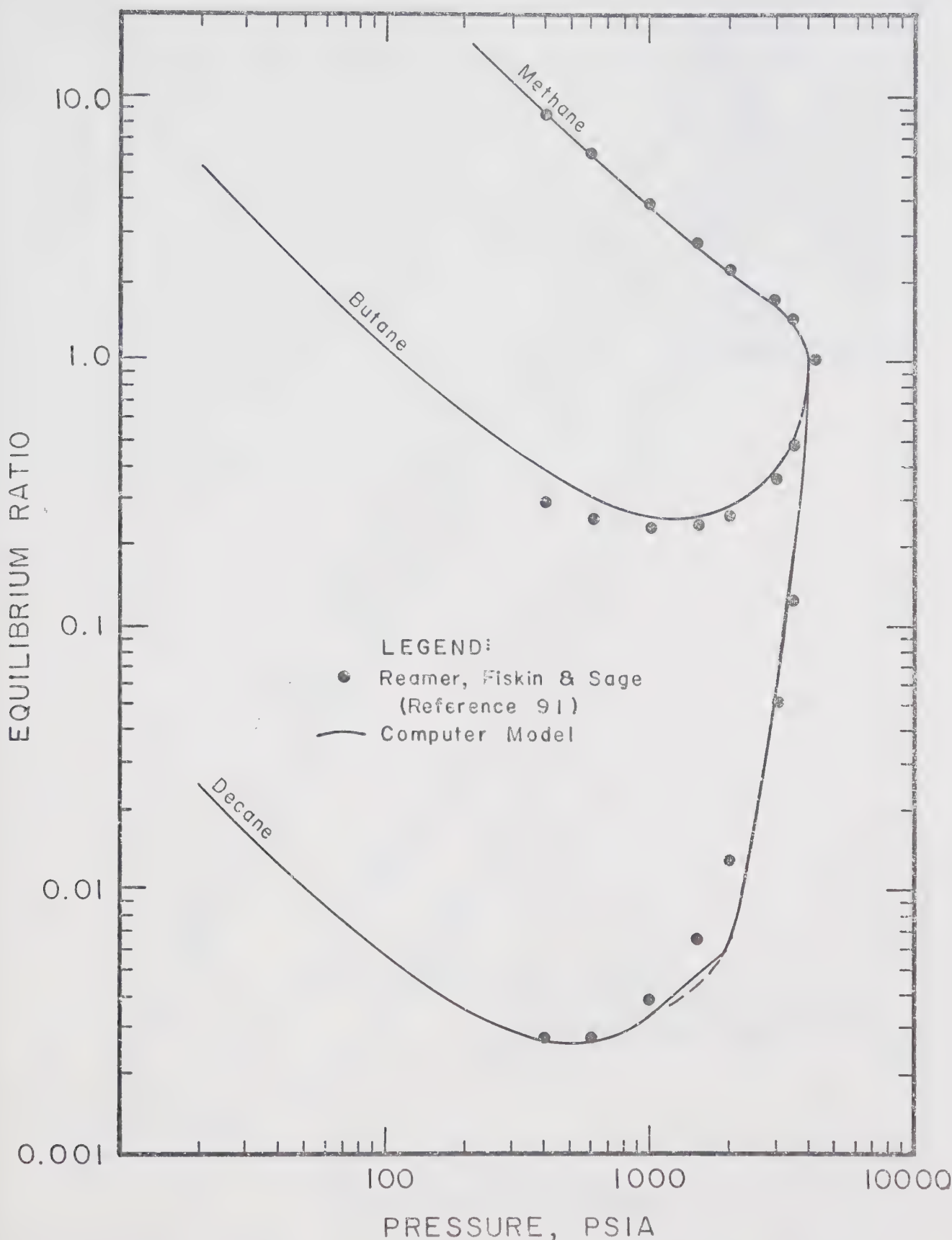


Figure 6-9. Comparison of Calculated and Literature Equilibrium Ratios for the Methane-n-Butane-Decane Mixtures of Table 6-7.

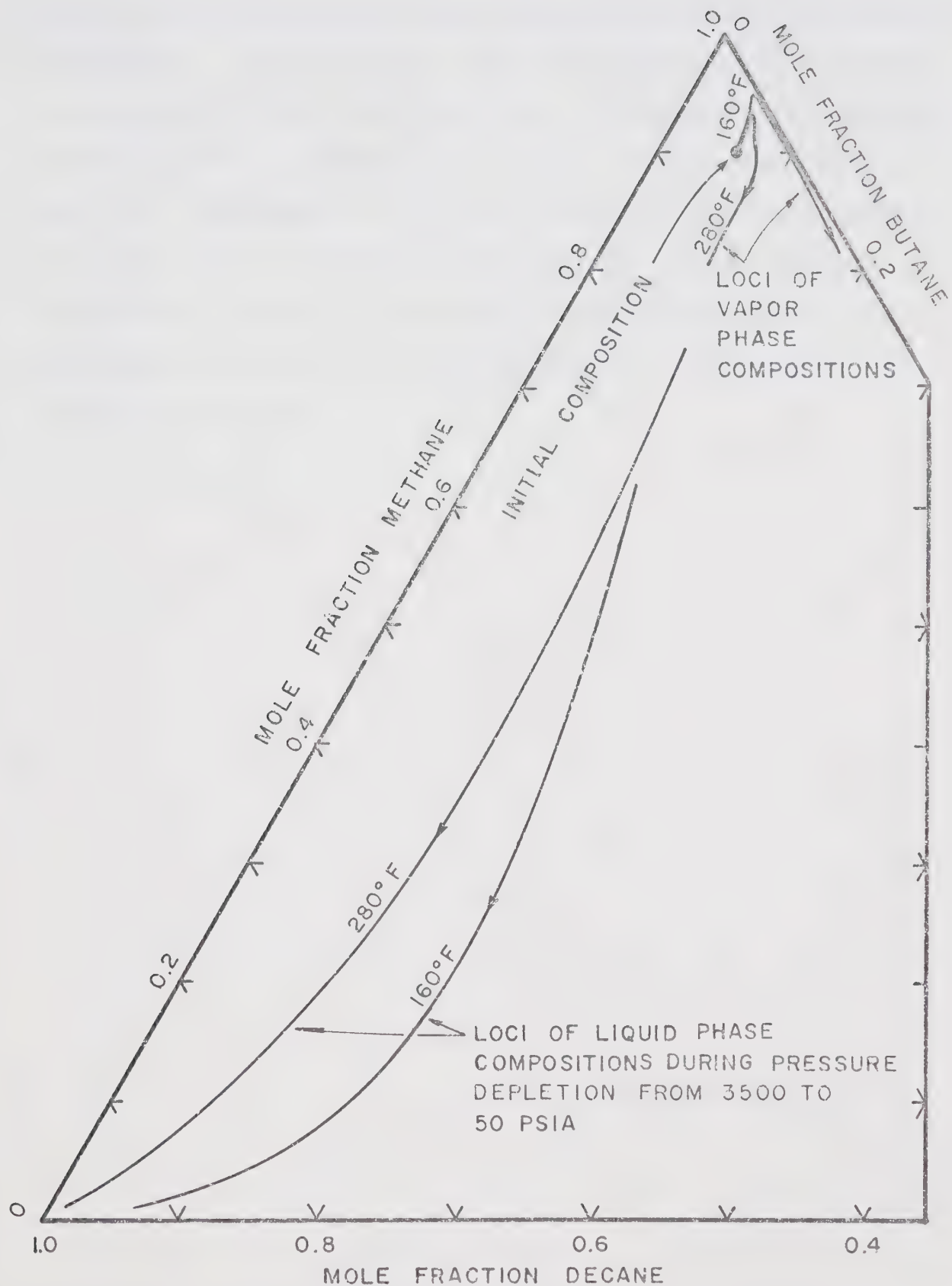


Figure 6-10. Loci of Phase Compositions for the Simulated Depletion Performance of the Mixtures given in Tables 6-7 and E-15.

phase to increase and the decane content of the liquid phase to decrease. The volume per cent retrograde liquid for the two examples is shown in Figure 6-11. The effect of increased temperature was to decrease the amount of retrograde liquid. There is a discrepancy in the calculated dew points inasmuch as the dew point at 280°F is indicated to be some 200 psi higher than at 160°F. This type of discrepancy might have been expected in view of the difficulties in extrapolating the decane K-values.

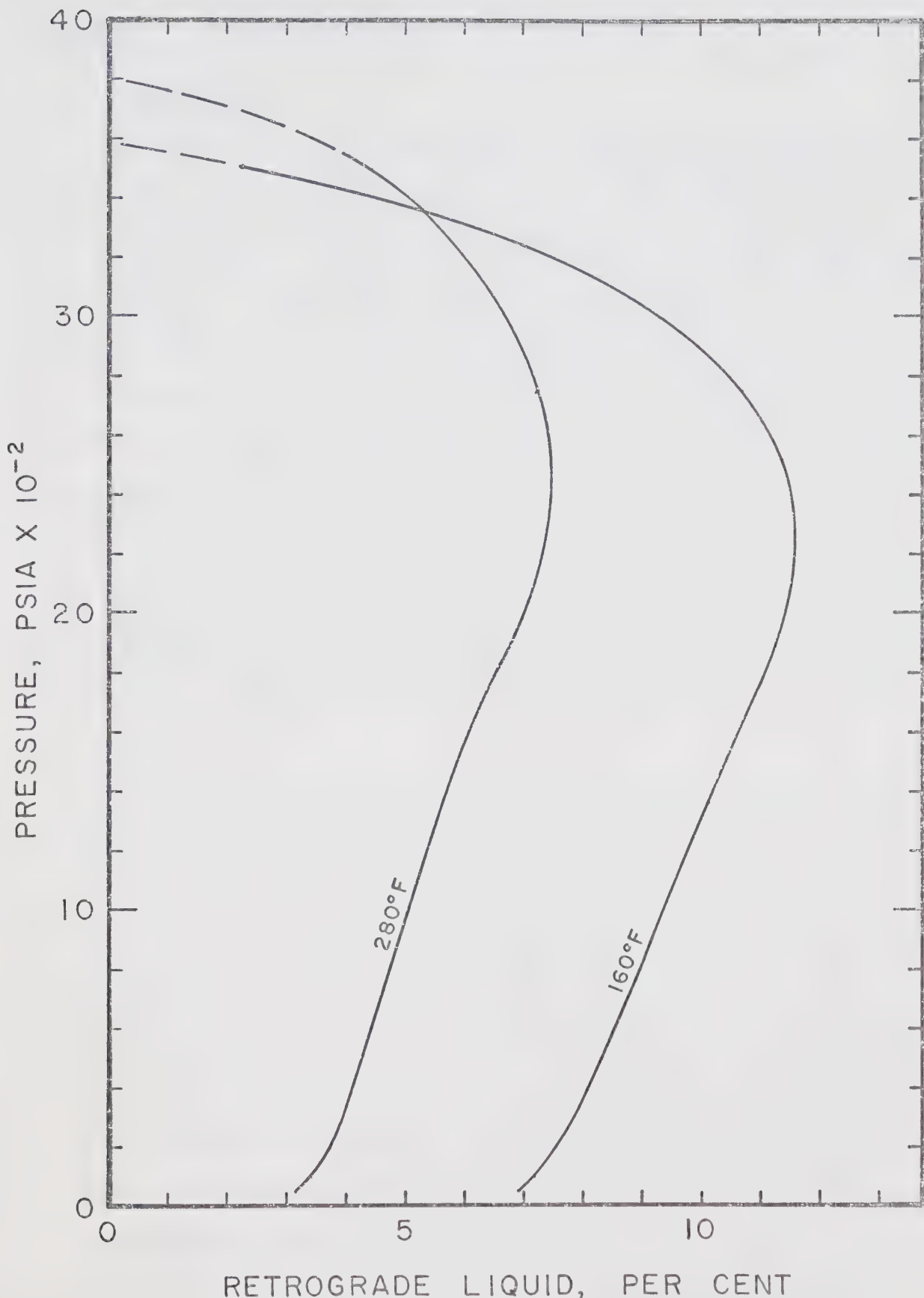


Figure 6-11. Volume Per Cent Retrograde Liquid for the Example Depletion Calculations Presented in Tables 6-7 and E-15.

Chapter 7. CONCLUSIONS AND RECOMMENDATIONS

7.1 Conclusions

The object of the experimental work was to design and construct an apparatus to study some of the effects that porous media have on the phase behavior of retrograde hydrocarbon mixtures. Except for some initial shakedown runs, the experimental work was directed toward obtaining photographs of retrograde liquid capillary structures in packs of uniform spheres. The photographs were used in a theoretical study of the effect of interface curvature on phase behavior carried out by the Petroleum Recovery Research Institute of Calgary. That study indicated that the curvature of the vapor-liquid interface would have a negligible effect on phase equilibrium except in a porous medium with a grain diameter of a few microns.

The conclusions with regard to the experimental aspect of this work are qualitative and generally pertain to the apparatus. The work concerning the calculation procedure developed to approximate the pressure depletion of retrograde hydrocarbon mixtures was carried on independently of the experimental program. Conclusions concerning this phase of the work are based on the results presented in this thesis.

1. The air bath enclosure proved to be a convenient means of maintaining good temperature control for the bulky equipment used in this study.
2. The general procedure for determining bubble or dew point pressures by using a differential pressure

transducer is believed to be an original innovation. The procedure may have some application in conventional PVT work.

3. The data of this work indicates that during the isothermal depletion of binary retrograde hydrocarbon mixtures, equilibrium between phases is spontaneous over the pressure interval that liquids are condensing.
4. The data of this work indicates that mass transfer from the liquid phase to the vapor phase in the packed cell did not appear to be enhanced by the forced convection of the vapor phase.
5. An explanation was developed for the tendency toward non-equilibrium between coexisting phases over the pressure interval that retrograde liquids vaporize. It was shown that the variation of phase fugacity with composition was important in this regard.
6. A new equation of state procedure was developed for the analytical representation of isochores. The method was demonstrated by applying it to the corresponding states correlation of Lydersen, Greenkorn and Hougen.
7. A calculation procedure was developed to extrapolate K-values from the Chao-Seader correlation over the high pressure region to the convergence pressure defined by the critical composition method.
8. The widely used Standing and Katz correlation was found to exhibit anomalous behavior along the isotherms $T_x = 1.05, 1.10$ and 1.15 . This behavior could be due to poor data or due to the failure of Kay's rule to correlate

the data in this region.

9. The BWR equation of state was found to give a good representation of the vapor region for various corresponding states compressibility factor correlations.
10. The Redlich-Kwong equation was found to give the best two-parameter equation of state approximation for the isochores of the reduced correlation by Rowlinson.
11. The work summarized in Appendix F shows that true Z_c factors for binary mixtures have significant and systematic departures from the mole averages of the pure component Z_c values.

7.2 Recommendations

1. Any future experimental program should use much smaller diameter glass beads (200 microns or less) in the packed cell. The smaller beads will prevent gravity segregation of liquids within the pack and should eliminate much of the anomalous non-equilibrium data.
2. Large cylinders of retrograde mixtures should be prepared and stored at pressures above their dew points. These cylinders could be used to obtain identical charges for experiments to determine the effects of rate, bead size and temperature on vaporization of retrograde liquids.
3. The mercury manometer for the gas density balance was a major cause of experimental difficulty and it should be replaced before an extensive experimental program is undertaken. A high precision pressure transducer or a quartz Bourdon tube could be used in place of the manometer.

4. The generalized equation of state procedure developed in this work should be applied to the raw data for some pure components which are known to be of high accuracy. This may involve development of temperature-explicit or pressure-explicit equations for the saturated state.
5. An improved procedure should be developed to insure that the upper pressure limit of the Chao-Seader correlation is never exceeded. This is particularly important for the points used to evaluate the coefficients in the extrapolation formula.
6. The accuracy of the phase density calculations should be improved. This might be achieved by using a more complex mixing rule to calculate pseudocritical temperature. The minimization of density errors is important since density is used to calculate the system composition for the next flash. Errors at any flash are carried forward and can accumulate to a significant amount.
7. The phase simulation program developed in this work should be modified so that it can be applied to more than three components. This would require a different search procedure for the mixture having a critical temperature equal to the system temperature.

NOMENCLATURE

A, B, C, D, E, F, G, H	= functions of specified arguments or coefficients depending upon usage
K	= equilibrium ratio or K-value
P	= pressure
P_k	= convergence pressure
R	= universal gas constant
T	= temperature
V	= volume
X	= dummy variable
Z	= compressibility factor
a, b	= coefficients in a two-parameter equation of state
f	= fugacity
k	= constant in Equation 5-4
ln	= natural logarithm
log	= logarithm, base other than e
n	= integer limit
v	= partial molar volume
x	= mole fraction in a liquid solution
y	= mole fraction in a vapor mixture

Greek Letters

α	= Riedel factor
γ	= activity coefficient
δ	= solubility parameter
δ_c	= parameter to characterize the orientational forces between molecules
ϵ	= small value used as a convergence criterion

ν = fugacity coefficient in the liquid solution
 ρ = density
 ϕ = fugacity coefficient in the vapor mixture
 ω = acentric factor

Subscripts

c = value at the critical state
 i, j, m, n = integer indices
 L = liquid phase property
 p = pseudo property
 r = reduced value of the variable
 s = value of the variable at saturation
 v = vapor phase property

$$\text{standard error} = \sqrt{\frac{1}{n} \sum_{i=1}^n \left(\frac{x_{\text{data}} - x_{\text{calc}}}{x_{\text{data}}} \right)^2}$$

REFERENCES

1. Katz, D.L., and Kurata, F., "Retrograde Condensation", *Ind. Eng. Chem.*, 32, 817, (1940).
2. Standing, M.B., Lindblad, E.N., and Parsons, R.L., "Calculated Recoveries by Cycling from a Retrograde Reservoir of Variable Permeability", *Pet. Trans. A.I.M.E.*, 174, 165, (1948).
3. Havlena, Z.G., Griffith, J.D., Pot, R., and Kiel, O.C., "Condensate Recovery by Cycling at Declining Pressure", *Proc. 7th. World Pet. Congress*, Vol. 6, 383, (1967).
4. Weinaug, C.F., and Cordell, J.C., "Revaporization of Butane and Pentane from Sand", *Pet. Trans. A.I.M.E.*, 179, 303, (1948).
5. Oxford, C.W., and Huntington, R.L., "Vaporization of Hydrocarbons from an Unconsolidated Sand", *Pet. Trans. A.I.M.E.*, 198, 318, (1953).
6. Gimatudinov, Sh.K., and Shedlovsky, A.N., "Saturation Pressure of Gas-Oil Systems in a Porous Medium", *Ivz. Vyssh. Ucheb. Zaved., Neft i Gaz*, No. 2, 29, (1963).
7. Tindy, R., and Raynal, M., "Are Test-Cell Saturation Pressures Accurate Enough?", *Oil and Gas J.*, 64, No. 49, 126, (1966).
8. Durmishyan, A.G., Mamedov, Yu.G., Mirzadzanzade, A.X., Rafibeili, N.M., and Sadykh-Zade, E.S., "Experimental Investigation of the Thermodynamic and Hydrodynamic Properties of Gas-Condensate Mixtures in Flow Through Porous Media", *Ivz. Akad. Nauk. SSSR, Mekh I Mashinostr.*, 1, 133, (1964).
9. Sadykh-Zade, E.S., Mamedov, Yu.G., and Rafibeili, N.M., "Determination of the Dynamic Pressure of the Beginning of Condensation in the Presence of a Porous Media", *Ivz. Vyssh. Ucheb. Zaved., Neft i Gaz*, No. 12, 33, (1963).
10. Mamedov, Yu.G., "The Experimental Study of the Depletion (Filtration) Process of Gas-Condensate Mixtures in Porous Media", *Dissertation Work, Azineftechim*, (1964).
11. Zadora, G.I., "An Apparatus for Studying Condensation and Evaporation of Gas-Condensate Mixtures in a Porous Medium", *Ivz. Vyssh. Ucheb. Zaved., Neft i Gaz*, No. 7, 39, (1965).

12. Trebin, F.A., and Zadora, G.I., "Experimental Study of the Effect of a Porous Media on Phase Changes in Gas-Condensate Systems", *Ivz. Vyssh. Ucheb. Zaved., Neft i Gaz*, No. 8, 37, (1968).
13. Smith, L.R., and Yarborough, L., "Equilibrium Revaporization of Retrograde Condensate by Dry Gas Injection", *Soc. Pet. Eng. J.*, 8, 87, (1968).
14. Sadykh-Zade, E.S., Aslanov, Sh.S., Ismailov, D.Kh., Khydyrkuliev, B., and Iskenderov, G.M., "Loss of Condensate During Complete Depletion of Gas-Condensate Fields", *Ivz. Vyssh. Ucheb. Zaved., Neft i Gaz*, No. 12, 45, (1968).
15. Rafibeili, N.M., and Sadykhov, A.M., "Effect of Inert Gas on Thermodynamic Nonequilibrium of Gas-Crude Oil Systems", *Dokl. Akad. Nauk. Azerbaidzh. SSSR*, 24, No. 5, 24, (1968).
16. Sadykh-Zade, E.C., Ismailov, D.Kh., Karakashev, V.K., and Abdullaev, A.A., "Study of the Process of Establishing Equilibrium in the Condensation of Gas-Condensate Systems", *Ivz. Vyssh. Ucheb. Zaved., Neft i Gaz*, No. 2, 41, (1968).
17. Clark, C.R., "Adsorption and Desorption of Light Paraffinic Hydrocarbons in Dry and Water-Saturated Sand-Clay Packs: Studies to Determine the Effect of these Phenomenon on the P-V-T Behavior of Natural Gases and Gas Condensates in the Reservoir", Ph.D. Thesis, Univ. of Kansas, Lawrence, (1969).
18. Ham, J.D., and Eilerts, C.K., "Effect of Saturation on Mobility of Low Liquid-Vapor Ratio Fluids", *Soc. Pet. Eng. J.*, 7, 11, (1967).
19. Efros, D.A., "Permeability of Porous Media During the Filtration of a Gassed Liquid", *Dokl. Akad. Nauk. SSSR*, 132, No. 2, 311, (1960).
20. Hurst, W., Goodson, W.C., and Leeser, R.E., "Aspects of Gas Deliverability", *Pet. Trans. A.I.M.E.*, 228, 668, (1963).
21. Weibe, R., and Gaddy, V.L., "Solubility of Carbon Dioxide in Water", *J. Am. Chem. Soc.*, 61, 315, (1939).
22. Selleck, F.T., Carmichael, L.T., and Sage, B.H., "Phase Behavior in the Hydrogen Sulfide-Water System", *Ind. Eng. Chem.*, 44, 2219, (1952).
23. Kobayashi, R., and Katz, D.L., "Vapor-Liquid Equilibria for Binary Hydrocarbon-Water Systems", *Ind. Eng. Chem.*, 45, 440, (1953).

24. Aslanov, Sh.S., Mamedov, Yu.G., Peisakhov, S.I., and Sadykh-Zade, E.S., "The Effect of Gas Sorption on Rock Permeability in the Presence of a Residual Water Saturation", *Ivz. Vyssh. Ucheb. Zaved., Neft i Gaz*, No. 8, 51, (1965).
25. Aslanov, Sh.S., Mamedov, Yu.G., Peisakhov, S.I., and Sadykh-Zade, E.S., "The Effect of Gas-Condensate Desorption on Rock Permeability in the Presence of a Residual Water Saturation", *Ivz. Vyssh. Ucheb. Zaved., Neft i Gaz*, No. 9, 53, (1965).
26. Morrow, N.R., Purvis, R.A., and Sigmund, P.M., "Retrograde Condensation in Porous Media", *Petroleum Recovery Research Report, RR-6*, Calgary, Dec., (1970).
27. Chao, K.C., and Seader, J.D., "A General Correlation of Vapor-Liquid Equilibria in Hydrocarbon Mixtures", *A.I.Ch.E.J.*, 7, 598, (1961).
28. Green, K.J., and Hachmuth, K.H., "An Analytic Correlation of Vapor-Liquid Phase Equilibria from Paraffin Hydrocarbon Binary Systems", *Nat. Gas Processors Assoc., Proc.* 41, 11, (1964).
29. Rowe, A.M., "The Critical Composition Method - A New Convergence Pressure Method", *Soc. Pet. Eng. J.*, 7, 54, (1967).
30. Standing, M.B., and Katz, D.L., "Density of Natural Gases", *Pet. Trans. A.I.M.E.*, 146, 140, (1942).
31. Lydersen, A.L., Greenkorn, R.A., and Hougen, O.A., "Generalized Thermodynamic Properties of Pure Fluids", *University of Wisconsin, Eng. Expt. Sta. Rept. No. 4*, Madison, Wisc., Oct., (1955).
32. Sage, B.H., Hicks, B.L., and Lacey, W.N., "Phase Equilibria in Hydrocarbon Systems. The Methane-n-Butane System in the Two-Phase Region", *Ind. Eng. Chem.*, 32, 1085, (1940).
33. Sage, B.H., Reamer, H.H., Olds, R.H., and Lacey, W.N., "Phase Equilibria in Hydrocarbon Systems. Volumetric and Phase Behavior of Methane-n-Pentane System", *Ind. Eng. Chem.*, 34, 1108, (1942).
34. Wagner, O.R., and Leach, R.O., "Effect of Interfacial Tension on Displacement Efficiency", *Soc. Pet. Eng. J.*, 6, 335, (1966).
35. Poston, R.S., and McKetta, J.J., "Vapor-Liquid Equilibrium in the Methane-n-Hexane System", *J. Chem. Eng. Data*, 11, 362, (1966).

36. Shim, J., and Kohn, J.P., "Multiphase and Volumetric Equilibria of Methane-n-Hexane Binary System at Temperatures Between -110° and 150°C.", *J. Chem. Eng. Data*, 7, 3, (1962).
37. Sage, B.H., and Lacey, W.N., Thermodynamic Properties of the Lighter Paraffin Hydrocarbons and Nitrogen, Am. Pet. Inst., New York, (1950).
38. NGSMA Data Book: 6th Ed., Natural Gasoline Supply Men's Assoc., Tulsa, Okla., (1951).
39. Hanson, G.H., and Brown, G.G., "Vapor-Liquid Equilibria in Mixtures of Volatile Paraffins", *Ind. Eng. Chem.*, 37, 821, (1945).
40. NGSMA Data Book: 7th Ed., Natural Gasoline Supply Men's Assoc., Tulsa, Okla., (1957).
41. NGPA Data Book: 8th Ed., Natural Gas Processors Suppliers Assoc., Tulsa, Okla., (1966).
42. NGAA - K Coefficients, I.B.M. Card Deck, Natural Gasoline Supply Men's Assoc., Tulsa, Okla., (1957).
43. Schlaudt, R.C., "Critical Convergence Pressure--A Criterion for Selecting Equilibrium Ratios for Complex Hydrocarbon Mixtures", Ph.D. Thesis, Texas A. and M. Univ., 1968.
44. Hadden, S.T., "Convergence Pressure in Hydrocarbon Vapor-Liquid Mixtures", *Chem. Eng. Prog. Symp. Series*, 49, No. 7, 53, (1953).
45. Grieves, R.B., and Thodos, G., "The Critical Temperatures of Ternary Hydrocarbon Systems", *Ind. Eng. Chem. Fund.*, 1, 45, (1962).
46. Chueh, P.L., and Prausnitz, J.M., "Vapor-Liquid Equilibria at High Pressures: Calculation of Critical Temperatures, Volumes, and Pressures of Nonpolar mixtures", *A.I.Ch.E.J.*, 13, 1107, (1967).
47. Grieves, R.B., and Thodos, G., "The Critical Temperatures and Pressures of Binary Systems: Hydrocarbons of All Types and Hydrogen", *A.I.Ch.E.J.*, 6, 561, (1960).
48. Grieves, R.B., and Thodos, G., "The Critical Temperatures of Multicomponent Hydrocarbon Systems", *A.I.Ch.E.J.*, 8, 550, (1962).
49. Grieves, R.B., and Thodos, G., "The Critical Temperatures and Critical Pressures of Binary Mixtures of the Fixed Gases and Aliphatic Hydrocarbons", *Soc. Pet. Eng. J.*, 2, 197, (1962).

50. Kurata, F., and Katz, D.L., "Critical Properties of Volatile Hydrocarbon Mixtures", *Trans. A.I.Ch.E.*, 38, 995, (1942).
51. Mayfield, F.D., "Critical States of Two-Component Paraffin Systems", *Ind. Eng. Chem.*, 34, 843, (1942).
52. Etter, D.O., and Kay, W.B., "Critical Properties of Mixtures of Normal Paraffin Hydrocarbons", *J. Chem. Eng. Data*, 6, 409, (1961).
53. Davis, P.C., Bertuzzi, A.F., Gore, T.L., and Kurata, F., "The Phase and Volumetric Behavior of Natural Gases at Low Temperatures and High Pressures", *Pet. Trans. A.I.M.E.*, 201, 245, (1954).
54. Grieves, R.B., and Thodos, G., "The Critical Pressures of Multicomponent Hydrocarbon Mixtures and the Critical Densities of Binary Hydrocarbon Mixtures", *A.I.Ch.E.J.*, 9, 25, (1963).
55. Simon, R., and Yarborough, L., "A Critical Pressure Correlation for Gas-Solvent-Reservoir Oil Systems", *Pet. Trans. A.I.M.E.*, 228, 556, (1963).
56. Sutton, J.R., "The Critical Pressure of Multi-Component Mixtures", *Advances in Thermophysical Properties at Extreme Temperatures and Pressures*, A.S.M.E., New York, N.Y., 76, (1965).
57. Curl, R.F., Jr., and Pitzer, K.S., "Volumetric and Thermodynamic Properties of Fluids - Enthalpy, Free Energy, and Entropy", *Ind. Eng. Chem.*, 50, 265, (1958).
58. Hildebrand, J.H., and Scott, R.L., The Solubility of Nonelectrolytes, 3 Ed., Reinhold, New York, (1950).
59. Redlich, O., and Kwong, J.N.S., "On the Thermodynamics of Solutions. V. An Equation of State. Fugacities of Gaseous Solutions", *Chem. Rev.*, 44, 233, (1949).
60. Besserer, G.J., Private Communication, (1971).
61. Beattie, J.A., and Bridgeman, O.C., "A New Equation of State for Fluids", *Proc. Natl. Acad. Sci., U.S.*, 63, 229, (1928).
62. Benedict, M., Webb, G.B., and Rubin, L.C., "An Empirical Equation for Thermodynamic Properties of Light Hydrocarbons and Their Mixtures", *J. Chem. Phys.*, 8, 334, (1940).
63. Su, G.J., and Chang, C.H., "Generalized Beattie-Bridgeman Equation of State for Real Gases", *J. Am. Chem. Soc.*, 68, 1080, (1946).

64. Opfell, J.B., Sage, B.H., and Pitzer, K.S., "Application of Benedict Equation to Theorem of Corresponding States", *Ind. Eng. Chem.*, 48, 2069, (1956).

65. Su, G.J., and Viswanath, D.S., "Generalized Benedict-Webb-Rubin Equation of State for Real Gases", *A.I. Ch.E.J.*, 11, 205, (1965).

66. Hirschfelder, J.O., Beuhler, R.J., McGee, H.A., and Sutton, J.R., "A Generalized Equation of State for Both Gases and Liquids", *Ind. Eng. Chem.*, 50, 375, (1955).

67. Yen, L.C., and Woods, S.S., "A Generalized Equation for Computer Calculation of Liquid Densities", *A.I.Ch. E.J.*, 12, 95, (1966).

68. Pitzer, K.S., "The Volumetric and Thermodynamic Properties of Fluids: I. Theoretical Basis and Virial Coefficients", *J. Am. Chem. Soc.*, 77, 3427, (1955).

69. Riedel, L., "Eine Neue Universelle Dampfdruckformel", *Chemie. Ing. Tech.*, 26, 83, (1954);
 "Die Flüssigkeitsdichte im Sättigungszustand", *Ibid*, 259;
 "Kritischer Koeffizient, Dichte des gesättigten Dampfes und Verdampfungswärme", *Ibid*, 679;
 "Kompressibilität, Oberflächenspannung und Wärmeleitfähigkeit im flüssigen Zustand", *Chemie. Ing. Tech.*, 27, 209, (1955);
 "Die Bestimmung unbekannter kritischer Daten von nicht assoziierenden Stoffen", *Ibid*, 475;
 "Die Zustandsfunktion des realen Gases", *Ibid*, 557.

70. Martin, J.J., and Hou, Yu-Chun, "Development of an Equation of State for Gases", *A.I.Ch.E.J.*, 1, 142, (1955).

71. Bono, J.L., and Starling, K.S., "Proper Selection of the Response Variate in Applied Regression Analysis", *Can. J. Chem. Eng.*, 48, 468, (1970).

72. Bishnoi, P.R., and Robinson, D.B., "An Evaluation of Methods for Determining Equation of State Parameters Using Volumetric and Heat Capacity Data", *Can. J. Chem. Eng.*, 49, 642, (1971).

73. Davis, B.W., and Rice, O.K., "Thermodynamics of the Critical Point: Liquid-Vapor Systems", *J. Chem. Phys.*, 47, 5043, (1967).

74. Rackett, H.G., "Equation of State for Saturated Liquids", J. Chem. Eng. Data, 15, 514, (1970).
75. Reid, R.C., and Sherwood, T.K., The Properties of Gases and Liquids, 2nd Ed., McGraw Hill, New York, (1966).
76. Bradford, M.L., and Thodos, G., "Densities of Hydrocarbons in their Saturated Vapor and Liquid States", Can. J. Chem. Eng., 46, 277, (1968).
77. Marquardt, D.W., "An Algorithm for Least Squares Estimation of Non-Linear Parameters", J. Soc. Ind. Appl. Math., 11, 431, (1963).
78. Brown, G.G., and Holcomb, D.E., "The Compressibility of Gases and Vapor-Liquid Phase Equilibria in Hydrocarbon Systems", Petroleum Engineer, 11, 23, (1940).
79. Kay, W.B., "Density of Hydrocarbon Gases and Vapors at High Temperature and Pressure", Ind. Eng. Chem., 28, 1014, (1936).
80. Poettmann, F.H., "The Calculation of Pressure Drop in the Flow of Natural Gas Through Pipe", Pet. Trans. A.I.M.E., 192, 317, (1951).
81. Sukkar, Y.K., and Cornell, D., "Direct Calculation of Bottom Hole Pressures in Natural Gas Wells", Pet. Trans. A.I.M.E., 204, 43, (1955).
82. Trube, A.S., "Compressibility of Natural Gases", Pet. Trans. A.I.M.E., 210, 355, (1957).
83. Katz, D.L., Cornell, D., Kobayashi, R., Poettman, F.H., Vary, J.A., Elenbaas, J., and Weinaug, C.F., Handbook of Natural Gas Engineering, McGraw-Hill, New York, 710, (1959).
84. Matthews, T.A., Roland, C.H., and Katz, D.L., "High Pressure Gas Measurement", Petrol. Refiner, 21, No. 6, 58, (1942).
85. Rowlinson, J.S., "The Reduced Equation of State", Trans. Far. Soc., 51, 1317, (1955).
86. Rowlinson, J.S., "The Equilibrium Properties of Assemblies of Non-Spherical Molecules", Trans. Far. Soc., 50, 647, (1954).
87. Wiese, H.C., Jacobs, J., and Sage, B.H., "Phase Equilibria in the Hydrocarbon Systems. Phase Behavior in the Methane-Propane-n-Butane System", J. Chem. Eng. Data, 15, 82, (1970).

88. Carter, R.T., Sage, B.H., and Lacey, W.N., "Phase Behavior in the Methane-Propane-n-Pentane System", Pet. Trans. A.I.M.E., 142, 170, (1941).
89. Dourson, R.H., Sage, B.H., and Lacey, W.N., "Phase Behavior in the Methane-Propane-n-Pentane System", Pet. Trans. A.I.M.E., 151, 206, (1942).
90. Wiese, H.C., Reamer, H.H., and Sage, B.H., "Phase Equilibria in Hydrocarbon Systems. Phase Behavior in the Methane-Propane-n-Decane System", J. Chem. Eng. Data, 15, 75, (1970).
91. Reamer, H.H., Fiskin, J.M., and Sage, B.H., "Phase Equilibria in Hydrocarbon Systems. Phase Behavior in the Methane-n-Butane-Decane at 160°F.", Ind. Eng. Chem., 41, 2871, (1949).
92. Reamer, H.H., Sage, B.H., and Lacey, W.N., "Phase Equilibria in Hydrocarbon Systems. Volumetric and Phase Behavior of the Methane-n-Butane-Decane System", Ind. Eng. Chem., 43, 1436, (1951).

APPENDIX A
LEAST SQUARES FITTING TECHNIQUES

A.1 Foreword

Several attempts were made to obtain suitable approximations for the various corresponding states correlations. Initially compressibility factors were approximated by power polynomials in reduced pressure and reduced temperature. The usual problem of the least squares normal equations forming an ill-conditioned matrix was avoided by using orthogonal polynomials. However, orthogonal polynomials had the disadvantage that values of the dependent variable were required at every point in the rectangular grid covered by the values selected for the independent variables. This disadvantage did not present any problem when reduced pressure and reduced temperature were used as independent variables since the correlations are normally tabulated in this fashion. The problem was that functional forms which used reduced temperature and reduced pressure were not very satisfactory for approximating the correlations.

The next attempt at approximating the correlations used power polynomials in reduced temperature and reduced density. These functions resulted in better approximations but orthogonal polynomials could not be used unless the data was plotted and extrapolated so that the dependent variable was known at every point in the grid formed by the independent variables. At this point linear programming was considered. This method was soon rejected because if the functional form was satisfactory it was tantamount to basing the approximation on the poorest data points (extreme points) in the correlation.

Finally, it was decided to attempt to use some of the well-known equations of state. These equations are usually non-linear with respect to their parameters. The parameters for non-linear equations can be conveniently estimated by an algorithm proposed by Marquardt⁷⁷ provided that the matrix that forms the normal equations is not ill-conditioned. This restriction has the effect of limiting the number of parameters to about twelve.

A.3 Computer Program

A listing of the FORTRAN program used to fit the Standing and Katz correlation to a reduced form of the B-W-R equation is reproduced on pages A-3 to A-9. The main program reads the data, calculates the matrix for the normal equations, uses Marquardt's algorithm to improve the current estimates for the least squares parameters, and controls the print out of the report. The reduced form of the B-W-R equation was specified in a function subprogram. The program could be adapted to other equations of state simply by changing the function subprogram and the statements containing the partial derivatives with respect to the least squares parameters.

The inverse of the matrix was calculated by two subroutines. Subroutine PARTN partitioned the matrix into upper and lower triangular matrices. Subroutine INVER calculated the inverses of the triangular matrices and multiplied them together to obtain the inverse matrix. This method of direct inversion may be subject to round-off error. A test was made to see if round-off was significant and, if necessary, subroutine IMPRO was used to improve the inverse matrix.


```

IMPLICIT REAL*8 (A-H, -Z)
DIMENSION R(75), F2(75,20), TR(20), PR(40), PE(75),
1 DF(10), D(10,10), U(10,10), ALHS(10,10), B(10), A(10), RHS(10),
2 C(10), L(10), M(75)
COMMON ALHS, D, U
1 FORMAT(20F4.3)
2 FORMAT(1X,6E20.8)
3 FORMAT(1 1)
4 FORMAT(1X,F5.2,1X,20F5.1)
5 FORMAT(1X,1s)
6 FORMAT(7X,20F5.2,/)
7 FORMAT('1'1)
8 FORMAT('CAUTION: IMPROV USED 10 ITERATIONS')
9 FORMAT('APPROXIMATION OF STANDING-KATZ CORRELATION WITH R48')
M=0
AN=4
N=0
S=0.0
Lc=75
LL=20
READ(5,1)W1
READ(5,1)(TR(L),L=1,LL)
READ(5,1)(PR(I),I=1,12)
DO 20 I=1,12
READ(5,1)(F2(I,L),L=1,LL)
DO 19 L=1,LL
1F(F2(I,L))19,19,19
1c N=N+1
S=S+F2(1,L)
19 CONTINUE
20 CONTINUE
AN=N
WRITE(6,2)S
WRITE(6,5)N
DO 95 IWT=2,3
WRITE(6,7)
A(1)=0.1743
A(2)=-0.609
A(3)=-0.421
A(4)=0.655
A(5)=-0.16
A(6)=-0.081
A(7)=0.985
A(8)=0.58
A(9)=1.0
A(10)=1.0
DO 70 ITER=1,11
VAR1=0.0
VAR2=0.0
DO 21 I=1,M
C(I)=A(I)
B(I)=0.0
RHS(I)=0.0
DO 21 J=1,I
ALHS(I,J)=0.0

```



```

21 CONTINUE
DO 40 I=1,IE
DO 40 L=1,LL
W=1.0
IF(L.EQ.1)W=W1(1)
IF(L.EQ.2)W=W1(1)
IF(L.EQ.3)W=2.0
IF(L.EQ.18)W=2.0
IF(L.EQ.19)W=0.0
IF(L.EQ.20)W=10.0
R(1)=R0(1)*0.2707*(F2(1,1)*TR(L))
32 F=FCALC(R(1),TR(L),A(1),A(2),A(3),A(4),A(5),A(6),A(7),A(8),A(9),
     A(10))
R2=R(1)**2
DF(1)=T(1)
DF(2)=R(1)/TR(L)
DF(3)=R(1)/TR(L)**3
DF(4)=R2
DF(5)=R2/TR(L)+A(6)*R(1)**5/TR(L)
DF(6)=A(5)*R(1)**5/TR(L)
DF(7)=R2/TR(L)**2*(1.0+A(8)*R2)*DEXP(-A(8)*R2)
DF(8)=-A(7)*A(8)*R(1)**6/TR(L)**3*DEXP(-A(8)*R2)
VAR1=VAR1+(F2(1,L)-F)**2*W
VAR2=VAR2+(1.0+r/F2(1,L))**2*W
DO 23 J=1,M
1F(1WT-Z)22,Z3,Z4
22 RHS(J)=RHS(J)+(F2(1,L)-F)*DF(J)
GO TO 25
23 RHS(J)=RHS(J)+(F2(1,L)-F)*DF(J)/F2(1,L)**2*W
GO TO 25
24 RHS(J)=RHS(J)+(F2(1,L)-F)*DF(J)*r
25 CONTINUE
DO 33 K=1,M
1F(1WT-Z)26,Z7,Z8
26 ALHS(J,K)=ALHS(J,K)+DF(J)*DF(K)
GO TO 29
27 ALHS(J,K)=ALHS(J,K)+DF(J)*DF(K)/F2(1,L)**2*W
GO TO 29
28 ALHS(J,K)=ALHS(J,K)+DF(J)*DF(K)**2
29 CONTINUE
33 CONTINUE
40 CONTINUE
1F(1WT-1)34,34,35
34 ALAS=0.01
35 DO 36 I=1,M
B(I)=ALHS(I,I)
36 CONTINUE
RMS1=DSQRT(VAR1/AN)
RMS2=DSQRT(VAR2/AN)
WRITE(6,2)(A(J),J=1,M),RMS1,RMS2
WRITE(5,3)
41 DO 42 I=1,M
ALAS(I,I)=R(I)+ALAS
42 CONTINUE
CALL PARIN(M)

```



```

CALL INVER(M)
CALL INPER(M,KEY)
10 WRITE(6,10)
11 READ(6,11)
12 IF(11.EQ.0,13,14)
13 ICOUNT=0
14 DO 15 J=1,M
15 E(J)=0.0
16 DO 17 K=1,M
17 E(J)=E(J)+D(J,K)*ABS(K)
18 CONTINUE
19 A(J)=C(J)+E(J)
20 TEST=0.000005
21 IF(TEST-0.000005)51,51,55
22 ICODE=1
23 CONTINUE
24 IF(ICODE)50,50,25
25 RMS1=0.0
26 RMS2=0.0
27 DO 44 I=1,15
28 DO 44 L=1,LL
29 W=1.0
30 IF(L.EQ.1)W=WL(1)
31 IF(L.EQ.2)W=WL(1)
32 IF(L.EQ.3)W=WL(1)
33 IF(L.EQ.4)W=WL(1)
34 IF(L.EQ.5)W=WL(1)
35 IF(L.EQ.6)W=WL(1)
36 IF(L.EQ.7)W=WL(1)
37 E(I)=PR(I)*0.27C/(E2(I,L)*TR(L))
38 F=FCALC(R(1),TR(L),A(1),A(2),A(3),A(4),A(5),A(6),A(7),A(8),A(9),
39 A(10))
40 RMS1=RMS1+(F2(I,L)-F)**2*W
41 RMS2=RMS2+(1.0+1/E2(I,L))**2*W
42 CONTINUE
43 WRITE(6,2)RMS1,VAR1,RMS2,VAR2
44 IF(1WT-2)45,46,45
45 IF(RMS1-VAR1)45,45,49
46 IF(RMS2-VAR2)45,45,49
47 ALAM=ALAM/10.0
48 GO TO 47
49 ALAM=ALAM*10.0
50 GO TO 41
51 WRITE(6,3)
52 CONTINUE
53 CONTINUE
54 VAR1=0.0
55 VAR2=0.0
56 LS=1
57 LE=20
58 WRITE(6,7)
59 WRITE(6,8)
60 WRITE(6,9)(TR(L),L=LS,LE)
61 DO 90 I=1,15
62 DO 92 L=LS,LE
63 PE(L)=0.0
64 R(I)=PR(I)*0.27C/(E2(I,L)*TR(L))

```



```

F=FCALC(R(1),TH(L),A(1),A(2),A(3),A(4),A(5),A(6),A(7),A(8),A(9),
1,A(10))
VAR1=VAR1+(F2(I,L)-F)**2
VAR2=VAR2+(1.0-F/F2(I,L))**2
PE(L)=100.0*(1.0-F/F2(I,L))
92 CONTINUE
WRITE(6,4)PR(I),(PE(L),L=LS,LL)
93 CONTINUE
WRITE(6,5)
RMS1=DSQRT(VAR1/NA)
RMS2=DSQRT(VAR2/NA)
WRITE(6,2)RMS1,RMS2
95 CONTINUE
STOP
END

```

```

DOUBLE PRECISION FUNCTION FCALC(R,T,A1,A2,A3,A4,A5,A6,A7,A8,A9,A10)
1) IMPLICIT REAL*8(A-H,O-Z)
R2=R**R
FCALC=1.0+(A1+A2/T+A3/T**2)*R+(A4+A5/T)+A6*T+A7*T**2+A8*T**3+A9*T**4+A10*T**5
1) A7*R2/T**3+(1.0+A8*R2)*DEXP(-A9*R2)
RETURN
END

```



```

SUBROUTINE PARTN(N)
  DOUBLE PRECISION A(10,10), D(10,10), U(10,10)
  COMMON A, D, U
  INTEGER I, J, K, N, KPI, KM1
  DO 1 I=1,N
  DO 1 J=1,N
  D(I,J)=0.0
  U(I,J)=0.0
1 CONTINUE
  DETERMINE D AND U TRIANGULAR MATRICES SUCH THAT A=UDU
  D(1,1)=1.0
  D(1,1)=A(1,1)
  DO 2 J=2,N
  U(1,J)=A(1,J)
  D(J,1)=A(J,1)/U(1,1)
2 CONTINUE
  DO 7 K=2,N
  KM1=K-1
  KPI=K+1
  DO 3 J=K,N
  U(K,J)=A(K,J)
  DO 3 I=1,KM1
  D(K,J)=U(K,J)-D(K,I)*U(I,J)
3 CONTINUE
  D(K,K)=1.0
  IF(KPI=N)4,6,7
4 DO 6 I=KPI,N
  D(I,K)=A(I,K)
  DO 5 J=1,KM1
  D(I,K)=D(I,K)-U(J,K)*D(I,J)
5 CONTINUE
  D(I,K)=D(I,K)/U(K,K)
6 CONTINUE
7 CONTINUE
  RETURN
  END

```



```

SUBROUTINE INVER(N)
DOUBLE PRECISION A(10,10), D(10,10), U(10,10), P(10,10), Q(10,10)
COMMON A, D, U
INTEGER I, J, K, N, IM1, IP1, JM1, IR
DO 2 I=1,N
DO 1 J=1,N
P(I,J)=0.0
Q(I,J)=0.0
1 CONTINUE
P(I,I)=1.0/U(I,I)
Q(I,I)=1.0/D(I,I)
2 CONTINUE
C CALCULATE P, THE INVERSE OF U
DO 4 J=2,N
JM1=J-1
DO 4 K=1, JM1
I=J-K
IP1=I+1
DO 3 IR=IP1,J
P(I,J)=P(I,J)+U(I,IR)*P(IR,J)
3 CONTINUE
P(I,J)=-P(I,J)/U(I,I)
4 CONTINUE
C CALCULATE Q, THE INVERSE OF D
DO 6 I=2,N
IM1=I-1
DO 6 K=1, IM1
J=I-K
DO 5 IR=J, I-1
Q(I,J)=Q(I,J)+D(I,IR)*Q(IR,J)
5 CONTINUE
Q(I,J)=-Q(I,J)/D(I,I)
6 CONTINUE
C MULTIPLY P*Q TO OBTAIN INVERSE OF A
DO 7 I=1,N
DO 7 J=1,N
U(I,J)=0.0
DO 7 K=1,N
D(I,J)=D(I,J)+P(I,K)*Q(K,J)
7 CONTINUE
RETURN
END

```



```

SUBROUTINE IMPRO(N,KEY)
COMMON /Matrices/ A,B,C,D,E,F,G,H,I,J,L,U,V,W,X,Y,Z
COMMON A, B, U
INTEGER I, J, K, L, N, KEY
KEY=0
DO 6 L=L,1,6
MAX=0.000
DO 4 I=1,N
DO 1 J=1,N
U(I,J)=0.000
DO 3 K=1,N
U(I,J)=U(I,J)+A(I,K)*D(K,J)
2 CONTINUE
DO 5 I=1,N
U(I,I)=U(I,I)+1.000
DO 3 J=1,N
IF(DABS(U(I,J))-MAX)>0.001
3 MAX=DABS(U(I,J)))
5 MAX=0.000
3 CONTINUE
1 IF(MAX-1.00>6)7,7,4
4 DO 6 I=1,N
DO 6 J=1,N
ERR=0.000
DO 5 K=1,N
ERR=ERR+D(I,K)*U(K,J)
5 CONTINUE
6 U(I,J)=U(I,J)-ERR
6 CONTINUE
KEY=1
7 RETURN
END

```


APPENDIX B
TWO-PARAMETER EQUATIONS OF STATE

B.1 Foreword

Some of the classical two-parameter equations of state are reviewed in this appendix. Particular attention was given to the functional forms these equations have for approximating isochores. The objective of this investigation was to gain some insight as to what functions might be appropriate for approximating the reduced isochores of various corresponding states density correlations. A test of the suitability of each equation was made by fitting the reduced form of the equation to the ZT_r isochores of Rowlinson's correlation.

B.2 van der Waals Equation

The early work of van der Waals forms the basis of the theorem of corresponding states. Based on kinetic considerations and the fact that on a pressure versus volume plot the critical isotherm has a slope equal to zero, and a point of inflection, at the critical state, van der Waals proposed the equation

$$P + a/V^2 = RT/(V - b) \quad (B-1)$$

The term a/V^2 was intended to account for the intermolecular attractive forces (cohesive pressure), and the parameter b was to allow for the volume occupied by the molecules. The two constraints on the critical isotherm at the critical point can be expressed in equation form.

$$(\partial P / \partial V)_T = -RT_c / (V_c - b)^2 + 2a/V_c^3 = 0 \quad (B-2)$$

$$(\partial^2 P / \partial V^2)_T = 2RT_c / (V_c - b)^3 - 6a/V_c^4 = 0 \quad (B-3)$$

Equations B-1, B-2 and B-3 can be solved for the critical

constants with the result

$$P_c = a/(27 b^2) \quad V_c = 3 b \quad T_c = 8 a/(27 bR) \quad (B-4)$$

These values for the critical constants imply that

$$Z_c = P_c V_c / (RT_c) = 3/8 \quad (B-5)$$

for all substances. Equations B-4 and B-5 can be used to develop the reduced form of van der Waals equation.

$$P_r + 3/V_r = 8 T_r / \{3(V_r - 1/3)\} \quad (B-6)$$

Equation B-6 is a cubic equation in V_r which can be rewritten in terms of the compressibility factor.

$$Z^3 + \left(\frac{P_r}{8 T_r} + 1 \right) Z^2 + \left(\frac{27 P_r}{64 T_r^2} \right) Z - \frac{27 P_r^2}{512 T_r^3} = 0 \quad (B-7)$$

Since a cubic equation can be solved explicitly, Equation B-7 illustrates that $Z = f(P_r, T_r)$, which is a statement of the law of corresponding states. This law states that when different substances are subjected to conditions such that they have the same reduced pressure and reduced temperature, they will have the same compressibility factor. An expression similar to Equation B-7 can be developed for every two-parameter equation of state provided it has an algebraic form capable of giving a point of inflection at the critical state.

Even though two-parameter equations of state fail to correctly describe the critical state and dense fluid regions, graphical representations of the relation $Z = f(P_r, T_r)$ have good accuracy. For desk calculations graphical representations are convenient, however, for computer applications an analytical formulation is required. Selection of P_r and T_r

for independent variables results in an explicit solution, but a difficult ZPT surface to approximate. When V_r is taken as one of the independent variables the solution becomes implicit, however, the ZVT or ZVP surfaces are not as difficult to approximate.

Two density-implicit formulations are possible for the compressibility factor. Selection of V_r and P_r as independent variables for van der Waals equation results in the following expression

$$Z = 3 P_r V_r^3 / (3 P_r V_r^3 - 9 V_r - P_r V_r^2 + 3) \quad (B-8)$$

When V_r and T_r are selected for independent variables Z can be calculated from the expression

$$Z = V_r / (V_r - 1/3) - 9 / (8 T_r V_r) \quad (B-9)$$

Equation B-8 predicts the P_r/Z isochores to have the following form

$$P_r/Z = P_r - 3/V_r^2 - P_r/(3 V_r) + 1/V_r^3 \quad (B-10)$$

Differentiation of Equation B-10 with respect to P_r indicates that van der Waals equation predicts linear isochores with slopes equal to

$$(\partial(P_r/Z)/\partial P_r)_{V_r} = 1 - 1/(3 V_r) = (V_r - 1/3)/V_r \quad (B-11)$$

A similar development for the ZT_r isochores results in

$$ZT_r = V_r T_r / (V_r - 1/3) - 9 / (8 V_r) \quad (B-12)$$

and differentiation with respect to T_r shows these isochores to have slopes which are the reciprocal of the P_r/Z isochores

$$(\partial(ZT_r)/\partial T_r)_{V_r} = V_r / (V_r - 1/3) \quad (B-13)$$

It should be noted that if $V_r < 1/3$, Equations B-11 and B-13 predict the absurd result that the isochores have a negative slope.

The ZT_r values calculated from Equation B-12 differ from the correlation of Rowlinson by a standard error of 7.81 per cent. As a further test of the suitability of the functional form given by Equation B-12 the two critical state parameters, $a = 9/8$ and $b = 1/3$, were replaced by least squares estimators A and B. After substitution of ρ_r^{-1} for V_r , the following equation was fitted to Rowlinson's correlation.

$$ZT_r = T_r / (1 - B\rho_r) - A\rho_r \quad (B-14)$$

For the 713 points in the reduced density range from 0.05 to 1.0, the standard error was 2.51 per cent, indicating the form to have considerable merit. Table B-1 gives the percentage differences, $100(1 - (ZT_r)_{\text{calc.}} / (ZT_r)_{\text{Rowl.}})$, for a representative number of points. It should be noted from Table B-1 that the largest errors occur along the critical isotherm.

When Equation B-14 was fitted to 893 points with reduced densities ranging from 0.05 to 1.50, the standard error increased to 5.49 per cent. Table B-2 summarizes the percentage errors for this case.

Tables B-1 and B-2 indicate that the largest differences with van der Waals equation occur as the saturated state is approached. Isochores exhibit the greatest curvature as the saturated state is approached, and since van der Waals equation predicts linear isochores, large errors result.

A summary of the pertinent data for approximations of

TABLE 3-1.

TABLE OF APPROXIMATION OF ZT ISOCORES FROM REDUCED CORRELATION BY ROWLINSON.
TABLE OF PERCENTAGE DIFFERENCES BETWEEN CORRELATION AND VAN DER WAALS EQUATION.

T	1.00	1.05	1.10	1.20	1.30	1.40	1.50	1.60	1.70	1.80	1.90	2.00	2.20	2.40	2.60	2.80	3.00
P	0.05	-0.5	-0.3	-0.1	-0.0	0.1	0.2	0.3	0.4	0.5	0.6	0.7	0.8	0.9	0.4	0.5	0.4
0.10	-1.0	-0.6	-0.3	0.1	0.3	0.6	0.9	1.1	1.2	1.3	1.4	1.5	1.6	1.7	1.4	1.5	1.3
0.15	-1.5	-0.9	-0.5	0.2	0.6	1.0	1.3	1.5	1.7	1.9	2.0	2.0	2.0	1.9	1.9	1.8	1.7
0.20	-2.0	-1.2	-0.5	0.4	1.0	1.3	1.5	1.7	1.9	2.1	2.3	2.4	2.4	2.4	2.2	2.2	2.0
0.25	-2.8	-1.5	-0.7	0.6	1.4	1.8	2.0	2.1	2.3	2.4	2.4	2.4	2.4	2.4	2.2	2.2	2.0
0.30	-3.5	-1.9	-0.7	0.7	1.7	2.1	2.5	2.6	2.7	2.9	2.9	2.9	2.9	2.8	2.8	2.5	2.4
0.35	-4.1	-2.4	-1.0	0.9	1.9	2.5	2.8	3.1	3.2	3.3	3.3	3.3	3.3	3.1	3.0	2.8	2.6
0.40	-4.5	-2.6	-1.3	1.0	2.2	2.8	3.3	3.4	3.5	3.5	3.5	3.5	3.5	3.4	3.3	3.1	2.7
0.45	-4.7	-2.7	-1.2	0.9	2.4	3.2	3.5	3.7	3.7	3.8	3.8	3.8	3.8	3.6	3.5	3.2	2.7
0.50	-4.9	-2.8	-1.2	0.9	2.3	3.2	3.5	3.9	3.8	4.0	4.0	4.0	4.0	3.9	3.8	3.5	2.6
0.55	-4.8	-2.7	-1.0	1.0	2.3	3.2	3.6	3.9	3.9	3.9	3.9	3.9	3.9	3.8	3.5	3.3	2.4
0.60	-4.1	-2.2	-0.7	1.1	2.4	3.2	3.6	3.9	4.0	3.9	3.9	3.9	3.9	3.7	3.4	3.2	2.7
0.65	-3.4	-1.7	-0.5	1.2	2.4	3.2	3.5	3.8	4.0	4.0	4.0	4.0	4.0	3.8	3.6	3.3	2.7
0.70	-2.9	-1.3	-0.3	1.2	2.3	3.0	3.3	3.6	3.6	3.7	3.6	3.5	3.5	3.3	2.9	2.5	2.1
0.75	-2.8	-1.4	-0.4	0.8	1.8	2.4	2.8	3.1	3.1	3.2	3.2	3.1	3.1	2.9	2.5	2.0	1.3
0.80	-2.9	-1.8	-0.9	0.3	1.2	1.8	2.1	2.4	2.6	2.6	2.6	2.5	2.5	2.3	1.9	1.3	0.1
0.85	-3.4	-2.3	-1.6	-0.4	0.4	1.0	1.3	1.6	1.7	1.8	1.8	1.8	1.8	1.5	1.2	0.5	-0.9
0.90	-4.6	-3.2	-2.6	-1.3	-0.3	0.1	0.5	0.7	0.8	0.9	0.9	0.9	0.9	0.6	0.2	-0.3	-1.0
0.95	-6.5	-5.1	-4.0	-2.6	-1.9	-1.1	-0.7	-0.4	-0.2	-0.2	-0.1	-0.1	-0.1	-0.3	-0.8	-1.4	-3.1
1.00	-9.4	-7.8	-6.5	-5.0	-3.8	-2.3	-1.9	-1.6	-1.5	-1.5	-1.4	-1.4	-1.4	-1.5	-2.0	-2.7	-4.4

TABLE B-2.

APPROXIMATION OF ZT ISOCHORES FROM REDUCED CORRELATION BY ROWLINSON.
TABLE OF PERCENTAGE DIFFERENCES BETWEEN CORRELATION AND VAN DER WAALS EQUATION.

PT	1.00	1.05	1.10	1.20	1.30	1.40	1.50	1.60	1.70	1.80	1.90	2.00	2.20	2.40	2.60	2.80	3.00
0.05	-1.0	-0.7	-0.5	-0.3	-0.1	0.1	0.2	0.3	0.4	0.5	0.6	0.7	0.8	0.9	0.4	0.5	0.5
0.10	-1.9	-1.5	-1.1	-0.5	-0.1	0.1	0.2	0.3	0.4	0.5	0.6	0.7	0.8	0.9	1.0	1.1	1.1
0.15	-2.0	-2.3	-1.7	-0.7	-0.1	0.1	0.2	0.3	0.4	0.5	0.6	0.7	0.8	0.9	1.0	1.0	1.0
0.20	-4.1	-3.0	-2.1	-0.8	-0.3	0.0	0.5	1.4	1.7	2.0	2.2	2.5	2.7	2.8	2.2	2.1	2.1
0.25	-5.4	-3.8	-2.7	-0.9	-0.2	0.5	1.6	2.0	2.2	2.4	2.7	2.9	3.1	3.1	2.1	2.1	2.1
0.30	-6.7	-4.7	-3.1	-0.9	-0.4	1.1	1.8	2.2	2.7	3.0	3.2	3.5	3.9	4.1	3.1	3.1	3.1
0.35	-7.9	-5.6	-3.7	-1.0	-0.5	1.6	2.2	2.7	3.1	3.6	3.9	4.0	4.3	4.5	4.7	4.7	4.7
0.40	-8.8	-6.2	-4.3	-1.1	-0.7	1.9	2.7	3.1	3.5	4.0	4.3	4.7	4.9	5.1	5.3	5.2	5.2
0.45	-9.5	-6.7	-4.4	-1.2	-0.9	2.3	3.1	3.6	4.0	4.3	4.6	4.9	5.1	5.3	5.5	5.5	5.5
0.50	-10.2	-7.0	-4.6	-1.1	-1.0	2.0	2.6	3.4	4.1	4.3	4.7	5.0	5.4	5.7	6.0	6.2	6.2
0.55	-10.5	-7.1	-4.4	-1.0	-1.0	2.2	2.8	3.7	4.5	4.9	5.2	5.6	5.9	6.3	6.7	6.6	6.5
0.60	-9.9	-6.5	-3.9	-0.5	-0.5	1.7	2.3	3.2	4.2	4.7	5.2	5.6	6.0	6.4	6.8	6.4	6.4
0.65	-9.1	-5.8	-3.5	-0.0	-0.0	2.2	2.8	3.8	4.2	4.7	5.0	5.3	5.7	6.0	6.4	6.7	6.7
0.70	-6.3	-4.9	-2.7	0.6	2.8	4.3	5.2	5.9	6.3	6.7	7.0	7.3	7.6	7.9	8.0	8.0	8.0
0.75	-7.5	-4.2	-1.9	1.0	3.2	4.6	5.6	6.3	6.7	7.0	7.3	7.5	7.7	7.9	8.2	8.2	8.2
0.80	-6.5	-3.4	-1.3	1.3	1.7	3.7	4.3	5.1	5.5	5.9	6.3	6.7	7.0	7.3	7.6	7.6	7.6
0.85	-5.3	-2.3	-0.3	2.4	3.3	4.3	5.0	5.5	6.0	6.3	6.7	7.0	7.3	7.6	7.9	7.9	7.9
0.90	-4.0	-1.0	0.6	3.3	5.0	5.9	6.6	7.1	7.4	7.7	8.0	8.3	8.6	8.9	9.2	9.2	9.2
0.95	-2.5	-0.0	1.8	4.2	5.4	6.5	7.2	7.5	7.8	8.0	8.3	8.6	8.9	9.2	9.5	9.5	9.5
1.00	-1.1	0.9	2.5	4.4	5.8	6.7	7.5	7.9	8.1	8.4	8.7	9.0	9.3	9.6	9.9	10.0	10.0
1.05	-0.1	1.5	2.7	4.3	5.8	6.6	7.4	7.8	8.1	8.4	8.7	9.0	9.3	9.6	9.9	10.0	10.0
1.10	0.2	1.6	2.8	4.1	5.4	6.3	7.0	7.4	7.7	8.0	8.3	8.6	8.9	9.2	9.5	9.8	9.8
1.15	0.2	1.6	2.3	3.7	4.0	5.5	6.3	6.8	7.1	7.4	7.7	8.0	8.3	8.6	8.9	9.2	9.2
1.20	-0.7	0.5	1.5	2.7	3.7	4.0	4.3	4.8	5.1	5.5	5.8	6.1	6.4	6.7	7.0	7.3	7.3
1.25	-3.5	-1.1	0.2	1.9	2.9	3.1	3.5	3.8	4.1	4.4	4.7	5.0	5.3	5.6	5.9	6.2	6.2
1.30	-7.9	-4.6	-2.2	0.1	1.7	2.1	2.7	3.1	3.5	3.9	4.2	4.6	5.0	5.4	5.8	6.2	6.2
1.35	-13.8	-8.4	-5.1	-1.9	0.1	1.7	2.1	2.7	3.1	3.5	3.9	4.2	4.6	5.0	5.4	5.8	5.8
1.40	-20.9	-13.2	-9.1	-4.3	-1.9	0.1	1.7	2.1	2.7	3.1	3.5	3.9	4.2	4.6	5.0	5.4	5.8
1.45	-27.9	-18.1	-12.8	-7.0	-3.1	-1.2	0.8	1.4	1.9	2.4	2.9	3.4	3.9	4.3	4.7	5.1	5.5
1.50	-37.4	-23.8	-16.8	-9.6	-4.6	-1.6	0.2	0.8	1.4	1.9	2.4	2.9	3.4	3.9	4.3	4.7	5.1

the ZT_r isochores by the various two-parameter equations of state is given in Table B-3.

B.3 Berthelot Equation

Berthelot's equation is simply a modified van der Waals equation in which the cohesive pressure term has been given a temperature dependence.

$$P + a/(TV^2) = RT/(V - b) \quad (B-15)$$

The two-parameters, a and b , are related to the critical temperature and critical pressure by the following equations.

$$a = 27 R^2 T_c^3 / (64 P_c) \quad b = RT_c / (8 P_c) \quad (B-16)$$

The reduced form of the equation is

$$P_r + 3/(v_r T_r) = 8 T_r / \{3(v_r - 1/3)\} \quad (B-17)$$

and $Z_c = 3/8$ the same as in van der Waals equation. A density-implicit form for the compressibility factor is

$$Z = v_r / (v_r - 1/3) - 9 / (8 T_r^2 v_r) \quad (B-18)$$

and the ZT_r isochores are given by

$$ZT_r = v_r T_r / (v_r - 1/3) - 9 / (8 T_r v_r) \quad (B-19)$$

When Equation B-19 is differentiated with respect to T_r the isochores are shown to be curved with tangent slopes defined by

$$(\partial(ZT_r) / \partial T_r)_{V_r} = v_r / (v_r - 1/3) + 9 / (8 T_r^2 v_r) \quad (B-20)$$

Equation B-19 predicts isochores which curve concave downward (i.e. $\partial^2(ZT_r) / \partial T_r^2 < 0$) for all reduced densities and temperatures. Since the critical isochore is essentially

TABLE B-3.

SUMMARY OF TWO-PARAMETER EQUATION OF STATE APPROXIMATIONS FOR THE
 z_{T_r} ISOCHORES OF ROWLINSON'S CORRELATION

Results Using Equation of State Critical Point Parameters

0.05 $\leq \rho_r \leq 1.00$				0.05 $\leq \rho_r \leq 1.50$			
Equation	a	b	rms. %	a	b	rms. %	max. %
van der Waals	1.1250	0.3333	6.41	28.1	1.1250	0.3333	7.81
Berthelot	1.1250	0.3333	14.78	34.5	1.1250	0.3333	19.78
Dieterici	2.0000	0.5000	15.94	32.6	2.0000	0.5000	20.45
Redlich-Kwong	1.2824	0.2599	3.71	13.9	1.2824	0.2599	4.60

Results Using Least Squares Estimators

0.05 $\leq \rho_r \leq 1.00$				0.05 $\leq \rho_r \leq 1.50$			
A	B	rms. %	max. %	A	B	rms. %	max. %
van der Waals	1.4419	0.4327	2.51	9.4	1.2835	0.3670	5.49
Berthelot	1.0837	0.2083	4.51	38.7	0.9605	0.2197	9.43
Dieterici	1.8235	0.6007	5.15	38.0	1.7519	0.5415	8.29
Redlich-Kwong	1.4933	0.2996	1.14	4.8	1.4420	0.2840	1.92

linear, and the isochores for $V < V_c$ curve concave upward, it might be expected that Berthelot's equation would result in greater error at high density than van der Waals equation. This was indeed the case since Equation B-19 differed from the reduced correlation of Rowlinson by a standard error of 19.78 per cent compared to 7.81 per cent for van der Waals equation.

When the following modification of Equation B-17

$$ZT_r = T_r / (1 - B\rho_r) - A\rho_r / T_r \quad (B-21)$$

was fitted to Rowlinson's correlation the standard errors were 4.51 per cent for $0.05 \leq \rho_r \leq 1.0$, and 9.43 per cent for $0.05 \leq \rho_r \leq 1.50$. Tables B-4 and B-5 show the percentage differences for these two density ranges. The least squares estimators for these density ranges and other pertinent data are summarized in Table B-3.

B.4 Dieterici Equation

Dieterici proposed a two-parameter equation of state which contained an exponential term.

$$P = RT \exp(-a/RTV) / (V - b) \quad (B-22)$$

The two constraints on the critical isotherm at the critical point may be used to evaluate the two parameters.

$$a = 4 R^2 T_c^2 / (e^2 P_c) \quad b = RT_c / (e^2 P_c) \quad (B-23)$$

The reduced form of Dieterici's equation can be written as

$$P_r = e^2 T_r \exp(-2/V_r T_r) / \{2(V_r - 1/2)\} \quad (B-24)$$

It should be noted that the equation predicts $Z_c = 2/e^2 \approx 0.271$ which is typical for a large number of substances.

TABLE B-4*

APPROXIMATION OF ZT ISOCHORES FROM REDUCED CORRELATION BY ROWLINSON.
TABLE OF PERCENTAGE DIFFERENCES BETWEEN CORRELATION AND BERTHELLOT EQUATION.

Pr	1.00	1.05	1.10	1.120	1.130	1.140	1.150	1.160	1.170	1.180	1.190	2.000	2.200	2.400	2.600	2.800	3.000
0.05	-1.2	-1.1	-1.1	-1.1	-1.0	-1.0	-0.9	-0.8	-0.7	-0.6	-0.6	-0.6	-0.4	-0.2	-0.1	-0.2	-0.1
0.10	-2.3	-2.3	-2.2	-2.1	-2.0	-2.0	-1.8	-1.7	-1.5	-1.5	-1.4	-1.2	-1.1	-0.8	-0.7	-0.5	-0.2
0.15	-3.5	-3.4	-3.4	-3.4	-3.1	-2.9	-2.7	-2.5	-2.4	-2.1	-1.9	-1.7	-1.5	-1.0	-0.7	-0.5	-0.3
0.20	-4.6	-4.5	-4.3	-4.0	-3.7	-3.7	-3.5	-3.2	-2.9	-2.3	-2.4	-2.2	-1.9	-1.4	-1.1	-0.8	-0.5
0.25	-5.9	-5.6	-5.4	-4.9	-4.5	-4.1	-3.9	-3.6	-3.2	-2.8	-2.8	-2.6	-2.2	-1.8	-1.2	-0.9	-0.5
0.30	-7.1	-6.7	-6.3	-5.7	-5.2	-4.8	-4.8	-4.4	-4.0	-3.7	-3.2	-2.9	-2.5	-1.9	-1.3	-0.8	-0.4
0.35	-8.0	-7.8	-7.4	-6.5	-5.9	-5.3	-4.9	-4.4	-4.0	-3.6	-3.0	-2.6	-2.0	-1.2	-0.7	-0.3	0.1
0.40	-8.6	-8.5	-8.3	-7.3	-6.5	-5.9	-5.2	-4.8	-4.3	-3.8	-3.3	-2.8	-2.0	-1.2	-0.6	-0.0	0.3
0.45	-8.7	-8.9	-8.7	-8.0	-7.0	-6.0	-5.6	-5.0	-4.5	-3.9	-3.4	-2.8	-2.4	-1.9	-1.1	-0.5	0.5
0.50	-8.5	-9.0	-9.0	-8.4	-7.6	-6.7	-6.1	-5.3	-4.8	-4.0	-3.5	-2.9	-2.2	-1.8	-0.9	-0.2	0.7
0.55	-7.7	-8.6	-8.6	-8.8	-8.7	-8.0	-7.0	-6.3	-5.4	-4.7	-4.1	-3.4	-2.7	-1.6	-0.7	0.0	0.7
0.60	-5.7	-7.3	-8.1	-8.5	-7.9	-7.1	-6.3	-5.4	-4.6	-3.9	-3.2	-2.5	-1.3	-0.3	0.5	1.0	1.4
0.65	-3.0	-5.6	-7.1	-7.9	-7.6	-6.8	-6.0	-5.1	-4.3	-3.5	-2.9	-2.1	-0.8	0.0	0.9	1.5	1.8
0.70	0.2	-3.3	-5.5	-7.1	-7.0	-6.4	-5.7	-4.8	-4.0	-3.1	-2.5	-1.7	-0.3	0.5	1.4	1.9	2.2
0.75	4.0	-0.8	-3.7	-6.2	-6.5	-6.1	-5.3	-4.4	-3.6	-2.7	-1.9	-1.2	0.1	1.2	2.0	2.4	2.7
0.80	8.7	2.2	-1.5	-4.8	-5.6	-5.3	-4.8	-3.8	-2.9	-2.2	-1.3	-0.5	0.8	1.9	2.6	3.1	3.4
0.85	14.5	6.2	1.3	-3.1	-4.3	-4.3	-4.0	-3.9	-3.1	-2.3	-1.2	-0.6	0.2	1.5	2.6	3.4	4.2
0.90	21.4	11.0	4.7	-0.7	-2.5	-2.5	-2.5	-1.9	-1.2	-0.3	0.3	1.1	2.4	3.5	4.2	4.8	5.0
0.95	29.4	16.3	9.0	1.9	-0.8	-1.4	-1.2	-0.7	-0.0	0.5	1.4	2.2	3.5	4.4	5.1	5.6	5.8
1.00	38.7	22.4	13.3	4.4	1.1	0.1	0.2	0.6	1.1	1.61	2.6	3.4	4.6	5.6	6.2	6.5	6.8

TABLE B-5.

APPROXIMATION OF ZT ISOCHORES FROM REDUCED CORRELATION BY ROWLINSON.
TABLE OF PERCENTAGE DIFFERENCES BETWEEN CORRELATION AND BERTHELLOT EQUATION.

Pr	1.00	1.05	1.10	1.15	1.20	1.30	1.40	1.50	1.60	1.70	1.80	1.90	2.00	2.10	2.20	2.30	2.40	2.50	2.60	2.70	2.80	2.90	3.00
0.05	-1.9	-1.8	-1.7	-1.6	-1.5	-1.4	-1.3	-1.2	-1.1	-1.0	-0.9	-0.8	-0.7	-0.6	-0.5	-0.4	-0.3	-0.2	-0.1	0.0	-0.1	-0.2	
0.10	-3.8	-3.6	-3.5	-3.4	-3.2	-2.9	-2.6	-2.4	-2.2	-2.0	-1.9	-1.7	-1.5	-1.2	-1.0	-0.8	-0.6	-0.4	-0.2	0.0	-0.6	-0.8	
0.15	-5.9	-5.6	-5.4	-4.9	-4.3	-3.9	-3.6	-3.3	-3.0	-2.7	-2.4	-2.2	-2.0	-1.8	-1.5	-1.1	-0.9	-0.6	-0.4	-0.2	0.0	-0.6	
0.20	-8.0	-7.6	-7.1	-6.3	-5.6	-5.2	-4.7	-4.2	-3.9	-3.5	-3.2	-3.0	-2.8	-2.6	-2.2	-1.8	-1.4	-1.1	-0.8	-0.5	-0.2	0.1	-0.8
0.25	-10.5	-9.6	-9.0	-8.0	-7.9	-7.0	-6.3	-5.6	-5.2	-4.7	-4.2	-3.8	-3.4	-3.0	-2.6	-2.1	-1.7	-1.2	-0.9	-0.5	-0.2	0.0	-0.9
0.30	-13.0	-11.9	-10.9	-9.4	-8.3	-7.5	-6.7	-6.0	-5.6	-5.0	-4.8	-4.5	-4.2	-3.8	-3.4	-3.0	-2.3	-1.7	-1.2	-0.7	-0.3	0.0	-0.8
0.35	-15.4	-14.2	-13.1	-11.0	-9.7	-8.6	-7.7	-6.8	-6.0	-5.1	-4.5	-4.0	-3.5	-3.0	-2.4	-1.8	-1.3	-0.7	-0.3	-0.1	0.0	-0.7	
0.40	-17.7	-16.3	-15.2	-12.7	-12.0	-10.9	-9.6	-8.5	-7.6	-6.8	-6.0	-5.4	-4.7	-4.0	-3.6	-3.0	-2.6	-1.9	-1.1	-0.7	-0.3	0.0	-0.7
0.45	-19.5	-18.2	-16.8	-14.3	-12.2	-10.5	-9.3	-8.2	-7.5	-6.4	-5.7	-5.0	-4.2	-3.8	-3.4	-2.7	-2.0	-1.4	-0.9	-0.5	-0.2	0.0	-0.6
0.50	-21.0	-20.0	-18.2	-15.8	-13.5	-11.6	-10.2	-8.9	-8.0	-7.0	-6.1	-5.2	-4.3	-3.5	-3.0	-2.4	-1.8	-1.0	-0.5	-0.2	0.0	-0.5	
0.55	-23.0	-21.0	-21.4	-19.7	-17.1	-14.7	-12.5	-11.0	-9.5	-8.3	-7.3	-6.3	-5.3	-4.3	-3.8	-2.8	-2.0	-1.4	-0.8	-0.4	-0.2	0.0	-0.4
0.60	-23.4	-22.1	-20.6	-17.9	-15.4	-13.3	-11.5	-9.9	-8.5	-7.4	-6.4	-5.4	-4.4	-3.7	-3.0	-2.4	-1.7	-1.3	-0.6	-0.2	0.0	-0.1	0.0
0.65	-23.5	-22.4	-21.3	-18.9	-16.5	-14.3	-12.0	-10.1	-8.5	-7.3	-6.3	-5.2	-4.2	-3.5	-2.8	-2.2	-1.7	-1.1	-0.6	-0.3	0.0	-0.3	0.0
0.70	-23.0	-22.2	-21.5	-18.9	-16.2	-13.9	-12.0	-10.1	-8.7	-7.2	-6.2	-5.1	-4.1	-3.2	-2.2	-1.7	-1.2	-0.7	-0.3	0.0	-0.3	0.0	0.0
0.75	-22.8	-22.4	-21.5	-19.3	-16.6	-14.2	-12.1	-10.2	-8.7	-7.2	-5.9	-4.8	-3.8	-2.8	-1.4	-0.8	-0.3	0.0	0.7	0.0	0.3	0.0	0.7
0.80	-21.8	-22.0	-21.4	-19.2	-16.6	-14.2	-12.1	-10.1	-8.3	-7.0	-5.6	-4.4	-3.4	-2.4	-1.4	-0.9	-0.5	-0.2	0.3	0.0	0.8	1.3	
0.85	-20.0	-20.7	-20.6	-18.7	-16.2	-13.8	-12.0	-10.8	-9.8	-8.1	-6.4	-5.1	-3.8	-2.8	-1.9	-0.9	-0.5	-0.2	0.7	1.5	1.9		
0.90	-17.5	-18.1	-8.19	-19.2	-17.6	-15.3	-13.1	-11.9	-9.0	-7.3	-5.7	-4.4	-3.2	-2.2	-1.2	-0.3	-0.1	0.4	2.2	2.6	3.3	4.2	
0.95	-14.0	-16.5	-17.1	-16.2	-14.5	-12.2	-10.1	-8.2	-6.2	-5.5	-5.0	-3.5	-2.3	-1.2	-0.2	-0.1	1.1	2.1	2.9	3.3	4.2		
1.00	-9.5	-13.6	-15.0	-15.0	-15.0	-12.3	-11.3	-9.1	-7.2	-5.6	-4.0	-2.6	-1.3	-0.6	-0.3	-0.1	2.1	2.1	3.1	3.7	4.1		
1.05	-4.3	-14.0	-13.1	-12.8	-13.7	-12.1	-11.0	-9.2	-8.1	-6.3	-4.7	-3.0	-1.7	-0.4	-0.1	1.6	3.1	4.1	4.1	4.2			
1.10	1.5	-6.5	-9.9	-12.0	-12.0	-10.3	-9.1	-7.3	-5.4	-3.9	-2.2	-0.7	0.5	-0.5	-0.2	2.7	4.2	5.2					
1.15	8.4	-1.8	-6.7	-9.7	-9.4	-8.1	-6.4	-4.5	-2.9	-1.3	0.1	1.4	3.8	5.4									
1.20	16.2	2.9	-3.1	-7.4	-7.6	-6.6	-5.1	-3.6	-1.9	-0.4	1.0	2.4	4.8										
1.25	24.3	6.4	0.9	-4.5	-5.5	-4.7	-3.5	-2.1	-0.6	0.8	2.3	3.7	4.8										
1.30	33.2	1.2	4.9	-1.8	-3.2	-2.9	-1.8	-0.6	0.1	0.8	2.1	3.5											
1.35	43.0	1.9	8.6	1.3	0.6	0.7	0.7	0.1	0.1	0.1	0.1	0.1											
1.40	53.8	2.6	4.8	2.3	1.2	0.6	0.6	0.1	0.1	0.1	0.1	0.1											
1.45	65.4	3.3	9.7	8.7	7.2	5.9	4.2	2.3	1.2	0.8	2.1	3.5											
1.50	76.8	41.6	25.9	13.2	0.1	0.7	2.3	0.1	0.1	0.1	0.1	0.1											

Dieterici's equation results in the following density-implicit form for the compressibility factor

$$z = v_r \exp(-2/v_r T_r) / (v_r - 1/2) \quad (B-25)$$

Thus, the zT_r isochores are given by the expression

$$zT_r = v_r T_r \exp(-2/v_r T_r) / (v_r - 1/2) \quad (B-26)$$

By differentiating Equation B-26 with respect to T_r the tangent slopes of the zT_r isochores are obtained.

$$\left[\frac{\partial (zT_r)}{\partial T_r} \right]_{v_r} = \left[\frac{v_r}{v_r - 1/2} + \frac{2}{(v_r - 1/2) T_r} \right] \exp(-2/v_r T_r) \quad (B-27)$$

The second derivative of zT_r with respect to T_r

$$\left[\frac{\partial^2 (zT_r)}{\partial T_r^2} \right]_{v_r} = \left[\frac{4}{(v_r - 1/2) v_r T_r} \right] \exp(-2/v_r T_r) \quad (B-28)$$

is positive for $v_r > 1/2$. Thus, Dieterici's equation predicts isochores which have curvature opposite to that of experimental evidence when $v_r > 1.0$.

When Equation B-26 was compared with Rowlinson's correlation for $1.0 \leq v_r \leq 20.0$ the standard error was 15.94 per cent. Equation B-26 may be written in terms of ρ_r

$$zT_r = T_r \exp(-A\rho_r/T_r) / (1 - B\rho_r) \quad (B-29)$$

and the parameters A and B evaluated using a least squares criterion. Tables B-6 and B-7 give the percentage errors for the least squares approximations. The equation gave a poor representation of the critical isotherm, and large errors occurred along each isochore since the equation predicted the wrong curvature. Table B-3 summarizes the results and it is

TABLE 3-6.

APPROXIMATION OF ZT ISOCHORES FROM REDUCED CORRELATION BY ROWLINSON.
TABLE OF PERCENTAGE DIFFERENCES BETWEEN CORRELATION AND DIETERICI EQUATION.

$\frac{P}{P_r}$	1.00	1.05	1.10	1.20	1.30	1.40	1.50	1.60	1.70	1.80	1.90	2.00	2.20	2.40	2.60	2.80	3.00
0.05	0.4	0.5	0.6	0.6	0.6	0.7	0.7	0.6	0.6	0.6	0.6	0.6	0.5	0.4	0.3	0.2	0.1
0.10	0.6	0.8	1.0	1.3	1.4	1.4	1.4	1.4	1.3	1.2	1.2	1.1	0.8	0.3	0.7	0.5	0.7
0.15	0.4	0.9	1.2	1.7	2.0	2.1	2.1	2.0	2.0	1.9	1.8	1.7	1.5	1.3	0.9	0.7	0.7
0.20	0.0	0.8	1.4	2.2	2.6	2.7	2.8	2.8	2.6	2.4	2.3	2.1	1.7	1.5	1.2	0.9	0.9
0.25	-0.8	0.4	1.3	2.5	3.1	3.4	3.3	3.3	3.2	3.0	2.9	2.4	2.1	1.7	1.4	1.0	1.0
0.30	-2.0	-0.2	1.0	2.7	3.5	3.9	4.0	4.0	3.8	3.6	3.4	2.9	2.5	2.1	1.7	1.3	1.3
0.35	-3.3	-1.2	0.4	2.7	3.8	4.4	4.5	4.5	4.2	4.1	3.9	3.3	2.9	2.4	1.8	1.3	1.3
0.40	-4.9	-2.2	-0.3	2.6	4.0	4.7	5.2	5.0	4.9	4.7	4.5	4.2	3.6	3.1	2.5	1.9	1.3
0.45	-6.5	-3.3	-0.9	2.3	4.1	5.1	5.4	5.5	5.3	5.2	4.9	4.6	3.9	3.3	2.5	1.9	1.4
0.50	-8.5	-4.6	-1.7	1.9	4.0	5.3	5.6	5.6	5.5	5.4	5.1	4.9	4.2	3.4	2.5	1.7	1.2
0.55	-10.6	-6.0	-2.5	1.5	3.9	5.3	5.3	5.1	5.0	5.0	5.4	5.1	4.3	3.4	2.5	1.6	0.4
0.60	-12.3	-7.1	-3.2	1.3	3.9	5.4	6.1	6.3	6.3	6.0	5.6	5.3	4.4	3.3	2.4	1.2	0.0
0.65	-14.2	-8.2	-4.2	1.1	4.0	5.6	6.3	6.6	6.6	6.3	5.8	5.5	4.4	3.2	2.0	0.7	0.6
0.70	-16.5	-9.5	-5.0	0.8	4.0	5.7	6.4	6.8	6.7	6.4	5.9	5.4	4.3	3.2	2.9	1.6	0.5
0.75	-19.4	-11.4	-6.0	0.2	3.8	5.6	6.4	6.8	6.6	6.3	5.9	5.3	4.0	3.0	2.6	1.0	0.4
0.80	-22.6	-13.4	-7.3	-0.1	3.5	5.5	6.2	6.6	6.5	6.1	5.6	5.0	3.5	2.9	2.0	-1.6	-3.5
0.85	-26.0	-15.3	-8.5	-0.6	3.2	5.4	6.1	6.4	6.2	5.9	5.2	4.6	3.9	3.1	2.7	-0.7	-4.9
0.90	-29.7	-17.2	-9.8	-1.0	3.2	5.3	6.2	6.5	6.5	6.2	5.9	5.5	4.7	3.9	3.1	-2.0	-6.5
0.95	-33.7	-19.6	-10.8	-1.4	2.7	4.9	5.7	5.8	5.5	4.8	4.0	3.9	3.5	3.1	2.2	-3.6	-6.1
1.00	-38.0	-22.1	-12.5	-2.6	2.0	4.2	5.1	5.5	4.5	3.9	3.0	2.9	2.3	1.8	1.2	-5.6	-8.4

TABLE B-7.

 APPROXIMATION OF 2T ISOCHORES FROM REDUCED CORRELATION BY ROWLINSON.
 TABLE OF PERCENTAGE DIFFERENCES BETWEEN CORRELATION AND DIETERICI EQUATION.

T_x	1.00	1.05	1.10	1.20	1.30	1.40	1.50	1.60	1.70	1.80	1.90	2.00	2.20	2.40	2.60	2.80	3.00
p_x	0.05	0.3	0.4	0.6	0.7	0.7	0.7	0.8	0.7	0.7	0.7	0.7	0.7	0.7	0.6	0.6	0.4
0.10	0.5	0.8	1.0	1.3	1.5	1.6	1.6	1.5	1.5	1.5	1.5	1.5	1.5	1.5	1.0	1.0	0.9
0.15	0.3	0.8	1.2	1.8	2.1	2.4	2.4	2.3	2.3	2.2	2.2	2.0	2.0	1.7	1.5	1.3	1.3
0.20	0.0	0.8	1.5	2.4	2.9	3.1	3.1	3.2	3.1	3.0	2.9	2.8	2.7	2.7	2.7	2.7	2.7
0.25	-0.8	0.5	1.4	2.8	3.5	3.9	3.9	3.9	3.9	3.8	3.7	3.3	3.1	2.7	2.5	2.2	2.2
0.30	-1.9	-0.0	1.2	3.0	4.1	4.5	4.7	4.8	4.7	4.5	4.4	4.0	4.0	3.8	3.0	2.7	2.7
0.35	-3.2	-1.0	0.7	3.2	4.5	5.2	5.4	5.6	5.5	5.4	5.3	5.2	4.7	4.4	3.9	3.4	3.1
0.40	-4.6	-1.8	0.1	3.3	4.9	5.7	6.2	6.2	6.3	6.2	6.0	5.8	5.3	4.9	4.4	3.9	3.3
0.45	-6.1	-2.7	-0.2	3.2	5.2	6.3	6.8	7.0	6.9	6.9	6.7	6.5	6.0	5.4	4.8	4.3	3.6
0.50	-7.9	-3.8	-0.8	3.1	5.4	6.8	7.3	7.6	7.5	7.5	7.3	7.1	6.6	5.9	5.2	4.5	3.7
0.55	-9.7	-4.9	-1.3	3.0	5.6	7.2	7.8	8.2	8.3	8.1	7.9	7.8	7.1	6.3	5.6	4.8	3.8
0.60	-11.0	-5.6	-1.6	3.1	6.0	7.6	8.4	8.9	9.0	8.8	8.6	8.4	7.6	6.8	6.0	4.9	3.9
0.65	-12.5	-6.4	-2.2	3.3	6.4	8.3	9.2	9.6	9.7	9.6	9.2	9.0	8.2	7.2	6.2	5.1	3.8
0.70	-14.3	-7.2	-2.5	3.5	7.0	8.8	9.7	10.2	10.3	10.2	9.8	9.5	8.6	7.5	6.4	5.0	3.6
0.75	-16.5	-8.4	-2.9	3.5	7.3	9.2	10.3	10.8	10.8	10.7	10.4	10.0	9.0	7.8	6.5	5.0	3.4
0.80	-18.9	-9.7	-3.6	3.7	7.6	9.6	10.8	11.8	11.5	11.2	10.7	10.4	9.3	8.0	6.5	4.9	3.2
0.85	-21.4	-10.7	-3.9	4.0	8.2	10.4	11.4	11.8	11.9	11.7	11.3	10.8	9.5	8.0	6.4	4.7	2.9
0.90	-23.9	-11.6	-4.2	4.5	8.9	11.1	12.2	12.6	12.5	12.2	11.7	11.1	9.7	8.0	6.2	4.4	2.4
0.95	-26.5	-12.7	-4.2	5.1	9.4	11.8	12.8	13.1	13.0	12.6	12.1	11.4	9.8	7.9	5.9	3.8	1.6
1.00	-29.0	-13.8	-4.5	5.1	9.9	12.2	13.3	13.6	13.6	12.9	12.3	11.5	9.7	7.7	5.4	3.0	0.8
1.05	-31.9	-15.1	-5.3	5.0	10.2	12.5	13.6	13.8	13.4	13.0	12.2	11.4	9.4	7.2	4.7	2.4	
1.10	-35.2	-16.6	-5.8	4.9	10.1	12.5	13.4	13.6	13.2	12.6	11.8	10.9	8.9	6.5	3.9		
1.15	-38.5	-17.8	-6.6	4.9	9.9	12.2	13.0	13.2	12.2	12.7	12.0	11.1	10.1	8.0	5.5		
1.20	-42.3	-19.7	-7.4	4.6	9.7	11.9	12.5	12.3	11.8	11.0	10.0	9.0	8.0	6.6			
1.25	-47.3	-21.6	-8.3	4.2	9.3	11.4	11.9	11.5	10.8	9.7	8.7	7.5	5.3				
1.30	-53.2	-24.8	-10.0	3.2	8.4	10.3	10.7	10.1	9.1	8.9	7.2	5.6					
1.35	-59.4	-27.7	-11.8	2.9	7.1	9.5	10.5	10.5	9.5	8.8	7.2	5.3					
1.40	-65.4	-31.0	-14.5	0.0	6.0	8.0	8.9	8.9	8.0	7.0	6.0	5.0					
1.45	-69.9	-34.0	-17.0	-2.3	5.0	7.0	7.0	7.0	6.0	5.0	4.0	3.0					
1.50	-76.5	-38.0	-20.3	-5.3	4.0	6.0	6.0	6.0	5.0	4.0	3.0	2.0					

apparent that Dieterici's equation gave the poorest representation of the correlation.

B.5 Redlich-Kwong Equation

The Redlich-Kwong equation represents a remarkable improvement over the van der Waals equation which it closely resembles.

$$P + a/\{T^{0.5}(V^2 + Vb)\} = TR/(V - b) \quad (B-30)$$

The parameters a and b are evaluated by applying the constraints $(\partial P/\partial V)_T = 0$ and $(\partial^2 P/\partial V^2)_T = 0$ at the critical point with the result

$$a = R^2 T_c^{2.5} / \{9(\sqrt[3]{2} - 1)P_c\} = c R^2 T_c^{2.5} / P_c \quad (B-31)$$

$$b = (\sqrt[3]{2} - 1)RT_c / (3P_c) = dRT_c / P_c \quad (B-32)$$

Substitution of Equations B-31 and B-32 into Equation B-30 leads to the reduced form of the Redlich-Kwong equation.

$$P_r = 3 T_r / (V_r - d) - 9 c / \{T_r^{0.5} (V_r^2 + 3 dV_r)\} \quad (B-33)$$

The critical compressibility factor is $1/3$, a value which is too large to be representative of most substances.

The density-implicit form for the compressibility factor in terms of V_r and T_r can be written

$$Z = V_r / (V_r - 3d) - 3 c / \{T_r^{1.5} (V_r + 3d)\} \quad (B-34)$$

and the ZT_r isochores are given by

$$ZT_r = V_r T_r / (V_r - 3d) - 3 c / \{T_r^{0.5} (V_r + 3d)\} \quad (B-35)$$

A comparison of Equation B-35 with the reduced correlation of Rowlinson resulted in standard errors of 3.71 per cent and

4.60 per cent for the density ranges $0.05 \leq \rho_r \leq 1.0$ and $0.05 \leq \rho_r \leq 1.50$, respectively. This represents a significant improvement over van der Waals equation. The chief reason for the improvement is the last term in Equation B-35 which contains $T_r^{-0.5}$. This term provides for the curvature of the isochores. It may be recalled that van der Waals equation predicted linear isochores, and that in Berthelot's equation the curvature was the result of a term containing T_r^{-1} .

The tangent slopes of the isochores predicted by Equation B-35 can be calculated from

$$\left. \left(\frac{\partial (ZT_r)}{\partial T_r} \right) \right|_{V_r} = \frac{V_r}{V_r - 3d} - \frac{1.5c}{T_r^{1.5}(V_r + 3d)} \quad (B-36)$$

which when again differentiated with respect to T_r gives

$$\left. \left(\frac{\partial^2 (ZT_r)}{\partial T_r^2} \right) \right|_{V_r} = - \frac{2.25c}{T_r^{2.5}(V_r + 3d)} \quad (B-37)$$

showing the isochores to be concave downward for all reduced volumes.

The constants in Equation B-35 were replaced with least squares estimators A and B, and the following equation

$$ZT_r = T_r / (1 - B\rho_r) - A\rho_r / \{ T_r^{0.5} (1 + B\rho_r) \} \quad (B-38)$$

was fitted to Rowlinson's correlation. For reduced densities in the range $0.05 \leq \rho_r \leq 1.0$, the standard error was 1.14 per cent, and Table B-8 shows the maximum error of 4.8 per cent to occur at the critical point. When Equation B-38 was fitted to reduced densities in the range $0.05 \leq \rho_r \leq 0.7$, all errors were less than one per cent.

TABLE B-8.

TABLE OF PERCENTAGE DIFFERENCES BETWEEN CORRELATION AND REDLICH-KWONG EQUATION.

ρ_{TR}	1.00	1.05	1.10	1.20	1.30	1.40	1.50	1.60	1.70	1.80	1.90	2.00	2.20	2.40	2.60	2.80	3.00
0.05	0.3	0.3	0.2	0.2	0.1	0.2	0.2	0.2	0.1	0.2	0.1	0.2	0.1	0.2	0.1	0.2	0.1
0.10	0.6	0.6	0.5	0.5	0.4	0.4	0.3	0.3	0.2	0.3	0.2	0.3	0.2	0.3	0.2	0.3	0.2
0.15	0.8	0.8	0.7	0.7	0.6	0.6	0.5	0.5	0.4	0.4	0.4	0.4	0.3	0.4	0.3	0.4	0.3
0.20	1.0	1.0	1.0	1.0	0.9	0.8	0.7	0.6	0.5	0.5	0.6	0.6	0.6	0.6	0.6	0.6	0.5
0.25	0.8	1.0	1.0	1.1	1.0	0.9	0.9	0.7	0.7	0.7	0.7	0.6	0.6	0.6	0.6	0.6	0.6
0.30	0.6	0.8	1.0	1.1	1.1	1.1	0.9	0.9	0.8	0.7	0.7	0.7	0.7	0.7	0.7	0.7	0.7
0.35	0.4	0.5	0.6	1.0	1.0	0.9	1.0	0.8	0.8	0.7	0.7	0.7	0.7	0.7	0.7	0.7	0.7
0.40	0.3	0.4	0.3	0.7	0.8	0.8	0.8	0.8	0.7	0.7	0.7	0.6	0.7	0.6	0.7	0.6	0.7
0.45	0.2	0.2	0.2	0.3	0.6	0.7	0.6	0.6	0.6	0.6	0.6	0.6	0.7	0.6	0.7	0.6	0.7
0.50	0.4	0.6	0.6	0.6	0.6	0.4	0.3	0.2	0.4	0.3	0.3	0.5	0.5	0.6	0.6	0.6	0.6
0.55	0.5	0.0	0.1	0.1	0.4	0.3	0.0	0.0	0.0	0.1	0.2	0.2	0.4	0.6	0.6	0.8	0.8
0.60	1.3	0.3	0.1	0.1	0.6	0.6	0.6	0.4	0.3	0.1	0.0	0.1	0.3	0.5	0.6	0.8	1.0
0.65	2.1	0.6	0.2	0.9	0.9	0.7	0.7	0.5	0.2	0.0	0.1	0.2	0.5	0.5	0.5	0.5	0.5
0.70	2.8	1.0	0.2	1.1	1.2	1.2	1.2	1.0	0.8	0.5	0.2	0.0	0.1	0.4	0.6	0.8	1.0
0.75	3.2	0.9	0.4	1.7	1.7	1.7	1.6	1.6	1.2	0.8	0.5	0.2	0.1	0.3	0.9	1.2	1.5
0.80	3.6	0.8	0.8	2.1	2.3	2.3	2.0	1.7	1.7	1.7	1.7	1.7	1.7	1.7	1.7	1.7	1.7
0.85	4.0	0.9	1.0	2.5	2.6	2.6	2.3	2.3	2.0	1.5	1.0	0.5	0.1	0.3	0.9	1.3	1.5
0.90	4.4	0.9	1.2	2.7	2.8	2.8	2.5	2.5	2.0	1.5	1.0	0.5	0.1	0.3	0.9	1.4	1.6
0.95	4.7	0.6	1.2	2.9	2.2	2.2	1.9	1.9	1.6	1.6	1.6	1.5	0.5	0.4	1.1	1.6	1.7
1.00	4.8	0.3	1.8	3.6	3.7	3.2	3.2	2.4	2.4	1.7	1.2	0.5	0.0	0.5	1.3	1.7	1.8

For the 893 points with densities ranging from $0.05 \leq \rho_r \leq 1.50$, the standard error was 1.92 per cent. The percentage differences for a representative number of points are presented in Table B-9. It should be noted that the largest errors occur along the critical isotherm and the isochores for $\rho_r \geq 1.0$. A better fit for the critical isotherm would be obtained if z_c was a property which was entered into the equation such that the critical point was without error. The region for $\rho_r \geq 1.0$ is in error primarily because the equation predicts isochores which curve concave downward for all densities.

Table B-3 summarizes the results of approximating Rowlinson's correlation with the common two-parameter equations of state. The Redlich-Kwong equation was significantly better than the other equations tested. It is apparent, however, that all two-parameter equations have difficulty when the reduced density is greater than one.

TABLE B-9.

TABLE I
APPROXIMATION OF ZT ISOCHORES FROM REDUCED CORRELATION BY ROWLINSON.
TABLE OF PERCENTAGE DIFFERENCES BETWEEN CORRELATION AND REDLICH-KWONG EQUATION.

APPENDIX C

COMPUTER PROGRAMS FOR CORRESPONDING STATES
DENSITY CORRELATIONS


```

SUBROUTINE ZROLL(DR,PR,TR,Z,ITER,IFLAG)
C *** X ***
C A REDUCED 3-TERM EQUATION IS USED TO APPROXIMATE THE Z
C FACTOR CORRELATION OF ROLLING (TRANS. FARADAY SOCIETY, *
C VOL. 51, PP. 1317-1326, 1955). IF IFLAG = 0, Z=Z(PR,TR) *
C IF IFLAG .GT. 0, Z=Z(DR,TR).
C *** X ***
      DIMENSION A(8)
      DATA A/0.36556695,0.99938220,0.55560621,0.35381582,
1 0.44327453,0.10240614,0.53546923,0.54684921/
      ITER=0
      IF(TR<0.9)11,1,1
1  IF(TR<4.5)2,2,11
2  IF(IFLAG)3,3,10
3  DR=1.0
      DO 8 ITER=1,10
      DR2=DR*DR
      T1=(A(1)*TR-A(2)-A(3)/TR**2)*DR
      T2=(A(4)*TR-A(5))*DR2
      T3=A(5)*A(6)*DR**5
      T4=A(7)*DR2/TR**2
      T5=A(8)*DR2
      T6=EXP(-T5)
      P=(TR+T1+T2+T3)*DR+T4*DR*(1.0+T5)*T6
      DP=TR+2.0*T1+3.0*T2+6.0*T3+T4*T6*(3.0+3.0*T5-2.0*T5*T5)
      DR1=DR-(P-0.293*PR)/DP
      IF(DR1)4,4,5
4  DR1=0.5*DR
5  IF(DR1-1.5)7,7,6
6  DR1=DR+0.9*(1.5-DR)
7  IF(ABS(DR-DR1)-0.00001)9,8,8
8  DR=DR1
9  Z=0.293*PR/(DR1*T6)
10 DR2=DR*DR
     ITER=1
     Z=1.0+(A(1)-A(2)/TR-A(3)/TR**3)*DR+(A(4)-A(5)/TR)*DR2
1  +A(5)*A(6)*DR**5/TR+A(7)*DR2/TR**3*(1.0+A(8)*DR2)*
2  EXP(-A(8)*DR2)
11 RETURN
     END

```


SUBROUTINE ZKATZ(PR,TR,Z,ITER)

```

C * * * * * * * * * * * * * * * * * * * * * * * * * * * * * * * * * * *
C A REDUCED B-W-R EQUATION IS USED TO APPROXIMATE THE Z
C FACTOR CORRELATION OF STANDING-KATZ (TRANS. AIME, VOL.
C 146, PP. 140-142, 1942). THE B-W-R COEFFICIENTS WERE
C CALCULATED FROM THE TABULAR DATA IN 'HANDBOOK OF NATURAL
C GAS ENGINEERING', McGRAW-HILL, 1959, PP. 710-717.
C * * * * * * * * * * * * * * * * * * * * * * * * * * * * * * * * * * *
C
C DIMENSION A(8)
C DATA A/0.31506237,1.0467099,0.57832729,0.53530771,
C 1 0.61232032,0.10488613,0.68157001,0.63446549/
C
C 1 ITER=0
C 2 DR=1.0
C 3 IF(TR=1.05)10,1,1
C 4 IF(TR=3.0)2,2,10
C 5 IF(PR=15.0)3,3,10
C 6 DO 8 ITER=1,10
C 7 DR2=DR*DR
C 8 T1=(A(1)*TR-A(2)-A(3)/TR**2)*DR
C 9 T2=(A(4)*TR-A(5))*DR2
C 10 T3=A(6)*A(6)*DR2**5
C 11 T4=A(7)*DR2/TR**2
C 12 T5=A(8)*DR2
C 13 T6=EXP(-T5)
C 14 P=(TR+T1+T2+T3)*DR+T4*DR*(1.0+T5)*T6
C 15 DP=TR+2.0*T1+3.0*T2+1.0*T3+T4*T6*(3.0+3.0*T5-2.0*T5*T5)
C 16 DR1=DR-(P-0.270*PR)/DP
C 17 IF(DR1)4,4,5
C 18 DR1=0.5*DR
C 19 IF(DR1-2.2)7,7,6
C 20 DR1=DR+0.5*(2.2-DR)
C 21 IF(ABS(DR-DR1)-0.00001)9,3,9
C 22 DR=DR1
C 23 Z=0.270*PR/(DR1*TR)
C 24 RETURN
C END

```



```

SUBROUTINE COMPZ(ALPHA,ZC,TR,PR,Z,KODE)
C * * * * * * * * * * * * * * * * * * * * * * * * * * * * * * * * * * * *
C THIS SUBROUTINE SOLVES THE DENSITY IMPLICIT FORMULATION, *
C DR-F(ALPHA,ZC,PR,DR,TR) = 0, BY INTERVAL HALVING *
C * * * * * * * * * * * * * * * * * * * * * * * * * * * * * * * * * * * *
C KODE = 1 FOR A NORMAL EXIT FROM THIS SUBROUTINE *
C KODE = 2 IF TR OR PR ARE OUTSIDE THE CORRELATION *
C KODE = 3 IF PR IS WITHIN 0.001 OF PRS *
C KODE = 4 IF MORE THAN 15 ITERATIONS ARE REQUIRED *
C * * * * * * * * * * * * * * * * * * * * * * * * * * * * * * * * * * * *
C STATEMENT OF RIEDEL'S SATURATED LIQUID EQUATION
DRSL(A,T)=1.0+0.85*(1.0-T)+(1.930+0.20*(A-7.0))*1 (1.0-T)**0.3333333
KODE=1
ITER=0
IF(TR-0.3)17,1,1
1 IF(TR-30.)2,2,17
2 IF(PR-30.0)3,3,17
3 IF(PR-1.0)4,4,9
4 IF(TR-1.0)5,5,9
C STATEMENT OF RIEDEL'S VAPOR PRESSURE EQUATION
5 PRS=EXP(ALPHA* ALOG(TR)-0.0838*(ALPHA-3.75)*1 (36.0/TR-35.0-TR**6+42.0*ALOG(TR)))
IF(ABS(PR-PRS)=0.001)6,6,7
6 DR=DRSL(ALPHA,TR)
KODE=3
GO TO 16
7 IF(PR-PRS)8,6,9
8 D1=0.0
F1=-PR*ZC/TR
D2=1.0
F2=1.0-PR/TR
GO TO 10
9 D1=0.0
F1=-PR*ZC/TR
D2=3.1+10.0*(0.3-ZC)
F2=FDR(ALPHA,ZC,PR,D2,TR)
10 DR=0.5*(D1+D2)
F3=FDR(ALPHA,ZC,PR,DR,TR)
IF(F3)11,16,12
11 D1=DR
F1=F3
GO TO 13
12 D2=DR
F2=F3
13 ITER=ITER+1
C TEST FOR CONVERGENCE
IF(ABS(D1-D2)/D1=0.001)16,14,14
14 IF(ITER-15)10,10,15
15 KODE=4
16 Z=PR*ZC/(DR*TR)
RETURN
17 KODE=2
RETURN
END

```



```

FUNCTION FDR(ALPHA,ZC,PR,DR,TR)
C * * * * * * * * * * * * * * * * * * * * * * * * * * * * * * * * * *
C THIS SUBPROGRAM RETURNS F(DR) = DR-F(ALPHA,ZC,PR,DR,TR) *
C * * * * * * * * * * * * * * * * * * * * * * * * * * * * * * * * * *
C IF(DR-1.0)1,1,2
1 TRS=1.0
  PRS=1.0-(5.0-1.0/ZC)*(1.0-DR)**4+(4.0-1.0/ZC)*(1.0-DR)**5
  PD=PR-PRS
  PZ=PD/(1.0+(ZC*ALPHA-1.0)*DR**0.8+0.05*PD))
  GO TO 3
2 TRS=TROOT(ALPHA,ZC,DR)
C STATEMENT OF RIEDEL'S VAPOR PRESSURE EQUATION
  PRS=EXP(ALPHA* ALOG(TRS)-0.0838*(ALPHA-3.75)*
1 (36.0/TRS-35.0-TRS**6+42.0*ALOG(TRS)))
  PD=PR-PRS
  BASE=1.0/(ALPHA*ZC)
  PZ=PD*BASE**((DR**((1.0+5.47736*(BASE-0.53811785))*
1 (5.07301*SQRT(DR)-5.37068*DR+1.66199*DR**1.5000)-
2 0.0427438*SQRT(PD)))
3 FDR=DR-(DR*TRS/ZC+PZ)*ZC/TR
  RETURN
  END

```

```

FUNCTION TROOT(ALPHA,ZC,DR)
C * * * * * * * * * * * * * * * * * * * * * * * * * * * * * * * * *
C THIS SUBPROGRAM USES NEWTON-RAPHSON ITERATION TO SOLVE *
C RIEDEL'S SATURATED LIQUID EQUATION FOR TRS *
C * * * * * * * * * * * * * * * * * * * * * * * * * * * * * * * * *
C T1=0.98
C RIEDEL'S SATURATED LIQUID EQUATION
1 F=1.0+0.85*(1.0-T1)+(1.93+0.2*(ALPHA-7.0))*(1.0-T1)***
1 0.3333333
C TR DERIVATIVE OF RIEDEL'S SATURATED LIQUID EQUATION
  DF=-0.85-(0.6433334+0.06666667*(ALPHA-7.0))/(1.0-T1)***
1 0.6666667
  T2=T1-(F-DR)/DF
  IF(T2-1.0)3,2,2
C TEST FOR CONVERGENCE
2 T2=T1+0.9*(1.0-T1)
3 IF(ABS(T2-T1)-0.000001)5,4,4
4 T1=T2
  GO TO 1
5 TROOT=T2
  RETURN
  END

```


APPENDIX D
COMPUTER PROGRAM TO SIMULATE
THE DEPLETION PERFORMANCE OF A CONSTANT VOLUME RESERVOIR

This appendix gives a listing of the FORTRAN computer program used to simulate the depletion performance of a constant volume reservoir containing a retrograde fluid. The liquid phase is assumed to be immobile and the reservoir pressure is depleted by stepwise removal of some of the vapor phase. The program uses the following calculation procedure. The system pressure is decreased to the next specified lower pressure, and the system composition is flashed. The moles of vapor and liquid are calculated and the resulting phase compositions are used to determine the phase densities from corresponding states correlations. Knowledge of these densities permits calculation of the retrograde liquid saturation, and the moles of vapor which must be removed to restore the system to the initial volume. A new system composition is calculated and the process repeated. The same calculation procedure is used for both binary and ternary mixtures. Since flash calculations need not be trial and error for binary mixtures, the program performs some unnecessary calculations for these mixtures.

The main program reads the input data, calculates certain variables required for the support subroutines, and provides the format for the printout. Several examples of the printout from this program are reproduced in Appendix E. The comment cards at the start of the main program provide a listing of all the support subroutines that are required. Some of the required subroutines were presented in Appendices A and C. Comment cards are also used to describe the function of each subroutine.


```

LINE=20+NCOMP
GO TO 18
17 WRITE(IRITE,11)NAME
WRITE(IRITE,8)
LINE=9+NCOMP
18 IP=IP+1
P=PP(IP)
CALL XTRAP(PK,IV)
IF(IV)20,24,22
20 DO 21 I=1,NCOMP
X(I)=Z(I)
Y(I)=0.0
C(I)=1.0
21 CONTINUE
DV=0.0
GO TO 28
22 DO 23 I=1,NCOMP
X(I)=0.0
Y(I)=Z(I)
C(I)=1.0
23 CONTINUE
DL=0.0
24 PPCV=0.0
PTCV=0.0
WV=0.0
C CALCULATE PSEUDOCRITICAL PROPERTIES FOR V PHASE
DO 25 I=1,NCOMP
PPCV=PPCV+Y(I)*PC(I)
PTCV=PTCV+Y(I)*TC(I)
WV=WV+Y(I)*WM(I)
25 CONTINUE
C CALCULATE VAPOR DENSITY VIA STANDING-KATZ CORRELATION
PRV=P/PPCV
TRV=T/PTCV
CALL ZKATZ(PRV,TRV,ZV,ITER)
IF(ITER)26,26,27
26 WRITE(IRITE,13)ITER
27 DV=ZV*10.73159*T/(WV*P)
IF(ZT)35,35,36
35 ZT=1.0/(DV*WV)
36 IF(IV)28,28,31
28 PPCL=0.0
PTCL=0.0
PZCL=0.0
PVCL=0.0
PACL=0.0
WL=0.0
C CALCULATE PSEUDOCRITICAL PROPERTIES FOR L PHASE
DO 29 I=1,NCOMP
PVCL=PVCL+X(I)*VC(I)
PACL=PACL+X(I)*AC(I)
PTCL=PTCL+X(I)*TC(I)
PZCL=PZCL+X(I)*ZC(I)
WL=WL+X(I)*WM(I)

```



```
29 CONTINUE
  PPCL=PZCL*10.73159*PTCL/PVCL
C   CALCULATE LIQUID DENSITY VIA L-G-H CORRELATION
  PRL=P/PPCL
  TRL=T/PTCL
  CALL COMPZ (PACL,PZCL,TRL,PRL,ZL,KODE)
  IF(KODE-1)34,30,34
34 WRITE(IRITE,14)KODE
30 DL=ZL*10.73159*T/(WL*P)
  IF(ZT)37,37,31
37 ZT=1.0/(DL*WL)
C   CALCULATE MOLES OF LIQUID (ZX)
31 ZX=(1.0-V)*ZT
  PL=100.0*DL*WL*ZX
  ZY=(1.0-PL/100.0)/(DV*WV)
C   ADD MOLES OF L AND V TO GET TOTAL MOLES (ZT)
  ZT=ZX+ZY
  WRITE(IRITE,9)COMP(1),Z(1),Y(1),X(1),C(1),P,PL,DV,DL
  WRITE(IRITE,10)(COMP(I),Z(I),Y(I),X(I),C(I),I=2,NCOMP)
  WRITE(IRITE,12)ZT,ZY,ZX,PK
  LINE=LINE+NCOMP+3
C   CALCULATE NEW SYSTEM COMPOSITION
  DO 32 I=1,NCOMP
    Z(I)=(ZY*Y(I)+ZX*X(I))/ZT
32 CONTINUE
  IF(ABS(P-PEND)-1.0)40,40,33
33 IF(LINE-56)18,17,17
40 CONTINUE
  GO TO 15
50 CALL EXIT
END
```



```

SUBROUTINE XTRAP(PK,IV)
C * * * * * * * * * * * * * * * * * * * * * * * * * * * * * * * * * * * *
C THIS SUBROUTINE USES THE APPROXIMATING FORMULA GIVEN BY *
C GREEN, K.J., AND HACKMUTH, K.H., PROC. 41ST ANNUAL CONV. *
C OF N.P.G.A., PP. 11-19, (1963), TO EXTEND THE K-VALUES *
C FROM KCHOA INTO THE RANGE FROM 0.7*PK TO PK. *
C * * * * * * * * * * * * * * * * * * * * * * * * * * * * * * * * * * * *
      DIMENSION SPACE(36), C(3), C1(4,3), C2(4), A(4,4),
1 D(4,4), U(4,4), P1(4)
      COMMON NCOMP, KATZ, T, P, V, SPACE, C
      SIGN=1.0
      IF(3000.0-PK)20,20,21
20 SIGN=-1.0
21 IF(P-(SIGN*0.1+0.6)*PK)1,1,2
1 CALL ROWE(PK,IV)
      RETURN
2 PSAVE=P
      P=500.0
      CALL ROWE(PK,IV)
      IF(PSAVE-PK)4,3,3
3 IV=1
      V=1.0
      GO TO 11
4 P=SIGN*0.1*PK
      DO 5 I=1,3
      P=P+PK*0.2
      CALL ROWE(PK,IV)
      P1(I)=P
      DO 5 J=1,NCOMP
      C1(I,J)=C(J)
      C1(4,J)=1.0
5 CONTINUE
      P1(4)=PK
      DO 10 J=1,NCOMP
      E=0.75
      IF(J-2)7,6,6
6 E=0.250
7 DO 8 I=1,4
      A(I,1)=(1.0-P1(I)/PK)**E
      A(I,2)=1.0/P1(I)
      A(I,3)=P1(I)
      A(I,4)=1.0
8 CONTINUE
      CALL PARTN(4,A,D,U)
      CALL INVER(4,A,D,U)
      DO 9 I=1,4
      C2(I)=0.0
      DO 9 K=1,4
      C2(I)=C2(I)+D(I,K)*C1(K,J)
9 CONTINUE
      C(J)=C2(1)*(1.0-PSAVE/PK)**E+C2(2)/PSAVE+C2(3)*PSAVE
1 +C2(4)
10 CONTINUE
      CALL FLASH(IV)
11 P=PSAVE
      RETURN
      END

```



```

SUBROUTINE ROWE(PK,IV)
C *****
C THIS SUBROUTINE CALCULATES THE CONVERGENCE PRESSURE OF *
C THE SYSTEM ACCORDING TO THE DEFINITION BY ROWE, A.M., *
C S.P.E.J. 7, PP. 54-60, (1967). *
C *****
DIMENSION WM(3), PC(3), TC(3), AF(3), DI(3), VI(3),
1 X(3), Y(3)
COMMON NCOMP, KATZ, T, P, V, WM, PC, TC, AF, DI, VI,
1 X, Y
1 FORMAT('OTIE LINE DOES NOT INTERSECT CRIT. TEMP. LOCUS!/')
  IF(NCOMP-2)2,2,3
2 Z3=0.0
  Z13=0.0
  GO TO 4
3 CALL CTEMP(Z13,1,3)
  Z31=1.0-Z13
  IF(T-TC(2))4,5,5
4 CALL CTEMP(Z12,1,2)
  Z1=Z12
  SLOPE=(Z13-Z12)/(Z12-1.0)
  ZZ=1.0-Z12
  GO TO 6
5 CALL CTEMP(Z23,2,3)
  SLOPE=-Z13/Z23
  ZZ=Z23
6 CALL KCHAO(IV)
  IF(IV)11,7,11
7 IF(NCOMP-2)10,10,8
8 SLANT=(Y(1)-X(1))/(Y(2)-X(2))
  Z2=(X(1)-SLANT*X(2)-Z13)/(SLOPE-SLANT)
  Z1=Z13+SLOPE*Z2
  Z3=1.0-Z1-Z2
  IF(Z2-ZZ)10,9,9
9 WRITE(6,1)
  Z1=Z12
  Z3=1.0-Z12
10 CALL CPRES(Z1,Z3,PK)
11 RETURN
END

```



```

SUBROUTINE KCHAO(IV)
C * * * * * * * * * * * * * * * * * * * * * * * * * * * * * * * * * * * *
C THIS SUBROUTINE CALCULATES EQUILIBRIUM RATIOS USING THE *
C METHOD OF CHAO, K.C., AND SEADER J.D., A.I.CHE.J., 7, *
C PP. 598-605, (1961). *
C * * * * * * * * * * * * * * * * * * * * * * * * * * * * * * * * * * * *
      DIMENSION WM(3), PC(3), TC(3), AF(3), DI(3), VI(3),
1 X(3), Y(3), Z(3), PHI(3), FNU(3), GAM(3), C(3), VC(3),
2 F(3)
      COMMON NCOMP, KATZ, T, P, V, WM, PC, TC, AF, DI, VI,
1 X, Y, Z, PHI, FNU, GAM, C, VC
1 FORMAT(' KCHAO ITER EQUAL 30')
      S1=0.0
      S2=0.0
      DO 2 I=1,NCOMP
      X(I)=TC(I)*VC(I)
      S1=S1+X(I)
2 CONTINUE
      DO 5 I=1,NCOMP
      X(I)=X(I)*Z(I)/S1
      S2=S2+X(I)
5 CONTINUE
      DO 6 I=1,NCOMP
      X(I)=X(I)/S2
6 CONTINUE
      CALL FGAM(0)
      DO 7 I=1,NCOMP
      Y(I)=GAM(I)*FNU(I)*X(I)
7 CONTINUE
      VOLD=0.1
      ITER=0
8 ITER=ITER+1
      SUMX=0.0
      SUMY=0.0
      DO 9 I=1,NCOMP
      SUMX=SUMX+X(I)
      SUMY=SUMY+Y(I)
9 CONTINUE
      DO 10 I=1,NCOMP
      X(I)=X(I)/SUMX
      Y(I)=Y(I)/SUMY
10 CONTINUE
      CALL FGAM(1)
      CALL PHIY
      DO 13 I=1,NCOMP
      FV=PHI(I)*Y(I)*P
      FL=GAM(I)*X(I)*FNU(I)
      F(I)=SQRT(FV*FL)
      Y(I)=F(I)/(PHI(I)*P)
      X(I)=F(I)/(GAM(I)*FNU(I))
      IF(X(I))11,11,12
11 C(I)=0.0

```



```
GO TO 13
12 C(I)=Y(I)/X(I)
13 CONTINUE
   IF(ITER=3)8,8,14
14 CONTINUE
   CALL FLASH(IV)
   IF(IV)19,15,19
15 IF(ABS(V-VOLD)=0.00001)19,19,16
16 VOLD=V
   ITER=ITER+1
   IF(ITER=30)10,10,18
18 WRITE(6,1)
19 RETURN
END
```


SUBROUTINE PHIY

```

C * * * * * * * * * * * * * * * * * * * * * * * * * * * * * * * * * * * *
C THIS SUBROUTINE CALCULATES THE VAPOR FUGACITY (PHI) AND *
C COMPRESSIBILITY FACTOR (Z) FROM THE REDLICK-KWONG EQUAT- *
C ION OF STATE. BY SETTING KATZ = 1, Z IS CALCULATED FROM *
C THE KATZ-STANDING CORRELATION INSTEAD OF REDLICK-KWONG. *
C * * * * * * * * * * * * * * * * * * * * * * * * * * * * * * * * * * * *
      DIMENSION WM(3), PC(3), TC(3), AF(3), DI(3), VI(3),
1 X(3), Y(3), Z(3), PHI(3), ARK(3), BRK(3)
      COMMON NCOMP, KATZ, T, P, V, WM, PC, TC, AF, DI, VI,
1 X, Y, Z, PHI
1 FORMAT(' Z R-K ITER EQUAL 30')
2 FORMAT(' Z KATZ ITER =',13)
      AMIX=0.0
      BМИX=0.0
      DO 3 I=1,NCOMP
      TR=T/TC(I)
      ARK(I)=SQRT(0.42748028/(PC(I)*TR**2.5))
      BRK(I)=0.08664035/(PC(I)*TR)
      BМИX=BМИX+BRK(I)*Y(I)
      AMIX=AMIX+ARK(I)*Y(I)
3  CONTINUE
      AOB=AMIX*AMIX/BМИX
      IF(KATZ)4,4,9
4  CON1=2.0
      CON2=BМИX*P+0.001
      DO 8 ITER=1,30
      ZAS=(CON1+CON2)/2.0
      H=BМИX*P/ZAS
      ZZ=1.0/(1.0-H)-AOB*(H/(1.0+H))
      DEL=ZZ-ZAS
      IF(ABS(DEL)-0.0001)12,12,5
5  IF(DEL)6,6,7
6  CON1=ZAS
      GO TO 8
7  CON2=ZAS
8  CONTINUE
      WRITE(6,1)
      RETURN
9  PPC=0.0
      PTC=0.0
      DO 10 I=1,NCOMP
      PPC=PPC+Y(I)*PC(I)
      PTC=PTC+Y(I)*TC(I)
10 CONTINUE
      PR=P/PPC
      TR=T/PTC
      CALL ZKATZ(PR,TR,ZZ,ITER)
      IF(ITER)11,11,12
11 WRITE(6,2)ITER
      GO TO 4
12 DO 13 I=1,NCOMP
      PHI(I)=EXP((ZZ-1.0)*BRK(I)/BМИX- ALOG(ZZ-BМИX*P)-
1 AOB*(2.0*ARK(I)/AMIX-BRK(I)/BМИX)*ALOG(1.0+BМИX*P/ZZ))
13 CONTINUE
      RETURN
      END

```



```

SUBROUTINE FGAM(KASE)
C * * * * * * * * * * * * * * * * * * * * * * * * * * * * * * * * * * *
C THIS SUBROUTINE CALCULATES LIQUID FUGACITY COEFFICIENTS *
C (FNU) FROM A CORRESPONDING STATES CORRELATION, AND THE *
C ACTIVIVITY COEFFICIENTS IN THE LIQUID SOLUTION (GAM) *
C FROM HILDEBRAND'S EQUATION FOR A REGULAR SOLUTION. *
C * * * * * * * * * * * * * * * * * * * * * * * * * * * * * * * * * * *
DIMENSION WM(3), PC(3), TC(3), AF(3), DI(3), VI(3),
1 X(3), Y(3), Z(3), PHI(3), FNU(3), GAM(3), A(15,2)
COMMON NCOMP, KATZ, T, P, V, WM, PC, TC, AF, DI, VI,
1 X, Y, Z, PHI, FNU, GAM
DATA A/2.43840,-2.24550,-0.34084,0.00212,-0.00223,
1 0.10486,-0.03691,0.0,0.0,0.0,0.0,0.0,0.0,0.0,0.0,0.0,
25.75748,-3.01761,-4.9850,2.02299,0.0,0.06427,0.26667,
3-0.31138,-0.02655,0.02883,-4.238930,8.65808,-1.22060,
4-3.15224,-0.025/
IF(KASE)6,1,6
1 DO 5 I=1,NCOMP
  J=2
  CORR=1.0
  IF(WM(I)-17.0)3,4,4
3 J=1
4 TR=T/TC(I)
  PR=P/PC(I)
  FPO=A(1,J)+A(2,J)/TR+A(3,J)*TR+A(4,J)*TR**2+A(5,J)*TR**3
  1+(A(6,J)+A(7,J)*TR+A(8,J)*TR**2)*PR+(A(9,J)+A(10,J)*TR
  2)*PR**2-ALOG(PR)/2.3025851
  FPI=A(11,J)+A(12,J)*TR+A(13,J)/TR+A(14,J)*TR**3+
  1 A(15,J)*(PR-0.60)
  FNU(I)=P*EXP((FPO+AF(I)*FPI)*2.3025851)
5 CONTINUE
6 CON1=0.0
  CON2=0.0
  DO 7 I=1,NCOMP
    DELMX=X(I)*VI(I)
    CON1=CON1+DELMX
    CON2=CON2+DELMX*DI(I)
7 CONTINUE
  DELMX=CON2/CON1
  RT=1.987*T/1.80
  DO 8 I=1,NCOMP
    GAM(I)=EXP(VI(I)*(DI(I)-DELMX)**2/RT)
8 CONTINUE
  RETURN
END

```



```

SUBROUTINE FLASH(KODE)
C ****
C THIS SUBROUTINE CHECKS IF THE SYSTEM IS IN THE TWO PHASE *
C REGION, THEN PERFORMS AN EQUILIBRIUM FLASH CALCULATION *
C USING A NEWTON-RAPHSON PROCEDURE TO LOCATE V.
C ****
      DIMENSION WM(3), PC(3), TC(3), AF(3), DI(3), VI(3),
1 X(3), Y(3), Z(3), PHI(3), FNU(3), GAM(3), C(3)
      COMMON NCOMP, KATZ, T, P, V, WM, PC, TC, AF, DI, VI,
1 X, Y, Z, PHI, FNU, GAM, C
      1 FORMAT(' FLASH ITER EQUAL 10')
C      CHECK IF SYSTEM CAN BE FLASHED
      BP=0.0
      DP=0.0
      DO 10 I=1,NCOMP
      BP=BP+C(I)*Z(I)
      DP=DP+Z(I)/C(I)
10 CONTINUE
      IF(BP-1.0)12,11,11
11 IF(DP-1.0)13,14,14
C      KODE = -1 SYSTEM IS A SINGLE PHASE LIQUID
12 KODE=-1
      V=0.0
      RETURN
C      KODE = 1 SYSTEM IS A SINGLE PHASE VAPOR
13 KODE=1
      V=1.0
      RETURN
14 KODE=0
C      KODE = 0 SYSTEM IS IN TWO PHASE REGION
      V=0.7
      DO 20 ITER=1,10
      F=0.0
      DF=0.0
      DO 15 I=1,NCOMP
      R=(C(I)-1.0)/((C(I)-1.0)*V+1.0)
      F=F+R*Z(I)
      DF=DF-R*R*Z(I)
15 CONTINUE
      V1=V-F/DF
      IF(V1)16,16,17
16 V1=V*0.5
      GO TO 19
17 IF(V1-1.0)19,18,18
18 V1=(V+1.0)*0.5
19 V=V1
      IF(ABS(F)-0.000001)21,20,20
20 CONTINUE
      WRITE(6,1)
21 DO 22 I=1,NCOMP
      X(I)=Z(I)/((C(I)-1.0)*V+1.0)
      Y(I)=C(I)*X(I)
22 CONTINUE
      RETURN
      END

```



```

SUBROUTINE CTEMP(Z,IL,IH)
C * * * * * * * * * * * * * * * * * * * * * * * * * * * * * * * * * * * *
C THIS SUBROUTINE DETERMINES THE COMPOSITION OF THE BINARY *
C MIXTURE WHOSE CRITICAL TEMPERATURE EQUALS THE SYSTEM *
C TEMPERATURE VIA THE CORRELATION OF ETER, D.O., AND KAY, *
C W.B., J. CHEM. ENG. DATA, VOL. 6, PP. 409-414, (1961). *
C * * * * * * * * * * * * * * * * * * * * * * * * * * * * * * * * * * * *
DIMENSION WM(3), PC(3), TC(3)
COMMON NCOMP, KATZ, T, P, V, WM, PC, TC
Z=1.0
DO 22 K=1,5
DO 20 J=1,10
Z=Z+0.1**K
WL=Z*WM(IL)
WH=(1.0-Z)*WM(IH)
AMW=(WM(IL)*WL+WM(IH)*WH)/(WL+WH)
IF(WM(IL)=17.0)10,11,11
10 A=420.0
B=WL/(WL+WH)
B=0.447-0.597*B**1.86
GO TO 18
11 IF(WM(IL)=31.0)12,13,13
12 A=565.0
B=0.454-10.0**((2.0/Z)**2.37)
GO TO 18
13 IF(WM(IL)=45.0)14,15,15
14 A=677.0
B=0.452-0.209*Z**1.85
GO TO 18
15 IF(WM(IL)=59.0)16,17,17
16 A=769.0
B=0.447-10.0**((0.842/Z)**1.78)
GO TO 18
17 A=TC(IL)
B=0.344-290.0/WM(IL)**2*Z**((15.0/WM(IL)**0.556)
18 TCM=A*(AMW/WM(IL))**B
IF(ABS(TCM-T)=0.1)23,23,19
19 IF(TCM-T)20,23,21
20 CONTINUE
21 Z=Z+0.1**K
22 CONTINUE
23 RETURN
END

```



```

SUBROUTINE CPRES(Z1,Z3,PK)
C * * * * * * * * * * * * * * * * * * * * * * * * * * * * * * * * * * * *
C THIS SUBROUTINE DETERMINES THE CRITICAL PRESSURE OF A * *
C SPECIFIED BINARY OR TERNARY MIXTURE VIA THE CORRELATION * *
C OF ETTER, D.O., AND KAY, W.B., J. CHEM. ENG. DATA, VOL. * *
C 6, PP. 409-414, (1961). * *
C * * * * * * * * * * * * * * * * * * * * * * * * * * * * * * * * * * * *
DIMENSION WM(3), PC(3), W(3), Z(3), X(3), A(3), B(3),
1 C(3)
COMMON NCOMP, KATZ, T, P, V, WM, PC
Z(1)=Z1
Z(2)=1.0-Z1-Z3
Z(3)=Z3
PK=0.0
S=0.0
WAV=0.0
DO 10 I=1,NCOMP
PK=PK+Z(I)*PC(I)
W(I)=Z(I)*WM(I)
S=S+W(I)
10 CONTINUE
DO 19 I=1,NCOMP
W(I)=W(I)/S
WAV=WAV+W(I)*WM(I)
X(I)=Z(I)
IF(WM(I)-17.0)11,12,12
11 A(I)=137.0
B(I)=1.073
C(I)=-3.07
X(I)=W(I)
GO TO 19
12 IF(WM(I)-31.0)13,14,14
13 A(I)=28.6
B(I)=1.595
C(I)=-4.0
GO TO 19
14 IF(WM(I)-45.0)15,16,16
15 A(I)=13.6
B(I)=1.225
C(I)=-4.3
GO TO 19
16 IF(WM(I)-59.0)17,18,18
17 A(I)=9.24
B(I)=1.284
C(I)=-3.5
GO TO 19
18 A(I)=9400.0/WM(I)**1.71
B(I)=2.06/WM(I)**0.115
19 CONTINUE
IF(NCOMP-2)20,20,21
20 PK=PC(1)+(A(1)*X(1)**B(1)+C(1))*(WAV-WM(1))
RETURN
21 PK=PK+A(1)*X(1)**B(1)*(WAV-WM(1))+A(2)*(Z(2)/(1.0-Z(1))
1 )**B(2)*(1.0-Z(1))*((WAV-W(1)*WM(1))/(1.0-W(1))-WM(2))
RETURN
END

```


Critical Temperature Calculations by the Method of Etter and Kay

Etter and Kay⁵² observed that a log-log plot of the critical temperatures of a series of binary mixtures of alkanes (all mixtures having a common component) versus the average molecular weight of the mixture resulted in a family of straight lines. These lines converged to a common point representing the critical temperature and molecular weight of the lightest component in the mixture. Thus, they were able to correlate critical temperatures to within about one per cent using equations having the form

$$T_C = A(M_{Av}/M_L)^B$$

where: T_C is the critical temperature of the binary mixture, °R,

A is a constant and represents the critical temperature of the light component in the mixture,

M_{Av} is the average molecular weight calculated on a weight basis,

M_L is the molecular weight of the light component,

B is the slope of the straight line expressed as a simple function of the composition.

Critical Pressure Calculations by the Method of Etter and Kay

Etter and Kay also observed that a plot of the critical pressures of a series of binary mixtures of alkanes (all mixtures having a common component) versus average molecular weight of the mixture resulted in a family of straight lines. These lines converged to a common point representing the critical pressure and molecular weight of the lightest component in the mixture. Thus, they were able to correlate critical pressures to within about two per cent by equations having the

form

$$P_C = P_{cL} + C(M_{Av} - M_L)$$

where: P_C is the critical pressure of the binary mixture, psia,

P_{cL} is the critical pressure of the light component in the mixture, psia,

C is the slope of the straight line expressed as a simple function of the composition,

M_{Av} is the average molecular weight, calculated on a weight basis for binaries containing methane, and on a mole basis for other systems,

M_L is the molecular weight of the light component.

Etter and Kay showed that the following relationship could be used to extend the procedure for binaries to multicomponent mixtures

$$P_C = \sum x_i P_{ci} + \sum \phi_i$$

where: $\sum x_i P_{ci}$ is the pseudocritical pressure of the mixture,

$\sum \phi_i$ is the excess critical pressure of every binary mixture with the light component in the system, excepting the binary made up of the lightest and heaviest components in the system.

APPENDIX E
COMPUTER PRINTOUT FOR
SIMULATION OF DEPLETION PERFORMANCE RUNS

TABLE E-1

RUN NO. 5, METHANE AND N-BUTANE AT 100 F.
DEPLETION OF A CONSTANT VOLUME RESERVOIR BY VAPOR PRODUCTION

PURE COMPONENT DATA								
COMP	MOLE WT LB/MOLE	PC PSIA	VC FT**3	TC DEG R	ZC	PITZER OMEGA	RIEDEL ALPHA	
C1	16.042	669.7	1.590	343.13	0.288	0.000	5.860	
C4	58.120	550.7	4.080	765.29	0.274	0.195	6.770	
SIMULATED DEPLETION PERFORMANCE								
COMP	SYSTEM COMP	VAPOR COMP	LIQUID COMP	K VALUE	P, PK PSIA	LIQ VOL %	VAPOR CF/LB	LIQUID CF/LB
C1	0.816	0.816	0.000	1.000	2250.	0.00	0.073	0.00000
C4	0.184	0.184	0.000	1.000				
MOLES	0.570	0.570	0.000		1934.			
C1	0.815	0.815	0.000	1.000	2000.	0.00	0.082	0.00000
C4	0.183	0.183	0.000	1.000				
MOLES	0.511	0.511	0.000		1934.			
C1	0.815	0.839	0.580	1.445	1750.	7.54	0.103	0.0475
C4	0.183	0.160	0.419	0.352				
MOLES	0.438	0.391	0.047		1934.			
C1	0.812	0.869	0.477	1.822	1500.	9.98	0.138	0.0407
C4	0.187	0.130	0.522	0.249				
MOLES	0.366	0.301	0.064		1934.			
C1	0.800	0.878	0.396	2.217	1250.	9.15	0.178	0.0373
C4	0.199	0.121	0.603	0.201				
MOLES	0.307	0.240	0.059		1934.			
C1	0.783	0.877	0.317	2.767	1000.	7.87	0.232	0.0348
C4	0.216	0.122	0.682	0.178				
MOLES	0.237	0.186	0.050		1934.			
C1	0.758	0.872	0.253	3.442	800.	6.88	0.298	0.0331
C4	0.241	0.127	0.746	0.170				
MOLES	0.189	0.145	0.043		1934.			

TABLE E-1 (CONT.)

RUN NO. 5, METHANE AND N-BUTANE AT 100 F.

SIMULATED DEPLETION PERFORMANCE									
COMP	SYSTEM	VAPOR COMP	LIQUID COMP	K VALUE	P, PSIA	LIQ VOL %	VAPOR CF/LB	LIQUID CF/LB	
C1	0.729	0.858	0.188	4.554	600.	5.81	0.401	0.0318	
C4	0.270	0.141	0.811	0.174					
MOLES	0.142	0.106	0.036		1934.				
C1	0.688	0.823	0.121	6.758	400.	4.46	0.582	0.0305	
C4	0.311	0.176	0.878	0.201					
MOLES	0.097	0.069	0.027		1934.				
C1	0.624	0.706	0.053	13.303	200.	2.01	0.988	0.0294	
C4	0.375	0.293	0.946	0.309					
MOLES	0.047	0.034	0.012		1934.				
C1	0.537	0.627	0.035	17.626	150.	1.19	1.184	0.0292	
C4	0.462	0.372	0.964	0.386					
MOLES	0.033	0.026	0.007		1934.				
ZKATZ ITER =	0								
C1	0.500	0.500	0.000	1.000	100.	0.00	1.520	0.0000	
C4	0.499	0.499	0.000	1.000					
MOLES	0.017	0.017	0.000		1934.				

TABLE E-2

RUN NO. 13, METHANE AND N-BUTANE AT 100 F.
DEPLETION OF A CONSTANT VOLUME RESERVOIR BY VAPOR PRODUCTION

PURE COMPONENT DATA							
COMP	MOLE WT LB/MOLE	PC PSIA	VC FT**3	TC DEG R	ZC	PITZER OMEGA	RIEDEL ALPHA
C1	16.042	669.7	1.590	343.13	0.288	0.000	5.860
C4	58.120	550.7	4.080	765.29	0.274	0.195	6.770
SIMULATED DEPLETION PERFORMANCE							
COMP	SYSTEM COMP	VAPOR COMP	LIQUID COMP	K VALUE	P, PK PSIA VOL %	VAPOR CF/LB	LIQUID CF/LB
C1	0.849	0.849	0.000	1.000	2000.	0.00	0.092
C4	0.151	0.151	0.000	1.000			
MOLES	0.482	0.482	0.000		1912.		
C1	0.848	0.848	0.000	1.000	1750.	0.00	0.107
C4	0.150	0.150	0.000	1.000			
MOLES	0.416	0.416	0.000		1934.		
C1	0.848	0.869	0.477	1.822	1500.	3.39	0.138
C4	0.150	0.130	0.522	0.249			
MOLES	0.345	0.323	0.021		1934.		
C1	0.844	0.878	0.396	2.217	1250.	3.74	0.178
C4	0.155	0.121	0.603	0.201			
MOLES	0.279	0.255	0.024		1934.		
C1	0.836	0.877	0.317	2.767	1000.	3.19	0.232
C4	0.163	0.122	0.682	0.178			
MOLES	0.216	0.196	0.020		1934.		
C1	0.824	0.872	0.253	3.442	800.	2.62	0.298
C4	0.175	0.127	0.746	0.170			
MOLES	0.168	0.152	0.016		1934.		
C1	0.811	0.858	0.188	4.554	600.	1.89	0.401
C4	0.186	0.141	0.811	0.174			
MOLES	0.122	0.111	0.011		1934.		

TABLE E-2 (CONT.)

RUN NO. 13, METHANE AND N-BUTANE AT 100 F.

SIMULATED DEPLETION PERFORMANCE									
COMP	SYSTEM	VAPOR COMP	LIQUID COMP	K VALUE	P, PSIA	P, PSIA	Liq Vol %	VAPOR CF/LB	LIQUID CF/LB
C1	0.793	0.823	0.121	6.758	400.	0.83	0.582	0.0305	
C4	0.206	0.176	0.878	0.201					
MOLES	0.077	0.072	0.005		1934.				
C1	0.776	0.776	0.000	1.000	200.	0.00	1.119	0.0000	
C4	0.223	0.223	0.000	1.000					
MOLES	0.035	0.035	0.000		1934.				

TABLE E-3

RUN NO. 1, METHANE AND N-PENTANE AT 99.5 F.
DEPLETION OF A CONSTANT VOLUME RESERVOIR BY VAPOR PRODUCTION

PURE COMPONENT DATA							
COMP	MOLE WT LB/MOLE	PC PSIA	VC FT**3	TC DEG R	ZC	PITZER OMEGA	RIEDEL ALPHA
C1	16.042	669.7	1.590	343.13	0.288	0.000	5.860
C5	72.146	487.3	4.730	845.08	0.254	0.238	7.030
SIMULATED DEPLETION PERFORMANCE							
COMP	SYSTEM COMP	VAPOR COMP	LIQUID COMP	K VALUE	P, PK PSIA VOL %	VAPOR CF/LB	LIQUID CF/LB
C1	0.881	0.881	0.000	1.000	2500.	0.00	0.074
C5	0.119	0.119	0.000	1.000			
MOLES	0.588	0.588	0.000		2410.		
C1	0.880	0.905	0.694	1.303	2250.	10.83	0.091
C5	0.118	0.094	0.305	0.308			
MOLES	0.527	0.457	0.069		2410.		
C1	0.878	0.927	0.587	1.576	2000.	11.62	0.113
C5	0.121	0.072	0.412	0.176			
MOLES	0.464	0.388	0.076		2410.		
C1	0.871	0.941	0.514	1.830	1750.	11.63	0.139
C5	0.128	0.058	0.485	0.121			
MOLES	0.403	0.327	0.075		2410.		
C1	0.860	0.946	0.447	2.114	1500.	10.74	0.169
C5	0.139	0.053	0.552	0.097			
MOLES	0.344	0.275	0.068		2410.		
C1	0.846	0.949	0.379	2.499	1250.	9.90	0.212
C5	0.153	0.050	0.620	0.081			
MOLES	0.286	0.224	0.062		2410.		
C1	0.825	0.951	0.310	3.069	1000.	9.13	0.276
C5	0.174	0.048	0.689	0.070			
MOLES	0.231	0.175	0.056		2410.		

TABLE E-3 (CONT.)

RUN NO. 1, METHANE AND N-PENTANE AT 99.5 F.

SIMULATED DEPLETION PERFORMANCE									
COMP	SYSTEM COMP	VAPOR COMP	LIQUID COMP	K VALUE	P, PSIA	PK VOL %	VAPOR CF/LB	LIQUID CF/LB	
C1	0.795	0.951	0.252	3.775	800.	8.52	0.355	0.0284	
C5	0.204	0.048	0.747	0.064					
MOLES	0.188	0.137	0.051		2410.				
C1	0.760	0.948	0.191	4.945	600.	7.89	0.482	0.0274	
C5	0.239	0.051	0.808	0.064					
MOLES	0.147	0.100	0.046		2410.				
C1	0.707	0.938	0.128	7.279	400.	7.22	0.722	0.0264	
C5	0.292	0.061	0.871	0.071					
MOLES	0.107	0.065	0.042		2410.				
C1	0.622	0.926	0.096	9.609	300.	6.85	0.943	0.0260	
C5	0.377	0.073	0.903	0.081					
MOLES	0.088	0.048	0.039		2410.				
C1	0.556	0.901	0.063	14.262	200.	6.39	1.341	0.0256	
C5	0.443	0.098	0.936	0.104					
MOLES	0.068	0.032	0.036		2410.				
C1	0.457	0.876	0.046	18.909	150.	6.13	1.688	0.0254	
C5	0.542	0.123	0.953	0.129					
MOLES	0.058	0.024	0.034		2410.				
C1	0.387	0.825	0.029	28.188	100.	5.76	2.264	0.0252	
C5	0.612	0.174	0.970	0.179					
MOLES	0.048	0.016	0.032		2410.				
C1	0.293	0.786	0.022	35.134	80.	5.57	2.617	0.0251	
C5	0.706	0.213	0.977	0.217					
MOLES	0.044	0.012	0.031		2410.				
C1	0.245	0.722	0.015	46.686	60.	5.32	3.096	0.0250	
C5	0.754	0.277	0.984	0.281					
MOLES	0.039	0.009	0.029		2410.				

TABLE E-4

RUN NO. 2, METHANE AND N-PENTANE AT 99.7 F.
DEPLETION OF A CONSTANT VOLUME RESERVOIR BY VAPOR PRODUCTION

PURE COMPONENT DATA								
COMP	MOLE WT LB/MOLE	PC PSIA	VC FT**3	TC DEG R	ZC	PITZER OMEGA	RIEDEL ALPHA	
C1	16.042	669.7	1.590	343.13	0.288	0.000	5.860	
C5	72.145	487.3	4.730	845.08	0.254	0.238	7.030	
SIMULATED DEPLETION PERFORMANCE								
COMP	SYSTEM COMP	VAPOR COMP	LIQUID COMP	K VALUE	P, PK PSIA	LIG VOL %	VAPOR CF/LB	LIQUID CF/LB
C1	0.911	0.911	0.000	1.000	2500.	0.00	0.084	0.0000
C5	0.089	0.089	0.000	1.000				
MOLES	0.561	0.551	0.000		2409.			
C1	0.910	0.910	0.000	1.000	2250.	0.00	0.093	0.0000
C5	0.088	0.088	0.000	1.000				
MOLES	0.508	0.503	0.000		2409.			
C1	0.910	0.927	0.587	1.577	2000.	3.66	0.113	0.0389
C5	0.088	0.072	0.412	0.176				
MOLES	0.446	0.422	0.024		2409.			
C1	0.908	0.940	0.513	1.831	1750.	5.17	0.139	0.0354
C5	0.091	0.059	0.486	0.121				
MOLES	0.385	0.351	0.033		2409.			
C1	0.903	0.945	0.447	2.115	1500.	5.09	0.169	0.0331
C5	0.096	0.054	0.552	0.097				
MOLES	0.325	0.292	0.032		2409.			
C1	0.895	0.949	0.379	2.500	1250.	4.85	0.212	0.0312
C5	0.104	0.050	0.620	0.081				
MOLES	0.267	0.237	0.030		2409.			
C1	0.884	0.951	0.309	3.070	1000.	4.54	0.276	0.0296
C5	0.115	0.048	0.690	0.070				
MOLES	0.211	0.183	0.028		2409.			

TABLE E-4 (CONT.)

RUN NO. 2, METHANE AND N-PENTANE AT 99.7 F.

SIMULATED DEPLETION PERFORMANCE									
COMP	SYSTEM COMP	VAPOR COMP	LIQUID COMP	K VALUE	P, PK PSIA	LIQ VOL %	VAPOR CF/LB	LIQUID CF/LB	
C1	0.866	0.951	0.251	3.776	800.	4.23	0.355	0.0284	
C5	0.133	0.048	0.748	0.065					
MOLES	0.169	0.143	0.025		2409.				
C1	0.845	0.948	0.191	4.948	600.	3.87	0.482	0.0274	
C5	0.154	0.051	0.808	0.064					
MOLES	0.128	0.105	0.022		2409.				
C1	0.812	0.937	0.128	7.283	400.	3.42	0.721	0.0264	
C5	0.187	0.062	0.871	0.071					
MOLES	0.088	0.068	0.019		2409.				
C1	0.755	0.926	0.096	9.614	300.	3.15	0.943	0.0260	
C5	0.244	0.073	0.903	0.081					
MOLES	0.069	0.050	0.018		2409.				
C1	0.707	0.901	0.063	14.270	200.	2.79	1.341	0.0256	
C5	0.292	0.098	0.936	0.105					
MOLES	0.049	0.033	0.015		2409.				
C1	0.631	0.876	0.046	18.920	150.	2.57	1.687	0.0254	
C5	0.368	0.123	0.953	0.129					
MOLES	0.039	0.025	0.014		2409.				
C1	0.571	0.824	0.029	28.204	100.	2.24	2.262	0.0252	
C5	0.428	0.175	0.970	0.180					
MOLES	0.029	0.016	0.012		2409.				
C1	0.482	0.786	0.022	35.154	80.	2.07	2.614	0.0251	
C5	0.517	0.213	0.977	0.218					
MOLES	0.025	0.013	0.011		2409.				
C1	0.429	0.721	0.015	46.712	60.	1.84	3.091	0.0250	
C5	0.570	0.278	0.984	0.282					
MOLES	0.020	0.010	0.010		2409.				

TABLE E-5

RUN NO. 8, METHANE AND N-PENTANE AT 100 F.
DEPLETION OF A CONSTANT VOLUME RESERVOIR BY VAPOR PRODUCTION

PURE COMPONENT DATA							
COMP	MOLE WT LB/MOLE	PC PSIA	VC FT**3	TC DEG R	ZC	PITZER OMEGA	RIEDEL ALPHA
C1	16.042	669.7	1.590	343.13	0.288	0.000	5.860
C5	72.146	487.3	4.730	845.08	0.254	0.238	7.030
SIMULATED DEPLETION PERFORMANCE							
COMP	SYSTEM COMP	VAPOR COMP	LIQUID COMP	K VALUE	P, PK PSIA VOL %	VAPOR CF/LB	LIQUID CF/LB
C1	0.936	0.936	0.000	1.000	2500.	0.00	0.094
C5	0.064	0.064	0.000	1.000			
MOLES	0.540	0.540	0.000		2409.		
C1	0.935	0.935	0.000	1.000	2250.	0.00	0.104
C5	0.063	0.063	0.000	1.000			
MOLES	0.488	0.488	0.000		2409.		
C1	0.935	0.935	0.000	1.000	2000.	0.00	0.117
C5	0.063	0.063	0.000	1.000			
MOLES	0.432	0.432	0.000		2409.		
C1	0.935	0.940	0.513	1.831	1750.	0.74	0.139
C5	0.063	0.059	0.486	0.121			
MOLES	0.372	0.367	0.004		2409.		
C1	0.935	0.945	0.446	2.116	1500.	1.22	0.169
C5	0.064	0.054	0.553	0.098			
MOLES	0.312	0.304	0.007		2409.		
C1	0.933	0.949	0.379	2.502	1250.	1.39	0.212
C5	0.066	0.050	0.620	0.081			
MOLES	0.254	0.245	0.008		2409.		
C1	0.929	0.951	0.309	3.072	1000.	1.39	0.276
C5	0.070	0.048	0.690	0.070			
MOLES	0.198	0.189	0.008		2409.		

TABLE E-5 (CONT.)

RUN NO. 8, METHANE AND N-PENTANE AT 100 F.

		SIMULATED DEPLETION PERFORMANCE						
COMP	SYSTEM COMP	VAPOR COMP	LIQUID COMP	K VALUE	P, PK PSIA	LIQ VOL %	VAPOR CF/LB	LIQUID CF/LB
C1	0.923	0.951	0.251	3.779	800.	1.29	0.355	0.0284
C5	0.076	0.048	0.748	0.065				
MOLES	0.155	0.147	0.007		2409.			
C1	0.915	0.947	0.191	4.951	600.	1.10	0.482	0.0274
C5	0.084	0.052	0.808	0.064				
MOLES	0.114	0.108	0.006		2409.			
C1	0.904	0.937	0.128	7.288	400.	0.80	0.721	0.0264
C5	0.095	0.062	0.871	0.071				
MOLES	0.075	0.070	0.004		2409.			
C1	0.886	0.900	0.063	14.282	200.	0.22	1.340	0.0256
C5	0.113	0.099	0.936	0.105				
MOLES	0.035	0.034	0.001		2409.			
C1	0.871	0.875	0.046	18.936	150.	0.02	1.685	0.0254
C5	0.128	0.124	0.953	0.130				
MOLES	0.025	0.025	0.000		2409.			
C1	0.870	0.870	0.000	1.000	100.	0.00	2.521	0.0000
C5	0.129	0.129	0.000	1.000				
MOLES	0.016	0.016	0.000		2409.			
C1	0.870	0.870	0.000	1.000	80.	0.00	3.164	0.0000
C5	0.129	0.129	0.000	1.000				
MOLES	0.013	0.013	0.000		2409.			
C1	0.870	0.870	0.000	1.000	60.	0.00	4.237	0.0000
C5	0.129	0.129	0.000	1.000				
MOLES	0.010	0.010	0.000		2409.			
C1	0.870	0.870	0.000	1.000	40.	0.00	6.382	0.0000
C5	0.129	0.129	0.000	1.000				
MOLES	0.006	0.006	0.000		2409.			

TABLE E-6

RUN NO. 9, METHANE AND N-PENTANE AT 100 F.
DEPLETION OF A CONSTANT VOLUME RESERVOIR BY VAPOR PRODUCTION

PURE COMPONENT DATA								
COMP	MOLE WT LB/MOLE	PC PSIA	VC FT**3	TC DEG R	ZC	PITZER OMEGA	RIEDEL ALPHA	
C1	16.042	669.7	1.590	343.13	0.288	0.000	5.860	
C5	72.146	487.3	4.730	845.08	0.254	0.238	7.030	
SIMULATED DEPLETION PERFORMANCE								
COMP	SYSTEM COMP	VAPOR COMP	LIQUID COMP	K VALUE	P, PK PSIA	LIQ VOL %	VAPOR CF/LB	LIQUID CF/LB
C1	0.878	0.878	0.000	1.000	2500.	0.00	0.074	0.0000
C5	0.122	0.122	0.000	1.000				
MOLES	0.590	0.590	0.000		2409.			
C1	0.877	0.905	0.694	1.303	2250.	12.03	0.091	0.0470
C5	0.121	0.094	0.305	0.309				
MOLES	0.528	0.451	0.077		2409.			
C1	0.874	0.926	0.587	1.577	2000.	12.35	0.113	0.0389
C5	0.125	0.073	0.412	0.177				
MOLES	0.465	0.384	0.081		2409.			
C1	0.867	0.940	0.513	1.831	1750.	12.24	0.139	0.0355
C5	0.132	0.059	0.486	0.121				
MOLES	0.404	0.324	0.079		2409.			
C1	0.856	0.945	0.446	2.116	1500.	11.26	0.169	0.0331
C5	0.143	0.054	0.553	0.098				
MOLES	0.345	0.273	0.072		2409.			
C1	0.841	0.949	0.379	2.502	1250.	10.37	0.212	0.0312
C5	0.158	0.050	0.620	0.081				
MOLES	0.288	0.223	0.065		2409.			
C1	0.820	0.951	0.309	3.072	1000.	9.55	0.276	0.0296
C5	0.179	0.048	0.690	0.070				
MOLES	0.232	0.174	0.058		2409.			

TABLE E-6 (CONT.)

RUN NO. 9, METHANE AND N-PENTANE AT 100 F.

		SIMULATED DEPLETION PERFORMANCE						
COMP	SYSTEM COMP	VAPOR COMP	LIQUID COMP	K VALUE	P, PSIA	PK VOL %	VAPOR CF/LB	LIQUID CF/LB
C1	0.789	0.951	0.251	3.779	800.	8.91	0.355	0.0284
C5	0.210	0.048	0.748	0.065				
MOLES	0.190	0.136	0.053					2409.
C1	0.752	0.947	0.191	4.951	600.	8.27	0.482	0.0274
C5	0.247	0.052	0.808	0.064				
MOLES	0.149	0.100	0.049					2409.
C1	0.699	0.937	0.128	7.288	400.	7.56	0.721	0.0264
C5	0.300	0.062	0.871	0.071				
MOLES	0.109	0.065	0.044					2409.
C1	0.612	0.900	0.063	14.282	200.	6.62	1.340	0.0256
C5	0.387	0.099	0.936	0.105				
MOLES	0.069	0.032	0.037					2409.
C1	0.449	0.875	0.046	18.936	150.	6.35	1.685	0.0254
C5	0.550	0.124	0.953	0.130				
MOLES	0.060	0.024	0.035					2409.
C1	0.379	0.823	0.029	28.228	100.	5.97	2.259	0.0252
C5	0.620	0.176	0.970	0.181				
MOLES	0.049	0.016	0.033					2409.
C1	0.286	0.785	0.022	35.184	80.	5.78	2.609	0.0251
C5	0.713	0.214	0.977	0.219				
MOLES	0.045	0.012	0.032					2409.
C1	0.238	0.720	0.015	46.751	60.	5.52	3.085	0.0250
C5	0.761	0.279	0.984	0.284				
MOLES	0.040	0.009	0.030					2409.

TABLE E-7

RUN NO. 10, UHP METHANE AND N-PENTANE AT 100 F.
DEPLETION OF A CONSTANT VOLUME RESERVOIR BY VAPOR PRODUCTION

PURE COMPONENT DATA								
COMP	MOLE WT LB/MOLE	PC PSIA	VC FT**3	TC DEG R	ZC	PITZER OMEGA	RIEDEL ALPHA	
C1	16.042	669.7	1.590	343.13	0.288	0.000	5.860	
C5	72.146	487.3	4.730	845.08	0.254	0.238	7.030	
SIMULATED DEPLETION PERFORMANCE								
COMP	SYSTEM COMP	VAPOR COMP	LIQUID COMP	K VALUE	P, PK PSIA	LIQ VOL %	VAPOR CF/LB	LIQUID CF/LB
C1	0.925	0.925	0.000	1.000	2500.	0.00	0.089	0.0000
C5	0.075	0.075	0.000	1.000				
MOLES	0.549	0.549	0.000		2409.			
C1	0.924	0.924	0.000	1.000	2250.	0.00	0.099	0.0000
C5	0.074	0.074	0.000	1.000				
MOLES	0.496	0.496	0.000		2409.			
C1	0.924	0.926	0.587	1.577	2000.	0.40	0.113	0.0389
C5	0.074	0.073	0.412	0.177				
MOLES	0.439	0.436	0.002		2409.			
C1	0.924	0.940	0.513	1.831	1750.	2.53	0.139	0.0355
C5	0.075	0.059	0.486	0.121				
MOLES	0.377	0.360	0.016		2409.			
C1	0.922	0.945	0.446	2.116	1500.	2.78	0.169	0.0331
C5	0.077	0.054	0.553	0.098				
MOLES	0.317	0.299	0.017		2409.			
C1	0.917	0.949	0.379	2.502	1250.	2.79	0.212	0.0312
C5	0.082	0.050	0.620	0.081				
MOLES	0.259	0.241	0.017		2409.			
C1	0.910	0.951	0.309	3.072	1000.	2.66	0.276	0.0296
C5	0.089	0.048	0.690	0.070				
MOLES	0.203	0.187	0.016		2409.			

TABLE E-7 (CONT.)

RUN NO. 10, UHP METHANE AND N-PENTANE AT 100 F.

SIMULATED DEPLETION PERFORMANCE									
COMP	SYSTEM COMP	VAPOR COMP	LIQUID COMP	K VALUE	P, PK PSIA	LIQ VOL %	VAPOR CF/LB	LIQUID CF/LB	
C1	0.899	0.951	0.251	3.779	800.	2.48	0.355	0.0284	
C5	0.100	0.048	0.748	0.065					
MOLES	0.161	0.146	0.015		2409.				
C1	0.885	0.947	0.191	4.951	600.	2.22	0.482	0.0274	
C5	0.114	0.052	0.808	0.064					
MOLES	0.120	0.106	0.013		2409.				
C1	0.864	0.937	0.128	7.288	400.	1.86	0.721	0.0264	
C5	0.135	0.062	0.871	0.071					
MOLES	0.080	0.069	0.010		2409.				
C1	0.828	0.900	0.063	14.282	200.	1.21	1.340	0.0256	
C5	0.171	0.099	0.936	0.105					
MOLES	0.041	0.034	0.006		2409.				
C1	0.759	0.875	0.046	18.936	150.	1.01	1.685	0.0254	
C5	0.240	0.124	0.953	0.130					
MOLES	0.031	0.025	0.005		2409.				
C1	0.723	0.823	0.029	28.228	100.	0.70	2.259	0.0252	
C5	0.276	0.176	0.970	0.181					
MOLES	0.020	0.016	0.003		2409.				
C1	0.673	0.785	0.022	35.184	80.	0.54	2.609	0.0251	
C5	0.326	0.214	0.977	0.219					
MOLES	0.016	0.013	0.003		2409.				
C1	0.644	0.720	0.015	46.751	60.	0.31	3.085	0.0250	
C5	0.355	0.279	0.984	0.284					
MOLES	0.011	0.010	0.001		2409.				
ZKATZ ITER =	0								
C1	0.615	0.615	0.000	1.000	40.	0.00	3.901	0.0000	
C5	0.384	0.384	0.000	1.000					
MOLES	0.006	0.006	0.000		2409.				

TABLE E-8

RUN NO. 11, METHANE AND N-PENTANE AT 160 F.
DEPLETION OF A CONSTANT VOLUME RESERVOIR BY VAPOR PRODUCTION

PURE COMPONENT DATA								
COMP	MOLE WT LB/MOLE	PC PSIA	VC FT**3	TC DEG R	ZC	PITZER OMEGA	RIEDEL ALPHA	
C1	16.042	669.7	1.590	343.13	0.288	0.000	5.860	
C5	72.146	487.3	4.730	845.08	0.254	0.238	7.030	
SIMULATED DEPLETION PERFORMANCE								
COMP	SYSTEM COMP	VAPOR COMP	LIQUID COMP	K VALUE	P, PK PSIA	LIQ VOL %	VAPOR CF/LB	LIQUID CF/LB
C1	0.882	0.882	0.000	1.000	2500.	0.00	0.093	0.0000
C5	0.118	0.118	0.000	1.000				
MOLES	0.472	0.472	0.000		2278.			
C1	0.881	0.881	0.000	1.000	2250.	0.00	0.103	0.0000
C5	0.117	0.117	0.000	1.000				
MOLES	0.426	0.426	0.000		2278.			
C1	0.881	0.881	0.000	1.000	2000.	0.00	0.116	0.0000
C5	0.117	0.117	0.000	1.000				
MOLES	0.377	0.377	0.000		2278.			
C1	0.881	0.891	0.477	1.865	1750.	1.48	0.139	0.0386
C5	0.117	0.108	0.522	0.208				
MOLES	0.326	0.318	0.008		2278.			
C1	0.880	0.896	0.407	2.203	1500.	1.90	0.169	0.0356
C5	0.119	0.103	0.562	0.173				
MOLES	0.275	0.265	0.010		2278.			
C1	0.877	0.897	0.339	2.641	1250.	1.75	0.208	0.0333
C5	0.122	0.102	0.660	0.155				
MOLES	0.225	0.216	0.009		2278.			
C1	0.873	0.896	0.272	3.290	1000.	1.50	0.267	0.0314
C5	0.126	0.103	0.727	0.142				
MOLES	0.177	0.168	0.008		2278.			

TABLE E-8 (CONT.)

RUN NO. 11, METHANE AND N-PENTANE AT 160 F.

SYSTEM		SIMULATED DEPLETION PERFORMANCE						
COMP	COMP	VAPOR COMP	LIQUID COMP	K VALUE	P, PK PSIA	LIQ VOL %	VAPOR CF/LB	LIQUID CF/LB
C1	0.866	0.891	0.217	4.091	800.	1.17	0.336	0.0302
C5	0.133	0.108	0.782	0.139				
MOLES	0.138	0.132	0.006		2278.			
C1	0.859	0.879	0.162	5.417	600.	0.68	0.445	0.0290
C5	0.140	0.120	0.837	0.144				
MOLES	0.101	0.097	0.003		2278.			
C1	0.852	0.852	0.000	1.000	400.	0.00	0.640	0.0000
C5	0.147	0.147	0.000	1.000				
MOLES	0.064	0.064	0.000		2278.			
C1	0.852	0.852	0.000	1.000	200.	0.00	1.324	0.0000
C5	0.147	0.147	0.000	1.000				
MOLES	0.031	0.031	0.000		2278.			
C1	0.852	0.852	0.000	1.000	150.	0.00	1.781	0.0000
C5	0.147	0.147	0.000	1.000				
MOLES	0.023	0.023	0.000		2278.			
C1	0.852	0.852	0.000	1.000	100.	0.00	2.693	0.0000
C5	0.147	0.147	0.000	1.000				
MOLES	0.015	0.015	0.000		2278.			

TABLE E-9

RUN NO. 12, METHANE AND N-PENTANE AT 100 F.
DEPLETION OF A CONSTANT VOLUME RESERVOIR BY VAPOR PRODUCTION

PURE COMPONENT DATA							
COMP	MOLE WT LB/MOLE	PC PSIA	VC FT**3	TC DEG R	ZC	PITZER OMEGA	RIEDEL ALPHA
C1	16.042	669.7	1.590	343.13	0.288	0.000	5.860
C5	72.146	487.3	4.730	845.08	0.254	0.238	7.030
SIMULATED DEPLETION PERFORMANCE							
COMP	SYSTEM COMP	VAPOR COMP	LIQUID COMP	K VALUE	P ₀ PSIA	PK VOL %	VAPOR CF/LB
C1	0.927	0.927	0.000	1.000	2500.	0.00	0.090
C5	0.073	0.073	0.000	1.000			
MOLES	0.547	0.547	0.000		2409.		
C1	0.926	0.926	0.000	1.000	2250.	0.00	0.100
C5	0.072	0.072	0.000	1.000			
MOLES	0.495	0.495	0.000		2409.		
C1	0.926	0.926	0.000	1.000	2000.	0.00	0.113
C5	0.072	0.072	0.000	1.000			
MOLES	0.438	0.438	0.000		2409.		
C1	0.926	0.940	0.513	1.831	1750.	2.17	0.139
C5	0.072	0.059	0.486	0.121			
MOLES	0.376	0.362	0.014		2409.		
C1	0.924	0.945	0.446	2.116	1500.	2.47	0.169
C5	0.075	0.054	0.553	0.098			
MOLES	0.316	0.300	0.015		2409.		
C1	0.920	0.949	0.379	2.502	1250.	2.50	0.212
C5	0.079	0.050	0.620	0.081			
MOLES	0.258	0.242	0.015		2409.		
C1	0.914	0.951	0.309	3.072	1000.	2.41	0.276
C5	0.085	0.048	0.690	0.070			
MOLES	0.202	0.187	0.014		2409.		

TABLE E-9 (CONT.)

RUN NO. 12, METHANE AND N-PENTANE AT 100 F.

SIMULATED DEPLETION PERFORMANCE								
COMP	SYSTEM COMP	VAPOR COMP	LIQUID COMP	K VALUE	P, PSIA	PK VOL %	VAPOR CF/LB	LIQUID CF/LB
C1	0.904	0.951	0.251	3.779	800.	2.24	0.355	0.0284
C5	0.095	0.048	0.748	0.065				
MOLES	0.159	0.146	0.013		2409.			
C1	0.891	0.947	0.191	4.951	600.	2.00	0.482	0.0274
C5	0.108	0.052	0.808	0.064				
MOLES	0.118	0.107	0.011		2409.			
C1	0.872	0.937	0.128	7.288	400.	1.65	0.721	0.0264
C5	0.127	0.062	0.871	0.071				
MOLES	0.079	0.069	0.009		2409.			
C1	0.839	0.900	0.063	14.282	200.	1.01	1.340	0.0256
C5	0.160	0.099	0.936	0.105				
MOLES	0.039	0.034	0.005		2409.			
C1	0.779	0.875	0.046	18.936	150.	0.81	1.685	0.0254
C5	0.220	0.124	0.953	0.130				
MOLES	0.030	0.025	0.004		2409.			
C1	0.748	0.823	0.029	28.228	100.	0.50	2.259	0.0252
C5	0.251	0.176	0.970	0.181				
MOLES	0.019	0.016	0.002		2409.			
C1	0.709	0.785	0.022	35.184	80.	0.35	2.609	0.0251
C5	0.290	0.214	0.977	0.219				
MOLES	0.015	0.013	0.001		2409.			
C1	0.688	0.720	0.015	46.751	60.	0.12	3.085	0.0250
C5	0.311	0.279	0.984	0.284				
MOLES	0.010	0.010	0.000		2409.			
C1	0.674	0.674	0.000	1.000	40.	0.00	4.303	0.0000
C5	0.325	0.325	0.000	1.000				
MOLES	0.006	0.006	0.000		2409.			

TABLE E-10

METHANE, PROPANE, AND N-BUTANE MIXTURE AT 100 F.
DEPLETION OF A CONSTANT VOLUME RESERVOIR BY VAPOR PRODUCTION

PURE COMPONENT DATA							
COMP	MOLE WT LB/MOLE	PC PSIA	VC FT**3	TC DEG R	ZC	PITZER OMEGA	RIEDEL ALPHA
C1	16.042	669.7	1.590	343.13	0.288	0.000	5.860
C3	44.094	616.3	3.210	665.68	0.276	0.153	6.540
C4	58.120	550.7	4.080	765.29	0.274	0.195	6.770
SIMULATED DEPLETION PERFORMANCE							
COMP	SYSTEM COMP	VAPOR COMP	Liquid COMP	K VALUE	P, PK PSIA VOL %	VAPOR CF/LB	LIQUID CF/LB
C1	0.700	0.700	0.000	1.000	1750. 0.00	0.073	0.0000
C3	0.180	0.180	0.000	1.000			
C4	0.120	0.120	0.000	1.000			
MOLES	0.518	0.518	0.000		1724.		
C1	0.699	0.705	0.501	1.407	1650. 2.06	0.080	0.0473
C3	0.179	0.177	0.267	0.663			
C4	0.119	0.117	0.231	0.506			
MOLES	0.484	0.471	0.013		1718.		
C1	0.699	0.707	0.450	1.570	1600. 2.35	0.083	0.0434
C3	0.180	0.176	0.287	0.615			
C4	0.120	0.115	0.262	0.440			
MOLES	0.466	0.450	0.015		1718.		
C1	0.699	0.723	0.396	1.824	1500. 5.12	0.096	0.0405
C3	0.180	0.170	0.307	0.553			
C4	0.120	0.106	0.295	0.360			
MOLES	0.424	0.390	0.034		1718.		
C1	0.696	0.755	0.326	2.317	1250. 8.76	0.137	0.0380
C3	0.181	0.156	0.335	0.468			
C4	0.121	0.087	0.338	0.257			
MOLES	0.333	0.274	0.058		1718.		
C1	0.680	0.771	0.273	2.826	1000. 9.26	0.194	0.0365
C3	0.187	0.150	0.353	0.426			
C4	0.131	0.077	0.373	0.206			
MOLES	0.259	0.198	0.060		1719.		

TABLE E-10 (CONT.)

METHANE, PROPANE, AND N-BUTANE MIXTURE AT 100 F.

SIMULATED DEPLETION PERFORMANCE								
COMP	SYSTEM COMP	VAPOR COMP	LIQUID COMP	K VALUE	P, PK PSIA	LIQ VOL %	VAPOR CF/LB	LIQUID CF/LB
C1	0.654	0.771	0.249	3.090	900.	8.84	0.222	0.0358
C3	0.198	0.152	0.359	0.422				
C4	0.146	0.076	0.390	0.195				
MOLES	0.231	0.174	0.057		1718.			
C1	0.641	0.766	0.224	3.415	800.	8.24	0.255	0.0351
C3	0.203	0.155	0.365	0.425				
C4	0.154	0.077	0.410	0.189				
MOLES	0.205	0.151	0.053		1718.			
C1	0.624	0.758	0.197	3.832	700.	7.52	0.295	0.0344
C3	0.210	0.160	0.368	0.436				
C4	0.164	0.080	0.433	0.186				
MOLES	0.179	0.130	0.048		1717.			
C1	0.605	0.743	0.169	4.385	600.	6.68	0.345	0.0337
C3	0.217	0.169	0.369	0.458				
C4	0.176	0.086	0.461	0.188				
MOLES	0.153	0.110	0.043		1715.			
C1	0.582	0.721	0.139	5.158	500.	5.73	0.410	0.0330
C3	0.225	0.181	0.365	0.496				
C4	0.192	0.096	0.494	0.195				
MOLES	0.127	0.091	0.036		1711.			
C1	0.554	0.687	0.108	6.318	400.	4.62	0.499	0.0323
C3	0.234	0.198	0.354	0.559				
C4	0.211	0.113	0.536	0.211				
MOLES	0.101	0.072	0.029		1704.			
C1	0.520	0.632	0.076	8.250	300.	3.26	0.630	0.0314
C3	0.243	0.221	0.329	0.673				
C4	0.236	0.145	0.594	0.244				
MOLES	0.074	0.054	0.020		1689.			
C1	0.479	0.534	0.044	12.115	200.	1.35	0.848	0.0305
C3	0.251	0.248	0.273	0.910				
C4	0.269	0.216	0.682	0.317				
MOLES	0.044	0.036	0.008		1657.			

TABLE E-11 (CONT.)

METHANE, PROPANE, AND N-BUTANE MIXTURE AT 160 F.

COMP	SYSTEM COMP	SIMULATED DEPLETION PERFORMANCE				VAPOR CF/LB	LIQUID CF/LB
		VAPOR COMP	LIQUID COMP	K VALUE	P, PK PSIA		
C1	0.534	0.588	0.201	2.924	1000.	6.46	0.157
C3	0.276	0.257	0.394	0.651			
C4	0.189	0.154	0.404	0.382			
MOLES	0.236	0.199	0.036		1443.		
C1	0.527	0.584	0.180	3.242	900.	5.80	0.181
C3	0.278	0.259	0.395	0.656			
C4	0.193	0.156	0.424	0.367			
MOLES	0.207	0.173	0.033		1444.		
C1	0.519	0.573	0.158	3.625	800.	4.71	0.207
C3	0.281	0.264	0.393	0.673			
C4	0.199	0.161	0.448	0.360			
MOLES	0.178	0.151	0.026		1444.		
C1	0.510	0.555	0.135	4.105	700.	3.31	0.237
C3	0.283	0.271	0.386	0.703			
C4	0.205	0.172	0.478	0.361			
MOLES	0.150	0.131	0.018		1445.		
C1	0.502	0.528	0.111	4.736	600.	1.66	0.275
C3	0.286	0.280	0.373	0.751			
C4	0.211	0.190	0.515	0.370			
MOLES	0.121	0.111	0.009		1445.		
C1	0.496	0.496	0.000	1.000	500.	0.00	0.325
C3	0.287	0.287	0.000	1.000			
C4	0.216	0.216	0.000	1.000			
MOLES	0.092	0.092	0.000		1445.		
C1	0.496	0.496	0.000	1.000	400.	0.00	0.427
C3	0.287	0.287	0.000	1.000			
C4	0.216	0.216	0.000	1.000			
MOLES	0.070	0.070	0.000		1445.		
C1	0.496	0.496	0.000	1.000	300.	0.00	0.595
C3	0.287	0.287	0.000	1.000			
C4	0.216	0.216	0.000	1.000			
MOLES	0.050	0.050	0.000		1445.		

TABLE E-12

METHANE, PROPANE, AND N-PENTANE MIXTURE AT 160 F.
DEPLETION OF A CONSTANT VOLUME RESERVOIR BY VAPOR PRODUCTION

PURE COMPONENT DATA								
COMP	MOLE WT LB/MOLE	PC PSIA	VC FT**3	TC DEG R	ZC	PITZER OMEGA	RIEDEL ALPHA	
C1	16.042	669.7	1.590	343.13	0.288	0.000	5.860	
C3	44.094	616.3	3.210	665.68	0.276	0.153	6.540	
C5	72.146	487.3	4.730	845.08	0.254	0.238	7.030	
SIMULATED DEPLETION PERFORMANCE								
COMP	SYSTEM COMP	VAPOR COMP	LIQUID COMP	K VALUE	P _s PSIA	PK LIQ VOL %	VAPOR CF/LB	LIQUID CF/LB
C1	0.675	0.675	0.000	1.000	2000.	0.00	0.073	0.0000
C3	0.195	0.195	0.000	1.000				
C5	0.130	0.130	0.000	1.000				
MOLES	0.471	0.471	0.000		1880.			
C1	0.674	0.689	0.441	1.559	1750.	4.78	0.088	0.0447
C3	0.194	0.190	0.273	0.695				
C5	0.129	0.120	0.284	0.423				
MOLES	0.407	0.380	0.026		1853.			
C1	0.672	0.722	0.334	2.160	1500.	8.97	0.120	0.0381
C3	0.195	0.180	0.297	0.606				
C5	0.131	0.096	0.367	0.263				
MOLES	0.337	0.285	0.052		1853.			
C1	0.662	0.738	0.280	2.631	1250.	9.74	0.159	0.0361
C3	0.198	0.177	0.306	0.579				
C5	0.138	0.083	0.413	0.202				
MOLES	0.275	0.220	0.056		1853.			
C1	0.645	0.739	0.230	3.212	1000.	8.89	0.210	0.0344
C3	0.203	0.180	0.306	0.587				
C5	0.150	0.080	0.463	0.173				
MOLES	0.219	0.168	0.050		1856.			
C1	0.621	0.729	0.185	3.923	800.	7.69	0.269	0.0330
C3	0.209	0.187	0.299	0.626				
C5	0.169	0.083	0.514	0.161				
MOLES	0.175	0.131	0.043		1857.			

TABLE E-12 (CONT.)

METHANE, PROPANE, AND N-PENTANE MIXTURE AT 160 F.

SYSTEM		SIMULATED DEPLETION			PERFORMANCE			
COMP	COMP	VAPOR COMP	LIQUID COMP	K VALUE	P, PSIA	LIG VOL %	VAPOR CF/LB	LIQUID CF/LB
C1	0.594	0.706	0.138	5.104	600.	6.18	0.358	0.0314
C3	0.215	0.199	0.278	0.715				
C5	0.190	0.093	0.582	0.161				
MOLES	0.131	0.097	0.034		1854.			
C1	0.556	0.687	0.113	6.047	500.	5.37	0.424	0.0306
C3	0.220	0.208	0.261	0.795				
C5	0.222	0.104	0.524	0.167				
MOLES	0.110	0.080	0.029		1848.			
C1	0.531	0.659	0.088	7.463	400.	4.46	0.515	0.0298
C3	0.222	0.218	0.237	0.921				
C5	0.245	0.122	0.674	0.181				
MOLES	0.088	0.063	0.024		1838.			
C1	0.500	0.616	0.062	9.824	300.	3.41	0.651	0.0290
C3	0.223	0.229	0.201	1.137				
C5	0.276	0.153	0.735	0.208				
MOLES	0.066	0.047	0.018		1820.			
C1	0.460	0.544	0.037	14.546	200.	2.03	0.882	0.0281
C3	0.221	0.236	0.149	1.579				
C5	0.317	0.218	0.813	0.269				
MOLES	0.042	0.031	0.010		1788.			
C1	0.414	0.482	0.025	19.259	150.	1.18	1.072	0.0276
C3	0.213	0.231	0.114	2.024				
C5	0.371	0.285	0.860	0.332				
MOLES	0.030	0.023	0.006		1762.			
ZKATZ	ITER = 0							
C1	0.386	0.386	0.000	1.000	100.	0.00	1.389	0.0000
C3	0.206	0.206	0.000	1.000				
C5	0.406	0.406	0.000	1.000				
MOLES	0.016	0.016	0.000		1762.			

TABLE E-13

METHANE, PROPANE, AND N-PENTANE MIXTURE AT 220 F.
DEPLETION OF A CONSTANT VOLUME RESERVOIR BY VAPOR PRODUCTION

PURE COMPONENT DATA							
COMP	MOLE WT LB/MOLE	PC PSIA	VC FT**3	TC DEG R	ZC	PITZER OMEGA	RIEDEL ALPHA
C1	16.042	669.7	1.590	343.13	0.288	0.000	5.860
C3	44.094	616.3	3.210	665.68	0.276	0.153	6.540
C5	72.146	487.3	4.730	845.08	0.254	0.238	7.030
SIMULATED DEPLETION PERFORMANCE							
COMP	SYSTEM COMP	VAPOR COMP	LIQUID COMP	K VALUE	P, PK PSIA VOL %	VAPOR CF/LB	LIQUID CF/LB
C1	0.500	0.500	0.000	1.000	1500. 0.00	0.080	0.0000
C3	0.300	0.300	0.000	1.000			
C5	0.200	0.200	0.000	1.000			
MOLES	0.346	0.346	0.000		1469.		
C1	0.500	0.558	0.324	1.719	1400. 19.22	0.106	0.0507
C3	0.299	0.280	0.359	0.780			
C5	0.199	0.161	0.316	0.510			
MOLES	0.315	0.229	0.086		1469.		
C1	0.494	0.563	0.255	2.202	1300. 14.54	0.120	0.0434
C3	0.301	0.281	0.371	0.758			
C5	0.203	0.155	0.372	0.416			
MOLES	0.288	0.217	0.070		1467.		
C1	0.487	0.565	0.236	2.388	1250. 13.81	0.127	0.0420
C3	0.303	0.282	0.372	0.757			
C5	0.208	0.152	0.390	0.390			
MOLES	0.275	0.207	0.067		1466.		
C1	0.484	0.565	0.221	2.557	1200. 13.20	0.135	0.0410
C3	0.304	0.283	0.372	0.761			
C5	0.211	0.150	0.406	0.370			
MOLES	0.263	0.197	0.065		1465.		
C1	0.480	0.562	0.196	2.863	1100. 11.80	0.150	0.0394
C3	0.305	0.287	0.368	0.780			
C5	0.213	0.150	0.435	0.345			
MOLES	0.238	0.180	0.058		1465.		

TABLE E-13 (CONT.)

METHANE, PROPANE, AND N-PENTANE MIXTURE AT 220 F.

SIMULATED DEPLETION PERFORMANCE								
COMP	SYSTEM COMP	VAPOR COMP	LIQUID COMP	K VALUE	P, PK PSIA	LIQ VOL %	VAPOR CF/LB	LIQUID CF/LB
C1	0.471	0.557	0.175	3.178	1000.	10.69	0.168	0.0384
C3	0.307	0.291	0.363	0.803				
C5	0.220	0.151	0.461	0.327				
MOLES	0.215	0.161	0.053		1465.			
C1	0.452	0.547	0.155	3.522	900.	9.33	0.189	0.0374
C3	0.309	0.296	0.354	0.835				
C5	0.228	0.155	0.489	0.317				
MOLES	0.191	0.144	0.046		1466.			
C1	0.451	0.534	0.135	3.948	800.	7.88	0.213	0.0364
C3	0.310	0.302	0.342	0.883				
C5	0.237	0.163	0.521	0.312				
MOLES	0.167	0.128	0.039		1467.			
C1	0.440	0.516	0.114	4.492	700.	6.34	0.242	0.0353
C3	0.312	0.308	0.326	0.947				
C5	0.247	0.174	0.559	0.312				
MOLES	0.143	0.111	0.031		1467.			
C1	0.427	0.493	0.094	5.214	600.	4.74	0.279	0.0342
C3	0.312	0.314	0.302	1.038				
C5	0.259	0.191	0.602	0.318				
MOLES	0.119	0.095	0.023		1465.			
C1	0.414	0.463	0.074	6.223	500.	3.02	0.327	0.0332
C3	0.312	0.318	0.271	1.170				
C5	0.273	0.218	0.653	0.333				
MOLES	0.094	0.079	0.015		1461.			
C1	0.401	0.423	0.054	7.735	400.	1.14	0.391	0.0320
C3	0.310	0.315	0.229	1.375				
C5	0.287	0.260	0.715	0.363				
MOLES	0.069	0.063	0.005		1454.			
C1	0.393	0.393	0.000	1.000	300.	0.00	0.514	0.0000
C3	0.308	0.308	0.000	1.000				
C5	0.297	0.297	0.000	1.000				
MOLES	0.046	0.046	0.000		1454.			

TABLE E-14

METHANE, PROPANE, N-DECANE MIXTURE AT 280 F.
DEPLETION OF A CONSTANT VOLUME RESERVOIR BY VAPOR PRODUCTION

PURE COMPONENT DATA							
COMP	MOLE WT LB/MOLE	PC PSIA	VC FT**3	TC DEG R	ZC	PITZER OMEGA	RIEDEL ALPHA
C1	16.042	659.7	1.590	343.13	0.288	0.000	5.860
C3	44.094	616.3	3.210	665.68	0.276	0.153	6.540
C10	142.276	304.0	9.660	1111.70	0.246	0.486	8.180
SIMULATED DEPLETION PERFORMANCE							
COMP	SYSTEM COMP	VAPOR COMP	LIQUID COMP	K VALUE	P, PK PSIA VOL %	VAPOR CF/LB	LIQUID CF/LB
C1	0.875	0.911	0.822	1.1086	3750. 41.51	0.095	0.0713
C3	0.075	0.059	0.096	0.6191			
C10	0.050	0.028	0.080	0.3509			
MOLES	0.486	0.285	0.200		3915.		
C1	0.874	0.903	0.735	1.2294	3500. 18.30	0.099	0.0581
C3	0.075	0.065	0.120	0.5426			
C10	0.050	0.030	0.144	0.2121			
MOLES	0.462	0.378	0.083		3914.		
C1	0.873	0.905	0.672	1.3462	3250. 14.47	0.107	0.0511
C3	0.075	0.066	0.130	0.5108			
C10	0.051	0.027	0.196	0.1418			
MOLES	0.434	0.371	0.063		3912.		
C1	0.871	0.908	0.618	1.4699	3000. 13.10	0.118	0.0461
C3	0.076	0.067	0.135	0.4961			
C10	0.052	0.024	0.246	0.0978			
MOLES	0.405	0.349	0.055		3909.		
C1	0.868	0.914	0.518	1.7638	2500. 11.66	0.147	0.0391
C3	0.076	0.068	0.137	0.5001			
C10	0.054	0.016	0.343	0.0485			
MOLES	0.345	0.298	0.047		3906.		
C1	0.860	0.916	0.421	2.1752	2000. 10.18	0.188	0.0343
C3	0.078	0.071	0.131	0.5437			
C10	0.061	0.012	0.447	0.0273			
MOLES	0.281	0.242	0.038		3903.		

TABLE E-14 (CONT.)

METHANE, PROPANE, N-DECANE MIXTURE AT 280 F.

SIMULATED DEPLETION PERFORMANCE									
COMP	SYSTEM COMP	VAPOR COMP	LIQUID COMP	K VALUE	P, PK PSIA	Liq VOL %	VAPOR CF/LB	LIQUID CF/LB	
C1	0.847	0.910	0.321	2.8367	1500.	8.38	0.248	0.0308	
C3	0.079	0.075	0.116	0.6444					
C10	0.072	0.013	0.562	0.0245					
MOLES	0.215	0.184	0.030		3926.				
C1	0.828	0.905	0.218	4.1451	1000.	7.20	0.373	0.0282	
C3	0.081	0.079	0.092	0.8592					
C10	0.090	0.014	0.688	0.0215					
MOLES	0.147	0.123	0.024		3941.				
C1	0.793	0.902	0.176	5.1217	800.	6.81	0.467	0.0273	
C3	0.081	0.082	0.079	1.0253					
C10	0.125	0.015	0.743	0.0209					
MOLES	0.120	0.098	0.022		3942.				
C1	0.768	0.897	0.133	6.7463	600.	6.43	0.520	0.0265	
C3	0.081	0.085	0.065	1.3078					
C10	0.149	0.017	0.801	0.0212					
MOLES	0.093	0.073	0.020		3939.				
C1	0.731	0.890	0.089	9.9912	400.	6.04	0.915	0.0257	
C3	0.080	0.088	0.047	1.8781					
C10	0.187	0.020	0.853	0.0237					
MOLES	0.067	0.048	0.018		3929.				
C1	0.668	0.873	0.044	19.7175	200.	5.55	1.717	0.0250	
C3	0.077	0.094	0.026	3.6011					
C10	0.253	0.032	0.929	0.0347					
MOLES	0.040	0.024	0.016		3906.				
C1	0.536	0.844	0.021	39.1565	100.	5.21	3.027	0.0246	
C3	0.066	0.098	0.013	7.0540					
C10	0.397	0.056	0.964	0.0590					
MOLES	0.027	0.012	0.015		3874.				
C1	0.384	0.794	0.010	77.9953	50.	4.90	4.885	0.0245	
C3	0.051	0.099	0.007	13.9564					
C10	0.564	0.106	0.982	0.1086					
MOLES	0.020	0.006	0.014		3838.				

TABLE E-15

METHANE, N-BUTANE, AND N-DECANE MIXTURE AT 280 F.
DEPLETION OF A CONSTANT VOLUME RESERVOIR BY VAPOR PRODUCTION

PURE COMPONENT DATA								
COMP	MOLE WT LB/MOLE	PC PSIA	VC FT**3	TC DEG R	ZC	PITZER OMEGA	RIEDEL ALPHA	
C1	16.042	669.7	1.590	343.13	0.288	0.000	5.860	
C4	58.120	550.7	4.080	765.29	0.274	0.195	6.770	
C10	142.276	304.0	9.660	1111.70	0.246	0.486	8.190	
SIMULATED DEPLETION PERFORMANCE								
COMP	SYSTEM COMP	VAPOR COMP	LIQUID COMP	K VALUE	P _s PSIA	PK VOL %	VAPOR CF/LB	LIQUID CF/LB
C1	0.900	0.907	0.734	1.2351	3500.	4.53	0.093	0.0543
C4	0.060	0.057	0.107	0.5401				
C10	0.040	0.034	0.158	0.2184				
MOLES	0.465	0.444	0.020		3897.			
C1	0.899	0.912	0.673	1.3544	3250.	5.59	0.102	0.0480
C4	0.060	0.056	0.115	0.4920				
C10	0.040	0.030	0.210	0.1449				
MOLES	0.435	0.411	0.024		3897.			
C1	0.899	0.918	0.621	1.4784	3000.	6.62	0.114	0.0437
C4	0.060	0.055	0.121	0.4613				
C10	0.040	0.025	0.257	0.0996				
MOLES	0.405	0.377	0.028		3896.			
C1	0.897	0.923	0.572	1.6143	2750.	7.20	0.128	0.0405
C4	0.060	0.055	0.125	0.4408				
C10	0.041	0.021	0.302	0.0696				
MOLES	0.374	0.344	0.029		3895.			
C1	0.895	0.927	0.524	1.7693	2500.	7.40	0.144	0.0379
C4	0.060	0.055	0.128	0.4279				
C10	0.043	0.017	0.346	0.0495				
MOLES	0.342	0.313	0.029		3894.			
C1	0.892	0.930	0.476	1.9522	2250.	7.31	0.163	0.0357
C4	0.061	0.055	0.130	0.4214				
C10	0.045	0.014	0.392	0.0361				
MOLES	0.310	0.282	0.028		3893.			

TABLE E-15 (CONT.)

METHANE, N-BUTANE, AND N-DECANE MIXTURE AT 280 F.

SIMULATED DEPLETION PERFORMANCE									
COMP	SYSTEM	VAPOR COMP	LIQUID COMP	K VALUE	P, PSIA	PK VOL %	VAPOR CF/LB	LIQUID CF/LB	
C1	0.888	0.932	0.428	2.1755	2000.	7.02	0.185	0.0339	
C4	0.062	0.055	0.131	0.4213					
C10	0.049	0.012	0.439	0.0278					
MOLES	0.278	0.251	0.026		3892.				
C1	0.883	0.930	0.378	2.4570	1750.	6.36	0.210	0.0322	
C4	0.062	0.055	0.131	0.4302					
C10	0.053	0.012	0.489	0.0264					
MOLES	0.244	0.221	0.023		3903.				
C1	0.877	0.928	0.328	2.8301	1500.	5.84	0.245	0.0308	
C4	0.063	0.057	0.129	0.4464					
C10	0.059	0.013	0.542	0.0248					
MOLES	0.211	0.190	0.021		3915.				
C1	0.868	0.927	0.276	3.3506	1250.	5.41	0.294	0.0295	
C4	0.064	0.058	0.124	0.4745					
C10	0.066	0.013	0.599	0.0231					
MOLES	0.177	0.158	0.018		3926.				
C1	0.857	0.925	0.224	4.1295	1000.	5.02	0.369	0.0283	
C4	0.065	0.060	0.115	0.5236					
C10	0.076	0.014	0.660	0.0217					
MOLES	0.143	0.126	0.017		3936.				
C1	0.841	0.922	0.180	5.1016	800.	4.73	0.461	0.0274	
C4	0.067	0.062	0.105	0.5916					
C10	0.091	0.015	0.713	0.0210					
MOLES	0.116	0.100	0.015		3943.				
C1	0.822	0.918	0.136	6.7208	600.	4.43	0.611	0.0266	
C4	0.068	0.065	0.091	0.7122					
C10	0.108	0.016	0.772	0.0213					
MOLES	0.089	0.074	0.014		3946.				
C1	0.793	0.915	0.114	8.0157	500.	4.28	0.729	0.0262	
C4	0.069	0.066	0.082	0.8119					
C10	0.136	0.017	0.803	0.0221					
MOLES	0.075	0.062	0.013		3945.				

TABLE E-15 (CONT.)

METHANE, N-BUTANE, AND N-DECANE MIXTURE AT 280 F.

SIMULATED DEPLETION PERFORMANCE									
COMP	SYSTEM	VAPOR COMP	LIQUID COMP	K VALUE	P, PSIA	LIQ VOL %	VAPOR CF/LB	LIQUID CF/LB	
C1	0.772	0.910	0.091	9.9582	400.	4.12	0.900	0.0258	
C4	0.069	0.069	0.071	0.9640					
C10	0.157	0.019	0.836	0.0238					
MOLES	0.062	0.049	0.012		3941.				
C1	0.742	0.903	0.068	13.1958	300.	3.94	1.173	0.0254	
C4	0.069	0.072	0.059	1.2207					
C10	0.187	0.023	0.872	0.0273					
MOLES	0.049	0.037	0.012		3931.				
C1	0.699	0.891	0.045	19.6719	200.	3.72	1.679	0.0251	
C4	0.069	0.076	0.043	1.7386					
C10	0.231	0.031	0.910	0.0349					
MOLES	0.035	0.024	0.011		3912.				
C1	0.627	0.880	0.033	26.1476	150.	3.59	2.139	0.0249	
C4	0.066	0.079	0.035	2.2586					
C10	0.305	0.039	0.931	0.0429					
MOLES	0.029	0.018	0.010		3893.				
C1	0.570	0.860	0.022	39.0972	100.	3.42	2.948	0.0247	
C4	0.063	0.083	0.025	3.3002					
C10	0.366	0.056	0.952	0.0592					
MOLES	0.022	0.012	0.010		3864.				
C1	0.482	0.806	0.010	77.9216	50.	3.12	4.763	0.0245	
C4	0.057	0.087	0.013	6.4258					
C10	0.460	0.106	0.976	0.1087					
MOLES	0.015	0.006	0.009		3810.				

APPENDIX F

CORRELATION OF CRITICAL COMPRESSIBILITY FACTORS
AND CRITICAL PRESSURES FOR BINARY MIXTURES

F.1 Foreword

Pseudocritical properties are extensively used to correlate thermodynamic data for mixtures. Pseudocritical z_c values are useful in some corresponding states correlations, however, their relationship to true z_c values has received little attention. This appendix summarizes the results of an attempt to correlate critical pressures of binary mixtures using true z_c values. Although the procedure was not sufficiently accurate for quantitative calculations it is of some academic interest.

The procedure used was a modification of a method proposed by Chueh and Prausnitz⁴⁶. They showed that the critical temperatures and the critical volumes of binary mixtures, and perhaps multicomponent mixtures, can be correlated by the relationships

$$T_c = \sum_i \phi_i T_{ci} + \sum_i \sum_j \phi_i \phi_j T_{cij} \quad (F-1)$$

$$V_c = \sum_i \phi_i V_{ci} + \sum_i \sum_j \phi_i \phi_j V_{cij} \quad (F-2)$$

where: ϕ_i , ϕ_j are weighting factors which reflect the composition of the mixture,

T_{ci} is the critical temperature of pure component i ,

T_{cij} is a correlation parameter which characterizes the effects of the $i-j$ interactions on the critical temperature, $T_{cii} = 0$,

V_{ci} is the critical volume of pure component i ,

V_{cij} is a correlation parameter which characterizes the effects of the $i-j$ interactions on the critical volume, $V_{cii} = 0$.

The interaction between each binary pair is characterized by a single correlating parameter and higher order interactions

are assumed to be small and are neglected. A functional form which used more correlating parameters would have improved the fit, however, it would have the serious disadvantage of restricting the method to those systems for which there is experimental data. The strength of Equations F-1 and F-2 lies in the fact that the correlation parameter for each binary system can usually be related to some other properties of the pure components. This makes it possible to estimate parameters for the systems for which there is no experimental data.

The chief disadvantage of Equations F-1 and F-2 is that the $i-j$ interactions are assumed to be symmetric with respect to the weighting. Chueh and Prausnitz tried several weightings and found that the surface fraction

$$\phi_i = x_i v_{ci}^{2/3} / \sum_i x_i v_{ci}^{2/3} \quad (F-3)$$

gave a satisfactory representation of the experimental data. They correlated critical pressures using Equations F-1, F-2 and F-3 in conjunction with a modified Redlich-Kwong equation of state.

The object of this investigation was to see if true z_c values could be easily correlated. If they could, the simple relationship

$$p_c = z_c R T_c / v_c \quad (F-4)$$

could be used to correlate critical pressures.

F.2 Correlation of Critical Compressibility Factors

A survey of the literature indicated that there were sufficient experimental data for 27 binary systems to permit

calculation of z_c . There were 8 binary systems containing methane and the experimental data (including z_c values calculated using Equation F-4) are presented in Table F-1. The experimental data for systems containing ethane and propane are presented in Tables F-2 and F-3, respectively. Table F-4 gives the data for several miscellaneous systems. The data presented in these tables indicates a systematic variation of z_c values with respect to composition and chemical species.

Since there were experimental data for only a few systems it was important that the correlation procedure could be generalized to systems for which there was no data. Thus, having regard for the work of Chueh and Prausnitz, the relationship

$$z_c = \sum_i \phi_i z_{ci} + \sum_i \sum_j \phi_i \phi_j z_{cij} \quad (F-5)$$

where: z_{ci} is the critical compressibility factor for pure component i ,

z_{cij} is a correlation parameter which characterizes the effects of the $i-j$ interactions on the critical compressibility factor.

was tried with various weightings (mole fraction, weight fraction, diameter fraction, surface fraction and volume fraction). The weight fraction weighting generally gave the best fit of the data to Equation F-5, however, there was some indication that the nature of z_c behavior is too complex to be approximated by a simple quadratic function such as Equation F-5.

The "z_c excess" defined by

$$z_c' = z_c - \sum_i \phi_i z_{ci} \quad (F-6)$$

are presented in Figure F-1 for the methane binaries. The z_{cij} parameters are simply one half the z_c' values at the

apex of the parabola. There is an orderly variation with chemical species, but the data for methane-n-butane, methane-n-pentane and methane-n-heptane show considerable scatter with respect to composition as reflected by the weight fraction methane in the mixture. Figure F-2 shows the z_{cij} correlation parameters to correlate remarkably well with the absolute value of the difference in critical temperatures of the chemical species.

Some caution must be exercised in extending the z_c correlation over the full range of composition. It is known that the methane-n-heptane and the methane-n-decane systems both exhibit complex liquid-liquid immiscibility and/or formation of solids at low temperatures.

The z_c' correlations for the ethane and propane binary systems are presented in Figures F-3 and F-4, respectively. There are wide variations from the curves predicted by Equation F-5. It should be appreciated, however, that z_c values are subject to considerable error since it is extremely difficult to determine critical volumes.

F.3 Correlation of Critical Pressures

The large discrepancies in the correlation of z_c values prevented quantitative estimation of critical pressures using Equation F-4. An independent test of the suitability of the general procedure was made by fitting

$$P_c = \frac{(\phi_1 z_{c1} + \phi_2 z_{c2} + 2\phi_1\phi_2 z_{c12}) R (\phi_1 T_{c1} + \phi_2 T_{c2} + 2\phi_1\phi_2 T_{c12})}{\phi_1 V_{c1} + \phi_2 V_{c2} + 2\phi_1\phi_2 V_{c12}} \quad (F-7)$$

to the data using a least squares criterion to minimize the error in P_c . The least squares estimators T_{cl2} , V_{cl2} and Z_{cl2} were very much different from the correlation parameters obtained using Equations F-1, F-2 and F-5, respectively. This showed that there are serious deficiencies in both the data and the model.

TABLE F-1. CRITICAL STATE DATA FOR SOME METHANE BINARIES

CRITICAL STATE DATA FOR METHANE AND PROPANE

AUTHOR(S) - SAGE, B.H., W.N. LACEY, AND J.G. SCHAAFS.

REFERENCE - I.E.C., 26, 214, (1934).

PURE COMPONENT DATA							
MOL FR	MOLE WT	PC	VC	TC	ZC	RIEDEL	PITZER
CH4	LB/MOLE	PSIA	FT**3	DEG R		ALPHA	OMEGA
1.0000	16.042	669.7	1.590	343.13	0.288	5.860	0.013
0.0000	44.094	616.3	3.210	665.68	0.276	6.540	0.152

MIXTURE CRITICAL DATA							
MOL FR	MOLE WT	PC	VC	TC	ZC	RIEDEL	PITZER
CH4	LB/MOLE	PSIA	FT**3	DEG R		ALPHA	OMEGA
0.1000	41.288	765.7	2.850	655.50	0.310	7.906	0.150
0.2000	38.483	890.6	2.660	637.90	0.346	7.662	0.141
0.3000	35.678	1018.4	2.460	619.30	0.373	7.621	0.131
0.4000	32.873	1153.0	2.280	598.40	0.411	7.702	0.120
0.5000	30.068	1291.6	2.085	575.00	0.436	7.694	0.117
0.6000	27.262	1436.4	1.907	547.70	0.426	7.596	0.0952
0.7000	24.457	1483.1	1.740	510.40	0.456	7.521	0.075

AUTHOR(S) - REAMERS, H.H., B.H. SAGE, AND W.N. LACEY.

REFERENCE - I.E.C., 42, 534, (1950).

PURE COMPONENT DATA							
MOL FR	MOLE WT	PC	VC	TC	ZC	RIEDEL	PITZER
CH4	LB/MOLE	PSIA	FT**3	DEG R		ALPHA	OMEGA
1.0000	16.042	669.7	1.590	343.13	0.288	5.860	0.013
0.0000	44.094	616.3	3.210	665.68	0.276	6.540	0.152

MIXTURE CRITICAL DATA							
MOL FR	MOLE WT	PC	VC	TC	ZC	RIEDEL	PITZER
CH4	LB/MOLE	PSIA	FT**3	DEG R		ALPHA	OMEGA
0.1400	40.108	757.0	3.240	649.69	0.356	7.869	0.147
0.2220	39.038	1020.0	2.555	619.69	0.391	7.793	0.120
0.4691	30.934	1218.0	2.307	589.69	0.444	7.736	0.111
0.5082	27.593	1353.0	2.082	559.69	0.469	7.616	0.094

TABLE F-1 (Cont.)

CRITICAL STATE DATA FOR ETHANE AND PROPANE

AUTHOR(S) = SAGE, Soren, L. B. MICHAELSON, AND J. C. LACHMAYR
 REFERENCE = I.E.C.C., 349, 1940, (1940).

		CRITICAL DATA					
MOL FR	MOLE AT	PC	VC	TC	ZC	RIEDEL	PITZER
CH4	LB/VOLE	PSIA	FTX*3	DEG R		ALPHA	OMEGA
1.0000	16.042	669.7	1.0590	343.13	0.288	5.860	0.013
0.6000	58.0120	529.1	4.8210	734.03	0.203	6.540	0.187

		MIXTURE CRITICAL DATA					
MOL FR	MOLE AT	PC	VC	TC	ZC	RIEDEL	PITZER
CH4	LB/VOLE	PSIA	FTX*3	DEG R		ALPHA	OMEGA
0.3600	42.971	1254.0	2.0700	709.09	0.449	8.003	0.172
0.4720	38.259	1521.0	2.057	679.00	0.491	7.928	0.156
0.5500	34.977	1520.0	2.021	649.00	0.516	7.859	0.142
0.5160	32.109	1520.0	1.924	619.09	0.531	7.791	0.128
0.6720	27.843	1730.0	1.810	589.09	0.536	7.726	0.116
0.7240	27.632	1512.0	1.860	529.09	0.538	7.653	0.103
0.7710	25.617	1923.0	1.894	525.00	0.539	7.580	0.090

CRITICAL STATE DATA FOR ETHANE AND PROPANE

AUTHOR(S) = GLDS, R. M., AND SAGE, A. C., AND LACHMAYR
 REFERENCE = I.E.C.C., 349, 1940, (1942).

		CRITICAL DATA					
MOL FR	MOLE AT	PC	VC	TC	ZC	RIEDEL	PITZER
CH4	LB/VOLE	PSIA	FTX*3	DEG R		ALPHA	OMEGA
1.0000	16.042	669.7	1.0590	343.13	0.288	5.860	0.013
0.6000	58.0120	529.1	4.8210	734.03	0.203	6.540	0.187

		MIXTURE CRITICAL DATA					
MOL FR	MOLE AT	PC	VC	TC	ZC	RIEDEL	PITZER
CH4	LB/VOLE	PSIA	FTX*3	DEG R		ALPHA	OMEGA
0.3369	43.943	1035.0	3.0180	672.09	0.432	7.743	0.163
0.2275	34.661	1457.0	2.0230	612.09	0.424	7.792	0.151
0.5895	29.157	1679.0	1.866	559.09	0.521	7.638	0.134

TABLE F-1 (Cont.)

CRITICAL STATE DATA FOR METHANE AND α -HEPTANE

AUTHOR(S) = SAGE, B.H., H.H. REATER, R.H. OLDS, AND W.H. LACEY.
 REFERENCE = I.E.C., 34, 1108, (1942).

PURE COMPONENT DATA							
OL	FR	MOLE WT	PC	VC	TC	ZC	RIEDEL PITZER
CH4		LB/MOLE	PSIA	FT**3	DEG R		ALPHA OMEGA
1.0000		16.042	669.7	1.690	343.13	0.268	5.860 0.013
0.0000		72.146	487.6	4.730	845.08	0.294	7.030 0.252

MIXTURE CRITICAL DATA							
OL	FR	MOLE WT	PC	VC	TC	ZC	RIEDEL PITZER
CH4		LB/MOLE	PSIA	FT**3	DEG R		ALPHA OMEGA
0.2950		55.595	1025.0	3.691	799.69	0.440	8.313 0.236
0.5211		42.910	1510.0	2.620	739.69	0.572	8.139 0.171
0.6705		34.528	2081.0	2.261	679.69	0.645	7.944 0.159
0.7665		29.142	2338.0	1.876	619.69	0.659	7.774 0.125
0.8236		25.938	2455.0	1.652	559.69	0.634	7.651 0.102

CRITICAL STATE DATA FOR METHANE AND α -HEPTANE

AUTHOR(S) = REATER, H.H., B.H. SAGE, AND W.H. LACEY.
 REFERENCE = J. CHEM. ENG. DATA, 1, 29, (1956).

PURE COMPONENT DATA							
OL	FR	MOLE WT	PC	VC	TC	ZC	RIEDEL PITZER
CH4		LB/MOLE	PSIA	FT**3	DEG R		ALPHA OMEGA
1.0000		16.042	669.7	1.690	343.13	0.268	5.860 0.013
0.0000		100.198	397.6	6.920	972.25	0.204	7.070 0.352

MIXTURE CRITICAL DATA							
OL	FR	MOLE WT	PC	VC	TC	ZC	RIEDEL PITZER
CH4		LB/MOLE	PSIA	FT**3	DEG R		ALPHA OMEGA
0.4410		63.036	1206.0	4.500	919.69	0.549	8.732 0.320
0.5550		50.966	1906.0	3.800	859.69	0.681	8.659 0.278
0.6720		43.645	2469.0	2.486	799.69	0.715	8.386 0.243
0.7320		38.595	2927.0	2.091	739.69	0.771	8.236 0.214
0.7780		34.724	3298.0	1.766	679.69	0.798	8.102 0.187
0.8170		31.442	3549.0	1.501	619.69	0.801	7.974 0.163
0.8550		28.244	3609.0	1.315	559.69	0.790	7.834 0.136
0.8940		24.932	3642.0	1.142	499.69	0.733	7.673 0.109

TABLE F-1 (Cont.)

CRITICAL STATE DATA FOR METHANE AND N-CLOE

AUTHOR(S) - SHINNAG, LEE, AND J.-P. KOFKE

REFERENCE - J. CHEM. ENG. DATA, 11, 176, (1966).

PURE COMPONENT DATA							
MOL FR	MOLE WT	PC	VC	TC	ZC	RIEDEL	PITZER
CH4	LB/MOLE	PSIA	FT*#3	DEG R		ALPHA	OMEGA
1.0000	16.042	669.7	1.590	342.13	0.288	5.860	0.013
0.0000	128.250	332.0	6.750	1070.21	0.254	7.940	0.430

MIXTURE CRITICAL DATA							
MOL FR	MOLE WT	PC	VC	TC	ZC	RIEDEL	PITZER
CH4	LB/MOLE	PSIA	FT*#3	DEG R		ALPHA	OMEGA
0.8500	31.751	4630.0	1.410	620.69	0.954	8.070	0.180
0.8720	30.424	4673.0	1.270	581.69	0.950	8.005	0.167
0.8930	29.506	4684.0	1.176	536.69	0.957	7.950	0.159
0.9150	28.945	4673.0	1.100	491.69	0.974	7.931	0.153

CRITICAL STATE DATA FOR METHANE AND N-DECANE

AUTHOR(S) - REAMER, H.H., ROH, GLDS, B.H. SAGE, AND W.H. LACEY.

REFERENCE - I.E.C., 34, 1526, (1942).

PURE COMPONENT DATA							
MOL FR	MOLE WT	PC	VC	TC	ZC	RIEDEL	PITZER
CH4	LB/MOLE	PSIA	FT*#3	DEG R		ALPHA	OMEGA
1.0000	16.042	669.7	1.590	342.13	0.288	5.860	0.013
0.0000	142.273	304.0	9.660	1111.70	0.246	8.180	0.466

MIXTURE CRITICAL DATA							
MOL FR	MOLE WT	PC	VC	TC	ZC	RIEDEL	PITZER
CH4	LB/MOLE	PSIA	FT*#3	DEG R		ALPHA	OMEGA
0.7389	49.001	2911.0	2.954	919.69	0.871	8.811	0.322
0.7979	41.553	3605.0	2.377	859.69	0.928	8.539	0.269
0.8333	37.035	4163.0	1.983	799.69	0.964	8.353	0.233
0.8574	34.042	4530.0	1.716	739.69	0.990	8.210	0.206
0.8767	31.606	4935.0	1.495	679.69	1.011	8.091	0.183
0.8912	29.776	5180.0	1.322	619.69	1.029	7.996	0.165
0.8979	28.930	5310.0	1.180	559.69	1.043	7.951	0.157

TABLE F-1 (Cont.)

CRITICAL STATE DATA FOR ETHYL CYANIDE AND CYANIDE SULFIDE

AUTHOR(S) = R. C. ELLIOTT, M. M. SAWYER, AND K. K. LACEY.
 REFER. ECF = IND. & C., 43, 576, (1951).

VOL. FR.	MOLE RT.	COPOLY CRITICAL DATA						MOLAL PVT213
		WC	VC	TC	ZC	ALP	PC	
C-4	LB/ MOLE	PSIA	FT ^{4/3}	DEG R	ALP	PC	PC	PC
1.0000	16.042	366.7	1.57	240.13	0.213	3.162	3.13	
0.9990	34.076	133.62	1.57	372.40	0.203	6.752	6.13	

VOL. FR.	MOLE RT.	LIQUID CRITICAL DATA						MOLAL PVT213
		WC	VC	TC	ZC	ALP	PC	
C-4	LB/ MOLE	PSIA	FT ^{4/3}	DEG R	ALP	PC	PC	PC
0.2000	20.0316	1600.0	1.293	312.00	0.322	7.031	6.037	
0.3000	27.0378	1907.0	1.134	329.00	0.375	7.097	6.171	
0.5000	24.157	1947.0	1.093	420.00	0.397	7.056	6.056	

TABLE F-2. CRITICAL STATE DATA FOR SOME ETHANE BINARIES

CRITICAL STATE DATA FOR ETHANE AND PROPANE

AUTHOR(S) = KRY, M.

REFERENCE = I.E.S.C., 32, 653, (1940).

		PURE COMPONENT DATA						
VL FR	MOLE WT	PC	VC	TC	ZC	RIEDEL	PITZER	
C2H6	LB/MOLE	PSIA	FT*#2	DEG K		ALPHA	OMEGA	
1.0000	30.058	70.02	2.0272	149.77	0.246	6.213	0.102	
0.9999	30.146	70.07	4.0120	150.29	0.274	6.276	0.101	

		MIXTURE CRITICAL DATA						
VL FR	MOLE WT	PC	VC	TC	ZC	RIEDEL	PITZER	
C2H6	LB/MOLE	PSIA	FT*#3	DEG K		ALPHA	OMEGA	
0.1749	50.212	546.1	3.0330	742.79	0.243	6.121	0.103	
0.4510	43.446	780.7	3.0325	697.67	0.319	8.037	0.114	
0.6277	39.673	841.6	2.0300	650.89	0.313	7.803	0.111	
0.8219	35.803	827.2	2.0300	607.27	0.312	7.612	0.112	
0.9472	31.949	75.162	2.0245	568.69	0.279	7.672	0.109	

CRITICAL STATE DATA FOR ETHANE AND IMPENTANE

AUTHOR(S) = REINER, H., SAGE, A. D., AND LACEY.

REFERENCE = J. CHEM. ENG. DATA, 5, 44, (1960).

		PURE COMPONENT DATA						
VL FR	MOLE WT	PC	VC	TC	ZC	RIEDEL	PITZER	
C2H6	LB/MOLE	PSIA	FT*#2	DEG K		ALPHA	OMEGA	
1.0000	30.058	739.3	2.0370	549.77	0.285	6.283	0.105	
0.9999	72.146	487.3	4.0730	545.08	0.254	7.033	0.262	

		MIXTURE CRITICAL DATA						
VL FR	MOLE WT	PC	VC	TC	ZC	RIEDEL	PITZER	
C2H6	LB/MOLE	PSIA	FT*#3	DEG K		ALPHA	OMEGA	
0.2946	59.745	741.6	3.0720	799.69	0.324	8.333	0.237	
0.5630	48.426	555.0	2.0505	739.01	0.344	8.177	0.201	
0.7189	41.323	470.1	2.0405	679.69	0.326	8.035	0.171	
0.8502	35.371	923.6	2.0100	619.59	0.303	7.934	0.141	
0.9778	31.002	756.0	2.0230	559.59	0.261	7.723	0.107	

TABLE F-2 (Cont.)

CRITICAL STATE DATA FOR ETHANE AND PROPANE

AUTHOR(S) = K.Y. LEE

REFERENCE = IND. ENG. CHEM., 50, 461, (1958).

		PURE CRITICAL DATA						
MOL FR	MOLE WT	PC	VC	TC	ZC	RIEDEL	PITZER	
C2H6	LB/MOLE	PSIA	FT*10 ³	DEG R		ALPHA	OMEGA	
1.0000	30.068	709.3	2.370	549.77	0.285	6.280	0.105	
0.0000	142.276	904.0	0.660	1111.70	0.246	8.180	0.466	

		MIXTURE CRITICAL DATA						
MOL FR	MOLE WT	PC	VC	TC	ZC	RIEDEL	PITZER	
C2H6	LB/MOLE	PSIA	FT*10 ³	DEG R		ALPHA	OMEGA	
0.2554	31.570	532.0	5.020	927.39	0.344	8.327	0.339	
0.5871	59.024	11.601	3.150	323.29	0.438	8.220	0.273	
0.7709	43.134	123.90	2.65	736.69	0.423	8.243	0.210	
0.871	37.32	1132.0	2.240	349.40	0.353	7.653	0.159	
0.9583	32.22	752.0	2.036	579.69	0.254	7.772	0.118	

CRITICAL STATE DATA FOR ETHANE AND TURPANE

AUTHOR(S) = REAMER, HAN, AND P.H. SAGE

REFERENCE = J. CHEM. ENG. DATA, 7, 161, (1962).

		PURE CRITICAL DATA						
MOL FR	MOLE WT	PC	VC	TC	ZC	RIEDEL	PITZER	
C2H6	LB/MOLE	PSIA	FT*10 ³	DEG R		ALPHA	OMEGA	
1.0000	30.068	709.3	2.370	549.77	0.285	6.280	0.105	
0.0000	142.276	904.0	0.660	1111.70	0.246	8.180	0.466	

		MIXTURE CRITICAL DATA						
MOL FR	MOLE WT	PC	VC	TC	ZC	RIEDEL	PITZER	
C2H6	LB/MOLE	PSIA	FT*10 ³	DEG R		ALPHA	OMEGA	
0.6980	63.954	1421.0	3.910	919.69	0.587	8.877	0.332	
0.7780	54.978	1540.0	3.249	159.69	0.577	8.622	0.281	
0.8350	45.922	1710.0	2.787	799.69	0.556	8.416	0.241	
0.8880	42.632	1887.0	2.407	739.69	0.511	8.204	0.199	
0.9270	38.259	1511.0	2.022	679.69	0.421	8.035	0.167	
0.9640	34.107	1184.0	1.755	619.69	0.314	7.865	0.134	
0.9950	30.629	778.0	2.142	559.69	0.277	7.715	0.105	

TABLE F-2 (Cont.)

CRITICAL STATE DENSITY AND THERMODYNAMIC COEFFICIENTS

AUTHOR(S) = KAM, S. & D. D. PRICE
 REFEREE = I. L. COOK, JR., 32, (1971)

COL FOR C2H6		COLS FOR C2H6				COLS FOR C2H6			
COL FOR C2H6	COL FOR C2H6	PC PSI	VC FT ³ /LB	TC DEG F	ZC	ALBEDO ALBEDO	RIBBED RIBBED	PLATE PLATE	
1.01000	30.6000	7.0000	2.0000	549.077	0.280	6.0210	6.0210	6.0210	
0.99999	34.0070	1.0000	1.0000	672.140	0.282	6.0210	6.0210	6.0210	
COL FOR C2H6		COLS FOR C2H6				COLS FOR C2H6			
COL FOR C2H6	COL FOR C2H6	PC PSI	VC FT ³ /LB	TC DEG F	ZC	ALBEDO ALBEDO	RIBBED RIBBED	PLATE PLATE	
0.91103	30.6000	1217.0	1.6450	649.673	0.284	7.0212	6.0212	6.0212	
0.82850	32.0917	1051.64	1.8100	614.689	0.287	7.0212	6.0212	6.0212	
0.64799	32.0000	912.0	1.9700	512.050	0.283	7.0212	6.0212	6.0212	
0.46544	31.0000	821.01	2.0300	435.034	0.279	7.0212	6.0212	6.0212	
0.27770	30.6000	710.07	2.0210	347.010	0.277	7.0212	6.0212	6.0212	
0.08971	30.6000	701.07	2.0210	221.004	0.274	7.0212	6.0212	6.0212	

TABLE F-3. CRITICAL STATE DATA FOR SOME PROPANE BINARIES

CRITICAL STATE DATA FOR PROPANE AND N-BUTANE

AUTHOR(S) - NYSEWANDER, C.H., P.H. SAGE, AND W.N. LACEY.

REFERENCE - I.E.C., 32, 118, (1940).

PURE COMPONENT DATA								
MOL FR	MOLE WT	PC	VC	TC	ZC	RIEDEL	PITZER	
C3H8	LB/MOLE	PSIA	FT**3	DEG R		ALPHA	OMEGA	
1.0000	44.094	616.3	3.210	665.68	0.276	6.540	0.152	
0.0000	58.120	550.7	4.080	765.29	0.274	6.770	0.201	

MIXTURE CRITICAL DATA								
MOL FR	MOLE WT	PC	VC	TC	ZC	RIEDEL	PITZER	
C3H8	LB/MOLE	PSIA	FT**3	DEG R		ALPHA	OMEGA	
0.2030	55.272	588.0	3.920	750.09	0.286	8.125	0.198	
0.3390	53.365	609.0	3.840	739.89	0.294	8.101	0.192	
0.5160	50.882	630.0	3.650	724.09	0.296	8.065	0.184	
0.6950	48.371	638.0	3.430	703.19	0.289	8.025	0.175	
0.8550	46.127	631.0	3.270	684.09	0.281	7.985	0.166	

CRITICAL STATE DATA FOR PROPANE AND N-PENTANE

AUTHOR(S) - SAGE, B.H., B.L. HICKS, AND W.N. LACEY.

REFERENCE - I.E.C., 32, 992, (1940).

PURE COMPONENT DATA								
MOL FR	MOLE WT	PC	VC	TC	ZC	RIEDEL	PITZER	
C3H8	LB/MOLE	PSIA	FT**3	DEG R		ALPHA	OMEGA	
1.0000	44.094	616.3	3.210	665.62	0.276	6.540	0.152	
0.0000	72.146	487.3	4.730	845.08	0.254	7.030	0.252	

MIXTURE CRITICAL DATA								
MOL FR	MOLE WT	PC	VC	TC	ZC	RIEDEL	PITZER	
C3H8	LB/MOLE	PSIA	FT**3	DEG R		ALPHA	OMEGA	
0.3498	62.333	608.0	4.360	798.69	0.309	8.291	0.233	
0.5557	56.557	648.0	3.960	760.59	0.314	8.207	0.213	
0.7921	49.926	671.0	3.440	715.49	0.300	8.081	0.186	
0.8190	49.171	664.0	3.390	710.09	0.295	8.065	0.183	

TABLE F-3 (Cont.)

CRITICAL STATE DATA FOR PROPANE AND 1-PENTANE

AUTHOR(S) - VAUGHN, W.E., AND F.C. COLLINS.

REFERENCE - I.E.C., 34, 885, (1942).

PURE COMPONENT DATA							
MOL FR C3H8	MOLE WT LB/MOLE	PC PSIA	VC FT**3	TC DEG R	ZC	RIEDEL ALPHA	PITZER OMEGA
1.0000	44.094	616.3	3.210	665.68	0.276	6.540	0.152
0.0000	72.146	494.7	4.900	828.70	0.273	6.870	0.215

MIXTURE CRITICAL DATA							
MOL FR C3H8	MOLE WT LB/MOLE	PC PSIA	VC FT**3	TC DEG R	ZC	RIEDEL ALPHA	PITZER OMEGA
0.1010	69.312	528.3	4.990	617.67	0.273	8.261	0.231
0.3930	61.121	614.0	3.780	780.00	0.277	8.197	0.214
0.5880	55.651	652.4	3.460	748.00	0.281	8.134	0.199
0.7940	49.872	652.8	3.220	710.20	0.280	8.049	0.180
0.8990	46.927	548.8	3.160	688.40	0.277	7.999	0.169

CRITICAL STATE DATA FOR PROPANE AND 1-PENTANE

AUTHOR(S) - REAMER, H.H., AND B.H. SAGE.

REFERENCE - J. CHEM. ENG. DATA, 11, 17, (1966).

PURE COMPONENT DATA							
MOL FR C3H8	MOLE WT LB/MOLE	PC PSIA	VC FT**3	TC DEG R	ZC	RIEDEL ALPHA	PITZER OMEGA
1.0000	44.094	616.3	3.210	665.68	0.276	6.540	0.152
0.0000	142.276	304.0	9.660	1111.70	0.246	8.180	0.466

MIXTURE CRITICAL DATA							
MOL FR C3H8	MOLE WT LB/MOLE	PC PSIA	VC FT**3	TC DEG R	ZC	RIEDEL ALPHA	PITZER OMEGA
0.7120	72.370	998.0	4.500	919.69	0.450	8.768	0.321
0.7993	63.799	1028.0	3.780	859.69	0.421	8.552	0.277
0.8673	57.122	980.0	3.270	799.69	0.373	8.363	0.240
0.9283	51.133	873.0	3.220	739.69	0.354	8.180	0.204
0.9870	45.370	678.0	3.210	679.69	0.298	7.989	0.166

TABLE F-3 (Cont.)

CRITICAL STATE DATA FOR TWO CO₂ / SULFUR AND PROPANE

AUTHOR(S) = KAY, W. B., AND GELMAN, A. NOSECK,

REFERENCE = I.E.E.C., 46, 221, (1956).

		PURE COMPOUND DATA						
VOL FR	MOLE WT	PC	VC	TC	ZC	RIEDEL	PITZER	
H ₂ S	LB/MOLE	PSIA	FT ^{4/3}	DEG R		ALPHA	OMEGA	
1.0000	34.076	1306.8	1.570	672.40	0.263	6.220	0.10	
0.0000	44.094	516.3	3.210	665.68	0.275	6.540	0.152	

		MIXTURE CRITICAL DATA						
VOL FR	MOLE WT	PC	VC	TC	ZC	RIEDEL	PITZER	
H ₂ S	LB/MOLE	PSIA	FT ^{4/3}	DEG R		ALPHA	OMEGA	
0.1633	42.458	693.6	2.079	657.94	0.263	8.351	0.164	
0.2986	41.132	735.2	2.079	631.04	0.291	8.095	0.163	
0.4342	39.744	821.7	2.079	616.12	0.295	8.110	0.157	
0.5641	38.442	857.6	2.079	643.95	0.282	8.112	0.148	
0.6755	37.328	956.3	2.079	664.50	0.269	8.102	0.139	
0.7817	36.262	1040.8	1.914	649.13	0.285	8.081	0.129	
0.8984	35.093	1129.2	1.720	658.63	0.282	8.016	0.117	

CRITICAL STATE DATA FOR CARBON DIOXIDE AND PROPANE

AUTHOR(S) = PFAFFEN, W., AND SAGE, A. D. AND LACEY.

REFERENCE = I.E.E.C., 46, 2515, (1956).

		PURE COMPOUND DATA						
VOL FR	MOLE WT	PC	VC	TC	ZC	RIEDEL	PITZER	
CO ₂	LB/MOLE	PSIA	FT ^{4/3}	DEG R		ALPHA	OMEGA	
1.0000	44.010	137.6	1.510	547.92	0.275	8.921	0.225	
0.0000	44.094	516.3	3.210	565.68	0.276	8.646	0.128	

		MIXTURE CRITICAL DATA						
VOL FR	MOLE WT	PC	VC	TC	ZC	RIEDEL	PITZER	
CO ₂	LB/MOLE	PSIA	FT ^{4/3}	DEG R		ALPHA	OMEGA	
0.4070	44.059	970.6	2.270	519.60	0.333	8.343	0.269	
0.5090	44.051	992.0	2.170	549.39	0.324	8.123	0.294	
0.7950	44.027	1317.6	1.700	529.69	0.285	9.287	0.367	

TABLE F-4. CRITICAL STATE DATA FOR SOME MISCELLANEOUS BINARIES

CRITICAL STATE DATA FOR N-BUTANE AND N-HEPTANE

AUTHOR(S) - KAY, W.B.

REFERENCE - I.E.C., 33, 590, (1941).

PURE COMPONENT DATA							
MOL FR	MOLE WT	PC	VC	TC	ZC	RIEDEL	PITZER
C4H10	LB/MOLE	PSIA	FT**3	DEG R		ALPHA	OMEGA
1.0000	58.120	550.7	4.080	765.29	0.274	6.770	0.201
0.0000	100.198	397.5	6.920	972.25	0.264	7.570	0.352

MIXTURE CRITICAL DATA							
MOL FR	MOLE WT	PC	VC	TC	ZC	RIEDEL	PITZER
C4H10	LB/MOLE	PSIA	FT**3	DEG R		ALPHA	OMEGA
0.1590	93.507	451.6	5.960	951.82	0.263	8.768	0.339
0.4249	82.319	538.0	5.050	908.62	0.278	8.638	0.308
0.6311	73.642	584.4	4.530	867.33	0.284	8.496	0.276
0.8010	66.493	596.1	4.220	825.86	0.283	8.353	0.246
0.9401	60.640	575.3	4.060	785.20	0.277	8.219	0.218

CRITICAL STATE DATA FOR N-BUTANE AND N-DECAINE

AUTHOR(S) - REAMER, H.H., AND B.H. SAGE.

REFERENCE - J. CHEM. ENG. DATA, 9, 24, (1964).

PURE COMPONENT DATA							
MOL FR	MOLE WT	PC	VC	TC	ZC	RIEDEL	PITZER
C4H10	LB/MOLE	PSIA	FT**3	DEG R		ALPHA	OMEGA
1.0000	58.120	550.7	4.080	765.29	0.274	6.770	0.201
0.0000	142.276	304.0	9.660	1111.70	0.246	8.180	0.466

MIXTURE CRITICAL DATA							
MOL FR	MOLE WT	PC	VC	TC	ZC	RIEDEL	PITZER
C4H10	LB/MOLE	PSIA	FT**3	DEG R		ALPHA	OMEGA
0.7390	80.084	714.0	4.970	919.69	0.359	8.719	0.318
0.8650	69.481	694.2	4.220	859.69	0.317	8.465	0.267
0.9560	61.822	616.3	4.000	799.69	0.287	8.262	0.226

TABLE F-4 (Cont.)

CRITICAL STATE DATA FOR CO₂ (SIXTEEN ADDENDA)

AUTOPSY(S) = GLODS, L. (1976) *TECHNOL. REV.*, 16, 1, SAGE, AND LINDEN, LUCY.
 REFERENCE = IeF-CO, 41, 473, (1949).

PURE COMPONENT DATA							
VOL FR	MOLE FR	PC	VC	TC	ZC	RIEDEL	PITZER
C ₂	LB/VCLE	PSIA	FT#*3	DEG R		ALPHA	OMEGA
1.0000	44.010	1070.6	1.021	247.43	0.275	6.021	0.322
0.8000	59.610	551.7	4.030	765.29	0.274	6.770	0.201

INTURE CRITICAL DATA							
VOL FR	MOLE FR	PC	VC	TC	ZC	RIEDEL	PITZER
C ₂	LB/VCLE	PSIA	FT#*3	DEG R		ALPHA	OMEGA
0.1727	15.610	741.1	3.480	742.59	0.323	8.491	0.255
0.3200	23.020	911.1	3.100	717.79	0.305	8.760	0.233
0.4816	31.330	1083.1	2.810	678.99	0.300	9.012	0.221
0.6446	40.710	1176.1	2.520	633.79	0.308	9.230	0.213
0.8000	48.410	1147.0	2.230	614.09	0.306	9.420	0.202

CRITICAL STATE DATA FOR C₅H₁₂ (SIXTEEN ADDENDA)

AUTOPSY(S) = GLODS, L. (1976) *TECHNOL. REV.*, 16, 1, SAGE, AND LINDEN, LUCY.
 REFERENCE = IeF-CO, 25, 723, (1933).

PURE COMPONENT DATA							
VOL FR	MOLE FR	PC	VC	TC	ZC	RIEDEL	PITZER
C ₅ H ₁₂	LB/VCLE	PSIA	FT#*3	DEG R		ALPHA	OMEGA
1.0000	72.146	487.3	4.730	845.09	0.254	7.030	0.252
0.8000	100.198	397.6	6.920	972.25	0.264	7.570	0.352

INTURE CRITICAL DATA							
VOL FR	MOLE FR	PC	VC	TC	ZC	RIEDEL	PITZER
C ₅ H ₁₂	LB/VCLE	PSIA	FT#*3	DEG R		ALPHA	OMEGA
0.2500	93.044	434.5	5.960	948.60	0.294	8.736	0.333
0.5580	94.544	479.1	5.080	911.00	0.268	8.614	0.306
0.7470	79.243	492.3	4.820	847.70	0.249	8.524	0.266

TABLE F-4 (Cont.)

CRITICAL STATE DATA FOR HYDROGEN SULFIDE AND CARBON DIOXIDE

AUTHOR(S) - BIERLEIN, J.A., AND W.R. KAY.

REFERENCE - I.E.C., 45, 618, (1953).

PURE COMPONENT DATA							
MOL FR	MOLE WT	PC	VC	TC	ZC	RIEDEL	PITZER
H ₂ S	LB/MOLE	PSIA	FT**3	DEG R		ALPHA	OMEGA
1.0000	34.076	1306.0	1.570	672.40	0.282	6.250	0.100
0.0000	44.010	1070.6	1.510	547.49	0.275	6.920	0.225

MIXTURE CRITICAL DATA							
MOL FR	OLE. WT	PC	VC	TC	ZC	RIEDEL	PITZER
H ₂ S	LB/MOLE	PSIA	FT**3	DEG R		ALPHA	OMEGA
0.0991	43.025	1075.6	1.503	552.04	0.272	9.381	0.375
0.1708	42.313	1085.0	1.498	556.42	0.272	9.228	0.346
0.3341	40.691	1129.8	1.491	570.39	0.274	8.914	0.266
0.5272	38.772	1206.5	1.490	594.25	0.281	8.593	0.224
0.6241	37.910	1245.0	1.491	598.22	0.284	8.449	0.187
0.7392	36.666	1283.6	1.499	625.75	0.286	8.290	0.146
0.8386	35.679	1301.7	1.509	643.18	0.284	8.164	0.142
0.9370	34.701	1304.5	1.523	659.99	0.281	8.047	0.119

CRITICAL STATE DATA FOR HYDROGEN SULFIDE AND N-PENTANE

AUTHOR(S) - REAMER, H.H., B.H. SAGE, AND W.R. LACEY.

REFERENCE - I.E.C., 45, 1805, (1953).

PURE COMPONENT DATA							
MOL FR	MOLE WT	PC	VC	TC	ZC	RIEDEL	PITZER
H ₂ S	LB/MOLE	PSIA	FT**3	DEG R		ALPHA	OMEGA
1.0000	34.076	1306.0	1.570	672.40	0.283	6.250	0.100
0.0000	72.145	487.3	4.730	845.08	0.254	7.030	0.252

MIXTURE CRITICAL DATA							
MOL FR	MOLE WT	PC	VC	TC	ZC	RIEDEL	PITZER
H ₂ S	LB/MOLE	PSIA	FT**3	DEG R		ALPHA	OMEGA
0.6260	51.740	1126.0	3.000	739.69	0.391	8.054	0.237
0.7260	44.807	1245.0	2.200	739.69	0.360	8.375	0.171
0.9360	35.370	1302.0	1.640	679.69	0.292	8.030	0.117

TABLE F-4 (Cont.)

CRITICAL STATE DATA FOR CYANIDE SULFIDE AND DECANE

AUTHOR(S) = RIEDEL, RIEDEL, SAGE, AND LACEY.

REFERENCE = INDUS. ENG. PROC., 1963, 11, 531.

MOL FR	MOLE AT	PC	VC	TC	ZC	RIEDEL	PITZER
CH ₃ S	LB/ CLE	PSIA	FTX*3	DEG F		ALPHA	OMEGA
1.0000	34.076	13.64	1.627	672.4	0.283	6.250	0.120
0.9999	142.276	304.0	9.660	1111.70	0.246	8.180	0.466

MOL FR	MOLE AT	PC	VC	TC	ZC	RIEDEL	PITZER
CH ₃ S	LB/ CLE	PSIA	FTX*3	DEG F		ALPHA	OMEGA
0.9999	44.093	1035.0	1.790	729.69	0.403	8.453	0.198
0.9490	34.559	1596.0	1.645	729.69	0.309	8.225	0.154
0.8440	34.672	1349.0	1.131	479.69	0.208	8.006	0.111

CRITICAL STATE DATA FOR CYANIDE OXIDE AND DECANE

AUTHOR(S) = RIEDEL, RIEDEL, SAGE.

REFERENCE = J. CHEM. ENG. DATA, 8, 502, (1963).

MOL FR	MOLE AT	PC	VC	TC	ZC	RIEDEL	PITZER
CO ₂	LB/ CLE	PSIA	FTX*3	DEG F		ALPHA	OMEGA
1.0000	44.010	1070.0	1.510	547.49	0.275	6.200	0.225
0.9999	142.270	304.0	9.660	1111.70	0.246	8.180	0.466

MOL FR	MOLE AT	PC	VC	TC	ZC	RIEDEL	PITZER
CO ₂	LB/ CLE	PSIA	FTX*3	DEG F		ALPHA	OMEGA
0.7281	70.736	3724.0	3.170	319.69	0.714	10.412	0.943
0.6050	63.171	2117.0	2.546	359.69	0.713	10.247	0.543
0.58480	57.437	2173.0	2.130	359.69	0.650	10.143	0.527
0.6705	56.473	2197.0	1.861	359.69	0.632	10.070	0.511
0.9346	52.314	2392.0	1.682	379.69	0.452	9.13	0.45
0.9477	49.14	1750.0	1.532	319.69	0.429	9.813	0.459
0.6946	44.547	1103.0	1.050	319.69	0.290	9.631	0.423

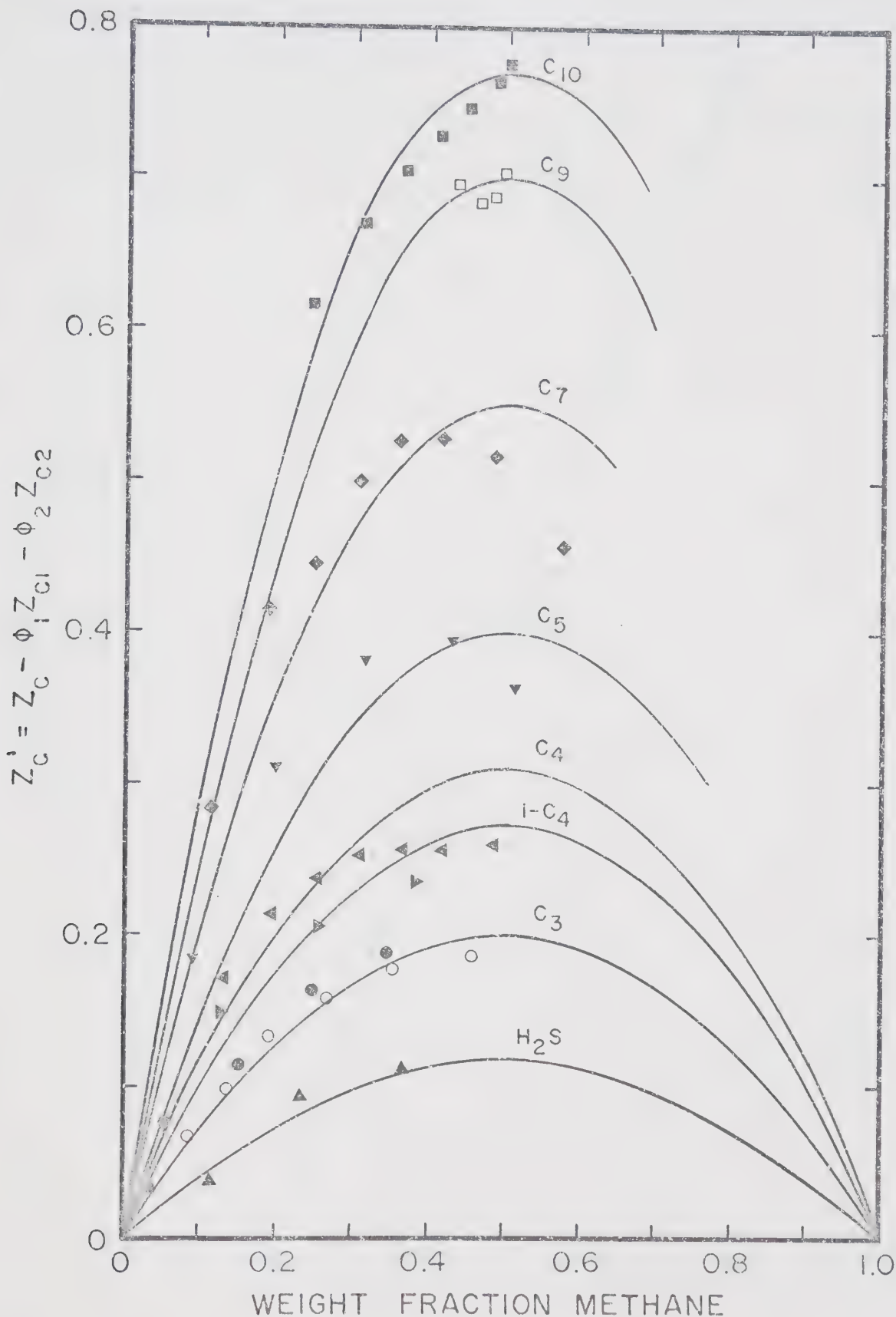


Figure F-1. Z_C' Excess Values for Binary Mixtures Containing Methane.

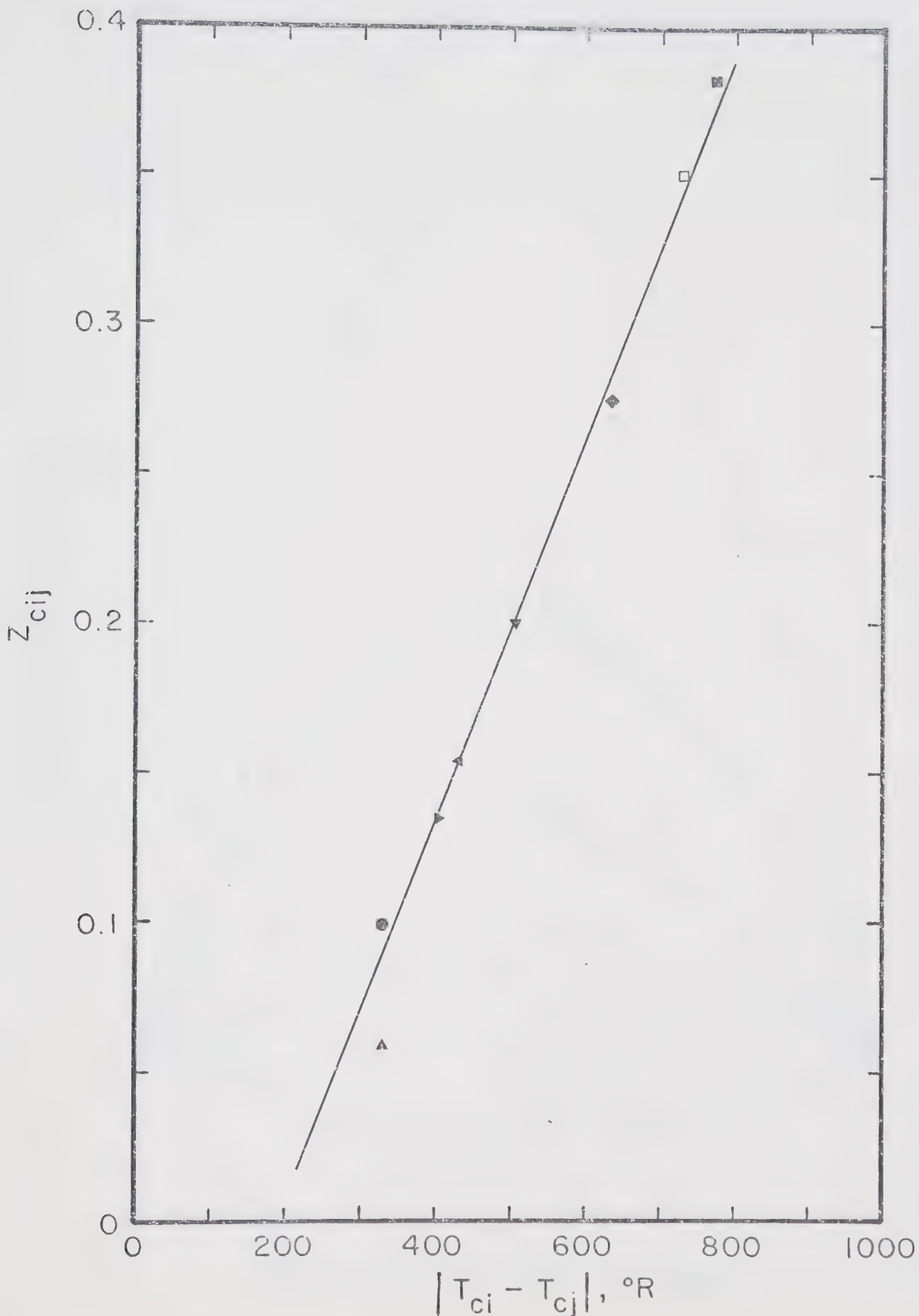


Figure F-2. Correlation of Z_{cij} with $|T_{ci} - T_{cj}|$ for Binary Mixtures Containing Methane.

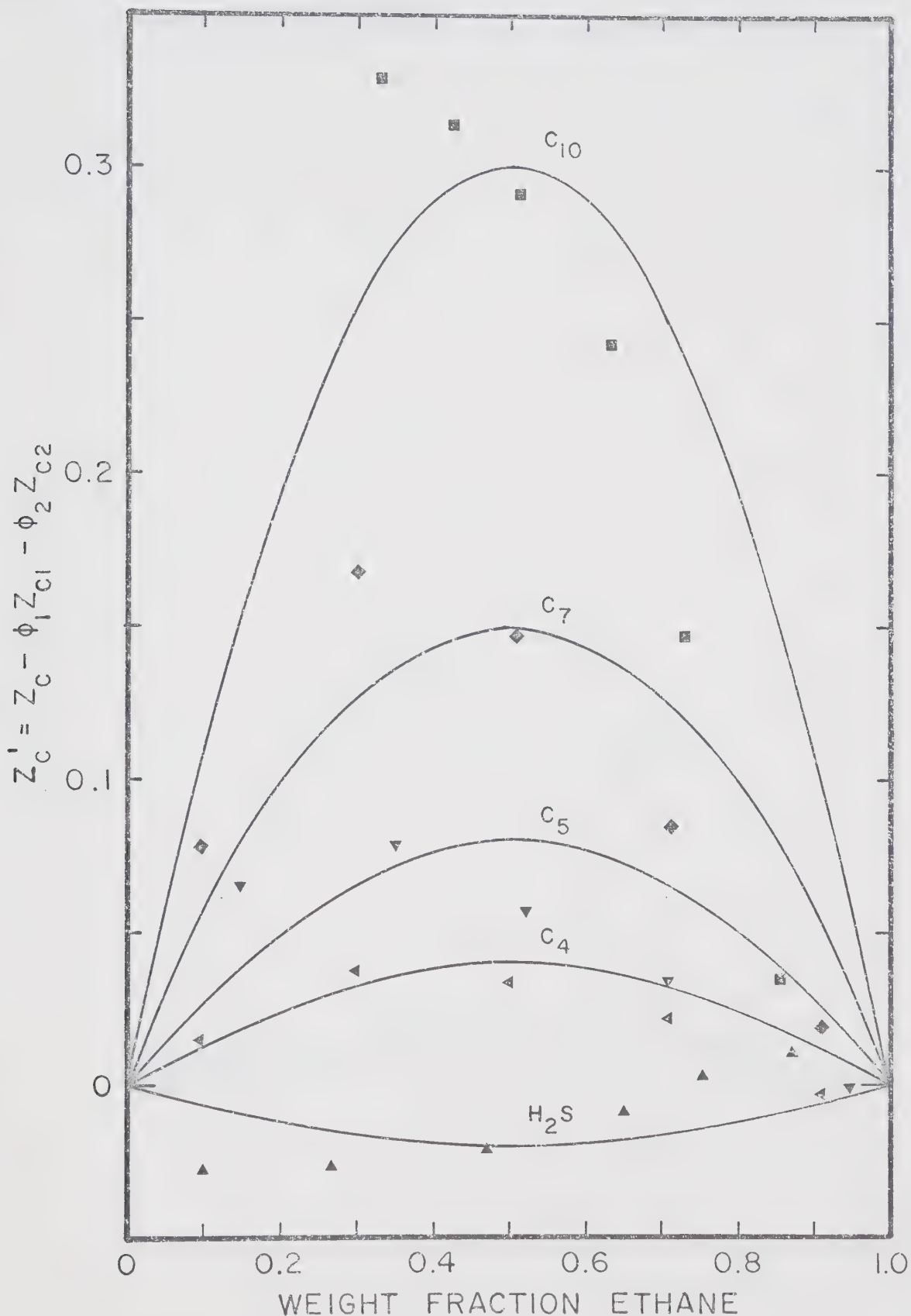


Figure F-3. Z_c' Excess Values for Binary Mixtures Containing Ethane.

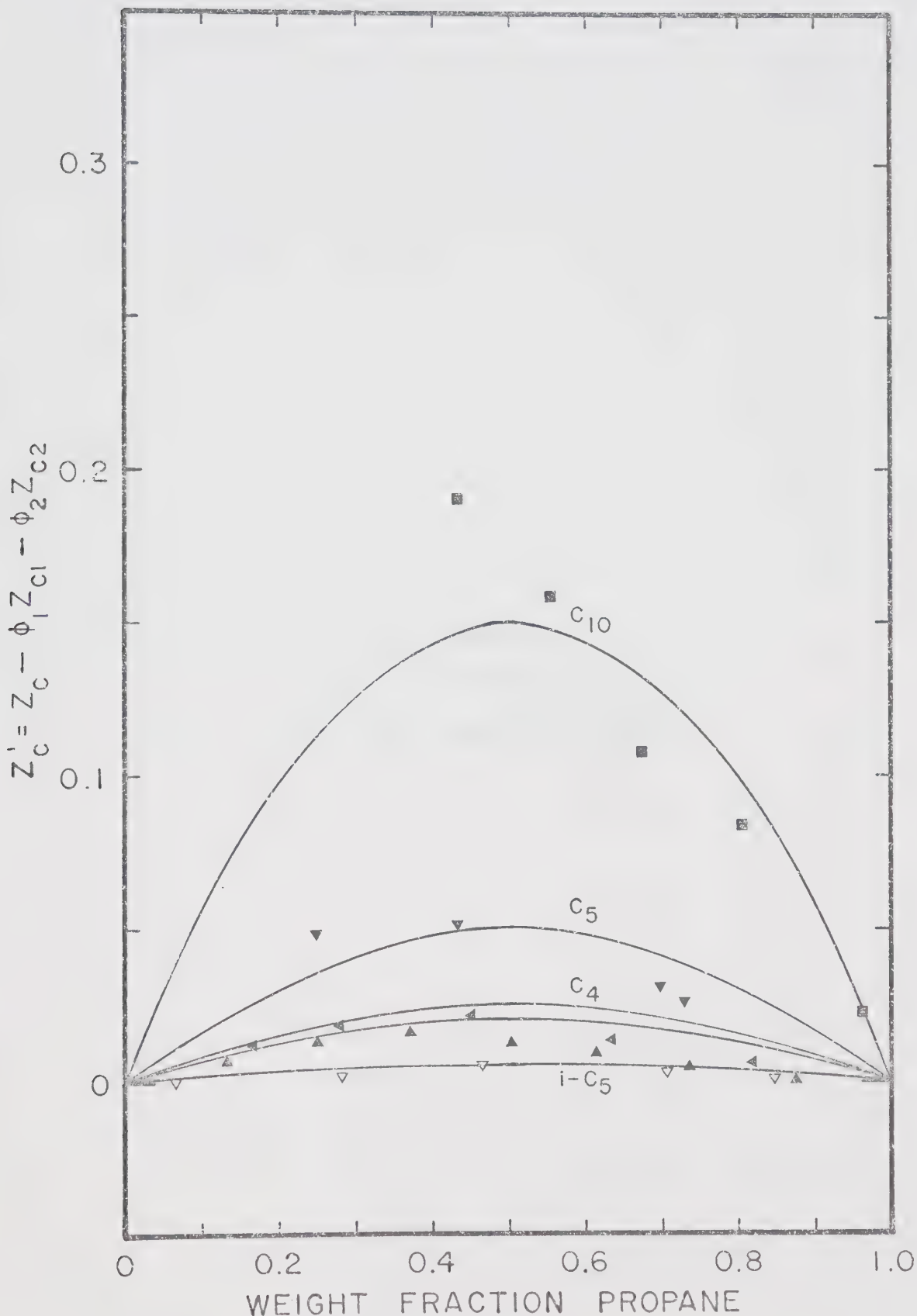


Figure F-4. Z_C' Excess Values for Binary Mixtures Containing Propane.

APPENDIX G
DENSITY BALANCE CALIBRATION
AND DATA REDUCTION PROGRAM

G.1 Foreword

Vapor phase samples were analyzed with an electro-magnetic gas density balance (R. Fuess Model 184). The density balance was calibrated using gases of known molecular weight. The calibrations were equivalent to preparing a plot of gas density versus the current required to balance the quartz bulb in the balance. The calibration was always made to pass through the origin (i.e. zero current in a high vacuum) by adjusting a small permanent magnet on the balance. Thus, the calibration could be expressed by a single constant representing the slope of the density versus current plot.

The composition of a binary mixture can be calculated from the relationship

$$x_1 = (M_m - M_2) / (M_1 - M_2) \quad (G-1)$$

where: M_m is the molecular weight of the mixture,
 M_1 is the molecular weight of pure component 1,
 M_2 is the molecular weight of pure component 2.

The molecular weight of the mixture was calculated from the equation

$$M_m = \rho ZRT/P \quad (G-2)$$

where: ρ is the calculated density using the calibration constant and the current reading,
 Z is the compressibility factor of the mixture,
 R is the universal gas constant,
 T is the absolute temperature of the gas sample in the density balance,
 P is the absolute pressure in the density balance based on the manometer reading.

G.2 Density Balance Calibration

The errors connected with the calibration of the balance

are either random or systematic. It was assumed that the errors in reading currents, pressures and temperatures were random and that by making several measurements they would tend to average out. Impurities in the calibration gases were assumed to cause systematic errors so various calibration gases were used.

The computer print out for two example calibrations using helium are presented in Table G-1. The helium was initially assumed to be pure so a molecular weight of 4.003 was used. The pressure column gives the balance pressures corrected to 0°C. The Z factors were estimated from data on second virial coefficients. The columns "current diff" and "density diff" give the discrepancies between the least squares straight line and the measured currents and the calculated gas densities, respectively. The slope of the calibration line is presented along with the r.m.s. errors in current and density. The first calibration gave a slope of 6.906 gm/m³/ma with a r.m.s. error of 0.0062 ma and 0.043 gm/m³. Tables G-2 and G-3 are calibrations using methane and nitrogen. The calibrations in Table G-4 were made with ultra high purity gases. The calibration constants for methane and carbon dioxide were 6.97 and 6.98, respectively. A value of 6.98 was used in all calculations in this thesis.

In order for the calibration presented in Table G-1 to give the same result the molecular weight of the gas must have been approximately 4.05. A mass spectrometer analysis of the helium used indicated the presence of some nitrogen. A nitrogen content of some 0.17 per cent would give the

TABLE G-1. DENSITY BALANCE CALIBRATIONS USING HELIUM

DATA REDUCTION FOR BALANCE CALIBRATION WITH HELIUM
JUNE 25, 1969DENSITY BALANCE CALIBRATION
GAS MOLE WT = 4.003 SCALE CORR = 0.00

PT	PRESSURE ATM	Z FACTOR	CURRENT MA	CURRENT DIFF	DENSITY GM/M**3	DENSITY DIFF
1	0.6017	1.0002	14.39	-0.002	99.397	0.0198
2	0.5401	1.0002	12.92	0.001	89.217	-0.0062
3	0.4869	1.0002	11.65	0.003	80.429	-0.0258
4	0.4320	1.0002	10.33	-0.002	71.359	0.0205
5	0.3774	1.0001	9.03	0.003	62.333	-0.0274
6	0.3252	1.0001	7.78	0.003	53.705	-0.0229
7	0.2678	1.0001	6.40	-0.004	44.227	0.0289
8	0.1993	1.0000	4.77	0.002	32.924	-0.0171
9	0.1355	1.0000	3.23	-0.010	22.375	0.0692
10	0.0658	1.0000	1.56	-0.014	10.872	0.0987
SLOPES		0.690602E 01		0.690602E 01		
RMS ERRORS		0.622942E-02		0.430211E-01		

DATA REDUCTION FOR BALANCE CALIBRATION WITH HELIUM
MARCH 20, 1970DENSITY BALANCE CALIBRATION
GAS MOLE WT = 4.003 SCALE CORR = 0.00

PT	PRESSURE ATM	Z FACTOR	CURRENT MA	CURRENT DIFF	DENSITY GM/M**3	DENSITY DIFF
1	0.5857	1.0002	14.05	-0.009	96.857	0.0625
2	0.5320	1.0002	12.77	-0.000	87.980	0.0039
3	0.4788	1.0002	11.50	0.007	79.178	-0.0492
4	0.4254	1.0002	10.22	0.010	70.333	-0.0752
5	0.3658	1.0001	8.78	0.001	60.481	-0.0072
6	0.3181	1.0001	7.63	-0.003	52.588	0.0231
7	0.2660	1.0001	6.38	-0.002	43.972	0.0184
8	0.2126	1.0001	5.10	-0.002	35.155	0.0195
9	0.1589	1.0000	3.81	-0.004	26.276	0.0283
10	0.1061	1.0000	2.55	0.003	17.541	-0.0262
11	0.0553	1.0000	1.33	0.002	9.148	-0.0144
SLOPES		0.688934E 01		0.688934E 01		
RMS ERRORS		0.536449E-02		0.369575E-01		

TABLE G-2. DENSITY BALANCE CALIBRATIONS USING METHANE

DATA REDUCTION FOR BALANCE CALIBRATION WITH METHANE
MAY 8, 1970DENSITY BALANCE CALIBRATION
GAS MOLE WT = 16.042 SCALE CORR = 0.15

PT	PRESSURE ATM	Z FACTOR	CURRENT MA	CURRENT DIFF	DENSITY GM/M**3	DENSITY DIFF
1	0.1558	0.9997	14.95	0.003	103.311	-0.0272
2	0.1394	0.9997	13.36	-0.002	92.366	0.0185
3	0.1127	0.9998	10.80	-0.002	74.654	0.0012
4	0.0878	0.9998	8.41	-0.002	58.147	0.0152
5	0.0737	0.9999	7.07	0.004	48.836	-0.0332
6	0.0583	0.9998	5.59	0.000	38.634	-0.0055
7	0.0424	0.9999	4.06	-0.007	28.118	0.0544
8	0.0299	0.9999	2.86	-0.002	19.786	0.0170
9	0.0223	0.9999	2.12	-0.019	14.791	0.1372
SLOPES		0.691231E 01		0.691231E 01		
RMS ERRORS		0.759720E-02		0.522393E-01		

DATA REDUCTION FOR BALANCE CALIBRATION WITH METHANE
MAY 8, 1970DENSITY BALANCE CALIBRATION
GAS MOLE WT = 16.042 SCALE CORR = 0.15

PT	PRESSURE ATM	Z FACTOR	CURRENT MA	CURRENT DIFF	DENSITY GM/M**3	DENSITY DIFF
1	0.1543	0.9997	14.76	-0.002	102.023	0.0180
2	0.1383	0.9997	13.24	0.012	91.413	-0.0873
3	0.1252	0.9997	11.97	-0.003	82.745	0.0215
4	0.1143	0.9997	10.92	0.001	75.526	-0.0095
5	0.1020	0.9998	9.75	-0.006	67.427	0.0455
6	0.0881	0.9998	8.42	-0.001	58.201	0.0114
7	0.0790	0.9999	7.55	-0.006	52.224	0.0471
8	0.0624	0.9998	5.97	0.004	41.225	-0.0326
9	0.0509	0.9999	4.87	0.003	33.634	-0.0214
10	0.0413	0.9999	3.95	-0.002	27.313	0.0156
11	0.0337	0.9999	3.21	-0.009	22.248	0.0645
12	0.0222	0.9999	2.12	-0.009	14.717	0.0559
SLOPES		0.691092E 01		0.691092E 01		
RMS ERRORS		0.636635E-02		0.439988E-01		

TABLE G-3. DENSITY BALANCE CALIBRATIONS USING NITROGEN

DATA REDUCTION FOR BALANCE CALIBRATION WITH NITROGEN,
MAY 7, 1970

DENSITY BALANCE CALIBRATION
GAS MOLE WT = 28.016 SCALE CORR = 0.15

PT	PRESSURE ATM	Z FACTOR	CURRENT MA	CURRENT DIFF	DENSITY GM/M**3	DENSITY DIFF
1	0.0925	0.9999	13.63	0.002	94.846	-0.0264
2	0.0731	0.9999	12.09	0.011	84.073	-0.0321
3	0.0689	0.9999	11.37	-0.004	79.176	0.0346
4	0.0626	0.9999	10.34	0.004	71.944	-0.0281
5	0.0567	0.9999	9.38	0.010	65.216	-0.0737
6	0.0483	0.9999	7.97	-0.014	55.577	0.1011
7	0.0390	0.9999	6.43	-0.018	44.883	0.1267
8	0.0320	0.9999	5.29	-0.000	36.825	0.0038
9	0.0238	0.9999	4.74	-0.020	33.134	0.1415
10	0.0232	0.9999	3.83	-0.010	26.733	0.0746
SLOPES			0.696063E 01		0.696062E 01	
RMS ERRORS			0.117102E-01		0.815186E-01	

DATA REDUCTION FOR BALANCE CALIBRATION WITH NITROGEN
JUNE 19, 1970

DENSITY BALANCE CALIBRATION
GAS MOLE WT = 28.016 SCALE CORR = 0.15

PT	PRESSURE ATM	Z FACTOR	CURRENT MA	CURRENT DIFF	DENSITY GM/M**3	DENSITY DIFF
1	0.0866	0.9999	14.33	0.000	99.976	-0.0065
2	0.0802	0.9999	13.27	-0.006	92.634	0.0479
3	0.0731	0.9999	12.12	0.014	84.459	-0.1034
4	0.0660	0.9999	10.93	0.010	76.184	-0.0756
5	0.0583	0.9999	9.64	-0.010	67.331	0.0720
6	0.0538	0.9999	8.88	-0.022	62.111	0.1545
7	0.0491	0.9999	8.14	0.018	56.664	-0.1295
8	0.0438	0.9999	7.24	-0.013	50.611	0.0967
SLOPES			0.697716E 01		0.697715E 01	
RMS ERRORS			0.137813E-01		0.961571E-01	

TABLE G-4. DENSITY BALANCE CALIBRATION USING UHP METHANE AND UHP CARBON DIOXIDE

DATA REDUCTION FOR BALANCE CALIBRATION WITH UHP C1
JULY 2, 1970DENSITY BALANCE CALIBRATION
GAS MOLE WT = 16.042 SCALE CORR = 0.25

PT	PRESSURE ATM	Z FACTOR	CURRENT MA	CURRENT DIFF	DENSITY GM/M**3	DENSITY DIFF
1	0.1468	0.9997	13.91	-0.004	97.036	0.0221
2	0.1340	0.9997	12.71	0.009	88.567	-0.0689
3	0.1284	0.9997	12.17	0.005	84.833	-0.0369
4	0.1188	0.9997	11.26	0.004	78.492	-0.0315
5	0.1122	0.9998	10.62	-0.006	74.108	0.0471
6	0.1041	0.9998	9.85	-0.011	68.773	0.0825
7	0.0966	0.9998	9.15	-0.002	63.826	0.0166
8	0.0885	0.9998	8.38	-0.001	58.447	0.0075
9	0.0820	0.9998	7.77	0.005	54.149	-0.0364
10	0.0739	0.9998	7.01	0.009	48.821	-0.0646
11	0.0678	0.9998	6.42	-0.002	44.790	0.0195
12	0.0604	0.9998	5.71	-0.011	39.897	0.0771
SLOPES			0.697373E 01		0.697372E 01	
RMS ERRORS			0.709188E-02		0.494576E-01	

DATA REDUCTION FOR BALANCE CALIBRATION WITH UHP CO2
JULY 16, 1970DENSITY BALANCE CALIBRATION
GAS MOLE WT = 44.010 SCALE CORR = 0.50

PT	PRESSURE ATM	Z FACTOR	CURRENT MA	CURRENT DIFF	DENSITY GM/M**3	DENSITY DIFF
1	0.0567	0.9997	14.70	-0.009	102.680	0.0693
2	0.0546	0.9997	14.19	0.007	98.998	-0.0526
3	0.0505	0.9997	13.12	-0.006	91.627	0.0449
4	0.0484	0.9997	12.57	0.006	87.700	-0.0427
5	0.0456	0.9997	11.84	0.008	82.590	-0.0570
6	0.0422	0.9997	10.94	-0.002	76.384	0.0196
7	0.0392	0.9998	10.17	0.006	70.941	-0.0485
8	0.0346	0.9998	8.98	-0.009	62.752	0.0689
SLOPES			0.698035E 01		0.698035E 01	
RMS ERRORS			0.754382E-02		0.526585E-01	

required molecular weight. Using similar reasoning, the results of Table G-2 indicate that the CP grade methane used had a true molecular weight of approximately 16.2. The calibration slopes for nitrogen given in Table G-3 are close to the accepted value of 6.98. This might have been expected since the molecular weights of any impurities are likely to be close to that of nitrogen.

G.3 Density Balance Data Reduction Program

A listing of the FORTRAN program used to calculate the composition of binary mixtures and to calibrate the density balance is reproduced on pages G-8 to G-10. Comment cards are used to assist the user. The program calls one subroutine called ZB. This subroutine calculates the compressibility factor for the various gases using simple approximations for second virial coefficients.


```

ATM(I)=HT*1.0005/760.0
60 CONTINUE
SUMX=0.0
IF(LABEL=3)70,140,70
70 DO 100 I=1,N
    TA=TB(I)+273.16
    AAA=ATM(I)
    XX=XL(I)
    CALL ZB(KEY,TA,AAA,XX,Z(I))
    IF(KEY=6)90,90,90
90 Z(I)=SLDR*EX(I)*Z(I)*2.04E-10*TA*ATM(I)
    XL(I)=(Z(I)-I)/(-2-1)
    XH(I)=1.0-XL(I)
    SUMX=SUMX+XL(I)
    GO TO 100
100 Y(I)=ATM(I)*WC/(Z(I)*82.054E-06*TA)
102 CONTINUE
    IF(KEY=3)110,120,120
110 SXX=0.0
    SXY=0.0
    SYY=0.0
C    CALIBRATION POINTS ARE WEIGHTED BY SQRT(DENSITY)
    DO 111 I=1,N
        SXY=SXY+X(I)*Y(I)*SQRT(Y(I))
        SXY=SXY+X(I)*Y(I)*SQRT(Y(I))
        SYY=SYY+Y(I)*Y(I)*SQRT(Y(I))
111 CONTINUE
    BX=SYY/SXY
    BY=SXY/SXX
    SDX=0.0
    SDY=0.0
    DO 112 I=1,N
        DX(I)=X(I)-Y(I)/BX
        DY(I)=Y(I)-BY*X(I)
        SDX=SDX+DX(I)*DX(I)
        SDY=SDY+DY(I)*DY(I)
112 CONTINUE
    SDX=SQRT(SDX/N)
    SDY=SQRT(SDY/N)
    WRITE(1,7)(I,ATM(I),Z(I),X(I),DX(I),Y(I),DY(I),I=1,1)
    WRITE(1,8)BX,BY,SDX,SDY
    GO TO 10
120 LAP=LAP+1
    IF(LAP=1)130,60,130
130 WRITE(1,9)(ITEST(I),P(I),ATM(I),Z(I),X(I),XL(I),
    1XH(I),I=1,N)
    IF(N-1)131,132,131
131 XX=SUMX/FLOAT(N)
    XIX=1.0-XX
    WRITE(1,10)XX,XIX
132 WRITE(1,11)XX,XIX
    GO TO 20
140 LAP=LAP+1
    GO TO 20
200 CALL EXIT
    END

```



```

SUBROUTINE ZB(KEY,TA,ATM,X,Z)
C *****
C THIS SUBROUTINE CALCULATES THE COMPRESSIBILITY FACTOR
C FOR THE PARTICULAR GAS SPECIFIED BY 'KEY' USING SECOND
C VIRIAL COEFFICIENT DATA WHICH APPLY AT ROOM TEMPERATURE
C *****
R=ATM/(82.054*TA)
GO TO(10,20,30,40,50,60,70,80,90),KEY
10 Z=1.0+12.0*R
RETURN
20 Z=1.0+(42.441-16711.3/TA-2501485.5/(TA*TA))*R
RETURN
30 Z=1.0-(8.6+0.191111*(TA-318.16))*R
RETURN
40 Z=1.0+255.0*(0.43-0.366*425.2/TA-0.694*(425.2/TA)**2
1-0.1125*(425.2/TA)**4.5)*R
RETURN
50 Z=1.0+(0.9*TA-389.7)*R
RETURN
60 E=244.0-1.5*(TA-273.16)
B22=255.0*(0.43-0.366*425.2/TA-0.694*(425.2/TA)**2
1-0.1125*(425.2/TA)**4.5)
GO TO 100
70 E=474.0-3.0*(TA-273.16)
B22=211.0*(0.43-0.366*469.8/TA-0.694*(469.8/TA)**2
1-0.15*(469.8/TA)**4.5)
GO TO 100
80 E=33.0-6.52*(TA-273.16)
B22=368.0*(0.43-0.586*507.9/TA-0.694*(507.9/TA)**2
1-0.175*(507.9/TA)**4.5)
GO TO 100
90 E=26.0-0.32*(TA-273.16)
B22=0.9*TA-389.7
100 S11=42.441-16711.3/TA-2501485.5/(TA*TA)
S12=5+0.5*(S11+B22)
XI=1.0-X
Z=X*X*(S11+2.0*X*XI*S12+XI*XI*B22
Z=1.0+R*R
RETURN
END

```


APPENDIX H
INSTRUMENT CALIBRATION DATA

TABLE H-1. PRESSURE GAUGE CALIBRATIONS

Serial No.	H26191	H19154R	H39687	H39217	H39217
CPE No.	1371	1390	1060	1344	1344
Range	0-1500	0-1500	0-5000	0-5000	0-5000
Date	Jan. 6/69	Jan. 6/69	Jan. 15/69	Jan. 15/69	June 4/69
DWG, psig	psig	psig	psig	psig	psig
0	0	0	0	0	0
200	200	200			
250			250	250	
400	400	400			
500			500	500	500
600	600	600			
750			750	750	
800	800	800			
1000	1000	1000	1005	1000	1000
1200	1200	1200			
1250			1250	1250	
1400	1400	1400			
1500	1500	1500	1500	1500	1500
1750			1750	1750	
2000			2000	2005	2000
2250			2250	2250	
2500			2500	2500	2500
2750			2756	2750	
3000			3000	3000	3000
3250			3250	3250	
3500			3505	3500	3500
3750			3755	3750	
4000			4000	4000	4000
4250			4250	4250	
4500			4505	4500	4500
4750			4750	4750	
5000			5000	5000	5000

Note: The Ruska dead weight gauge in the Department of Chemical and Petroleum Engineering Standards Laboratory was used in all calibrations.

Errors smaller than 0.1 per cent of full scale reading were not recorded.

TABLE H-2. THERMOCOUPLE CALIBRATION

Serial No.	#1 (Cell II)		#4 (Cell I)		#3 (Cell III)	
Type	Fe-constantan		Fe-constantan		Fe-constantan	
Date	May 8, 1970		May 8, 1970		May 8, 1970	
Water Bath Temp. °F	emf, millivolts Ref. J.	TC	emf, millivolts Ref. J.	TC	emf, millivolts Ref. J.	TC
100	1.951	1.956	1.951	1.956	1.951	1.956
130	2.821	2.827	2.821	2.826	2.821	2.826
160	3.700	3.705	3.706	3.712	3.704	3.711
190	4.607	4.612	4.607	4.612	4.605	4.612

Note: Ref. J. refers to the emf measured with respect to the reference junction used on the equipment.

TC refers to the emf measured at the thermocouple.

All voltages were measured with a Leeds-Northrup Model K-3 potentiometer.

APPENDIX I

PHOTOGRAPHS OF RETROGRADE LIQUID CAPILLARY STRUCTURES

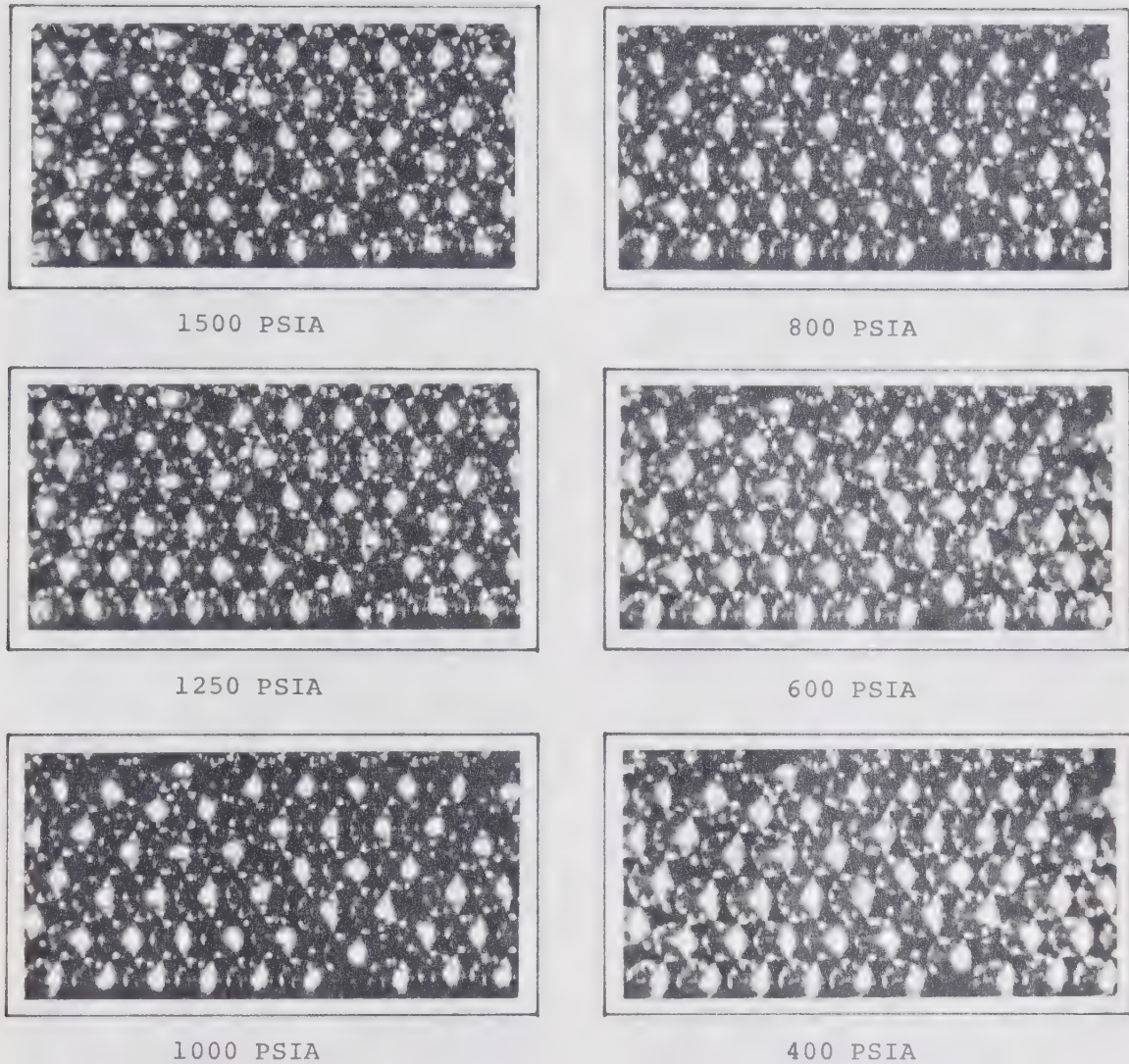


Figure I-1. Photographs of Liquid Capillary Structures Formed During Pressure Depletion of the Methane-n-Butane Mixture in Run 4.

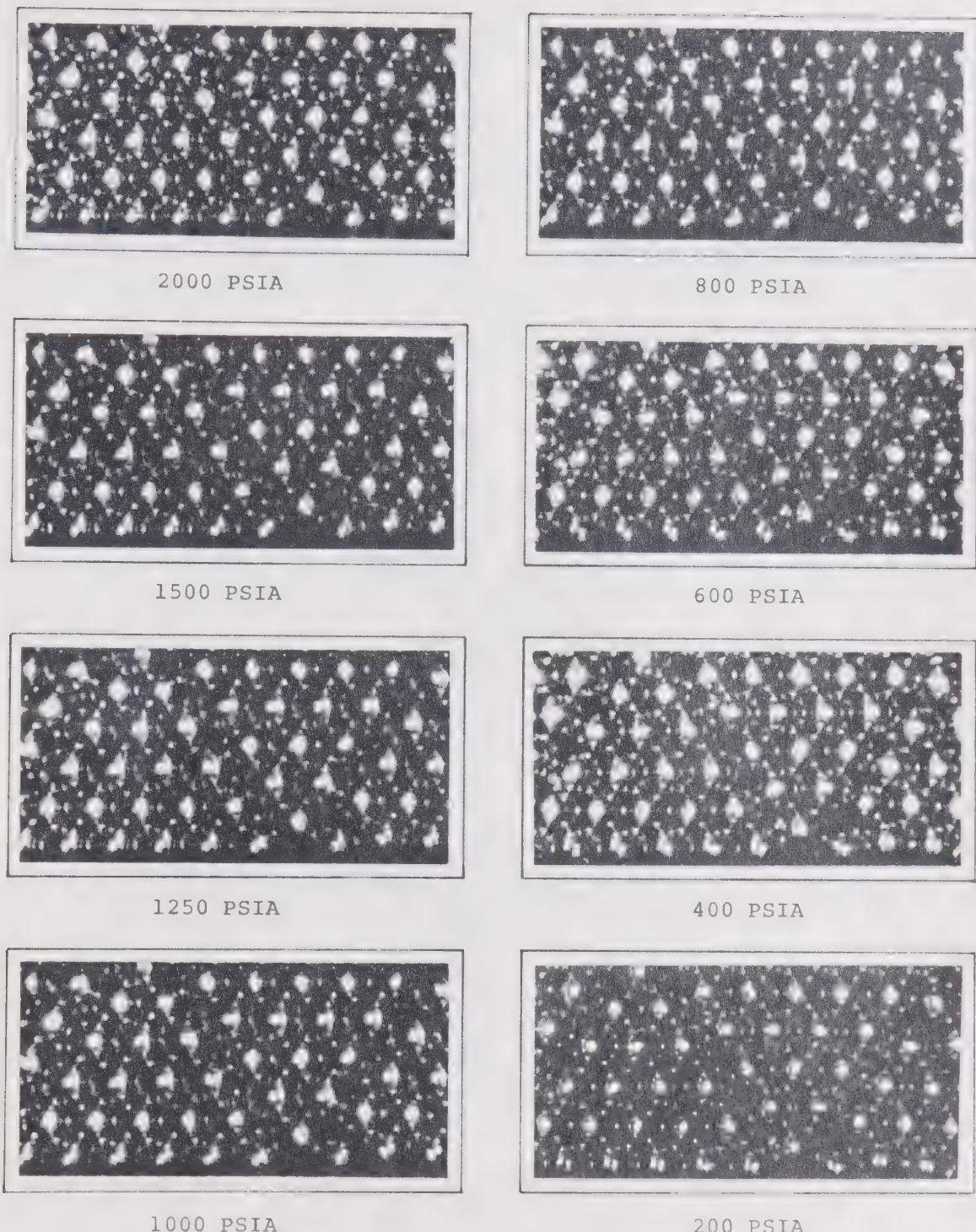


Figure I-2. Photographs of Liquid Capillary Structures Formed During Pressure Depletion of the Methane-n-Butane Mixture in Run 5.

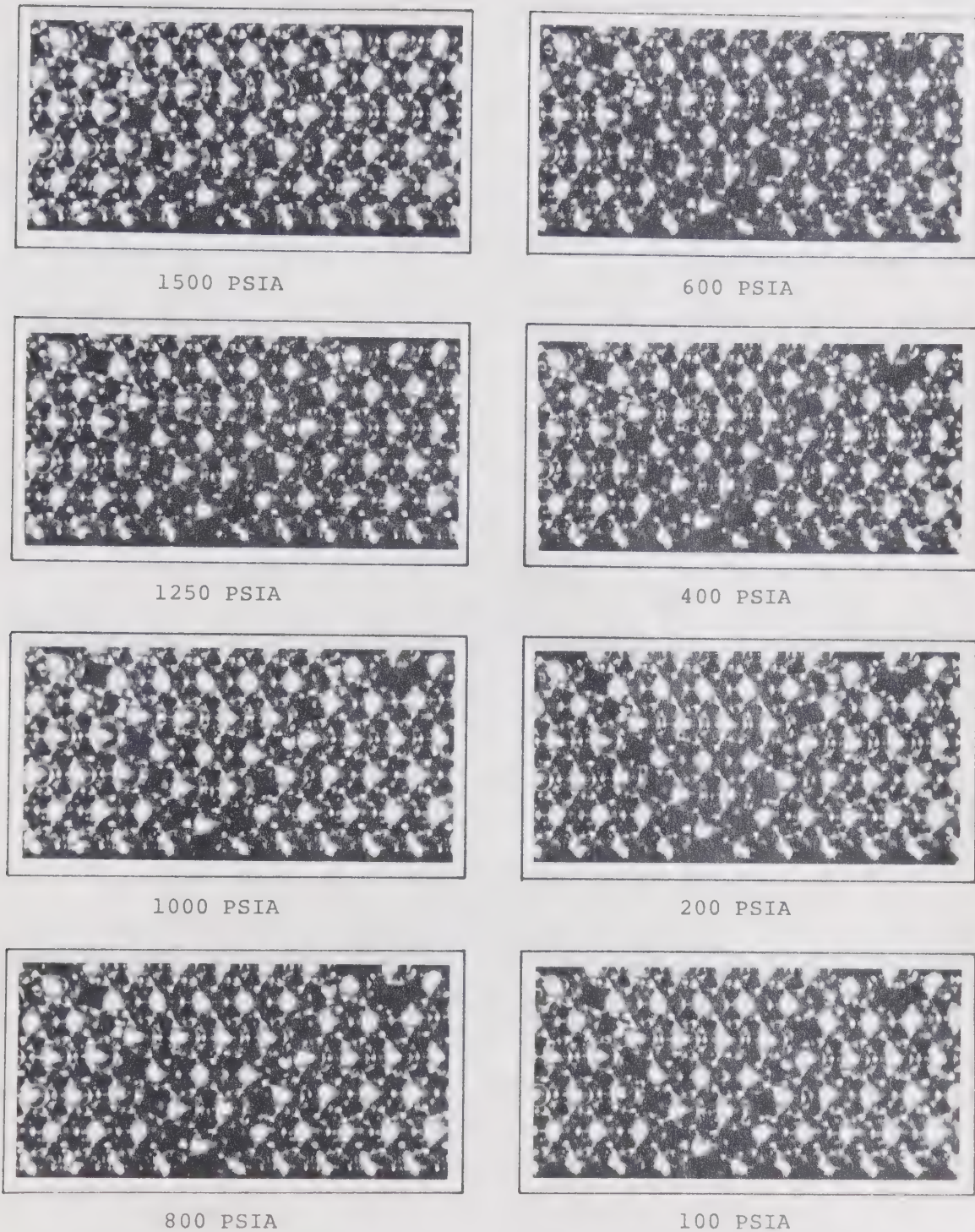


Figure I-3. Photographs of Liquid Capillary Structures Formed During Pressure Depletion of the Methane-n-Hexane Mixture in Run 7.

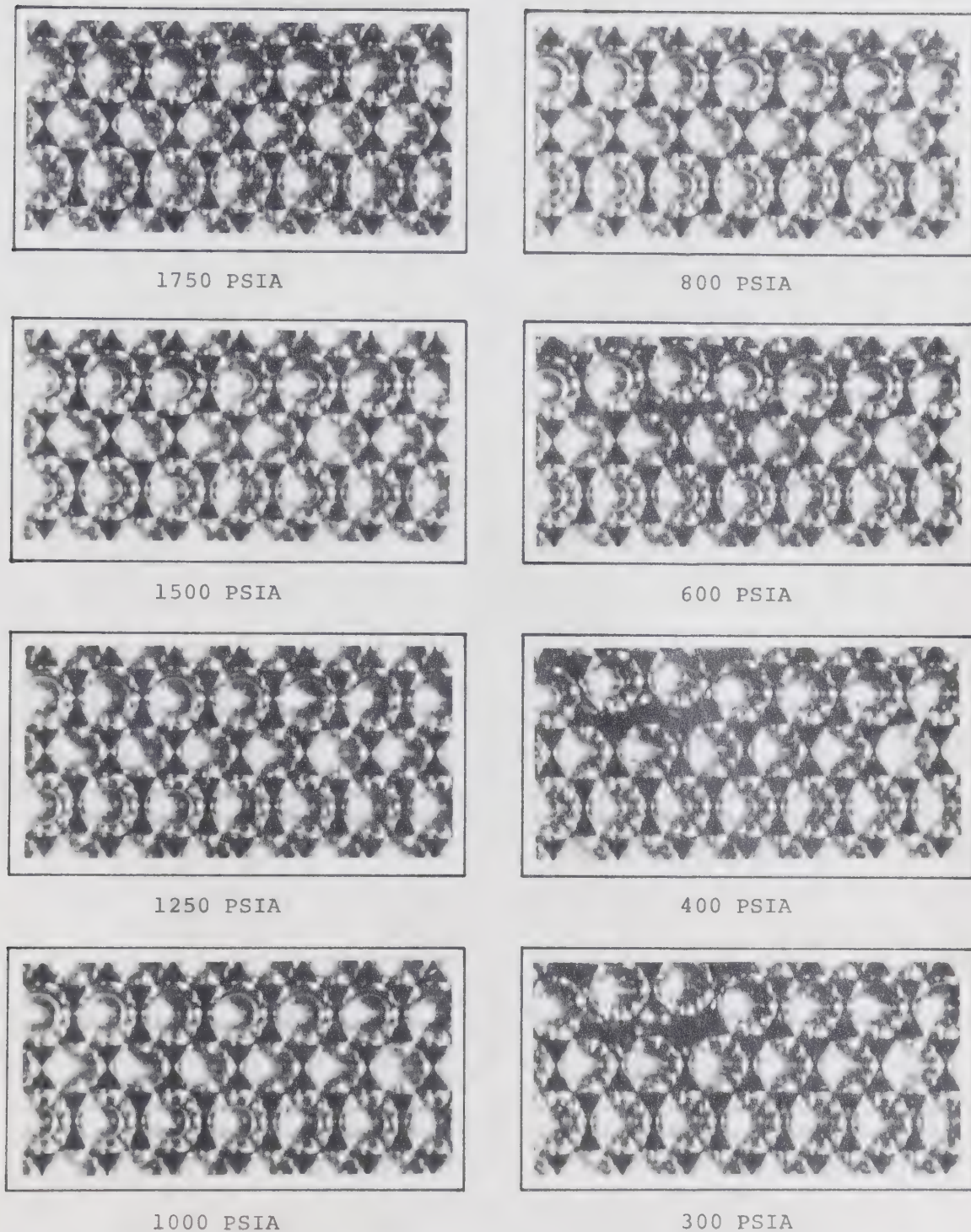


Figure I-4. Photographs of Liquid Capillary Structures Formed During Pressure Depletion of the Methane-n-Butane Mixture in Run 13.

B30043